PB83-144501

UMTRI-82-42

SUPERIOR-INFERIOR HEAD IMPACT TOLERANCE LEVELS

Nabih M. Alem
Guy S. Nusholtz
John W. Melvin

FINAL REPORT
NOVEMBER 1982

UNIVERSITY OF MICHIGAN
TRANSPORTATION RESEARCH INSTITUTE
FORMERLY HIGHWAY SAFETY RESEARCH INSTITUTE

UMTRI-82-42

SUPERIOR-INFERIOR HEAD IMPACT TOLERANCE LEVELS

Nabih M. Alem
Guy S. Nusholtz
John W. Melvin

University of Michigan Transportation Research Institute
Biomechanics Department
Ann Arbor, Michigan 48109

Contract No. 210-79-0028

FINAL REPORT
November 1982

U.S. Department of Health and Human Services
Public Health Service
Center for Disease Control
National Institute for Occupational Safety and Health
Rockville, Maryland 20857

1. Report No.	2. Government Accession No.	3. Recipient's Catalog No.
		PB83 144501

4. Title and Subtitle	5. Report Date
SUPERIOR-INFERIOR HEAD IMPACT TOLERANCE LEVELS	November 1982
	6. Performing Organization Code

7. Author(s)	8. Performing Organization Report No.
N.M. Alem, G.S. Nusholtz, J.W. Melvin	UMTRI-82-42

9. Performing Organization Name and Address	10. Work Unit No.
University of Michigan Transportation Research Institute 2901 Baxter Road Ann Arbor, Michigan 48109	11. Contract or Grant No. 210-79-0028
	13. Type of Report and Period Covered FINAL
12. Sponsoring Agency Name and Address National Institute for Occupational Safety and Health U.S. Department of Health and Human Services Rockville, Maryland 20857	14. Sponsoring Agency Code

15. Supplementary Notes

16. Abstract

The objectives of this research project were first to generate experimental kinematic response and injury data resulting from axial (superior-inferior) head impacts, then to use the generated results to establish a head/neck tolerance level to be used in the design and testing of protective industrial helmets. Fourteen impact tests were conducted on cadaveric specimens. Parameters of impact were the impactor weight (10 kg), its velocity at impact (7 to 11 m/s), padding of the impactor (0- to 5-cm ensolite), and the neck alignment with the spinal column. Peaks of the impact force ranged from 3 to 17 kN. Measured responses were the head 3-D motion and the spinal column accelerations.

The autopsies performed indicated that four tests failed to produce any neck or head damage. In one of the remaining tests, basal skull fracture (with no neck damage) was produced, while the skull fractured under the impactor in another test. In the remaining eight tests, cervical spinal injuries of various types were produced under varying impact conditions. The size of the sample of tests available for determining S-I tolerance levels remains too small for accurate assessment. This sample must be enlarged by conducting more S-I head impacts, and by widening the scope of experimental documentation to focus on measurement of the neck motion.

17. Key Words	18. Distribution Statement
	Unlimited

19. Security Classif.(of this report)	20. Security Classif.(of this page)	21. No. of Pages	22. Price
None	None	279	

Form DOT F 1700.7 (8-69)

DISCLAIMER

The contents of this report are reproduced herein as received from the contractor. The opinions, findings, and conclusions expressed herein are not necessarily those of the National Institute for Occupational Safety and Health, nor does mention of company names or products constitute endorsement by the National Institute for Occupational Safety and Health.

NIOSH Project Officer: Donald Campbell
Project Director: Nabih Alem

LIST OF TABLES

LIST OF FIGURES

1.0 INTRODUCTION

A research project entitled "Superior-Inferior Head Impact Tolerance Levels" was carried out at the University of Michigan Transportation Research Institute (UMTRI[1]) and sponsored by the National Institute of Occupational Safety and Health. The objective of the study was to generate experimental injury data that would lead to the establishment of an injury tolerance criterion in testing the effectiveness of protective industrial safety helmets. This document is the final report on this project, contract No. NIOSH-210-79-0028.

1.1 Historical Background

Currently, industrial safety helmets are evaluated for injury protection effectiveness using the American National Standard Institute ANSI Z89.1 guideline. The procedure is to drop an eight-pound hemispherical impactor onto the top of a helmet mounted on a rigid headform. The peak force, transmitted through the helmet to the base of the headform, is then measured and compared with the requirement specified in the ANSI standard.

Recent investigations have shown that the use of peak transmitted force as a criterion for industrial helmet performance evaluation does not account for the biomechanical characteristics of the human head, nor does it predict head injuries which are predicted by the majority of head injury criteria.

---

[1]Formerly the Highway Safety Research Institute (HSRI).

Further investigations have shown that, in superior-inferior impacts to the head, the weakest link is the neck where serious damage is likely to occur long before any injuries to the head and/or brain are inflicted. These investigations were limited in scope but have generated reasonable cause for concern over the injury mechanisms and tolerance of the neck to the S-I mode of impact.

A biomechanically defensible criterion is therefore urgently needed as a basis for developing a standard for evaluating the performance of industrial safety helmets. The current state of the art suggests two approaches. The first is to adapt one of the many head injury criteria currently available in the literature to S-I impacts to human heads, whereas the second is to develop a criterion based on actual S-I impacts in which both brain and neck injuries are monitored and correlated with the kinematics of impact.

The historical background of each approach is discussed in the next sections, followed by a discussion of their respective shortcomings and merits.

1.2 Head Injury-Based Criteria

The head injury criteria which are currently validated and available in the research literature draw their formulations from two basic sources of experimental head injuries. The first source is the Wayne State Tolerance Curve (WSTC) obtained from laboratory rigid impacts to cadaver foreheads in the anterior-posterior A-P direction [1,2].[2] In these tests, the A-P acceleration of the head was measured at the occiput, directly opposite and in-line with the impact. From each test, the average measured acceleration (a single number) was calculated and plotted

---

[2]Numbers is brackets indicate references listed in Section 7.0.

against the acceleration duration for that test to produce a single data point on the WSTC. For each test, fracture of the skull was used as an indication of potential hazard to live humans. The result was a curve separating the hazardous and non-hazardous cases, which was interpreted as the Tolerance Curve.

The second source of basic data for injury criteria was a series of impacts to live sub-human primates generated by Stalnaker et al. [3,4]. In order to correlate the kinematics of impacts (i.e., resultant head accelerations) with produced injuries, it was necessary to model the head with a four-parameter mechanical model and estimate the parameters of this model by driving point impedance techniques.

Once a model was defined for a given species, the acceleration measured from the impact tests on that species was used to drive its model and produce a maximum displacement. This displacement was then normalized to the length of the head in the direction of impact and called the resulting Maximum Strain. The results indicated that the primates could tolerate impacts whose maximum strain (obtained from the model) did not exceed a certain level; hence the name Maximum Strain Criterion (MSC).

In addition to human cadavers, as many as five sub-human primate species were tested. For each of the species a different model was generated both in the A-P and L-R direction, and a different Maximum Strain Criterion was obtained. Attempts to scale the results to live humans had limited success, and efforts to generate an S-I model and criterion were limited in scope.

1.3 Neck Injury-Based Criteria

The majority of published data related to neck tolerance levels is based on "whiplash" type impacts; for example, see [5,6,7]. Although useful for characterizing

the dynamic bending strength of the neck, it is not possible to extrapolate this tolerance data to S-I impact situations without the risk of making some modeling assumptions which may not hold in many cases.

The bulk of the data on the mechanisms, tolerances, and responses of head and neck under S-I impacts were generated in a pilot study at the Highway Safety Research Institute of The University of Michigan (now the University of Michigan Transportation Research Institute) in May 1978. In this study [8], eleven cadavers were subjected to S-I impacts to the skull vertex, and autopsies were performed on the cervical spine to determine the extent of damage to the base of the skull and the cervical vertebrae. No basal skull fractures were produced, but compressive fractures of the vertebrae began to occur for peak forces over 5.7 kN, for an impactor velocity of 7.5 m/s and initial impact work of 380J.

The UMTRI pilot study singled out the initial neck orientation with respect to the impact direction as the most important factor in influencing the mechanisms of injury and the thresholds of impact that can be tolerated by the head/neck complex. A subsequent study was carried out at UMTRI to define the kinematics of head/neck response to low levels of S-I impacts [9]. Although the study was not tailored to obtain injury information, most conclusions reached during the initial pilot study were confirmed. Thus, the neck orientation became a critical factor in loading the head/neck without producing injury.

The data base generated in both studies is not statistically sufficient for establishing a valid neck injury criterion. However, it provides an excellent nucleus for work toward that goal. Furthermore, these studies have indicated the direction that current and future similar investigations should take.

1.4 Shortcomings and Merits

The use of a head injury or neck injury criterion, or a combination thereof, as a basis for a Helmet Impact Performance Evaluation Standard (HIPES) can be justified with various arguments, all amenable to some human biomechanical response characteristics.

Head injury criteria that are derived from the WSTC fall into two categories. The first uses the tolerance curve to generate constants of a one degree-of-freedom model which is then driven by a measured acceleration history to produce a maximum displacement or velocity. Each model claims a given tolerance level based on the WSTC and on some impact characteristics (other than acceleration), such as the impacted subject (dummy or cadaver head). Like the WSTC, these models were originally developed for A-P impacts to be used with the A-P component of the head acceleration. Later, some of these models were extended (by modifying the model constants and defining different tolerance levels) to be used with resultant accelerations measured at various locations of the head.

The justification and validation of these newer models is essentially theoretical since only few case histories were employed in generating the new versions [3]. Therefore, the statistical value of their prediction is questionable even though their biomechanical justification may be valid. The use of these models as a HIPES basis offers the advantages of conceptual simplicity, prior use and validation, and ease of application. They must, however, be remodeled for application to S-I impacts and verified with some experimental and clinical case histories.

The second category of head injury criteria derived from the WSTC is purely mathematical and may be described as weighted impulse criteria. The first such criterion was the Gadd Severity Index (GSI) which was a successful curve-fitting of a portion of the WSTC. The GSI works as long as

one is using it under the same conditions as that of the WSTC, i.e., frontal rigid impacts to human cadavers in the A-P direction, and as long as its application is restricted to the A-P component of the head acceleration.

Such was not the case in the early widespread usage of the GSI as a head/brain injury criterion. Thus, researchers generalized the GSI to apply to resultant acceleration under any type of direct impact or indirect impulsive loading of the head. This generalization proved to be misleading, so a modified version of GSI was introduced to account for discrepancies between the predictions and the actual experimental injuries produced. The outcome was the Head Injury Criterion, or HIC.

The HIC attempted to weigh only the most significant portion of the resultant acceleration by searching for an interval (within the total pulse duration) for which a weighted impulse is the greatest. The weighting factor (2.5) and the tolerance threshold (1000) used in the HIC were retained from the GSI formulation, even though the calculation procedures were changed.

The initial success of the HIC in dealing with multiple pulses overshadowed its shortcomings as a general-purpose head injury criterion. Thus, the HIC was used, again indiscriminately, for all types of head accelerations produced under all types of impacts to all kinds of human surrogates. Only recently did HIC users realize that, any time the conditions under which a given criterion was developed change, the criterion is no longer fully applicable and misleading predictions may result.

The merits of the GSI and HIC is the automatic generation of an impact severity index which must then be interpreted correctly based on the impact circumstances. Both may be calculated on digital computers, but only the GSI may be analog-calculated.

The final head injury criterion derived from experimental head injury is the MSC based on a two-mass, spring-dashpot mechanical model. Unlike its single degree-of-freedom counterparts discussed earlier in this section, whose constants were derived from the WSTC, the constants for the MSC model were derived from mechanical impedances of human cadavers and of subhuman live primates. Injury-predictions of this model were shown to coincide with other models and with the WSTC, but the model goes one further step: injury prediction of lateral impacts. While other models (and the WSTC) can only claim statistical validity for A-P impacts, lateral versions of these models are merely reasonable speculations.

On the other hand, the MSC model parameters were not speculated but extracted from mechanical impedance data of the head driven at a point on the skull (with an electromagnetic shaker) in A-P as well as L-R directions. Unfortunately, no extensive testing was done in the S-I direction so that experimental justifications for any S-I model are weaker than those for A-P and L-R models. The use of this model as a foundation for a HIPES requires additional S-I driving impedance data and validation against experimental and, if possible, clinical case histories. Furthermore, it may be necessary to expand the MSC two-mass model to allow for simulation of the helmet attenuating effects on the impact severity.

As far as a neck injury-based HIPES, current research literature is simply not sufficient for development and validation of such a standard. The 1978 UMTRI-generated data represents the bulk of the data describing the human biomechanical response to S-I impacts, and can only be described as a first attempt at a complete and full understanding and documentation of this type of impact response.

The advantages of such a criterion as a foundation for a HIPES are numerous. The most obvious merit is that any criteria that is to be developed will draw the information directly from S-I impacts without resorting to speculations and extrapolations from non S-I impacts. Such an approach is generally recognized as the most valid research methodology, while the speculative approach, employed in cases where direct results cannot be obtained, usually decreases the confidence in the results.

In order to develop a neck injury criterion for S-I impacts (or any other criterion, for that matter), a data base must be available, or augmented if the current size of the base is not statistically acceptable. Once a data base is available, the various kinematic, dynamic, and physiological human responses, as well as the impact conditions, must be examined to point out any correlations that may exist. This process is as painstaking as the data generation itself and may or may not result in a simple or practical injury tolerance criterion.

These two processes (data generation and establishment of a tolerance level) have been extensively carried out during the last two decades and applied to automotive impact situations. (For example, see references [10-17] for a wide range of topics related to neck injury.) This means that most of the well-established and widely-used criteria are primarily concerned with A-P or L-R direct impacts, and in some cases, with whiplash-type indirect impacts. The experience gained from that research is certainly an invaluable resource to draw from and to shed some light on the methodology which must be employed to generate an S-I impact data base and to model and correlate the results.

2.0 EXPERIMENTAL METHODS

The immediate objective of this research project was to generate kinematic and dynamic data along with their associated injury information. Ultimately, a realistic injury tolerance criterion would be formulated, upon which a helmet impact performance evaluation standard could be adopted.

In this section, the experimental methods will be described. The test protocol is included as Appendix A of this report. The methods used have either been developed and applied in other projects at The University of Michigan and elsewhere or have been specifically developed for this S-I head impact project.

2.1 Test Subject Selection

Unembalmed cadavers provide reasonably good surrogates to live humans. Although some arguments may be presented against the validity of test results from these subjects, stronger arguments may be made against any other alternatives, such as sub-human primates or human volunteers. The response of unembalmed cadavers to identical impacts varies with age, size, time after death, strength and integrity of skeletal structure, and medical history. Therefore, every effort was made to keep the variability of these factors to a minimum by carefully selecting (or rejecting) an available subject. The final selection used in the testing phase includes fourteen cadavers described in Table 1.

TABLE 1. TEST SUBJECT BIOMETRICS

Test No.	Age	Wt(kg)	Ht(cm)	Cause of Death
81H401	59	74.9	169.8	Acute myocardial infarction
81H402	41	52.3	170.8	Lung cancer
81H403	64	44.7	171.5	Aspiration
81H404	65	62.9	183.8	Natural
81H405	49	85.9	181.8	Ventricular fibrillation
81H406	72	64.7	166.3	Cerebral vascular accident
81H407	63	55.9	169.2	Cardiac arrest
81H408	63	69.9	175.0	Cardiac arrest
81H409	54	--	--	Pneumonia, Carcinoma of spinal cord and kidney
81H410	66	81.5	177.2	Cardiac arrest
81H411	63	50.5	171.2	Cardiac arrest
81H412	66	54.5	177.7	Cardiac arrest
81H413				
81H414				

2.2 Subject Preparation[3]

The test cadavers were obtained from The University of Michigan Anatomy Department. Upon arrival at UMTRI, the subject was weighed and X-rayed to determine the integrity of the upper thorax, cervical spine, and head structure. Once the subject was approved for testing, it was appropriately prepared and stored in a cooler at 4° for the next day's surgical preparation.

2.3 Surgical Procedures

In this series of tests, surgical implantation of transducers consisted of three distinct groups of activities. These are described in the following sections.

[3]The protocol for the use of cadavers in this study was reviewed by the Committee to Review Grants for Clinical Research and Investigation Involving Human Beings of The University of Michigan Medical Center and follow guidelines established by the U.S. Public Health Service and recommended by the National Academy of Science/National Research Council.

2.3.1 Head Instrumentation. The three-dimensional rigid body motion of the head was measured using the UMTRI nine-accelerometer platform. This platform was screwed directly into the skull in the occipital region, leaving the top of the head exposed for impact. The method of attachment briefly follows. Several metal self-tapping screws are threaded directly into the occipital bones of the skull through small pilot holes. Anchors are attached to the magnesium accelerometer mounting plate (Figure 1) and are positioned near the screws on the exposed skull. To ensure rigidity, plastic acrylic is molded around the screws, feet, and plate such that the plate becomes rigidly attached to the skull. Three triaxial clusters of accelerometers are then attached to their positions on the plate.

2.3.2 Spinal Accelerometers. The spinal motion was monitored with triaxial acceleration clusters mounted at T1/C7, at T6 and at T12/L1 vertebrae. An incision was made over the vertebra, then an accelerometer mount was screwed right into the spinous process. Stabilizing hooks and tie wraps were used to anchor the mount to the vertebra. A spinal accelerometer mount is shown in Figure 2.

2.3.3 Cervical X-Ray Targets. In order to highlight the vertebral bodies of C2 through C7, specially fashioned lead targets were implanted on these six cervical vertebrae. The targets were soldered on stainless steel wire that was looped around each spinous process and its ends twisted until taut and the targets secured. Sheet metal screws with soldered heads were screwed into each lamina on the right, allowing both position and angle of the cervical spine to be determined.

2.3.4 Post-Test Procedures. A gross autopsy was performed on the head and neck. The scalp was reflected and the calvarium removed for examination. The epidural and subdural areas of the brain were inspected. The brain and

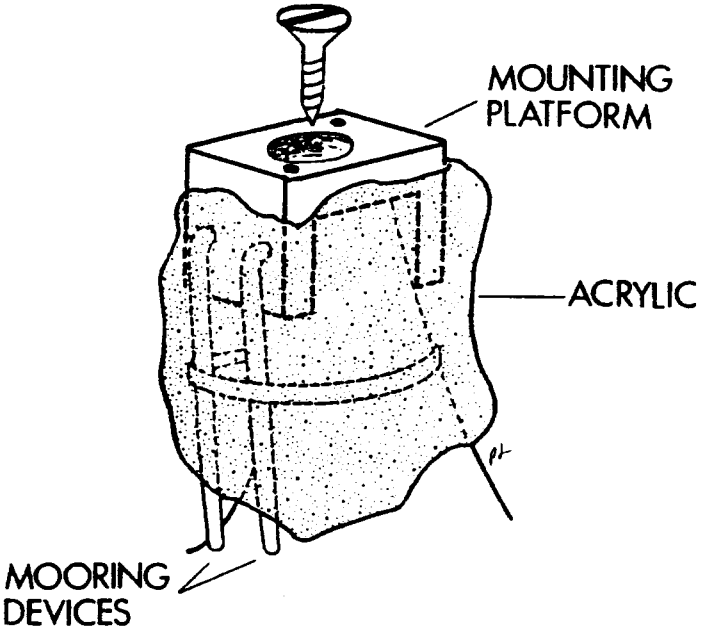

FIGURE 2. Schematic Representation of Spinal Mounting Platform

dura were extracted and the base of the skull examined. The cervical spine and adjacent musculature were removed and dissected. All observed injuries were recorded by sketches and photographs, and tentatively classified. After careful review of the results of autopsy, final classification of the injuries were determined.

A post-test three-dimensional X-ray procedure was followed to determine the location of the two occipital condyles with respect to the Frankfort Plane-based anatomical reference frame. This information is necessary for future computation of the reaction forces and moments at condyles.

2.4 Testing Equipment

Two testing devices were used during this project: the UMTRI impact air cannon and the UMTRI high-speed cineradiograph. A brief description of each device follows.

2.4.1 Impact Cannon. The UMTRI "air cannon," shown in Figure 3, was used to deliver the impact to the subject. This is a pneumatically operated testing machine designed and constructed especially to move a striking mass at a specific velocity for impact studies at UMTRI. The machine consists of an air reservoir and a ground and honed cylinder with two carefully fitted pistons. The transfer piston is propelled by compressed air through the cylinder and transfers its momentum to the impact piston. A striker plate attached to the impact piston travels a distance of about four inches, at which point an inversion tube absorbs the energy of the impact piston and halts it movement. The machine may be operated over a velocity range of 3 to 60 miles per hour with a 20-pound impact piston, and 6 to 120 miles per hour with a 6-pound impact piston, using a maximum of 100 psi pressure in the air reservoir. The maximum available energy is 22,000 foot-pounds when a compressed air bottle is used to pressurize the reservoir to 500 psi. An

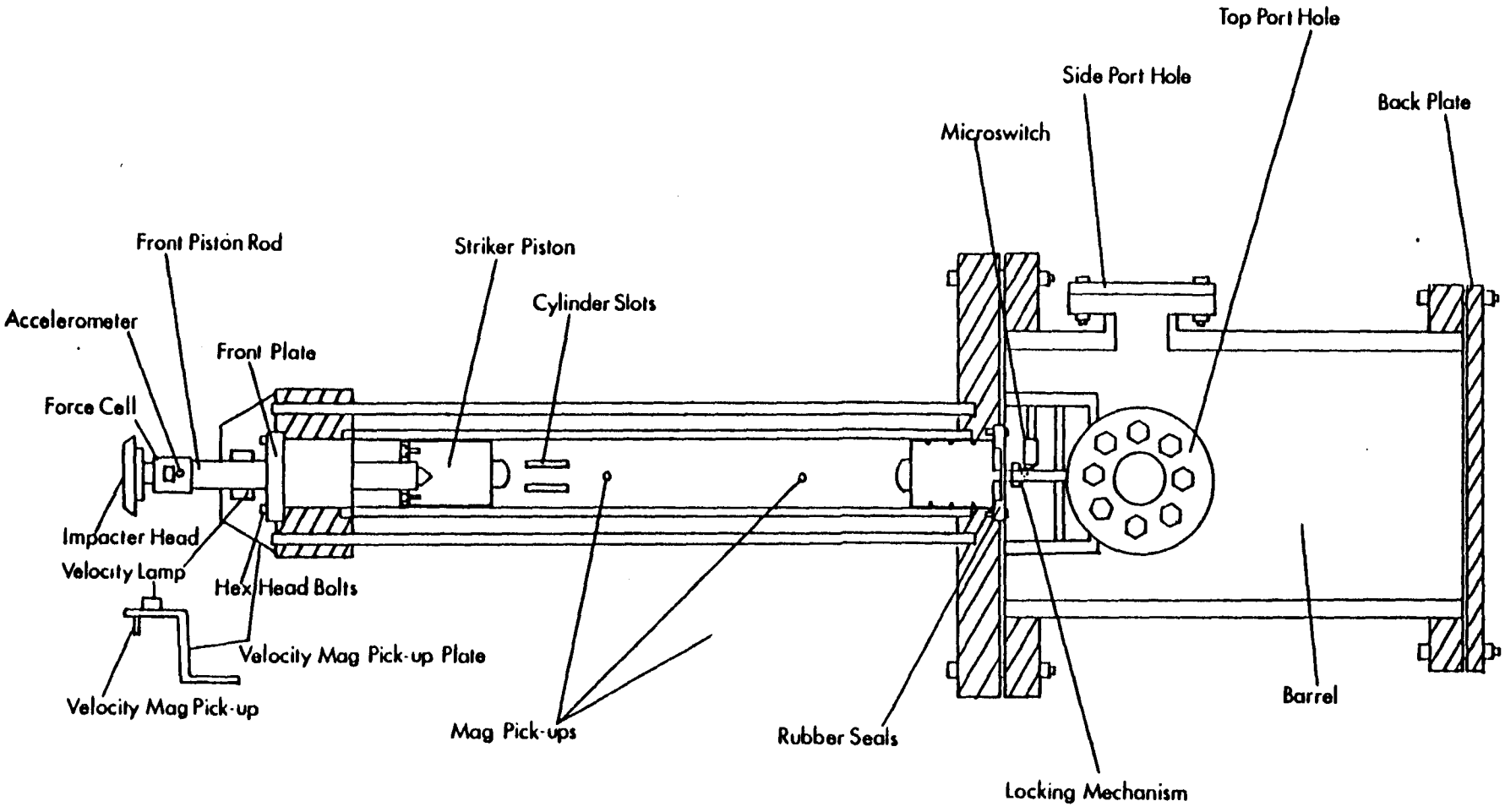

FIGURE 3. UMTRI Pneumatic Impact Device

accelerometer and inertia-compensated force transducer are mounted directly behind the striker plate.

2.4.2 High-Speed Cineradiography. This device is capable of taking up to 1000 frames/second of X-ray pictures, thus capturing the motion of skeletal structures under impact. In order to use it for documenting the motion of the cervical spine, the UMTRI cineradiograph was modified to increase the size of the imaged screen to a 14x17-inch area, and to include a mechanism for using a 35-mm camera. This modification was the first attempt at improving the visibility and definition of imaged bony structure. Although some improvement was achieved, the device remains in need of further development and testing.

The unmodified system [18] consists of a Photosonics 1B high-speed, 16-mm motion-picture camera which views a two-inch diameter output phosphor of a high-grain, four-stage, magnetically focused image intensifier tube, gated on and off synchronously with shutter pulses from the motion-picture camera. A lens optically couples the input photocathode of the image intensifier tube to X-ray images produced on a fluorescent screen by a smoothed direct-current X-ray generator. Smoothing of the full-wave rectified X-ray output is accomplished by placing a pair of high-voltage capacitors in parallel with the X-ray tube. The degree of ripple, or unsmoothness, of the X-ray output is directly proportional to X-ray tube current and inversely proportional to anode potential. At best, ripple in this system is approximately 8% of peak output. Particularly when no contrast medium is used, ripple can become as large as 30%. Ripple frequency occurs at the same frequency as full-wave rectification (120 Hz), so over a period of 8 milliseconds, or one cycle, density variation on the resulting eight frames of motion picture film can be as large as 50%. However, even with this density variation on

the film, it is still possible to discern changes in contrast boundaries caused by the impact event.

2.5 Subject-Impactor Alignment

The subject initial positioning allowed for most of the impact motion to occur in the midsagittal plane. The first ten subjects were placed prone on four layers of 10-cm seating foam atop an adjustable table as shown in Figure 4. This soft cushion allowed for a relatively free motion of the cervical spine. The head was either supported on breakaway styrofoam blocks or suspended with paper tape that offered minimal resistance during impact. The feet were blocked against the edge of the fixed table to simulate standing or seating reaction of the whole body to head-crown axial impacts. The last four tests were conducted with the subject supine as shown in Figure 5. The suspension rope was cut just as the impact was taking place, so that the significant part of the impact response was obtained with unappreciable vertical dropping velocity.

3.0 ANALYTICAL METHODS

The experimental design of the tests in this project was based on the ability to analytically extract useful kinematic and dynamic response parameters which could later be correlated with physiological response and injury. The groundwork preceding the establishment of such correlation, eventually leading to the adoption of a helmet impact performance evaluation standard, is a painstaking phase of the overall process. During this phase, the raw data obtained from the testing phase has to be cleaned and polished, then manipulated in order to generate new parameters which could be used in the concise definition of an injury tolerance level. In this section some of this analytical groundwork is described.

3.1 Signal Processing

Processing of the recorded transducer signals began by converting the analog signals into digital ones at the rate of 6400 samples/second. The frequency spectrum of each signal was examined to determine the highest significant frequency contained in the signal. Loss-pass digital filters were applied to all signals before analysis. Thus, 100-Hz filters were applied to impactor force and acceleration signals, while 250- and 400-Hz filters were used on the spinal and head acceleration signals, respectively.

3.2 Impact Severity

The impact severity was characterized by the velocity of the impactor, the peak and duration of contact force, the

force impulse, and the energy of the impactor at impact time. The velocity of the impactor was accurately measured from pulses generated by equally-spaced, impactor-mounted probes as they passed near a stationary magnetic pick up. All other impact parameters were calculated from the force pulse time-history.

The pulse duration (or length) was defined as the time interval between the formal beginning and end of the pulse. These two formal points were obtained by fitting straight lines to the rise and fall portions of the pulse and locating their intersections with the zero-force time axis. The impulse was obtained by integrating the force time-history. Finally, the transferred energy was defined as half the ratio of the square of the impulse over the impactor mass. The available pre-impact energy (half the product of the impactor mass times its squared velocity) is not presented, since only a portion of this energy is transferred to the subject, the other portion being absorbed by a crush tube installed in the impactor device.

3.3 Head Response

The description of the impact response of the human head requires that the kinematic quantities measured experimentally be described in reference frames which vary from one instrumentation method to another. One method for comparing mechanical responses between subjects is to refer all results to a "standard" anatomical frame which may be easily identified. However, it may be impractical to require that transducers be aligned with this anatomical frame, since this creates physical problems for which satisfactory solutions may not exist.

An alternative is to mount transducers in an arbitrary and convenient reference frame and then describe the transformation necessary to convert the data from this instrumentation frame to a desired anatomical one.

A three-dimensional X-ray technique is used to accomplish this for head impacts. Four anatomical landmarks (two superior edges of the auditory meati and two infraorbital notches) are marked with four mutually distinguishable lead pellets. The nine-accelerometer plate is marked with lead pellets at the center of mass of each triaxial accelerometer cluster and also at the plate center of mass. The head containing this instrumentation is then radiographed in two orthogonal directions (the x-z and y-z planes). On each of the two radiographs the optical center and the laboratory vertical z-axis are simultaneously X-rayed. The subsequent computations reconstruct the laboratory coordinates of each of the lead targets. The Frankfort plane is determined and the anatomical reference frame is reconstructed from the four anatomical points. The instrumentation frame and its origin are determined from the three triaxial accelerometer centers. Finally, the transformation matrix between the instrumentation frame and the anatomical frame is obtained.

Following this procedure, all input to the three-dimensional motion analysis program is available, so that the three-dimensional computation can proceed. This results in as many as 86 time-histories which can potentially be used in correlation with injury and/or to understand the motion of the head during impact. The UMTRI method has been fully documented in [19].

3.4 Spinal Response

The motion of the spine was documented by instrumenting three vertebrae along the upper and middle regions: at T1, T6, and T12. The instrumentation was for a triaxial acceleration measurement. Since this was not sufficient to fully document the three-dimensional motion of the instrumented vertebra, a mathematical realignment scheme was developed to "align" the three orthogonal axes of the

triaxial accelerations in such a way that the primary motion is along the resultant. The method has been successfully used for head impacts [20,21].

3.5 Mechanical Impedance

The areas of the human body affected by S-I impacts include the head itself, the neck and spine, and the upper thorax. These areas may be considered as one physical system consisting of many interacting elements.

It is a usual practice in complex system analyses to consider some input-output relationship as a means to characterize such a system. This relationship is called the transfer function of the system and may or may not be independent of time. This transfer function is a process which transforms the given input into an output. It is assumed here that this process is stationary or time-invariant.

There are a number of input and output parameters which have been measured. Thus, the measured impact force is an input quantity, while acceleration and velocity responses at the head anatomical center, at T1, and at T12 are all output quantities. It is therefore legitimate to characterize the upper portion of the body by transfer functions or processes which transform the impact force into any one of the resulting responses. The usefulness of such characterization is that it makes it possible to develop a "black box" model that predicts the human response to impact, given the impact force.

One such transfer function is the mechanical impedance, defined as the ratio of "force" over "velocity." Here the "force" and "velocity" are assumed to be those occurring when the system has reached a steady state under sinusoidal excitation. Mechanical impedance (with a magnitude and phase angle) is usually generated by exciting a given system with a given frequency, then sweeping the frequency over a

desired range. At each frequency, the magnitude of the steady-state velocity (also sinusoidal) results in an impedance which is a function of the frequency.

Unorthodox techniques are used in this project to obtain the mechanical impedance of the system as a function of frequencies. The method assumes that the system is time-invariant and linear, so that the principle of superposition may be applied. The method further assumes that the initial conditions of the system are all zero, allowing one to conclude that the magnitude of response at any given frequency is the result of an excitation of the same frequency.

Armed with these reasonable assumptions, and with the understanding that any irregular function of time (e.g., impact force, acceleration response) may be considered as one period of a periodic function, each of the input and output quantities were transformed to the frequency domain, resulting in a frequency spectrum at discrete frequencies ranging from the fundamental to the Nyquist rate. The fundamental is equal to the inverse of the signal duration, while the Nyquist rate is equal to half of the sampling rate. However, because of rounding errors of the Fast Fourier Transform (FFT), and since magnitudes of components in the upper frequency range are small and approach the rounding error, output/input ratio is noisy and should not be considered highly reliable.

Once all signals of interest have been transformed via FFT to the frequency domain, the spectrum is smoothed using a Hamming window. Finally, it is possible to characterize the system at each discrete frequency, resulting in an overall impedance curve which is a function of frequency. Finally, note that the input to the mechanical system may be at any location and in any direction, and the output can also be in any different (or same) direction and location.

4.0 RESULTS OF TESTING AND ANALYSIS

This section is primarily devoted to presentation of the results of cadaver axial impact tests. These results consist of characterization of input parameters, such as peak force and duration, and of output parameters which include kinematic, dynamic, and physiological responses. This section will also document the test peculiarities encountered during the testing which led to the modification of procedures initially described in Sections 2.0 and 3.0.

4.1 Subject Initial Conditions

The initial position and alignment of the head and spinal column were carefully adjusted to simulate the natural curvatures of the upper spine during normal seating or standing postures. In some tests, attempts were made to align the cervical and thoracic spines as close as possible along the axis of impact. This was done to confirm the suspected effects of the initial alignment on the resulting injuries. In all cases, in-place lateral X-rays were used to document the initial angles, with respect to the horizontal, of the head anatomical posterior-anterior axis, and of the neck using the tangent to its mid-portion as a reference line. The convention used in defining these alignment angles is diagrammed in Figure 6, and the measured angles are given in Table 2. Parameters extracted from impact force defining the severity of impact are summarized in Table 3.

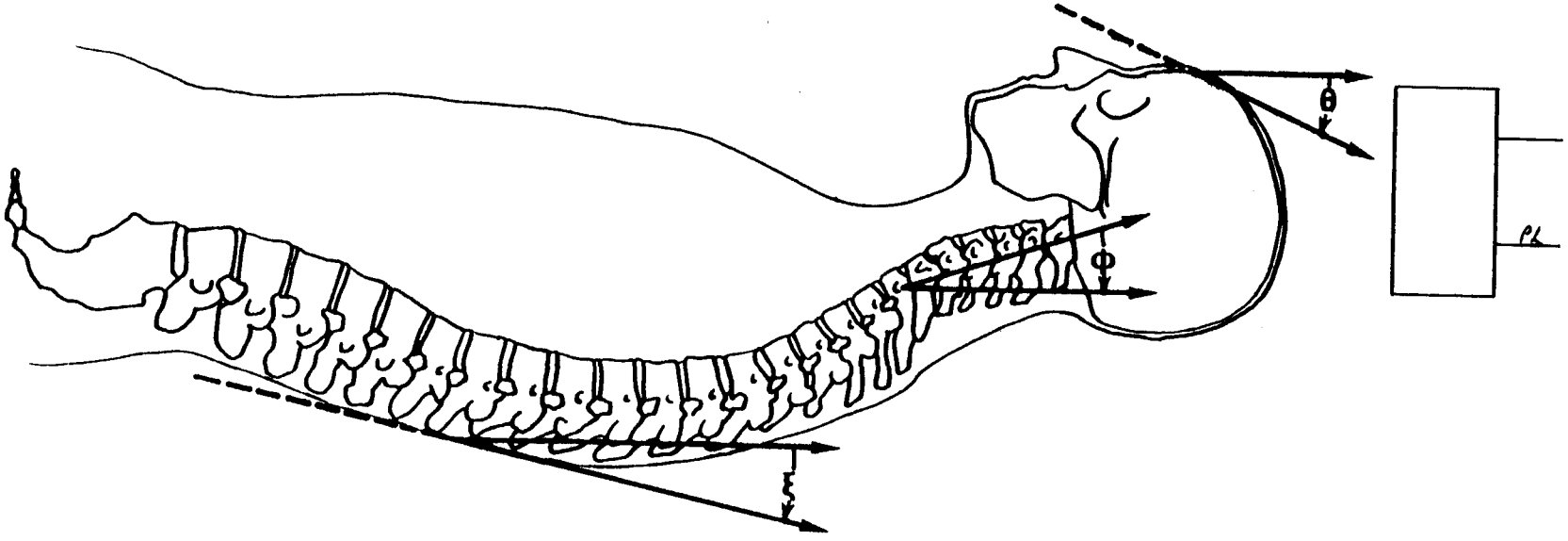

FIGURE 6. Definitions of Head/Neck/Thorax Angles

TABLE 2. SUBJECT INITIAL AND IMPACT CONDITIONS

Test Number	Neck Angle	Head Angle	Impactor	
			Velocity (m/s)	Padding (cm)
81H401*	30°	--	8.4	5.1
81H402	20°	--	10.9	5.1
81H403	25°	100°	10.9	5.1
81H404	25°	95°	7.8	5.1
81H405*	5°	80°	7.7	5.1
81H406	5°	80°	8.0	5.1
81H407	5°	--	9.2	5.1
81H408	10°	100°	9.7	5.1
81H409•	5°	--	10.4	0.0
81H410	30°	--	9.0	5.1
81H411*	---	--	7.2	5.1
81H412	10°	--	7.1	5.1
81H413•	0°	--	9.0	0.5
81H414*	---	--	6.9	0.5

TABLE 3. IMPACT FORCE PARAMETERS

Test Number	Force			
	Max (N)	Duration (ms)	Impulse (N-s)	Energy (N-m)
81H401*	4,200	15	34	61
81H402	11,000	9	49	122
81H403	10,500	6	40	82
81H404	4,000	14	36	65
81H405*	4,100	15	35	61
81H406	4,000	22	48	115
81H407	4,500	13	40	82
81H408	6,000	16	49	118
81H409•	15,000	3	36	66
81H410	5,200	20	42	88
81H411*	4,100	19	35	61
81H412	3,000	20	35	61
81H413•	17,000	3	26	33
81H414*	16,000	3	24	29

NOTE: *=No injuries; •=Skull fracture only.

4.2 Subject Kinematic Response

The detailed results of various analyses and data processing are included in Appendix A. In this section, these responses are briefly described and summarized.

4.2.1 Head Response. The UMTRI standard three-dimensional analysis of an instrumented rigid body yields some 86 variables. It was therefore necessary to limit the selection of those which could be correlated with injuries. The variables chosen were the resultant linear and angular accelerations and velocities of the head anatomical center and the accelerations of the T1, T6, and T12 (or L1) vertebrae. The HIC was also calculated, and the peaks of all these parameters are tabulated in Table 4.

TABLE 4. HEAD KINEMATIC RESPONSE

Test Number	HIC	Acceleration		Velocity	
		Linear (g)	Angular (Rad/S²)	Linear (m/s)	Angular (Rad/s)
81H401*	--	130	7,500	8.4	41
81H403	1031	160	8,100	8.1	41
81H405*	145	48	4,000	3.7	39
81H406	288	70	4,200	5.8	29
81H407	503	99	3,692	6.9	25
81H408	316	85	5,077	5.9	28
81H410	238	72	2,200	5.0	16
81H411*	76	48	1,150	3.5	7
81H412	61	45	1,400	3.5	12

NOTE: *=No injuries.

4.2.2 Cervical Spine Motion. High-speed X-ray movies taken at 1000 frames/second of the neck during impact on 35-mm film were not quantitatively analyzed due to the poor quality of the image. Qualitative analysis of each film was conducted, primarily to confirm the findings of the post-test autopsies. It should be noted that sophisticated

digital image enhancement could be applied to these movies so that the outline of the neck could be followed throughout the 10 to 20 millisecond duration of impact.

4.2.3 Thoracic Spine Response. Accelerations at T1, T6, and at T12 (or L1) vertebrae were "aligned" so that the primary axis of the realigned triad was along the resultant of the original non-aligned triad. The underlying assumption is that when motion is at its maximum, as indicated by the peak resultant acceleration, the actual motion at that instant is along the resultant regardless of how the orthogonal triad of measurement was initially oriented. Results of spinal accelerations are summarized in Table 5.

TABLE 5. SPINAL RESPONSE

Test No.	Acceleration (g)			Velocity (m/s)		
	T1	T6	T12	T1	T6	T12
81H401*	49	44	22	1.6	2.7	1.3
81H403	130	91	27	2.4	3.0	1.6
81H404	180	64	24	3.5	3.5	1.3
81H405*	46	41	12	1.7	2.0	1.0
81H406	70	54	15	2.4	2.5	1.0
81H408	59	88	20	2.2	1.7	1.1
81H410	48	17	7	---	---	---
81H411*	12	15	7	---	---	---

NOTE: *=No injuries.

4.3 Results of Autopsies

The detailed results of autopsies are included in Appendix A. However, these results are summarized here in Table 6.

TABLE 6. SUMMARY OF AUTOPSIES

Test No.	Injuries
81H402	Bilateral fracture of lamina of T2 at base of spinous process. Anterior body of T2 extremely compressed.
81H403	Ruptured C2-C3 and C3-C4 discs, with anterior longitudinal ligament torn between C3-C4. Anterior-inferior chip fracture of C2 body. Vertical fracture of posterior C2 body. C3 and C4 spinous process tip fractures. Ruptured T1-T2 disc with wedge fracture of T2 body. Rupture of posterior longitudinal ligament between T1-T2 producing complete bilateral dislocation between T1 and T2. Fracture of left transverse process of T2. Partial separation of anterior longitudinal ligament at upper T2 body. All interspinal ligaments torn between T1-T2. Left first rib fractured adjacent to T1.
81H404	Nearly complete tear of anterior longitudinal ligament at disc between C3-C4.
81H406	Bilateral fracture of posterior C1 arch. Fracture of C2 dens. Fracture of spinous process of C3 and C4. Fracture of right lamina of C7. Fracture of anterior-superior body of T1.
81H407	Rupture of anterior longitudinal ligament and disc between C5 and C6.
81H408	Tear of anterior longitudinal ligament between C3 and C4. Tear of anterior longitudinal ligament between disc of C4 and C5. Bilateral fracture of C1 posterior arch. Fracture of anterior inferior C2 body extending through C2-C3 disc. Compression fracture of upper body of T2. Compression fracture of lower body of T3.
81H409	Circular depressed fracture at apex of skull (beneath impactor).
81H410	Anterior longitudinal ligament torn at discs C3-C4 and C4-C5. Rupture of discs C3-C4 and C4-C5. Rupture of central portion of discs C5-C6 and C6-C7. Fracture of anterior of C4 body.
81H412	Teardrop fracture of lip of C5 with complete anterior longitudinal ligament tear. Bilateral tears of anterior longitudinal ligament at C4. Rupture of disc at C4 and C5.
81H413	Basal skull fracture. Foramen magnum area to bilateral temporal areas.

NOTE: No injuries were produced in Tests 81H401, 81H405, 81H411, and 81H414.

5.0 DISCUSSION OF RESULTS

The test conditions and impact modes were designed to answer specific questions concerning the production of damage to skull and neck structures. These conditions and modes were also selected in light of recently published S-I impact injury data, generated here at UMTRI and sponsored by NIOSH in one study [9] and by General Motors in another study [12]. The following discussion and arguments are based on results presented in this report (Section 4.0 and Appendix A), as well as on results of the two studies cited above, all of which are related to S-I head impacts.

5.1 Discussion of Injuries

In this section, injuries to the skull, neck, and thoracic spine are discussed separately. Non-injurious impacts are also reviewed here.

5.1.1 Skull Injuries. In looking for impact conditions that produce skull injuries under the impactor, one finds that localized fractures can occur for impacts in the R-L and P-A direction [20] when there is no padding to distribute the impact force and reduce local stress. Similar injuries are produced in impacts in the S-I direction when no padding is used (Test 81H409).

When a thin pad (0.5 cm ensolite) was added to the impactor surface while maintaining approximately the same velocity and producing approximately the same peak impact force, the local skull fracture was avoided but a basal skull fracture was produced (Test 81H413). A similar type of injury was produced in a previous study [9] for Test

79H200 in which the impact velocity was 12 m/s and impactor surface padding was 2.5-cm ensolite.

Although exact knowledge of the mechanisms of basal skull fracture cannot be directly observed, two mechanisms may be postulated on the basis of the system morphology. The first mechanism suggests that the neck reactive forces are transmitted to the relatively thin skull floor through the occipital condyles and the relatively strong ring opening of the foramen magnum, causing a basal skull ring fracture.

The second mechanism is the inition of a crack in the skull (due to excessive bending and stressing of the cranial shell) at a location removed from the skull base itself, that propagates towards the skull base and precipitates the basal skull fracture in question.

In a previous study [8,22], six unembalmed cadaveric subjects were impacted in the S-I direction. In an attempt to position the test subject such that the maximum possible force is transmitted to the spinal column through the head and neck, the test subject was placed in a supine position and the cervical spine was aligned along the line of action of the impact force. In this test series an in-position X-ray was used to align as best as possible the "general spinal axis." The underlying assumption for this type of initial positioning is that if the force level is high enough to exceed the strength of the skull floor near the foremen magnum, and the force is sufficiently distributed so as to avoid a local depressed fracture on the crown of the head, then direct loading of the condyles by the neck could cause the skull base to fracture. Despite these efforts, no skull fracture occurred. The injuries observed were fractures of the vertebral bodies and processes in the cervical and upper thoracic spine and increased force only resulted in more severe spinal damage.

In the follow-up study [9] and in several cases of the tests of the current study, an attempt was made to orient the impact line of action along the spinal column in a similar manner to the above-mentioned study. In Tests 81H405 and 81H406 of the current study, the impact velocity was nominally 8 m/s, the impactor surface padding was 5-cm ensolite, and the cervical spine was aligned approximately along the impactor axis. The peak forces in these tests were about 4 kN. While the padding and impactor velocity remained the same, Tests 81H401 and 81H404 had a significantly different alignment of the cervical spine, but the peak forces produced remained at the same 4 kN level. This indicates that the angle formed between the axis of the cervical spine and the axis of the impactor for a supine test subject may not significantly effect peak force. However, the angle does profoundly effect both the impact force-time waveform and the head acceleration time history (see [12] and Appendix B).

Although, in general, for a supine test subject the cervical spinal angles does not effect peak force, it has been suggested [12] that peak force may be increased by a combination of cervical and thoracic spinal angles (Figure 7) which compensate the effects of the normal lordotic curvature of the cervical spine and the kyphotic curvature of the upper thoracic spine on the force load path.

The second mechanism of basal skull fracture, in which deformation in the skull causes stress distal to the point of impact, has been discussed by Gurdjian [23]. He postulates that as long as the cranial skull remains intact under the impact, the shell undergoes an inbending under the impacted surface as well as an outbending away from the impacted region. It is at the outermost point of the bent cranial shell that a crack is initiated due to tension. The crack then propagates downwards toward the foramen magnum

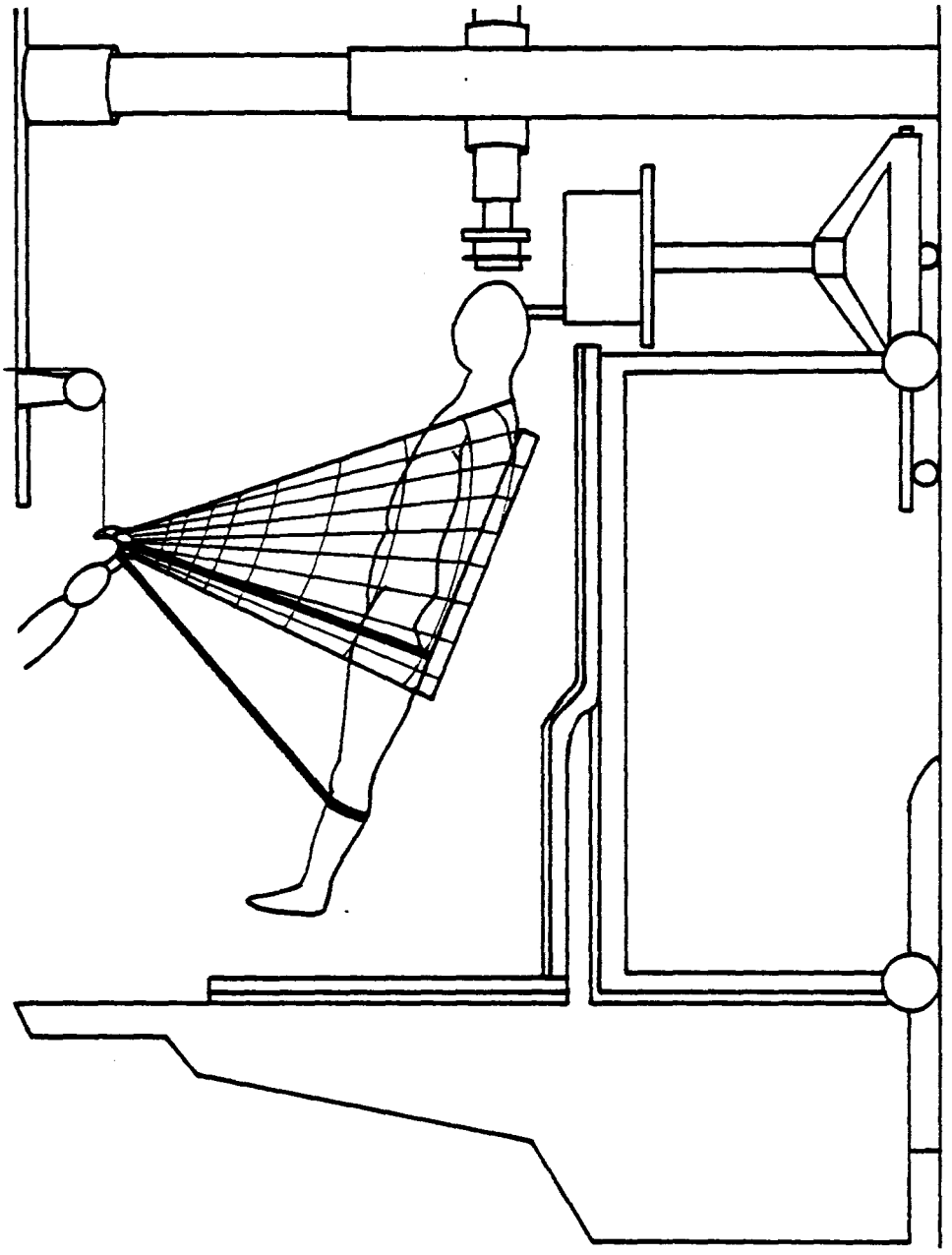

FIGURE 7. Set Up for Impact Test in Reference [12]

where the skull base is weakest and a basal skull fracture is precipitated.

The tests in which basal skull fracture occurred were characterized by large forces of short durations. This type of force-time history is significantly different from the force-time history of the rest of the tests in this study. The implication is that, although skull deformation may be a necessary condition for basal skull fracture, it may not be the sole cause in S-I impacts.

5.1.2 Cervical Injuries. In order for the forces to reach levels sufficient to cause the above-mentioned skull deformation, padding on the impactor surface must be of sufficient depth to eliminate local skull fracture but not great enough to spread the transfer of energy from the 10 Kg impactor to the skull over an extended time interval. When local or basal skull fractures occurred, neck injures were absent (79H200, 81H409, 81H413).

From this observation it would seem that if the available energy of the impactor is small enough not to overdrive the system, then to produce damage to the neck, the skull must remain intact throughout the impact. The implication is that when the skull remains intact the initial curvature of the neck allows it to "buckle" under the load from the condyles which results in extension or hyperextension motion of the neck.

Injuries to one or more cervical vertebrae occurred virtually in all the other tests where the neck "buckled" under the impact load. The common feature of these tests is that there was no attempt at aligning the neck with the spine and impactor axes. Instead, an initial curvature of the neck was allowed to simulate the natural attitude of normally standing or sitting persons.

Some observations could be made about the impact parameters and kinematic responses of these tests. In tests

81H402 and 81H403, fractures to the lower cervical vertebrae were caused. Both tests had peak forces of about 11 kN, an impactor velocity of 10.9 m/s, and a padding of 5 cm thickness. In the other tests (81H404, 81H406, 81H407, 81H408, 81H410, and 81H412), the force level dropped to 4 to 5 kN. Yet injury was produced under a variety of impact conditions, including different paddings and different head/neck angles. Most of the injuries occurred in C3-C4, i.e., in the region of maximum neck bending with occasional damage done to the C1/C2 area or to the T1/T2 thoracic region.

While the available sample is too small to conduct any sophisticated statistical analysis, it is clear that injuries to the cervical spine are occurring at impact force levels much lower than those required to produce skull fractures.

5.1.3 Non-Injurious Impacts. Four impact tests conducted in this research project did not produce any damage to the neck or the head. These were Tests 81H401, 81H405, 81H411, and 81H414. It might seem reasonable to draw a line between impact levels and kinematic parameters observed in these four tests and those observed in the remaining tests and call that line a threshold of tolerance. However, a closer look at these parameters reveals certain inconsistencies.

Thus, based on Tests 81H401, 81H405, and 81H411, a peak force level of about 4 kN seems at first glance to be just below the tolerance level of the neck. An exception is the level of 3 kN of Test 81H412 where injury did occur. Another exception at the upper spectrum is Test 81H414 where no injury occurred even for a force level of 16 kN, while identical test conditions and parameters produced a basal skull fracture in Test 81H413.

5.2 Injury Predictive Parameters

The search for a threshold that separates injurious from non-injurious impacts must be based on one or more impact parameters that could be measured and/or derived from kinematic and dynamic responses.

5.2.1 Impact Parameters. The tables presented in Section 4.0 include such impact force parameters as peak force, its duration, the area under the force curve, and the energy of impact that is absorbed by the head, as determined from conservation of momentum principles. By comparing these parameters to the results of autopsies, one should arrive at the critical value of some of the parameters previously mentioned below which no injury should occur.

A hard look at the data produced in this study indicates that none of the parameters chosen as predictors of injury is consistently resulting in a fail-proof criterion. For example, based on three non-injurious impacts, it seems that a peak force of 4.2 kN is about the maximum that could be tolerated without injury. Two exceptions are Tests 81H414 where no injury occurred even when force reached a peak of 16 kN, and Test 81H412 where injury was observed at a much lower peak force of 3 kN.

Because these tests had different force pulse durations, it was thought that a parameter that accounts for both duration and peak force may be more appropriate as an injury predictive measure. Thus, the impulse of the force, defined as the integral of the force-time history, was calculated. Another related parameter that was computed was the impact energy transferred to the head. Of the two parameters, the impulse offers less inconsistency in predicting non-injury than energy. Thus, an impulse level of 35 N.s seems to separate injurious from non-injurious impacts.

5.2.2 Response Parameters. The two potential tolerance criteria discussed above (peak force and impulse) define tolerable levels of impact in the S-I direction. Tolerable levels of kinematic response may also be defined based on kinematic head and neck response during impact. Such a parameter is the HIC, which was below 500 for all but one injurious as well as the non-injurious impacts. Although many researchers have suggested a HIC of 1000 as a threshold of injury, the current study does not support this suggestion. Further, examination of the data generated in this study and in other recent studies, indicates that the HIC is not a better predictor of injury than the impulse (integral of the force) or any other parameter that was considered for that purpose.

Two other kinematic responses were considered as predictors of injury. The first is the peak head linear acceleration, and the other is the peak head linear velocity. These two parameters can easily be monitored in helmet impact test devices. Of the two measures, the velocity offers a better predictive power than the acceleration, because it takes into account the duration of the impact. However, the number of tests available for determining a velocity threshold level is too small for that purpose.

5.3 Other Response Parameters

Two additional response measures could be used as injury predictors. These are briefly discussed here for the sake of completeness, even though their measurement could not be satisfactorily accomplished during this research project.

The first measure is the intracranial brain pressure which can be used, under appropriate assumptions, as an injury predictor. There are two problems associated with this parameter: (1) the difficulty with which brain pressure

can be monitored experimentally, and (2) the determination of a pressure level below which impact can be tolerated. Although many experimental and mathematical models support the concept of pressure-related brain injury, the actual implementation of a pressure measurement device in a helmet testing system is not feasible.

The other kinematic response which could be used as an injury predictor is the neck deformation, defined by the gross motion of the cervical spine. The current study indicates that low-level impacts produce significant neck injuries in most of the cases in which the initial neck orientation and curvature are close to the normal posture. Although a major part of this project was geared toward documenting the cervical spine motion during impact using high-speed X-ray movies, the outcome of this effort was less than expected in terms of the quality of the pictures and the ability to clearly document the neck motion.

6.0 SUMMARY AND RECOMMENDATIONS

Although some difficulties were encountered during the conduct of this project, some important facts were added to the knowledge and understanding of superior-inferior head impact mechanics.

The difficulties concerned the measurement of neck motion using high-speed cineradiography. A major effort was expended to improve the current device by increasing the size of the image to 35-mm and by using an improved X-ray to light a rare-earth screen. This effort was not, however, rewarded with improved image quality, so that no neck motion analysis was conducted.

The work on the X-ray device and the problems encountered in securing a steady supply of test subjects during the first year of the project led to curtailment of the scope of the testing, so that tests with a pressurized brain and vascular system were not conducted, even though considerable time was spent preparing and designing a detailed protocol for such tests.

Results of the limited series of tests indicate certain new findings and confirm some old suspicions about S-I head impact tolerance levels. The following is a summary of these findings along with the recommendations that could be drawn from these findings.

1. Padding is essential in distributing the impact force and eliminating localized skull fracture.
2. Load-distributing materials are effective methods of reducing localized skull fractures. However they do not necessarily eliminate skull fractures in general.

3. The use of Head Injury Criterion (HIC) is not recommended for predicting the injury potential of S-I head impacts.

4. Of the response parameters that were examined, head velocity seems the best suitable indicator for injury. Of the response parameters that were not examined, the neck gross motions (either deflection or angle) may offer the greatest potential for accurate injury prediction.

5. Of the impact parameters that were examined, the integral of the force-time curve, i.e., the force impulse, seems to be the most consistent injury indicator.

6. The size of the sample of tests available for determining S-I tolerance levels remains too small for accurate assessment. This sample must be enlarged by conducting more S-I head impacts, and by widening the scope of experimental documentation to focus on measurement of the neck motion.

7.0 REFERENCES

1. Gurdjian, E.S., Lissner, H.R., Evans, F.G., Patrick, L.M., and Hardy, W.G. "Intracranial Pressure and Acceleration Accompanying Head Impacts in Human Cadavers." Surgery, Gynecology, and Obstetrics, 113:185-190, 1961.

2. Hodgson, V.R. and Thomas, L.M. "Comparison of Head Acceleration Injury Indices in Cadaver Skull Fracture." Proc. 15th Stapp Car Crash Conf., 1972.

3. McElhaney, J.E., et al. "Biomechanical Aspects of Head Injury." In Human Impact Response Measurement and Simulation. Edited by W.F. King and H.J. Mertz. New York: Plenum Press, 1973.

4. Stalnaker, R.L., et al. Validation--Studies for Head Impact Injury, Final Report. Report No. UM-HSRI-76-14. Highway Safety Research Institute, June 1976.

5. Cammack, K.V. "Whiplash Injuries to the Neck." American Journal of Surgery, 93:663-666 (1957).

6. Mertz, H.J. and Patrick, L.M. "Investigation of the Kinematics and Kinetics of Whiplash." SAE Paper No. 670919, Proc. 11th Stapp Car Crash Conf., 1967.

7. Patrick, L.M. and Chou, C.C. Response of the Human Neck in Flexion, Extension and Lateral Flexion. SAE Vehicle Research Institute, Report No. VRI 7.3, 1976.

8. Culver, R.H., Bender, M., and Melvin, J.W. Mechanisms, Tolerances, and Response Obtained Under Dynamic Superior-Inferior Head Impact, Final Report. Highway Safety Research Institute, May 1978.

9. Alem, N.M. Helmet Impact Test System Development, Final Report. Highway Safety Research Institute, August 1980.

10. Hodgson, V.R. and Thomas, L.M. "Mechanisms of Cervical Spine Injury During Impact to the Protected Head." Paper No. 801300. Proc. 24th Stapp Car Crash Conf., 1980.

11. Huelke, D.F., Moffatt, E.A., Mendelsohn, R.A., and Melvin, J.W. "Cervical Fracture and Fracture Dislocations--An Overview." The Human Neck--Anatomy Injury Mechanisms and Biomechanics. Warrendale, Pa., Society of Automotive Engineers, Inc., 1979.

12. Nusholtz, G.S., Melvin, J.W., Huelke, D.F., Alem, N.M., and Blank, J.G. "Response of the Cervical Spine to Superior-Inferior Head Impact." Paper 811005. Proc. 25th Stapp Car Crash Conference, 1981.

13. Snyder, R.G., Chaffin, D.B., Schneider, L.W., Foust, D.R., Bowman, B.M., Abdelnour, T.A., and Baum, J.K. Basic Biomechanical Properties of the Human Neck Related to Lateral Hyperflexion Injury, Final Report. Highway Safety Research Institute, 1975.

14. Melvin, J.W. "Human Neck Injury Tolerance." The Human Neck--Anatomy, Injury Mechanisms and Biomechanics. Warrendale, Pa., Society of Automotive Engineers, Inc., 1979.

15. King, A.I. and Hodgson, V.R. Tolerance of the Neck to Indirect Impact. Technical Report No. 9, N00014-75-C-1015, March 5, 1979.

16. Goldsmith, W. "Some Aspects of Head and Neck Injury and Protection." Progress in Biomechanics. Sijthoff and Noordhoff, The Netherlands, 1979.

17. Foust, D.R., Chaffin, D.B., Snyder, R.G., and Baum, J.K. "Cervical Range of Motion and Dynamic Response and Strength of Cervical Muscles." Paper No. 730975. Proc. 19th Stapp Car Crash Conf., 1973.

18. Bender, M., Melvin, J.W., and Stalnaker, R.L. "A High-Speed Cineradiograph Technique for Biomechanical Impact." Paper No. 700824. Proc. 20th Stapp Car Crash Conf., 1976.

19. Alem, N.M. Measurement of 3-D Motion. Fifth Annual International Workshop on Human Subjects for Biomechanical Research, 1977.

20. Stalnaker, R.L., Melvin, J.W., Nusholtz, G.S., Alem, N.M., and Benson, J.B. "Head Impact Response." Paper No. 770921. Proc. 21st Stapp Car Crash Conf., 1977.

21. Nusholtz, G.S., Melvin, J.W., and Alem, N.M. "Head Impact Response Comparisons of Human Surrogates." Paper No. 791020. Proc. 23rd Stapp Car Crash Conf., 1979.

22. Culver, R.H. "Pilot Study of Basal Skull Fracture, Interim Letter Report." Highway Safety Research Institute, January 1978 (unpublished).

23. Gurdjian, E.S., Gonzales, D., Hodgson, V.R., Thomas, L.M., and Greenberg, S.W. "Comparisons of Research in Inanimate and Biologic Material: Artifacts and Pitfalls." In Impact Injury and Crash Protection, pp. 234-53. Edited by E.S. Gurdjian, W.A. Lange, L.M. Patrick, and L.M. Thomas. Springfield: Ill., C.C. Thomas, 1970.

APPENDICES

APPENDIX A

RESULTS OF AUTOPSIES

In this appendix, results of autopsies conducted on the subjects after the completion of tests are presented.

This presentation includes only those subjects where impact damage to the head or neck were observed. Therefore, since no injuries were observed in Tests 81H401, 81H405, 81H411, and 81H414, no autopsy summaries will be found for these tests in this appendix.

Some of the autopsy summaries are accompanied by close-up photographs that document a particular damage due to the impact. Arrows are used to point out a precise location on the photograph. These arrows are labeled with letters A, B, C, etc., and are referred to in the summary text [A], [B], [C], etc.

AUTOPSY SUMMARY

FOR TEST NO. 81H402

Injuries to Neck:

Bilateral fracture through lamina of T2 at base of spinous process [A].

Fracture of body of T2 [B].

NOTE: Hemorrhage above right eye due to head hitting balsa wood <u>after</u> impact.

Scoliosis between T1 and T4 (Hunchback).

TEST NO. 81H402

THORACIC VERTEBRAE (T1 - T4)

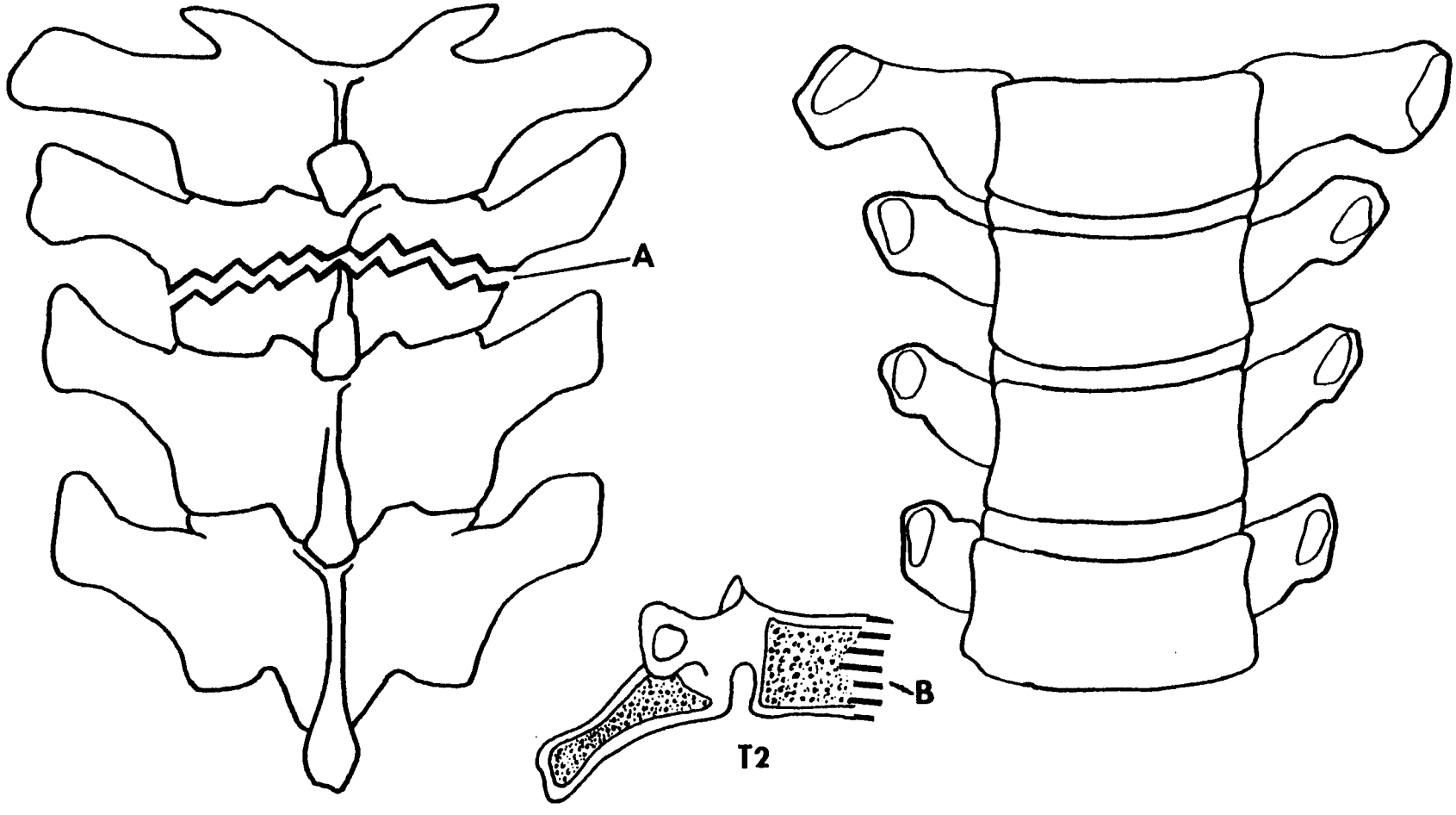

Reproduced from
best available copy.

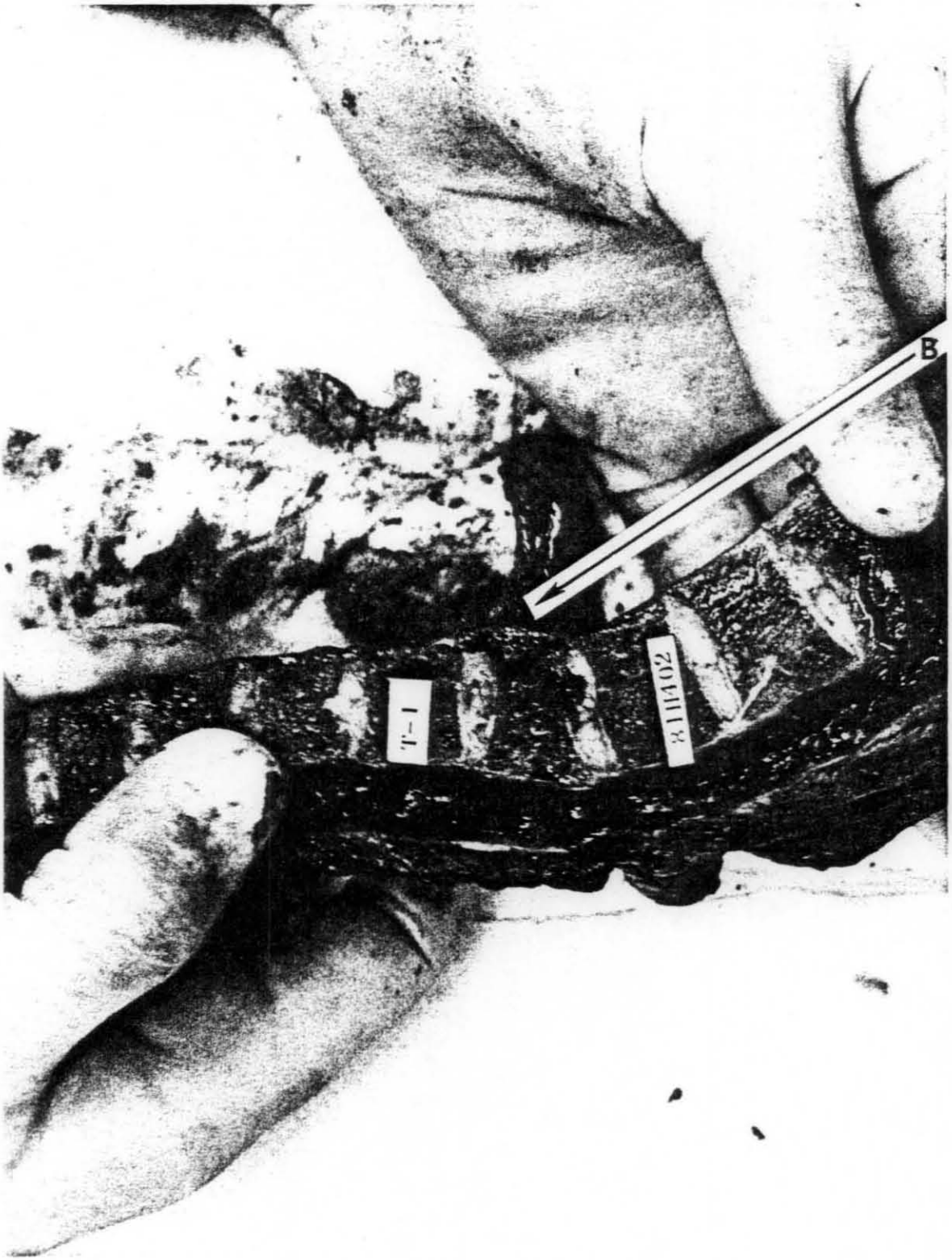

AUTOPSY SUMMARY

FOR TEST NO. 81H403

Injuries to Cervical and Thoracic Vertebrae:

Ruptured disc between C2 and C3 [A].

Ruptured disc between C3 and C4 [B].

Anterior-inferior chip fracture of C2 body [C].

Vertical fracture of posterior of C2 body [D].

Fracture of C3 spinous process at tip [E].

Fracture of C4 spinous process at tip [F].

Ruptured disc between T1 and T2 with wedge fracture of T2 body [G].

Complete bilateral dislocation between T1 and T2 [H].

Fracture of left transverse process of T2 [I].

Anterior longitudinal ligament torn between C3 and C4 [J].

Partial tear of anterior longitudinal ligament at upper T2 body [K].

Ruptured posterior longitudinal ligament between T1 and T2 [L].

All spinous ligaments torn between T1 and T2 [M].

NOTE: Left first rib fractured adjacent to T1.

TEST NO. 81H403

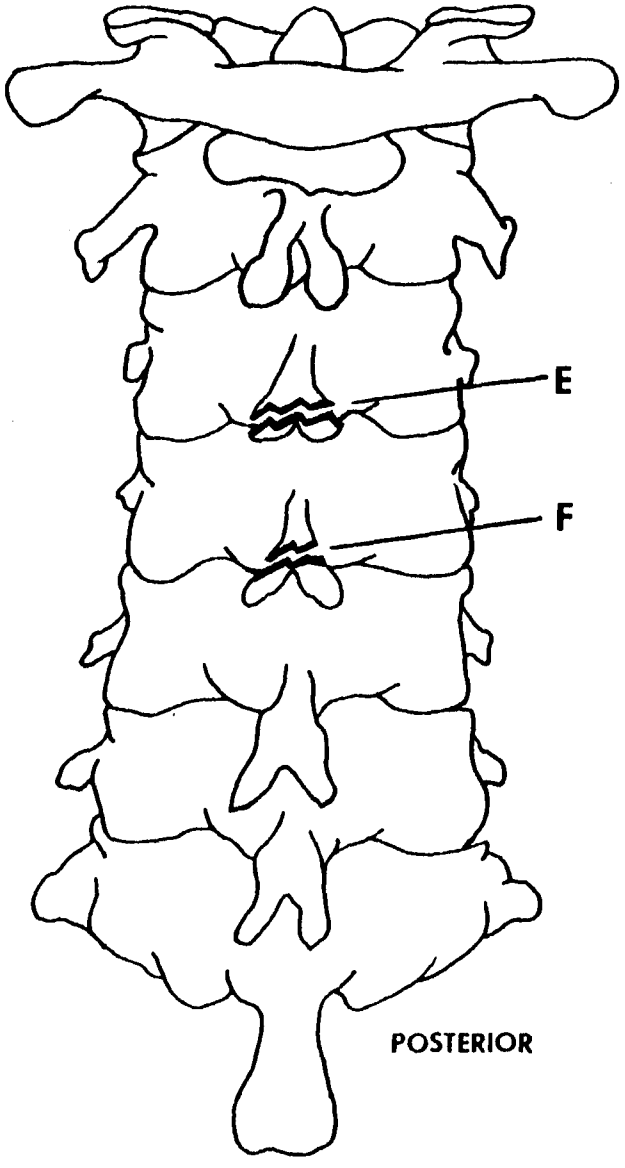

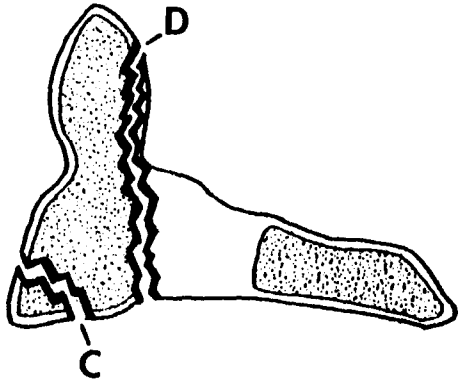

C2 CROSS SECTION

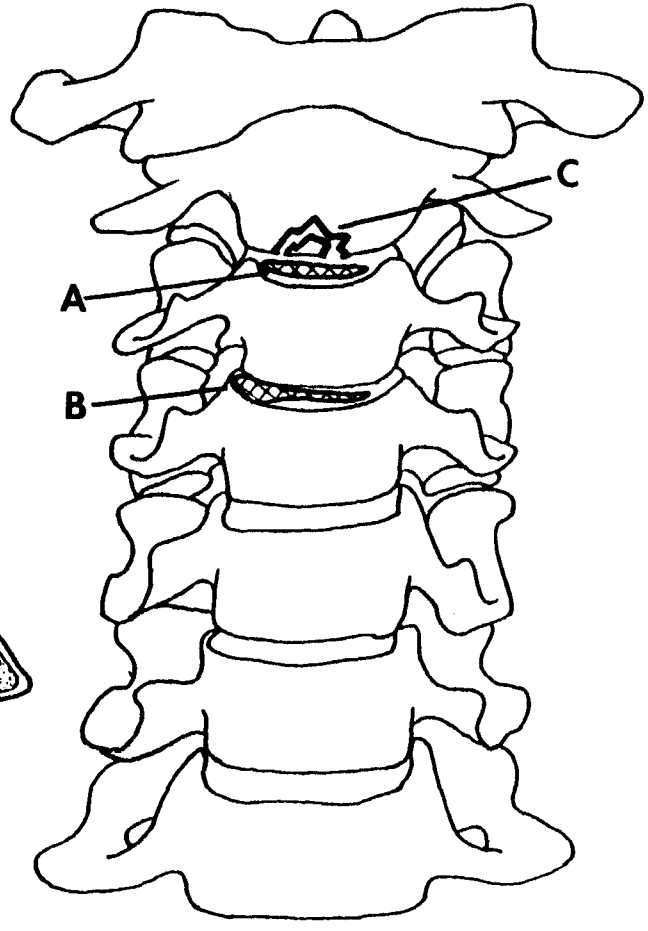

CERVICAL VERTEBRAE

TEST NO. 81H403

THORACIC VERTEBRAE (T1 - T4)

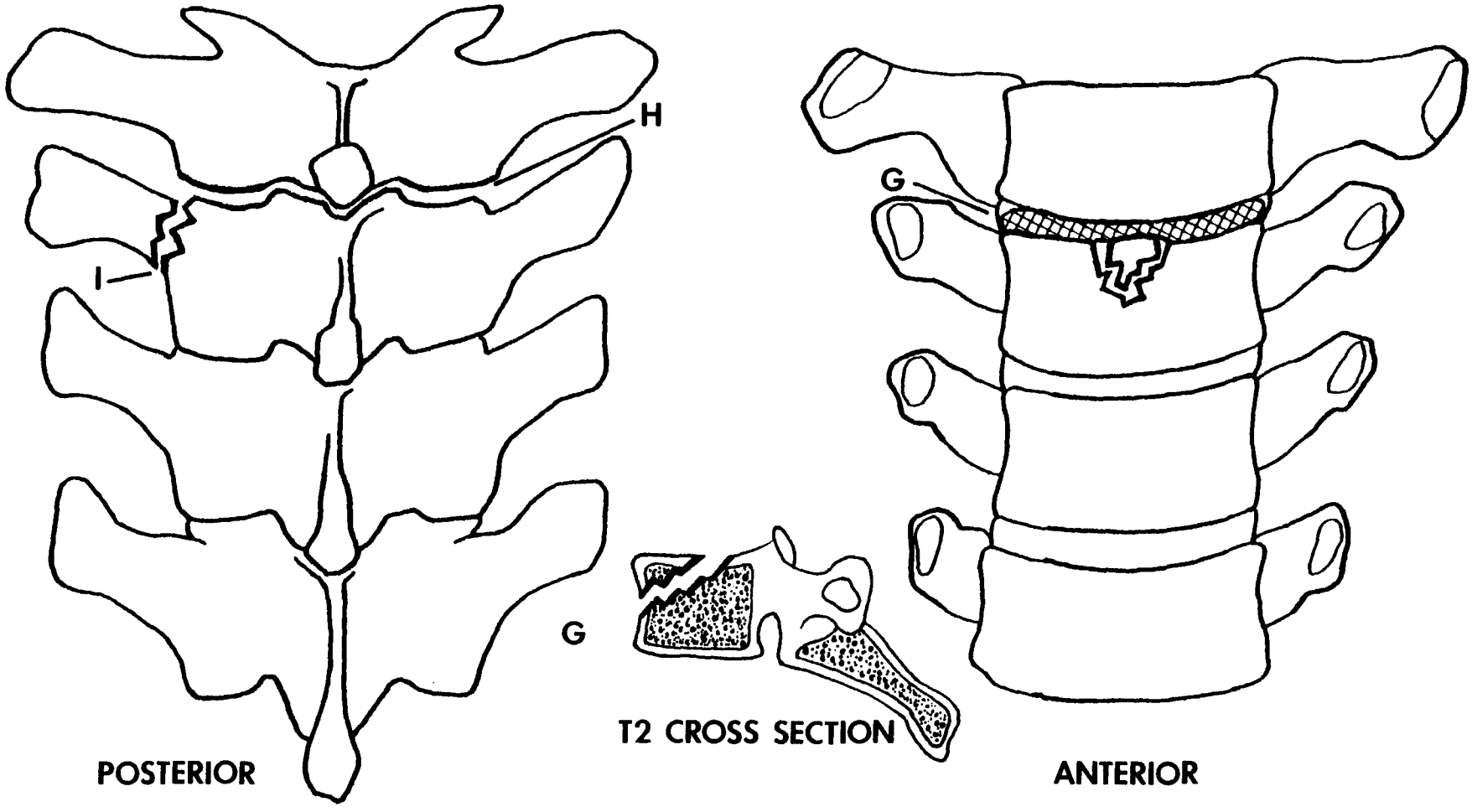

TEST NO. 81H403

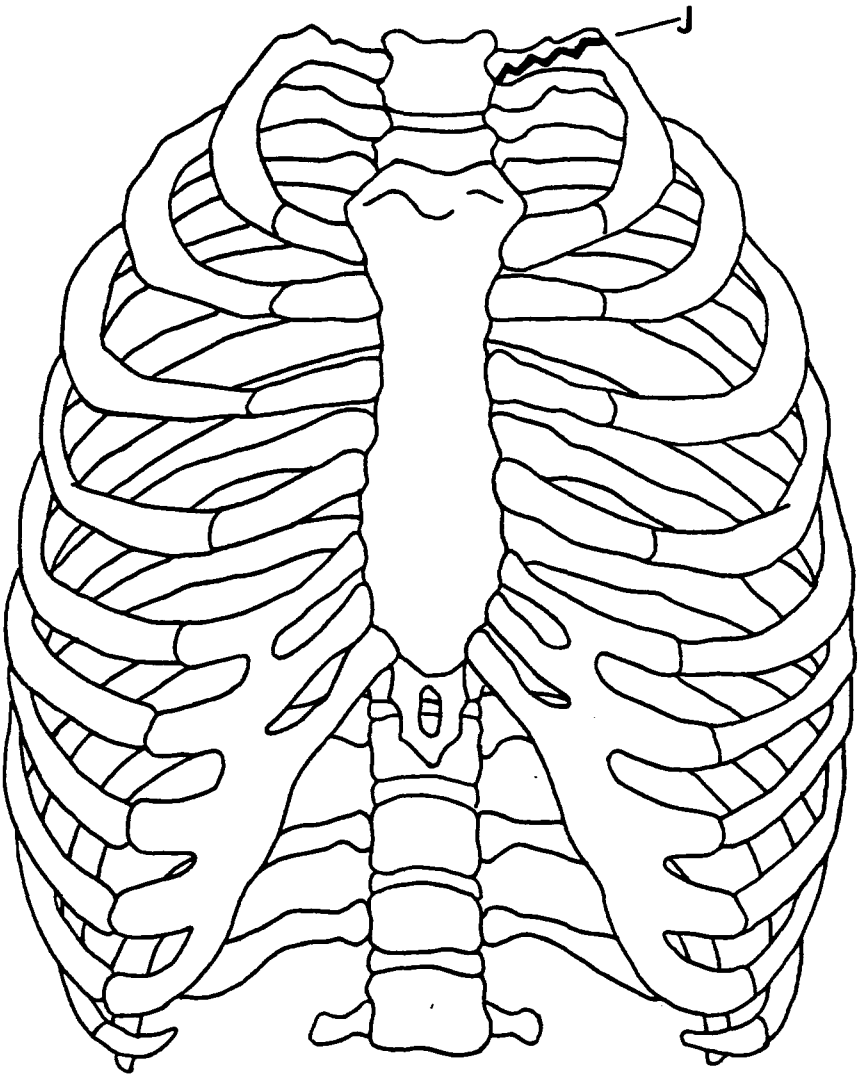

ANTERIOR THORAX

AUTOPSY SUMMARY

FOR TEST NO. 81H404

Injuries to Neck:

Nearly complete tear of anterior longitudinal ligament at disc between C3 and C4 [A].

NOTE: Lump on lamina of C4 and part of C5 (left side).

TEST NO. 81H404

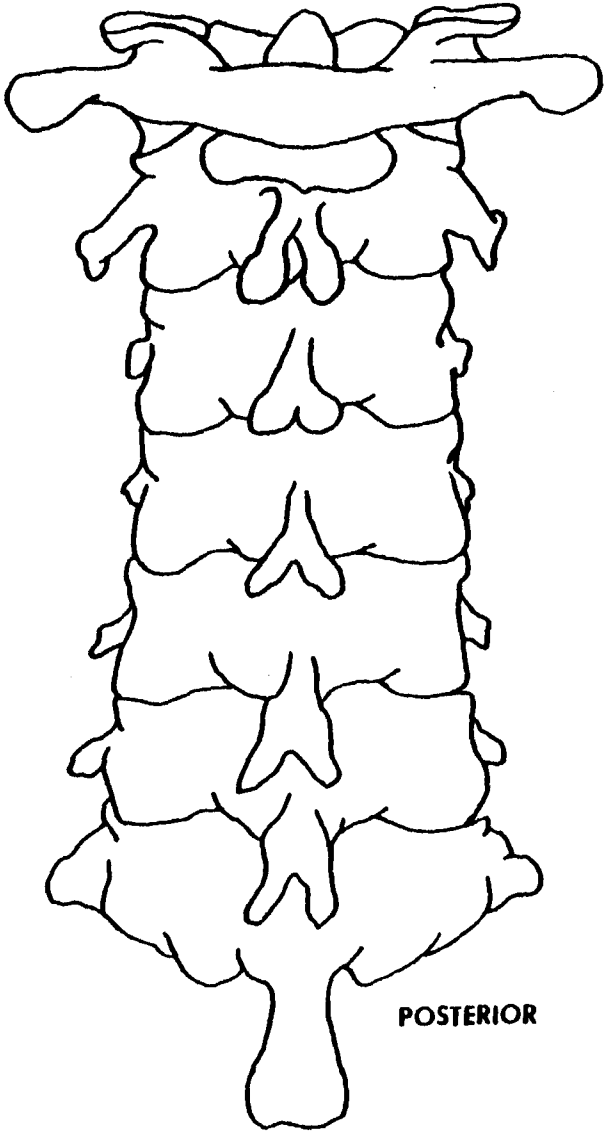

POSTERIOR

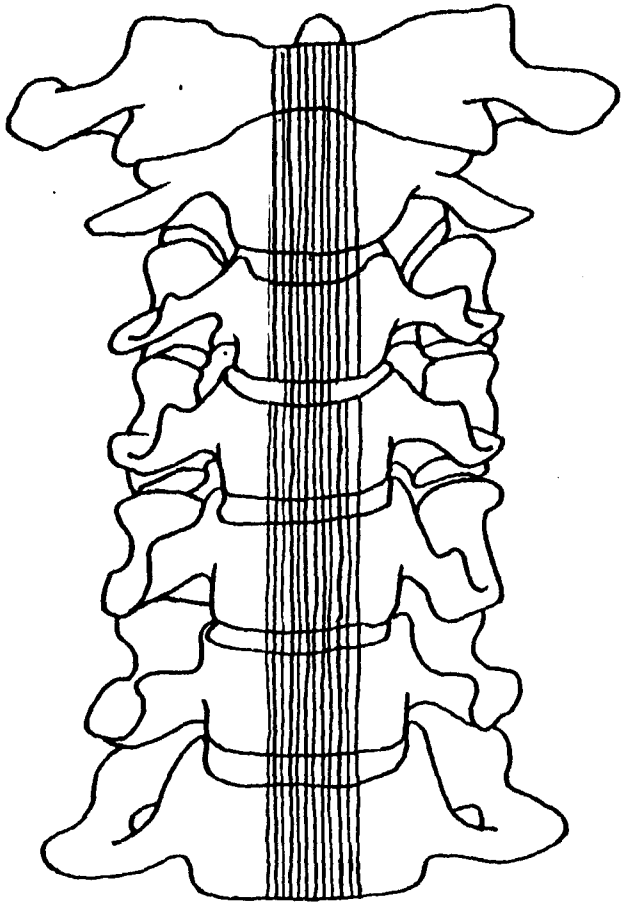

ANTERIOR

CERVICAL VERTEBRAE

Reproduced from
best available copy.

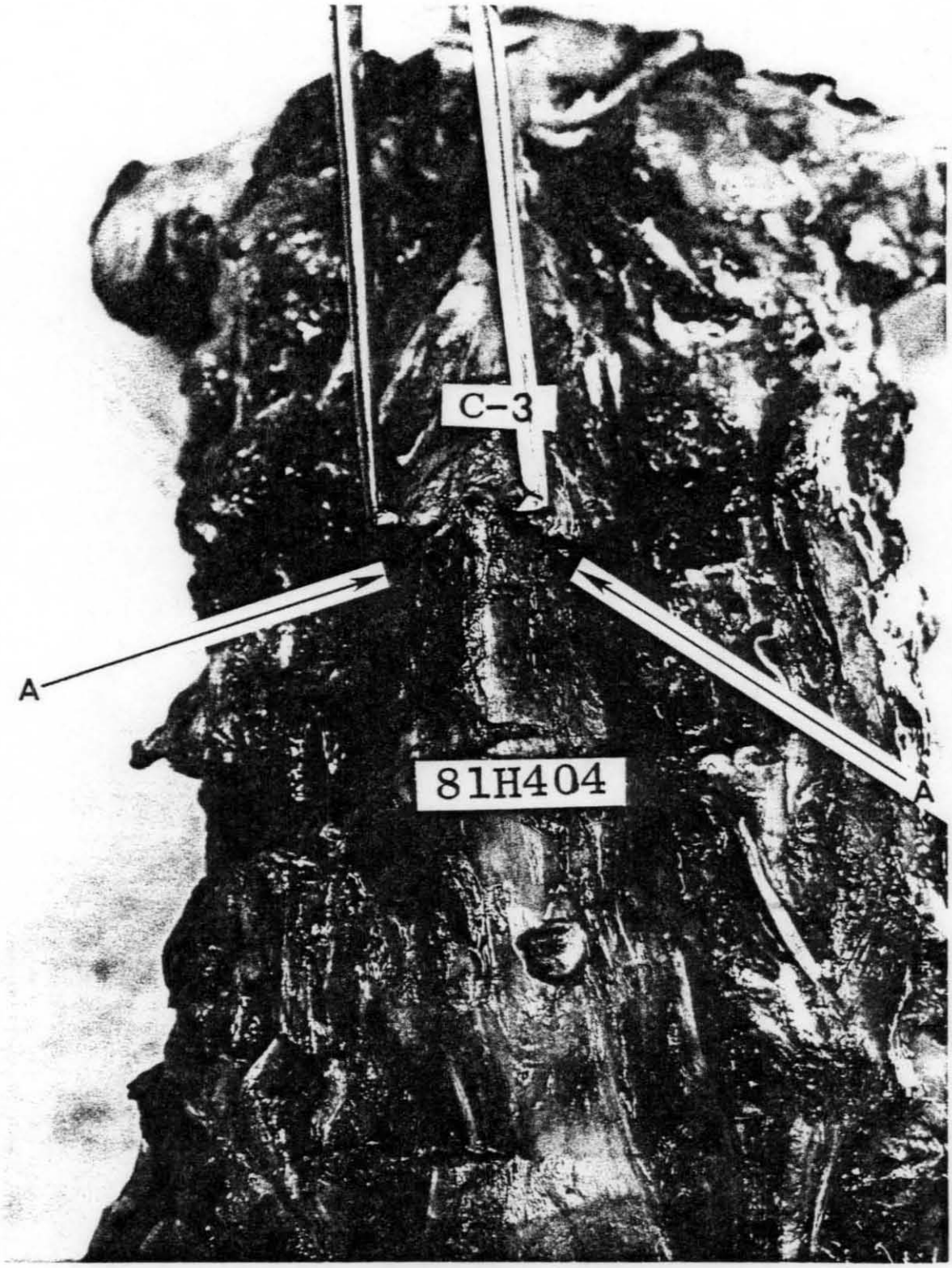

AUTOPSY SUMMARY

FOR TEST NO. 81H406

Injuries to Neck:

Bilateral fracture of posterior C1 arch [A].

Fracture of C2 dens [B].

Fracture of spinous process of C3 [C].

Fracture of spinous process of C4 [D].

Fracture of right lamina of C7 [E].

Fracture of anterior-superior body of T1 [F].

TEST NO. 81H406

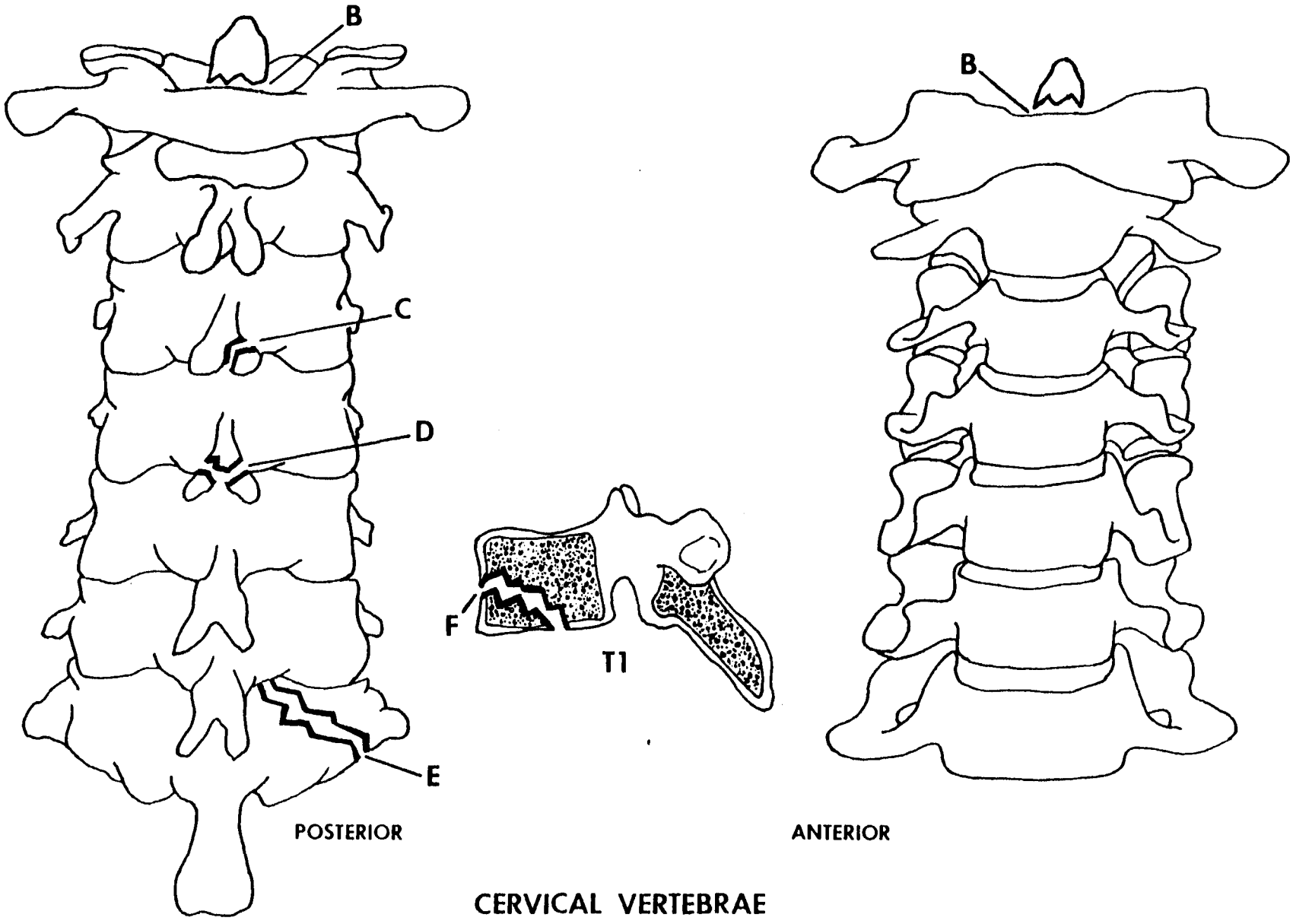

CERVICAL VERTEBRAE
AND T1 CROSS SECTION

TEST NO. 81H406

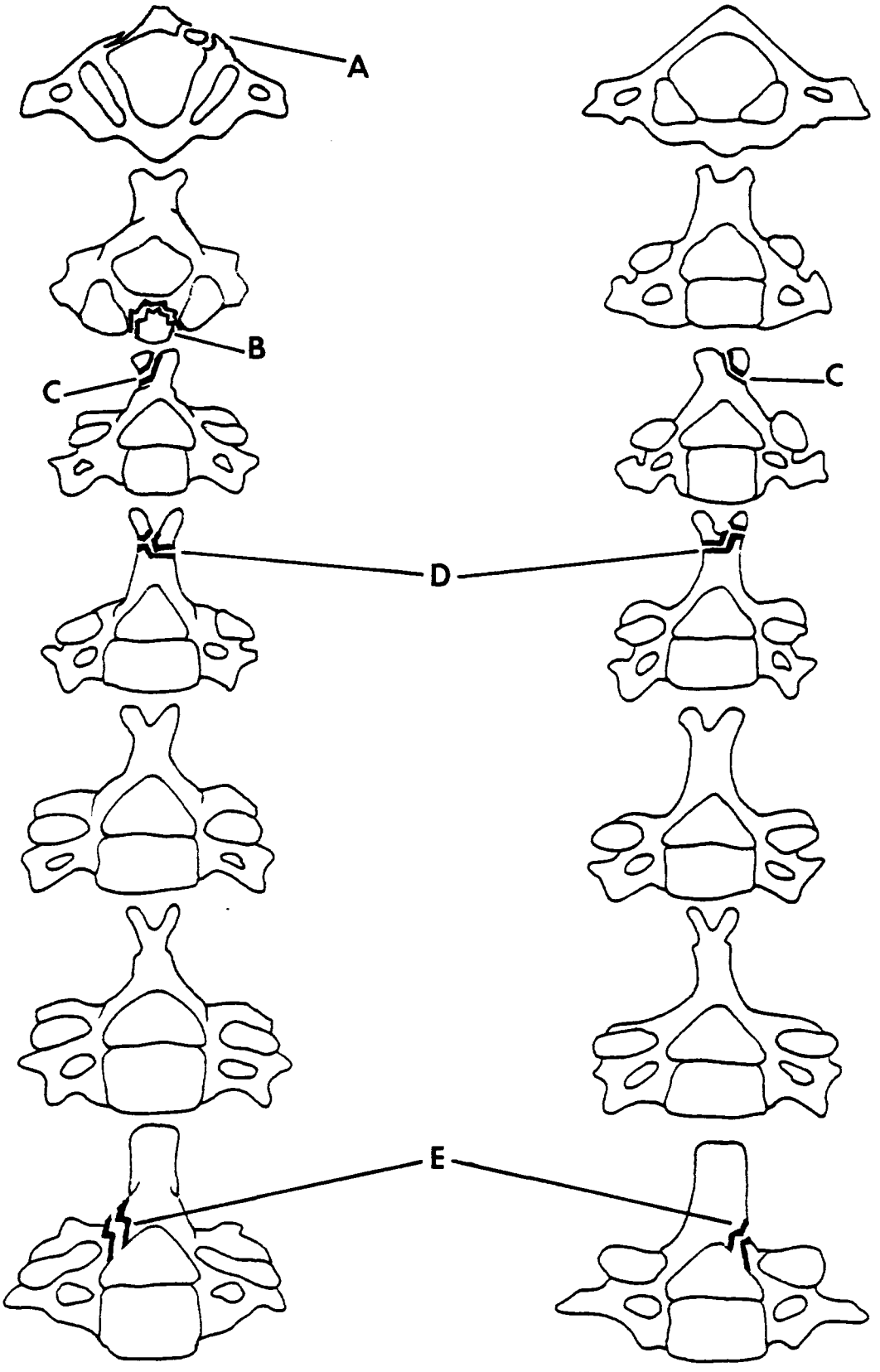

Reproduced from
best available copy.

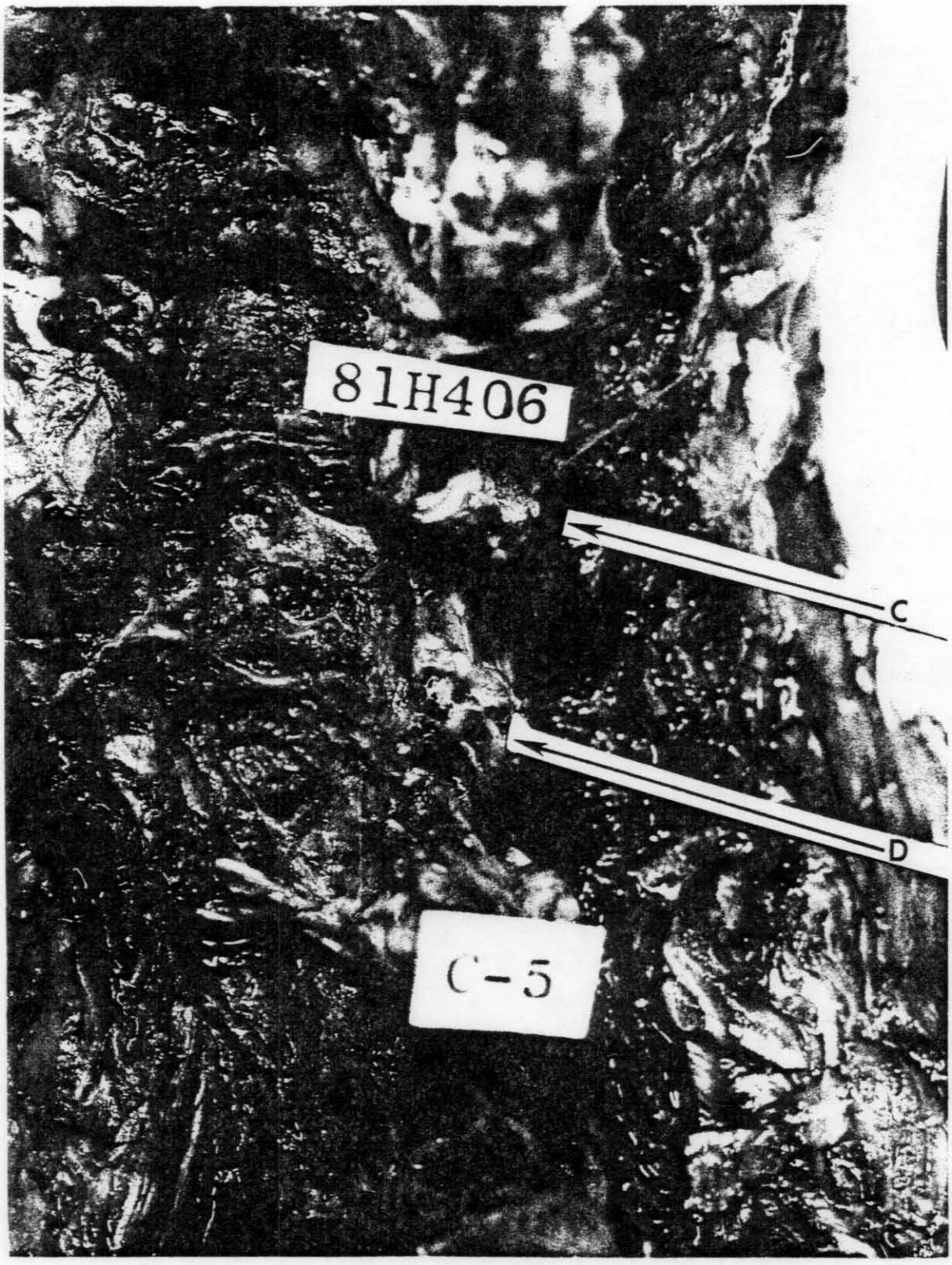


G
81E406

Reproduced from
best available copy.

AUTOPSY SUMMARY

FOR TEST NO. 81H407

Injuries to Neck:

Rupture of disc between C5 and C6 (A).

Tear on anterior longitudinal ligament at disc between C5 and C6 (B).

NOTE: Recent surgery indicated by large, fresh incision from substernal to symphysion.

Reproduced from
best available copy.

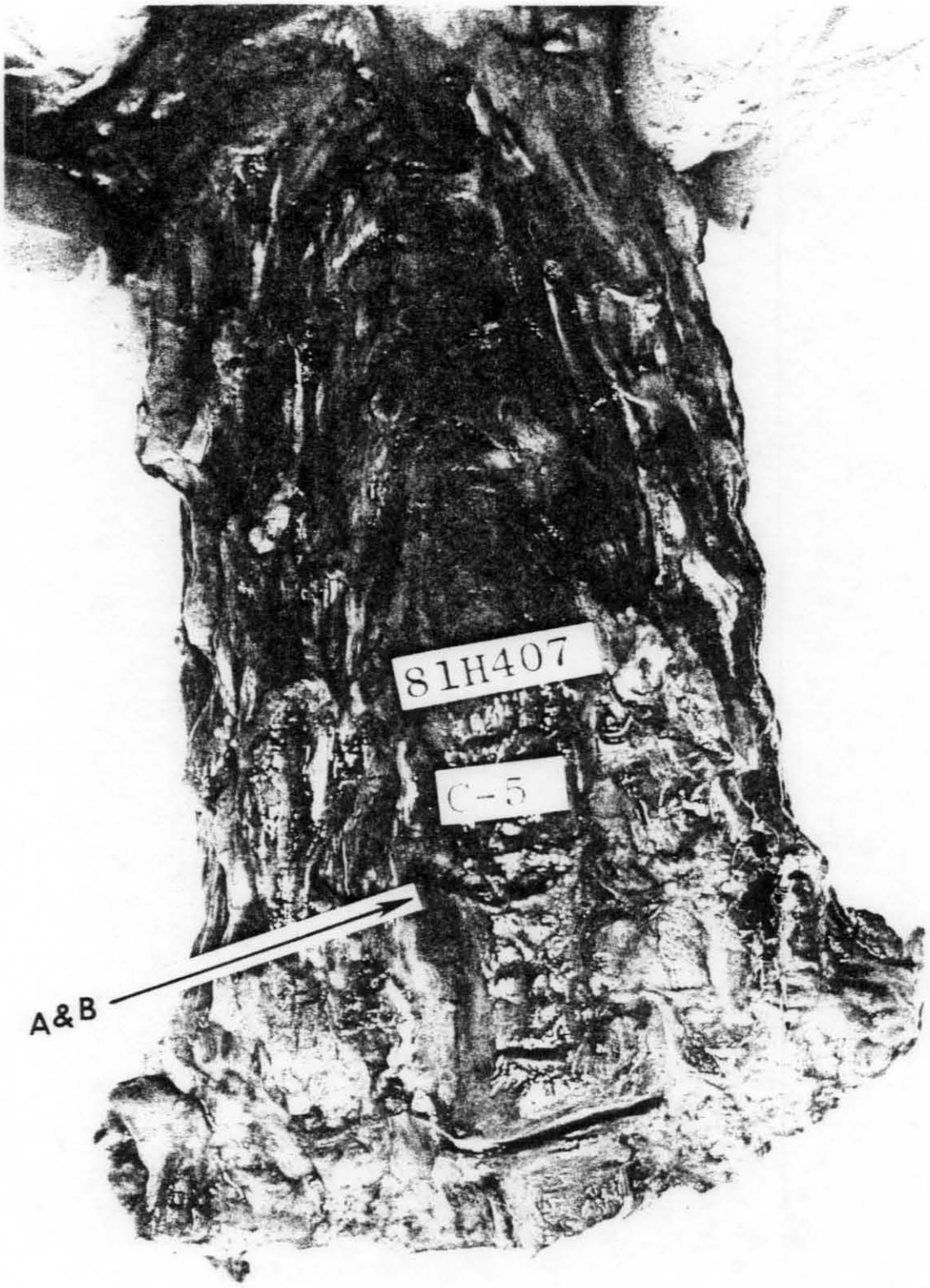

TEST NO. 81H407

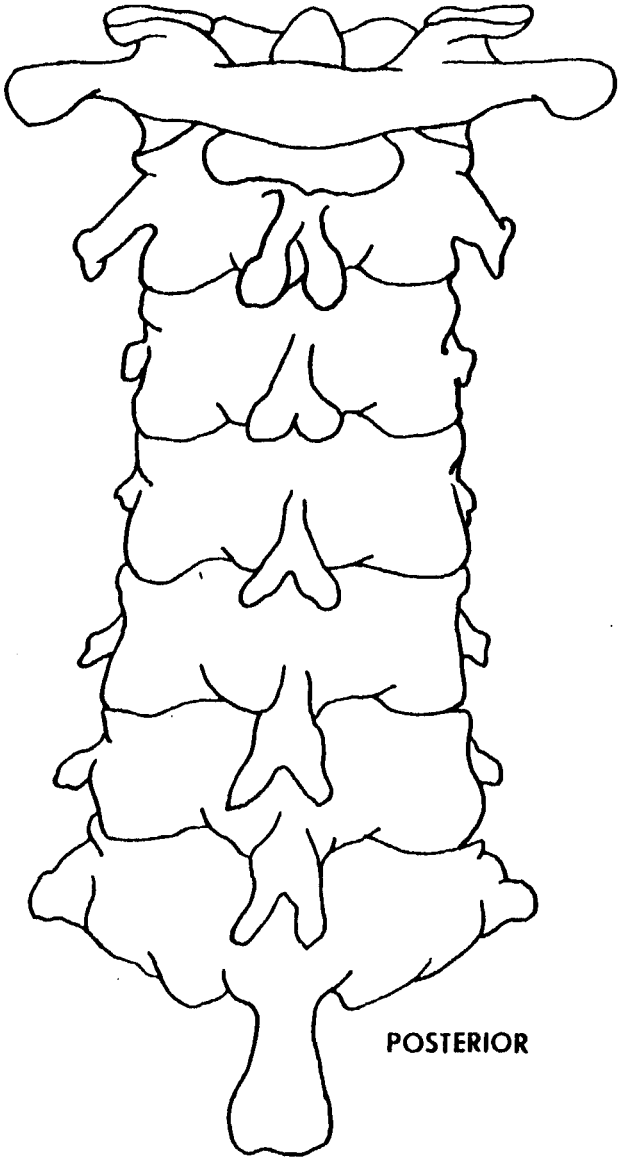

POSTERIOR

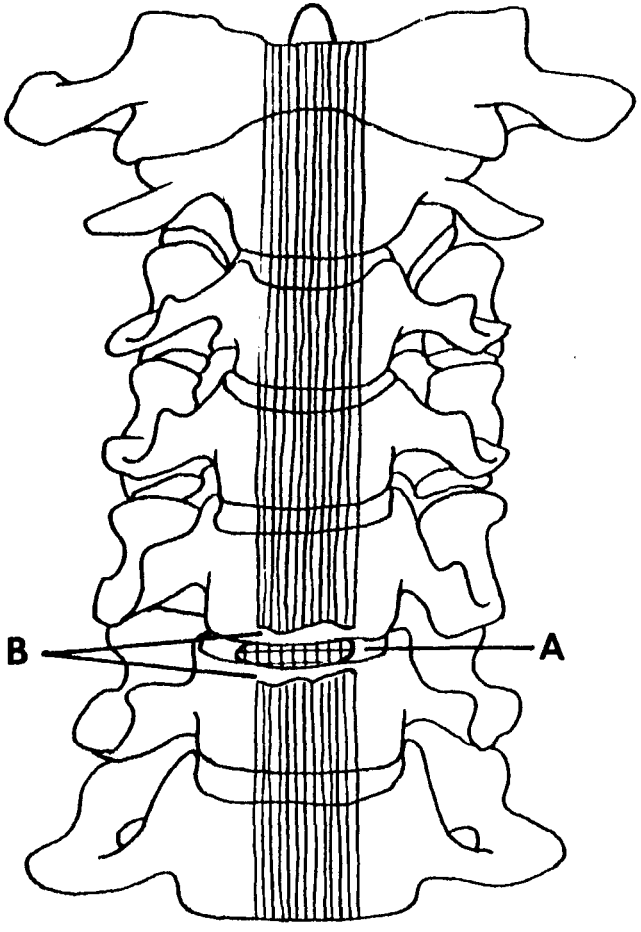

ANTERIOR

CERVICAL VERTEBRAE

AUTOPSY SUMMARY

FOR TEST NO. 81H408

Injuries to Neck:

Tear of anterior longitudinal ligament between C3 and C4 [A].

Tear of anterior longitudinal ligament between disc C4 and C5 [B].

Bilateral fracture of C1 posterior arch [C].

Fracture of anterior-inferior C2 body extending through C2-C3 disc [D].

Compression fracture of upper body of T2 [E].

Compression fracture of lower body of T3 [F].

TEST NO. 81H408

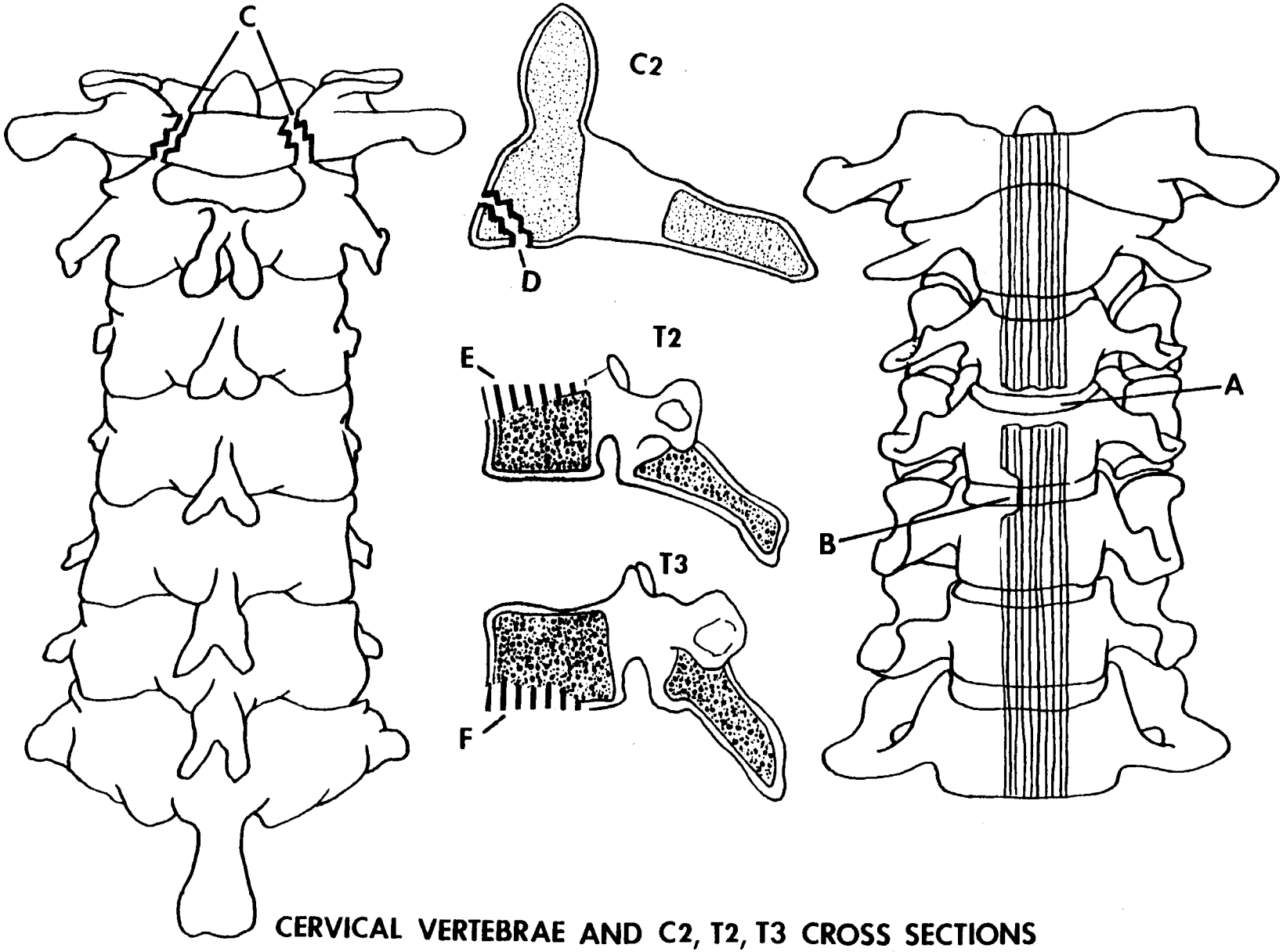

CERVICAL VERTEBRAE AND C2, T2, T3 CROSS SECTIONS

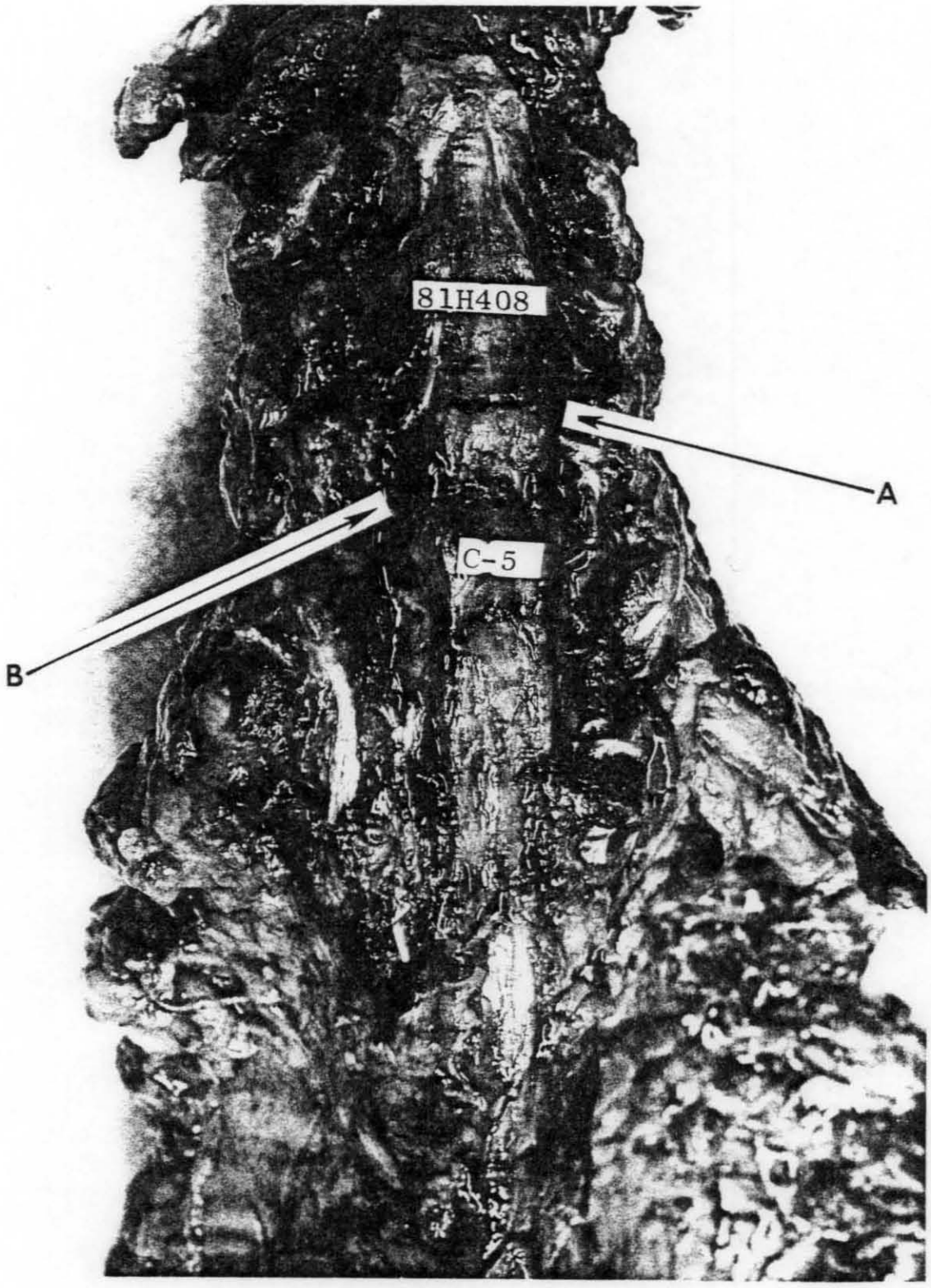
81H408
A
B
C-5

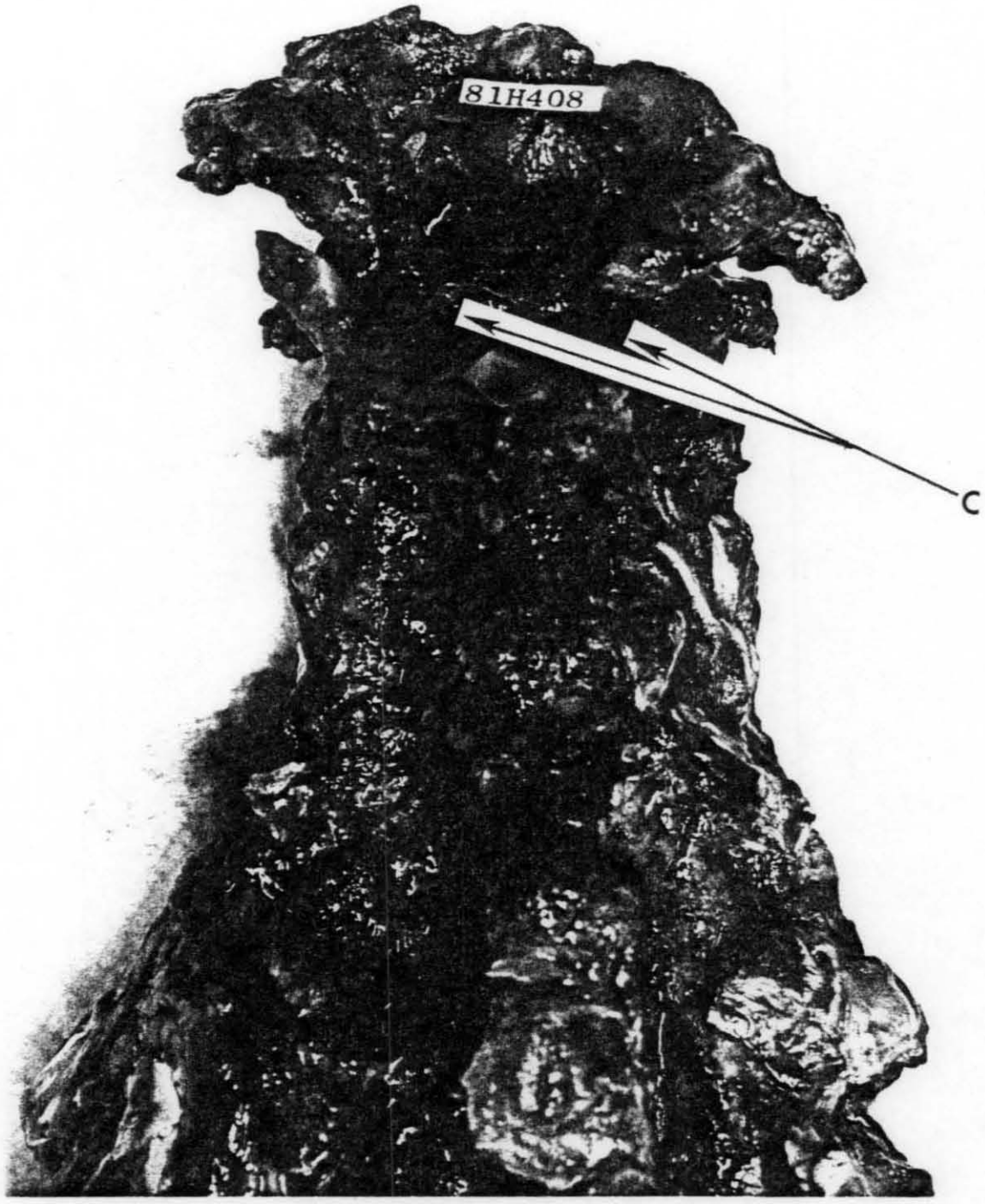
81H408
C


D
81H408
C-3

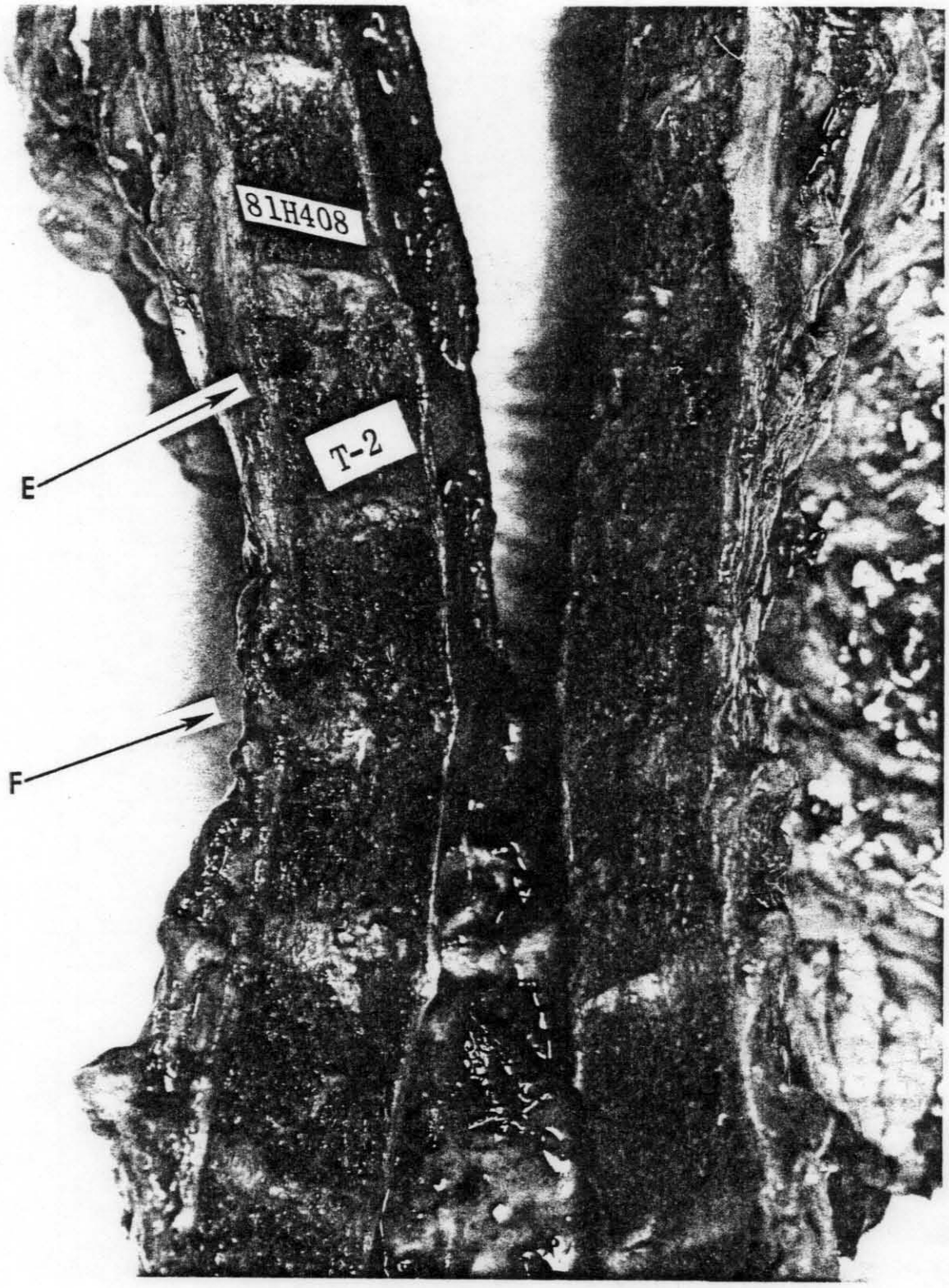
81H408
T-2
E
F

AUTOPSY SUMMARY

FOR TEST NO. 81H409

Injuries to Head:

Circular depressed fracture at apex of skull (beneath impact site).

NOTE: Cause of death was a carcinoma on the spinal cord. X-rays and scar tissue revealed surgical tampering with the cervical and upper thoracic vertebrae, thus deeming the subject unsuitable for data comparison. An uninstrumented test was performed which served as a trial test for 81H408.

TEST NO. 81H409

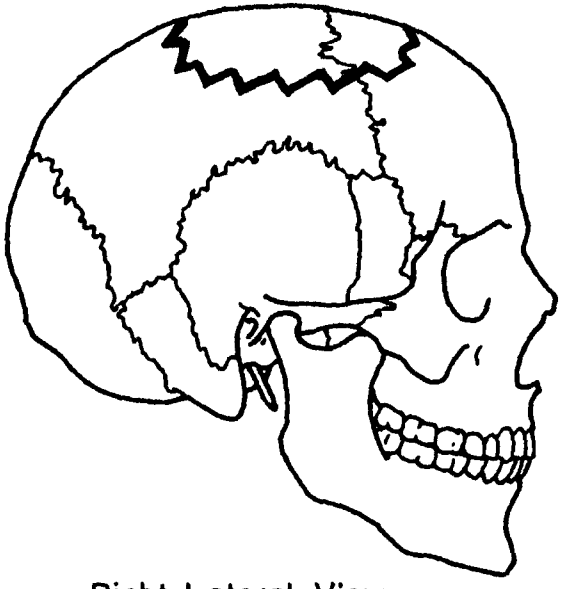

Right Lateral View

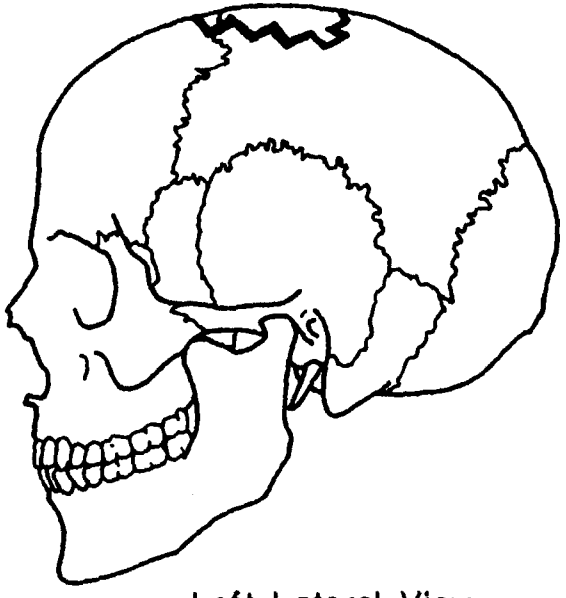

Left Lateral View

AUTOPSY SUMMARY

FOR TEST NO. 81H410

Injuries to Neck:

Anterior longitudinal ligament torn at disc C3/C4 [A].

Anterior longitudinal ligament torn at disc C4/C5 [B].

Rupture of disc C3/C4 [C].

Rupture of disc C4/C5 [D].

Rupture of central portion of disc C5/C6 [E].

Rupture of central portion of disc C6/C7 [F].

Fracture of anterior of C4 body [G].

NOTE: Spinous process of C5 partially broken during preparatory surgery; skull fracture incurred during transport.

TEST NO. 81H410

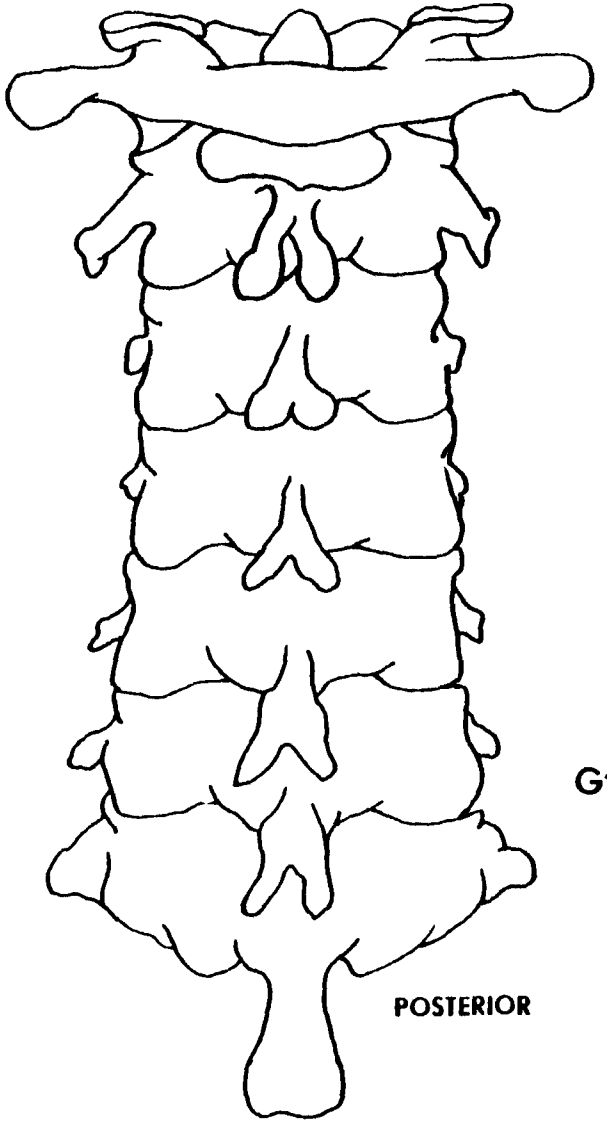

POSTERIOR

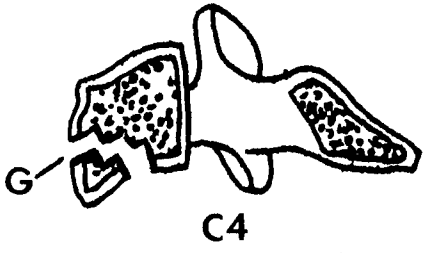

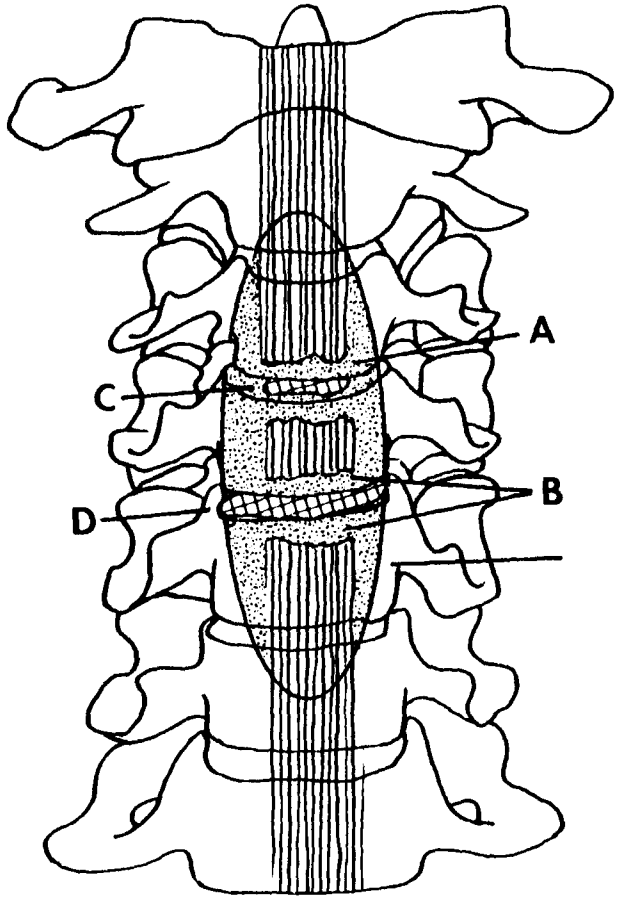

ANTERIOR

CERVICAL VERTEBRAE

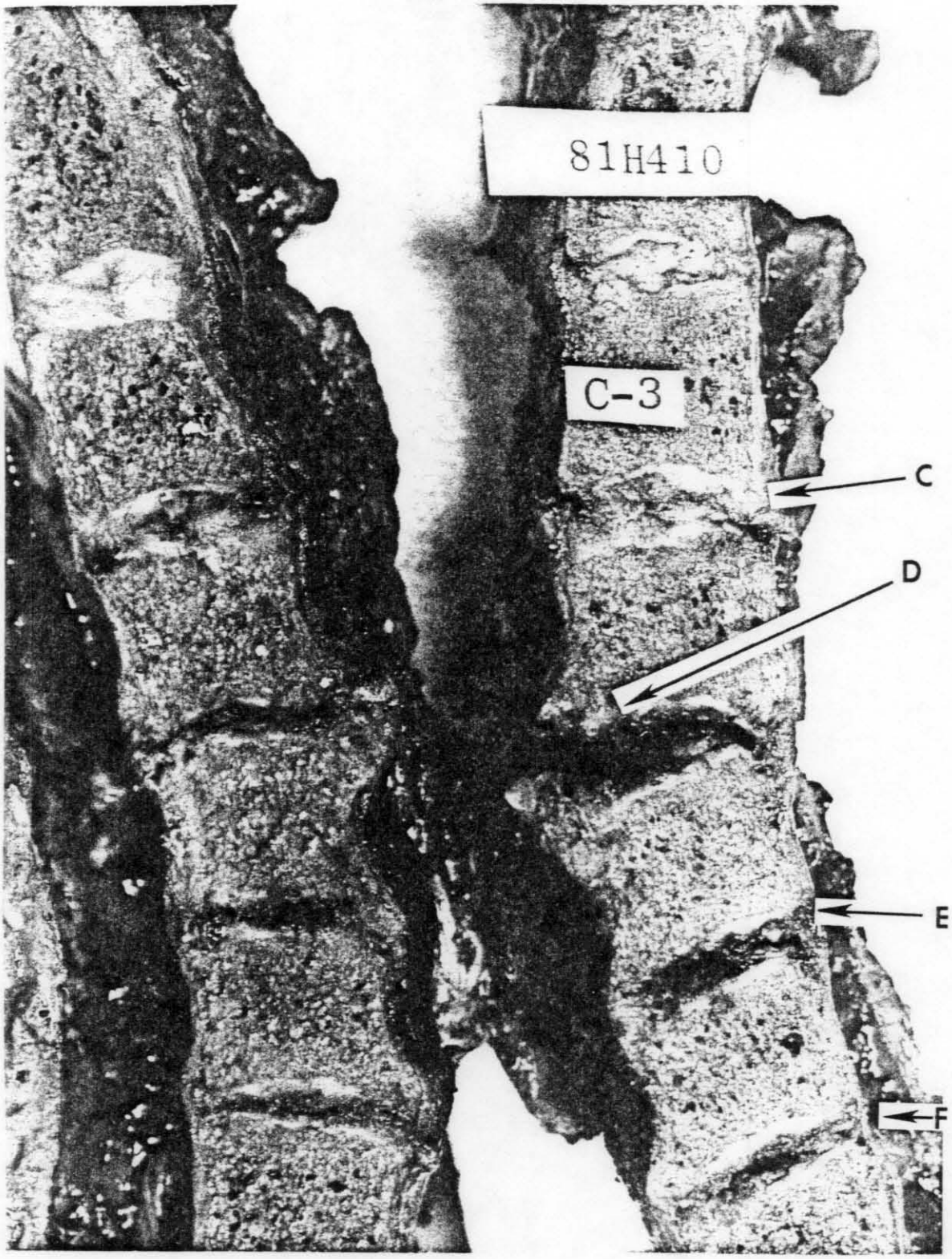
81H410
C-3
C
D
E
F

AUTOPSY SUMMARY

FOR TEST NO. 81H412

Injuries to Neck:

Teardrop fracture of C5 [A].

Anterior longitudinal ligament torn at C5 [B].

Bilateral tears of anterior longitudinal ligament at C4 [C].

Rupture of disc at C4 [D].

Rupture of disc at C5 [E].

TEST NO. 81H412

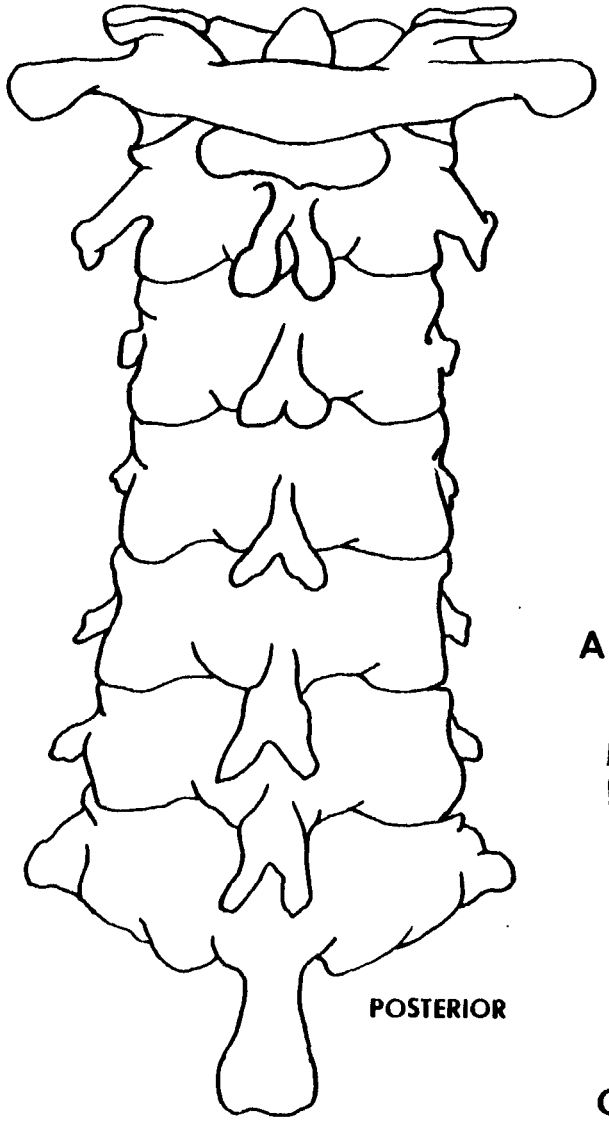

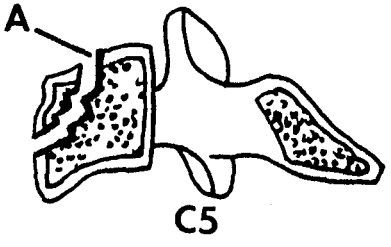

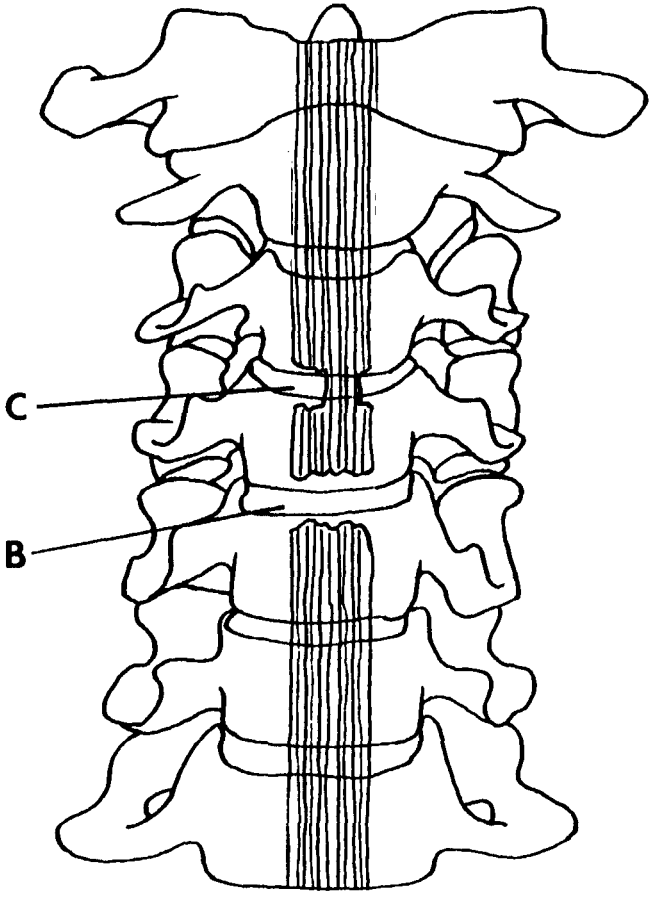

CERVICAL VERTEBRAE

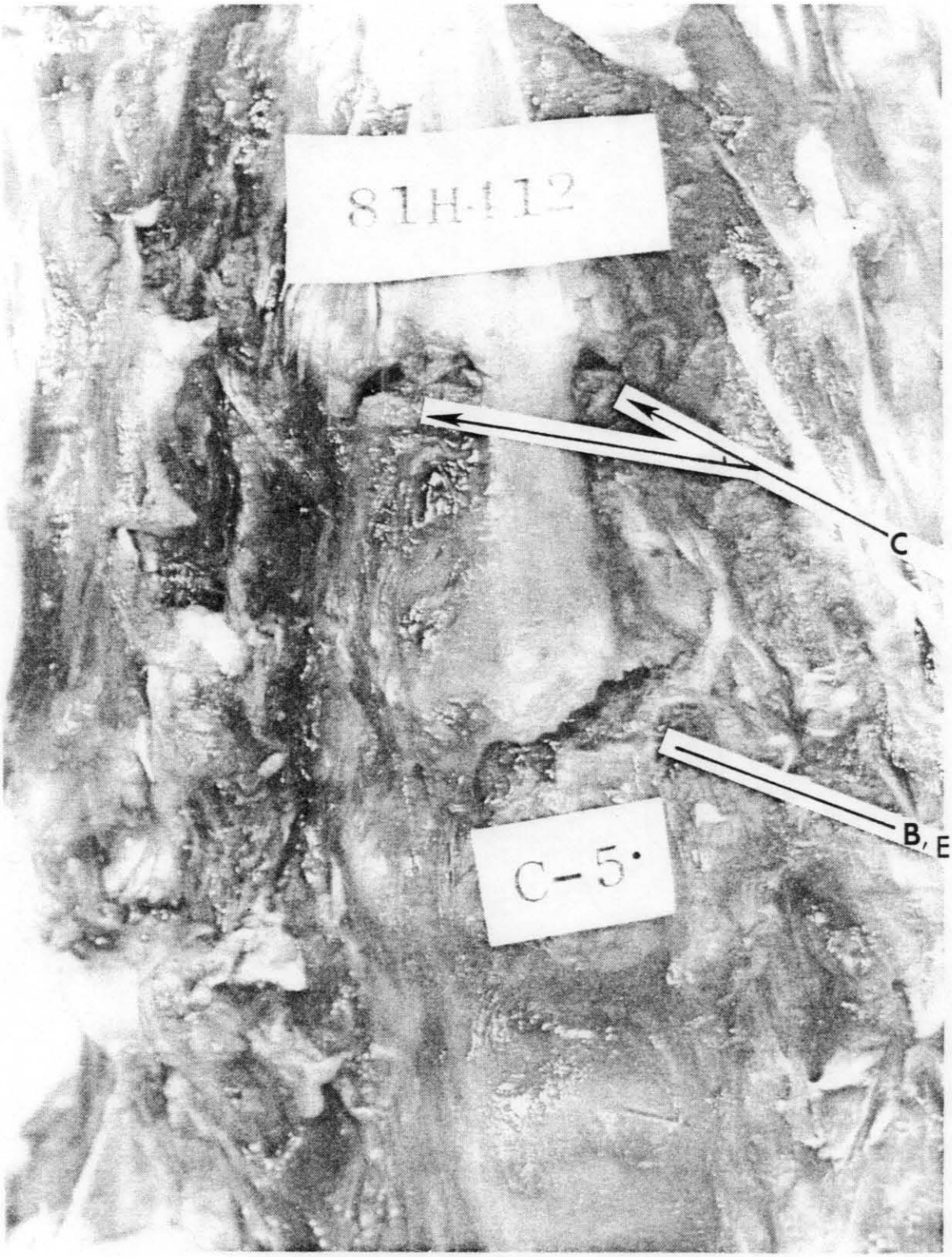
81H-112
C
B, E
C-5°

AUTOPSY SUMMARY

FOR TEST NO. 81H413

Injuries to head:

Bilateral basal skull fracture from temporal bone to foramen magnum.

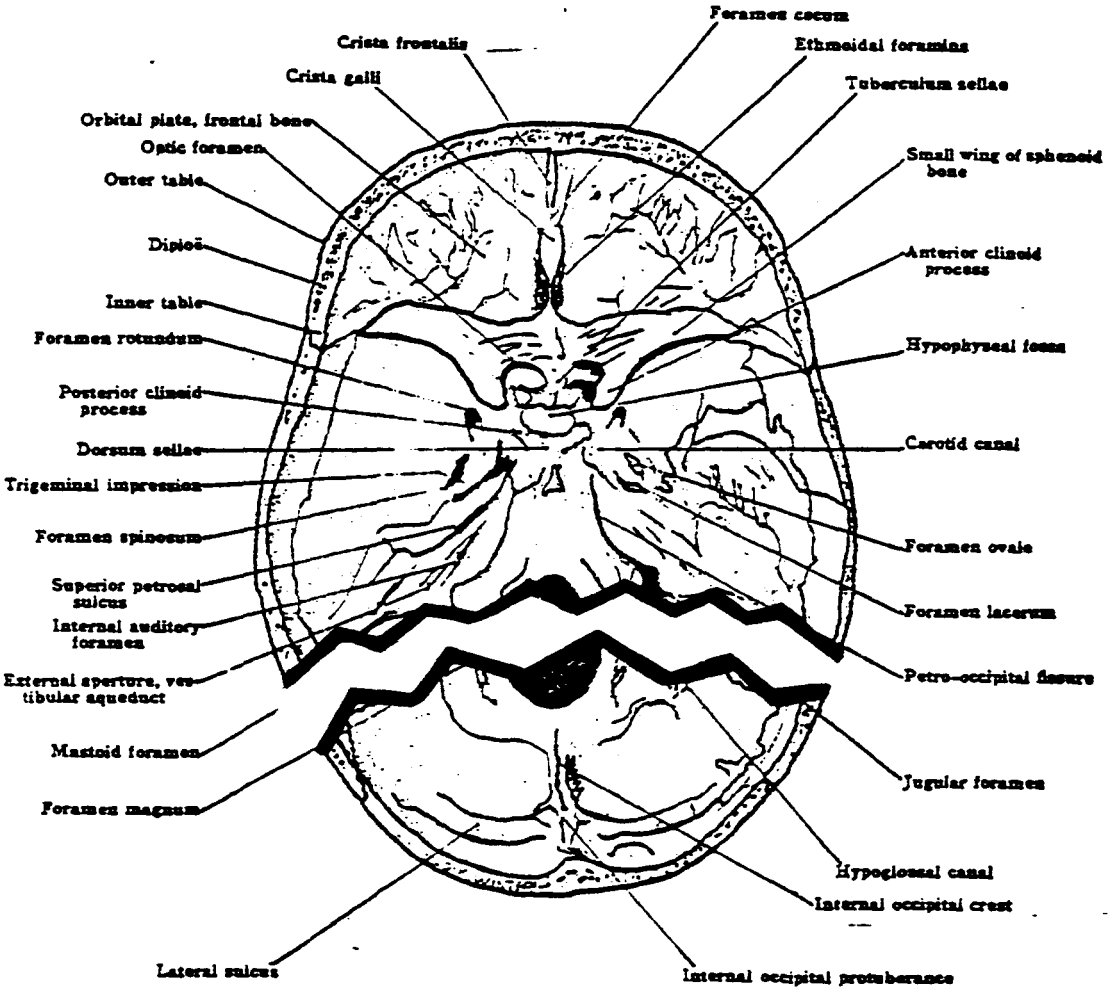

FIG. 109.—THE SKULL, INTERNAL ASPECT OF THE BASE.

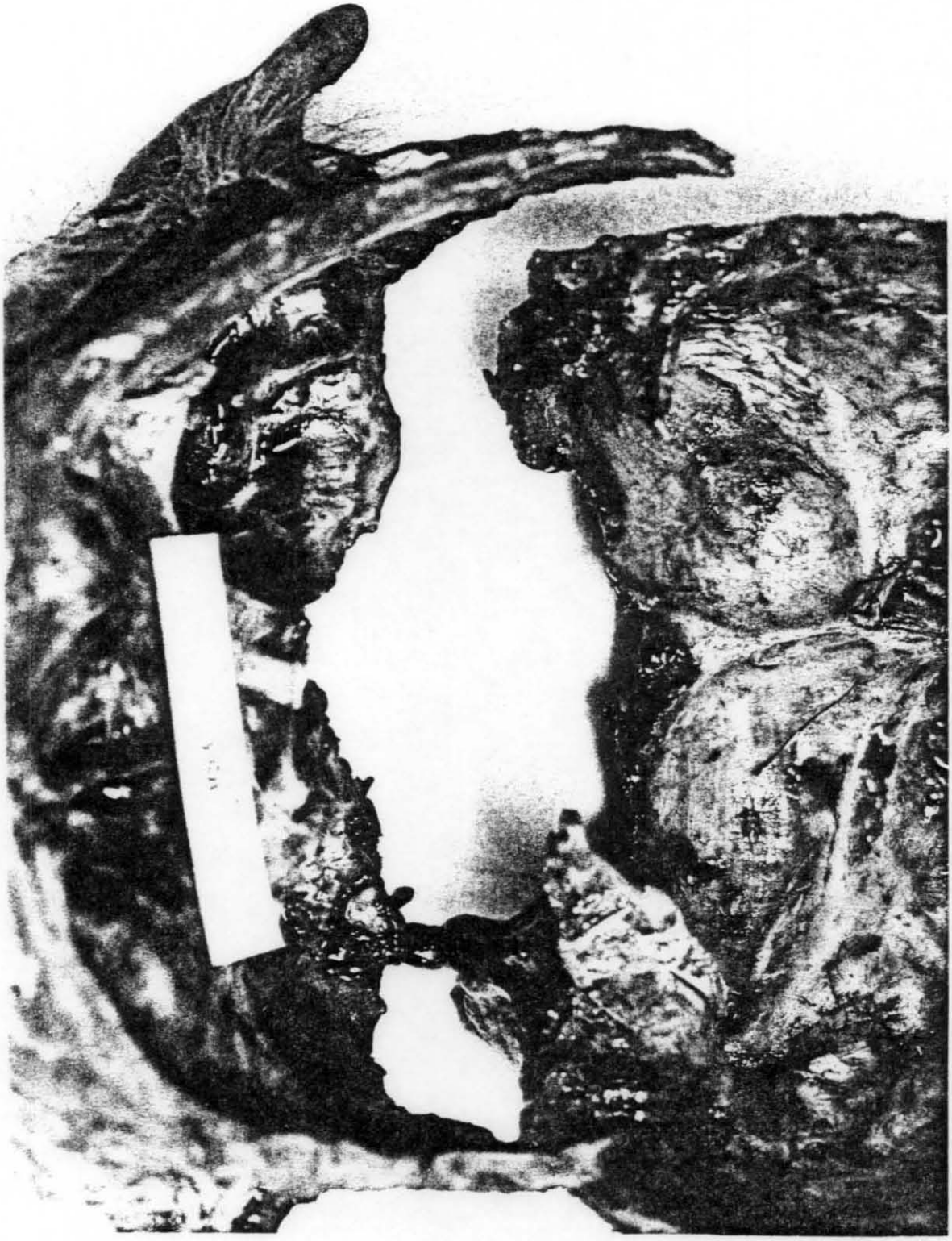

APPENDIX B

KINEMATIC RESPONSE: TIME HISTORIES

This appendix contains the results of signal processing of the kinematic response of the head and instrumented thoracic vertebra T1, T6, T12 and/or L1.

Up to 84 variables related to the 3-D motion of the head are derived from nine acceleration signals. These variables are briefly described below.

Var. 1-9: Signals obtained after filtering the nine raw head accelerations and realigning them in standard Posterior-Anterior (P-A), Right-Left (R-L), and Inferior-Superior (I-S) anatomical directions. These signals form the basic input to the "3D9X" computer program at UMTRI.

Var. 10-12: Linear acceleration of the instrumentation plate reference point (the centroid of the three triaxial accelerometers), in the standard anatomical reference frame.

Var. 13-18: Components of the head angular acceleration and velocity vectors along the anatomical (moving) reference directions.

Var. 19-24: Euler angles (ψ, θ, and ϕ) and their rates (time derivatives). These are used to describe the orientation of the head in three-dimensional space.

Var. 25-33: Time histories of the 3x3 transformation matrix (direction cosines) of the moving anatomical frame with respect to the fixed laboratory frames.

Var. 34-39: The head angular acceleration and velocity vectors (same as Var. 13-18) expressed in the fixed laboratory reference frame.

Var. 40-41: Resultant angular acceleration and angular velocity vectors.

Var. 42: Resultant linear acceleration vector at the instrumentation reference point.

Var. 43-45: Components of linear acceleration vectors of the head anatomical center which is the origin of the standard (PA, RL, IS) reference frame. This body point is selectable so that in some analysis the head estimated center of gravity may be used as the "body point" to be monitored.

Var. 46-48: Same acceleration vector as Var. 43-45, expressed along the fixed laboratory reference frame.

Var. 49-51: Linear velocity vector of the head anatomical center, expressed along the fixed axes of the laboratory frame.

Var. 52-54: Same linear velocity vector as above, expressed along the moving anatomical reference frame.

Var. 55-57: Linear displacement (position) of the body point (here, anatomical center) along the fixed laboratory axes. Note that these are obtained by direct integration of the corresponding velocities, since they are all expressed as inertial ccordinates.

Var. 58-60: The linear jerk vector, defined as the time-derivative of the acceleration time histories of the body point in question. Since the computations were entered at the acceleration level, determination of the jerk is accomplished by numerical differentiation performed in the frequency domain.

Var. 61-69: Nine time histories of the elements of 3x3 transformation matrix between the Frenet triad and the laboratory reference frame. The Frenet triad consists of the tangent (along the motion), the normal (perpendicular to the tangent), and the binormal which completes the right-handed orthogonal triad.

Var. 70-75: Head angular acceleration and velocity vectors expressed along the moving Frenet (T,N,B) triad.

Var. 76-77: Linear acceleration vector expressed as two components only: tangential and centripetal.

Var. 78: Resultant of linear acceleration vector, and the HIC of that pulse.

Var. 79: Resultant of linear velocity vector.

Var. 80-82: Instantaneous values of the curvature, torsion, and sphericity of the 3-D space curve along which the head body-point is moving.

Var. 83-84: The time derivatives of the Tangent and Normal, obtained by numerical differentiation.

Additional kinematic response and/or impact parameters are included in this appendix. Finally, some of the variables obtained from head three-dimensional motion

analysis were substituted by time histories of thoracic vertebrae. This was done in Tests 81H401 through 81H408, by executing "3DSIMP," one version of the "3D9X" general-purpose program that was tailored specifically for SI impacts.

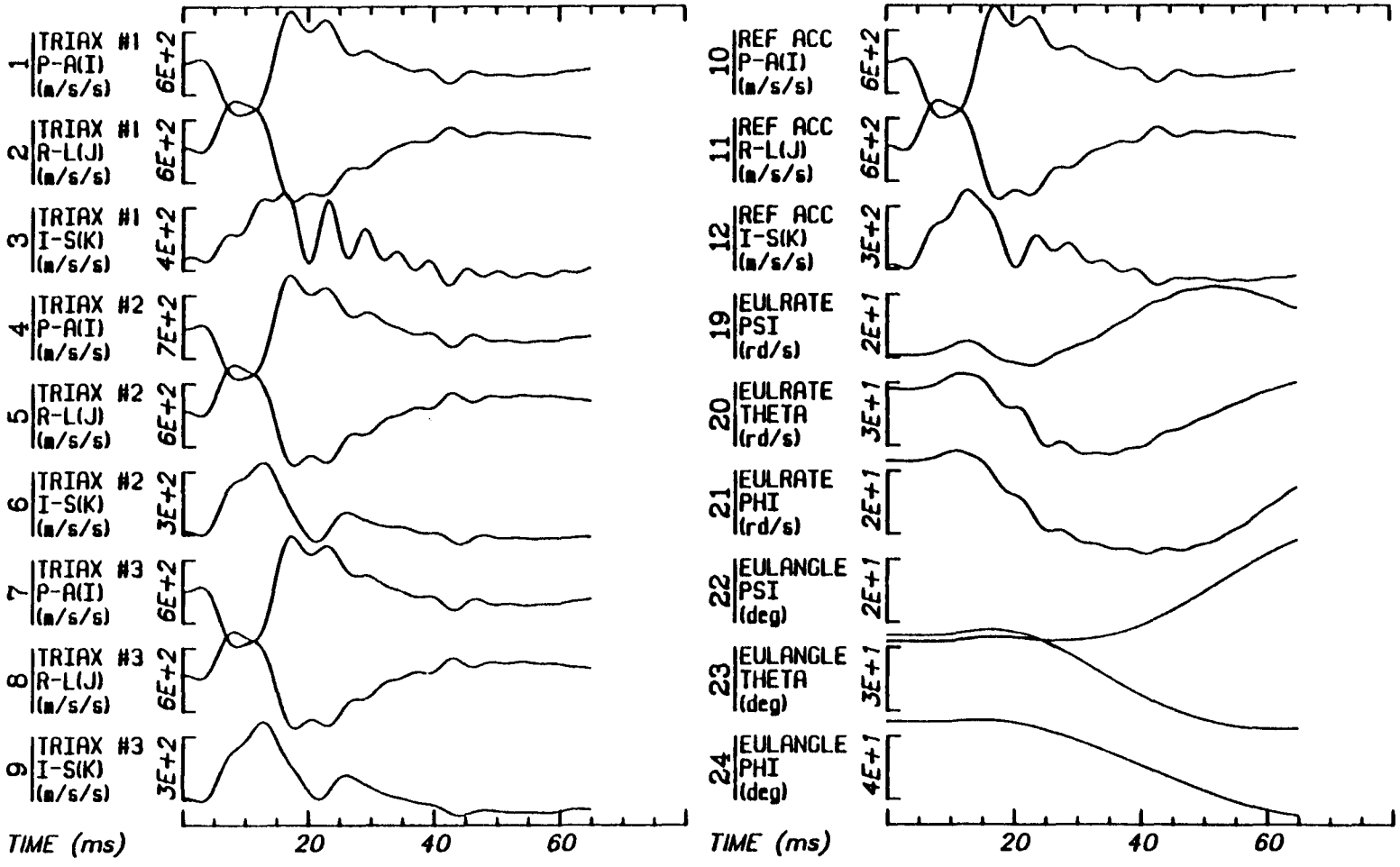

Run ID: 81H401 Tape: 3DSIMP.O File: 1 Date: MAR 31, 1981 Sheet: 1/5

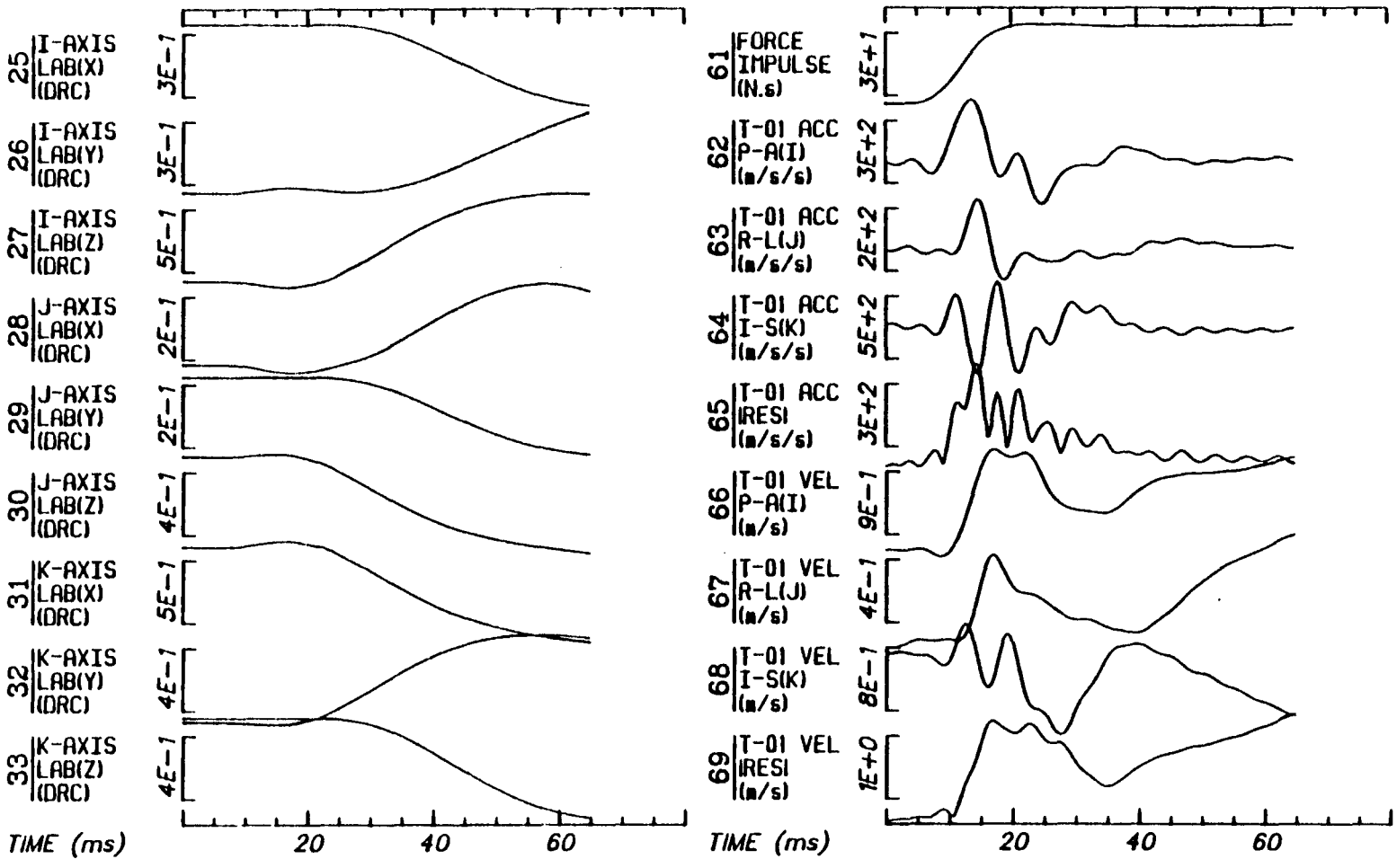

Run ID: 81H401 Tape: 3DSIMP.0 File: 1 Date: MAR 31, 1981 Sheet: 2/5

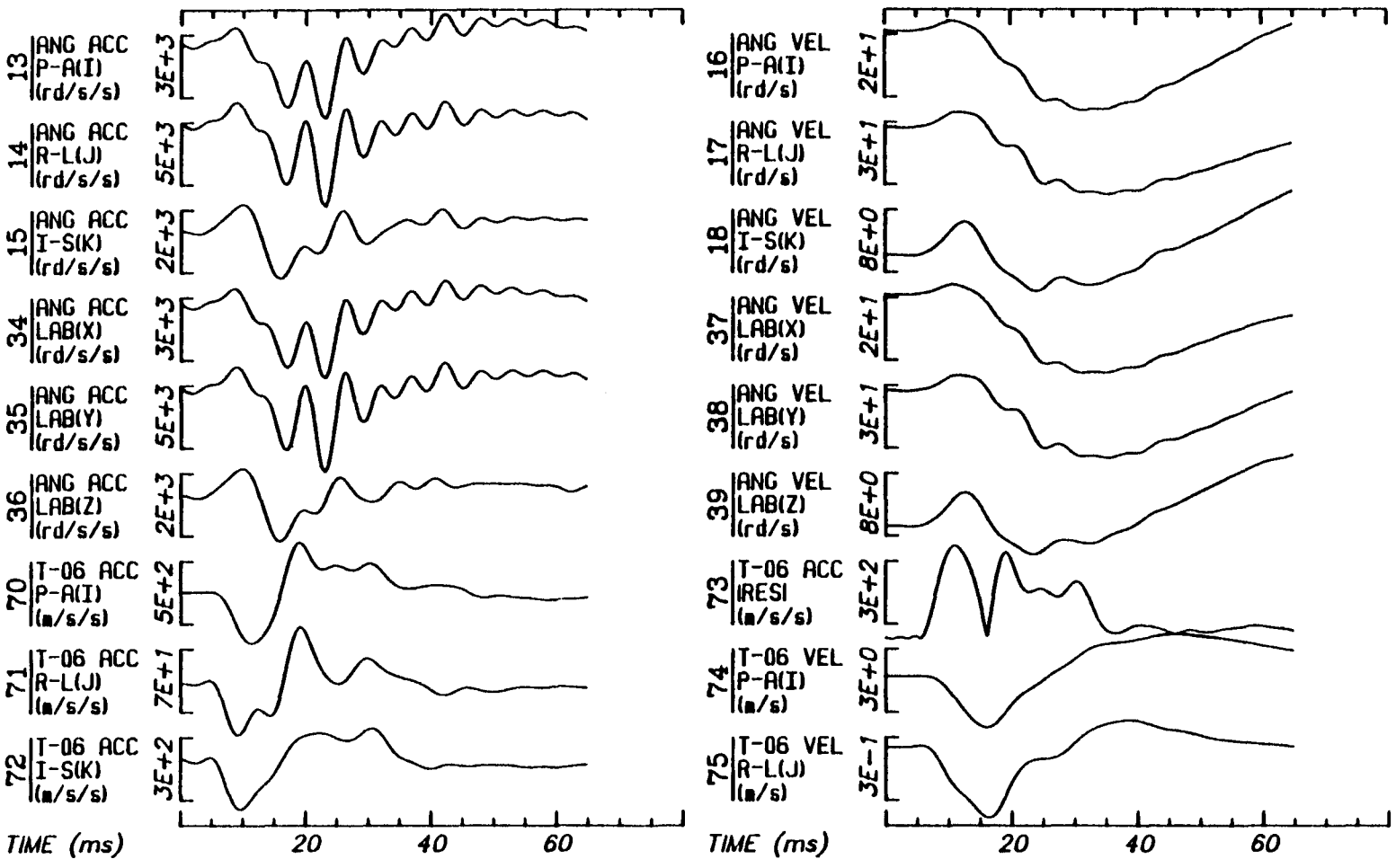

Run ID: 81H401 Tape: 3DSIMP.0 File: 1 Date: MAR 31, 1981 Sheet: 3/5

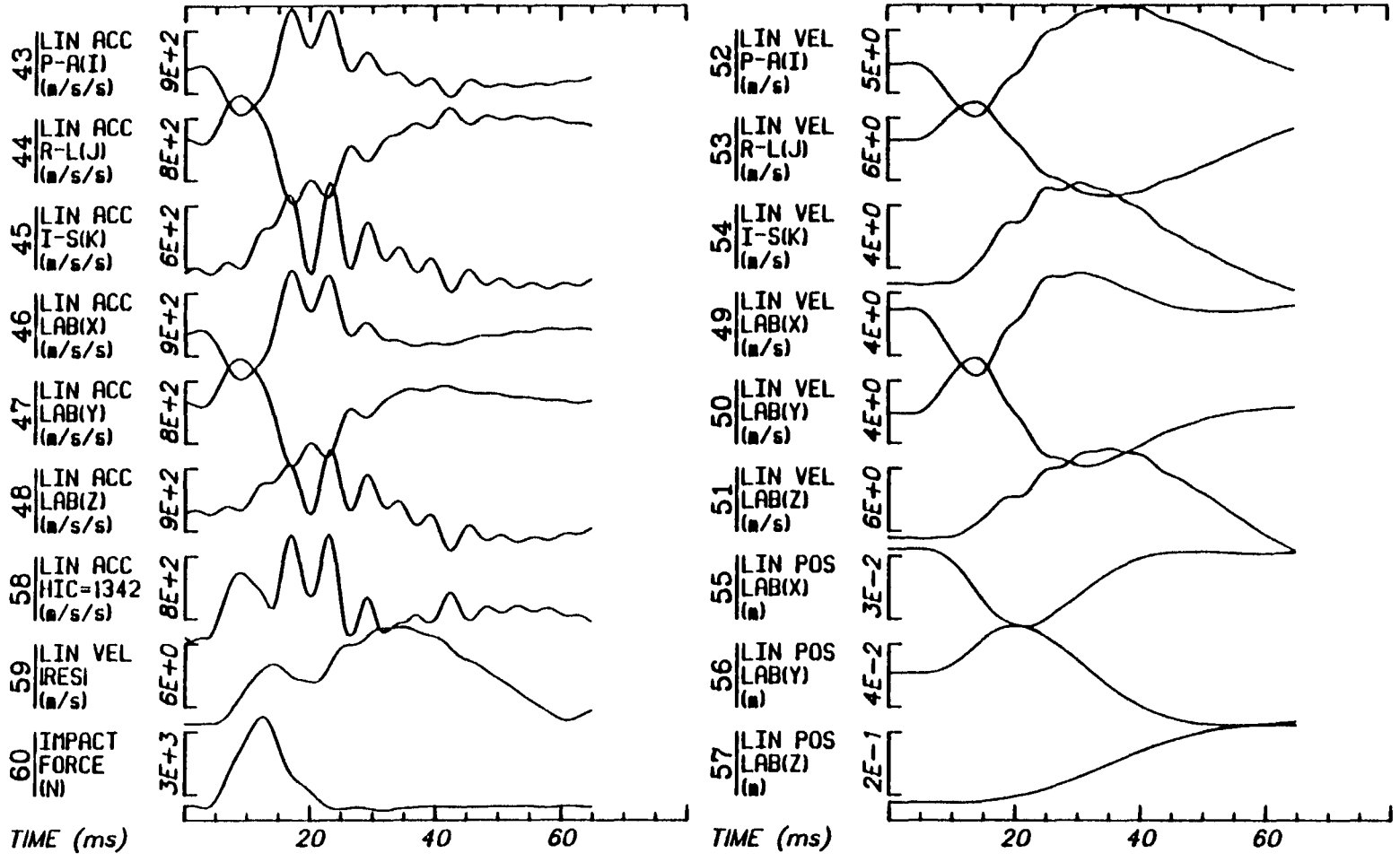

Run ID: 81H401 Tape: 3DSIMP.O File: 1 Date: MAR 31, 1981 Sheet: 4/5

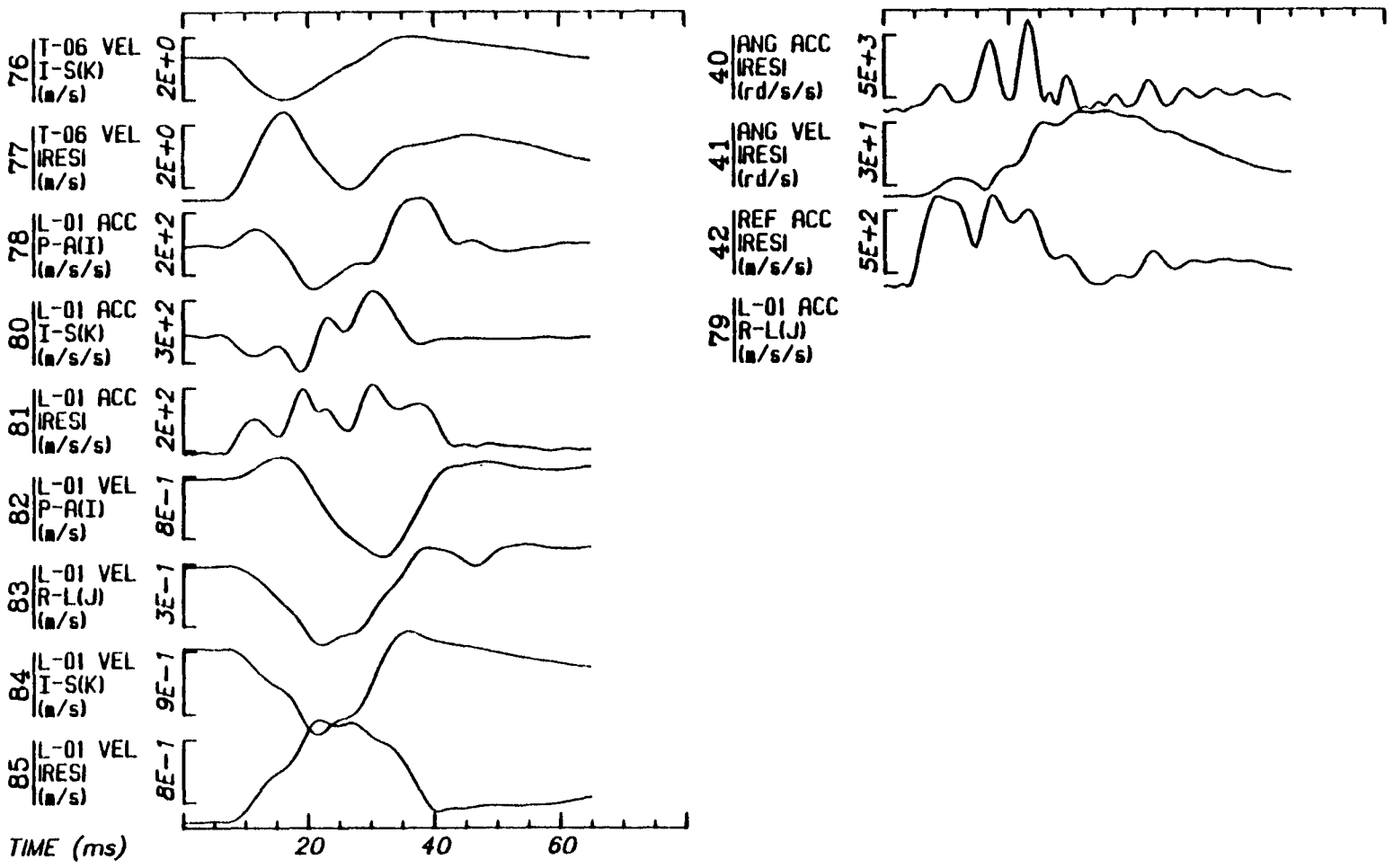

Run ID: 81H401 Tape: 3DSIMP.O File: 1 Date: MAR 31, 1981 Sheet: 5/5

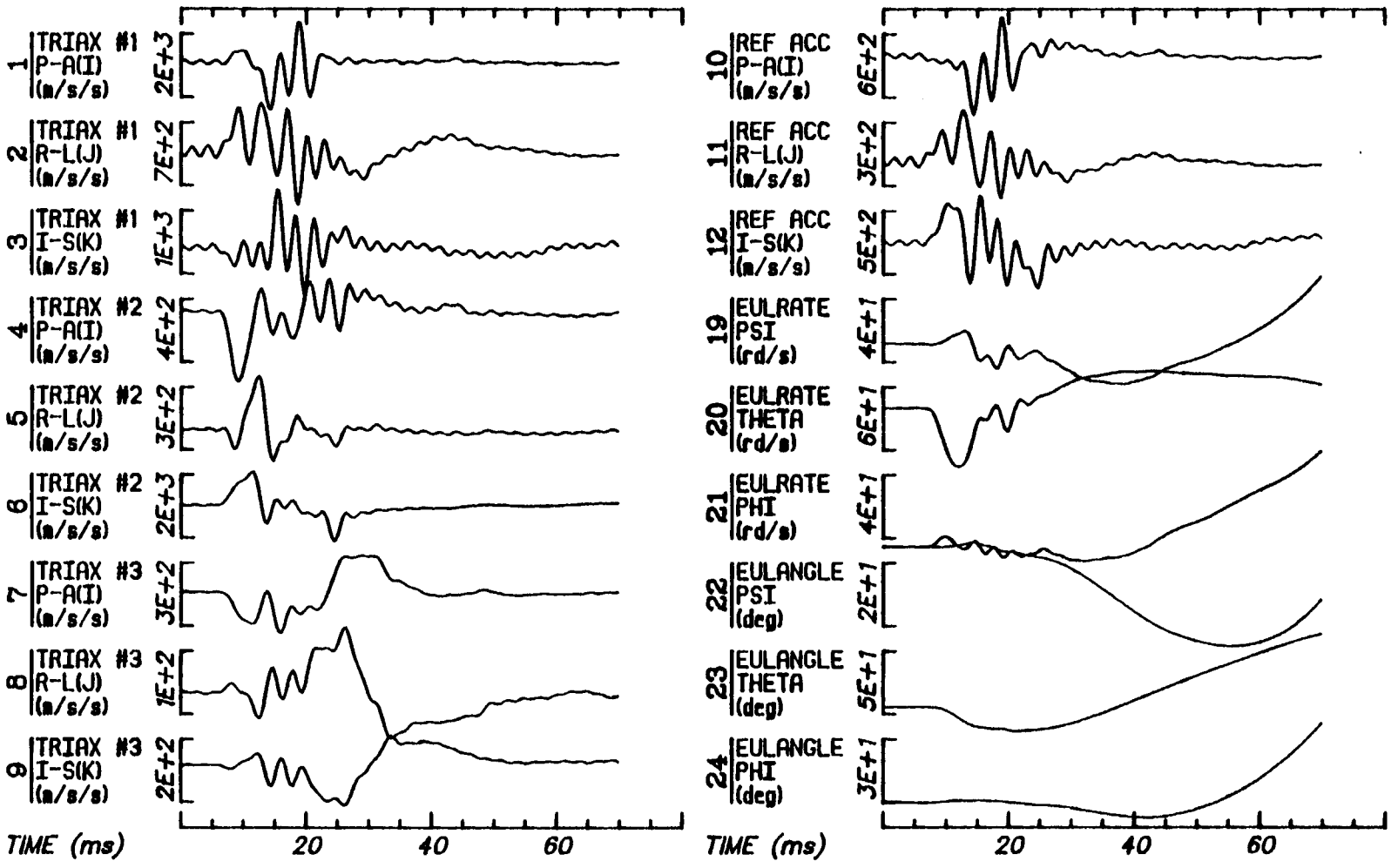

Run ID: 81H402 Tape: 3D9X-RES File: 73 Date: NOV 5, 1982 Sheet: 1/5

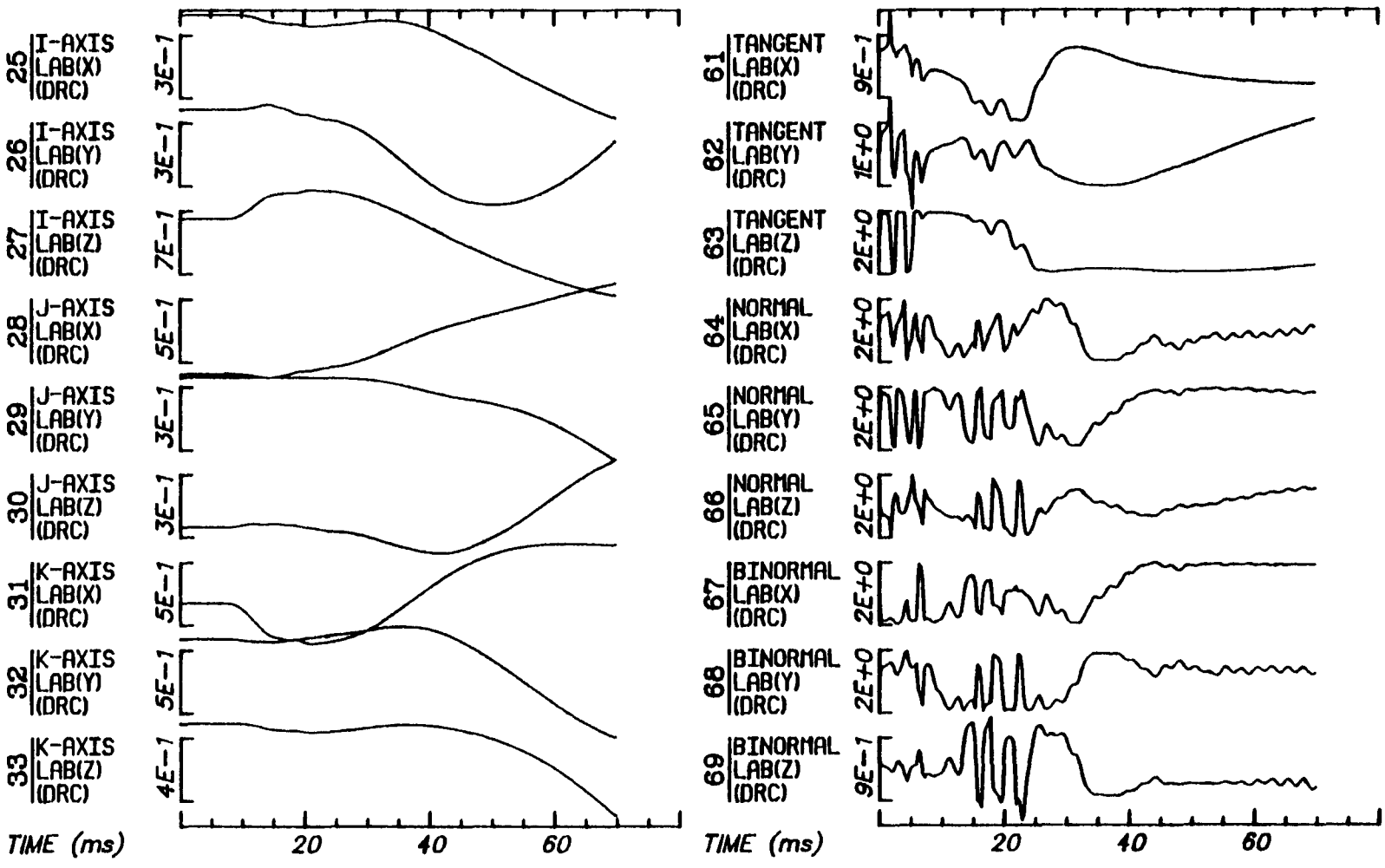

Run ID: 81H402 Tape: 3D9X-RES File: 73 Date: NOV 5, 1982 Sheet: 2/5

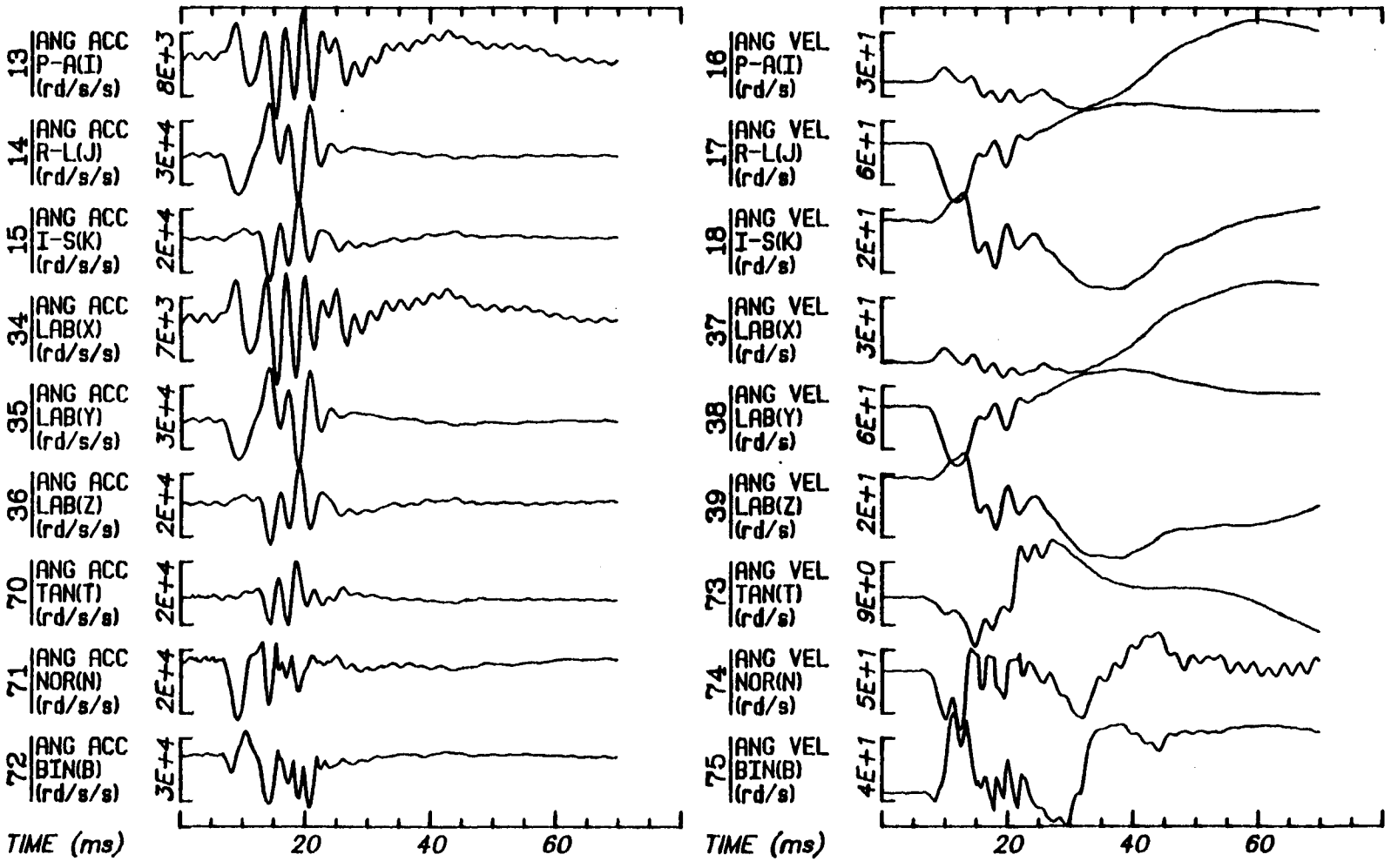

Run ID: 81H402 Tape: 3D9X-RES File: 73 Date: NOV 5, 1982 Sheet: 3/5

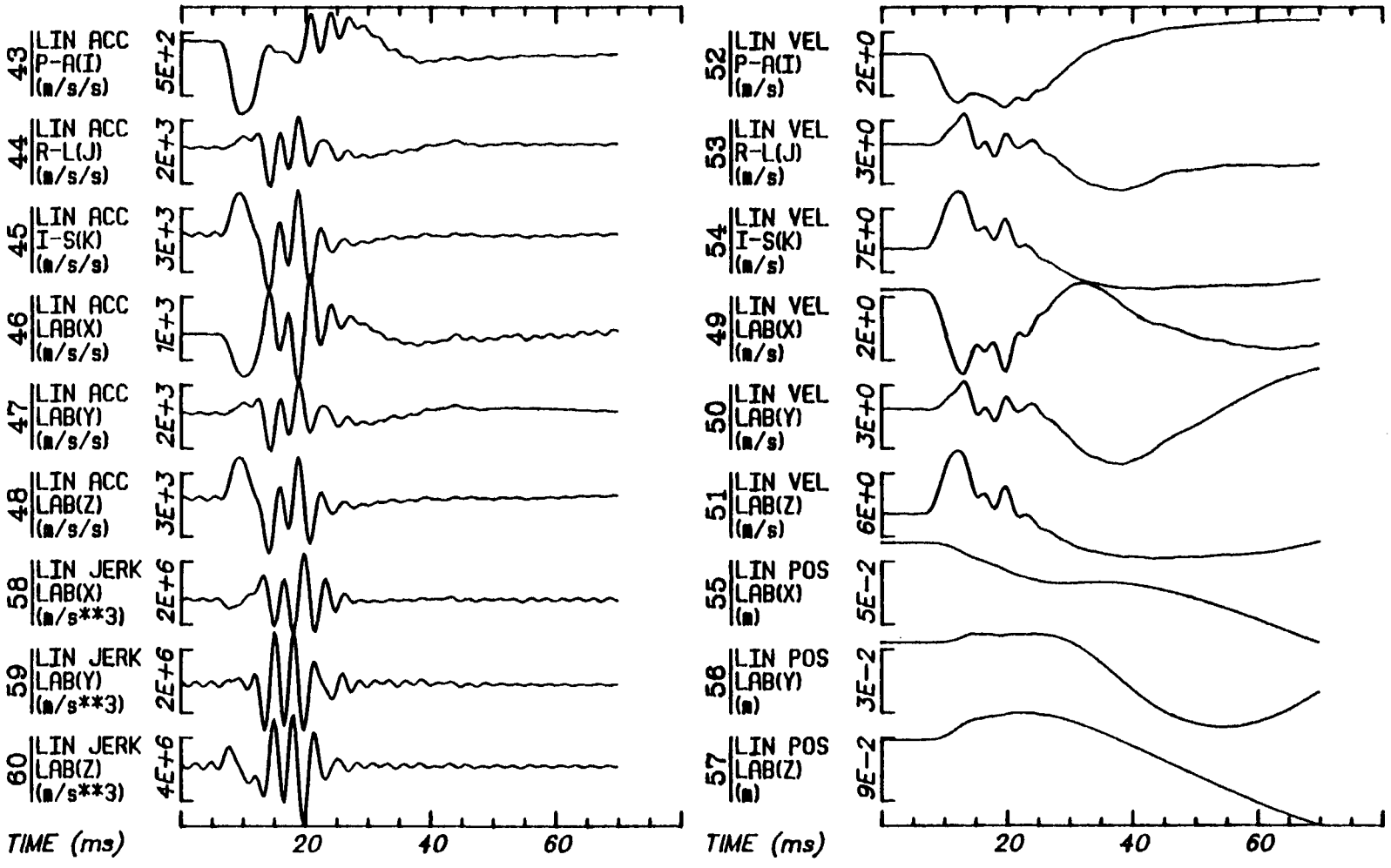

Run ID: 81H402 Tape: 3D9X-RES File: 73 Date: NOV 5, 1982 Sheet: 4/5

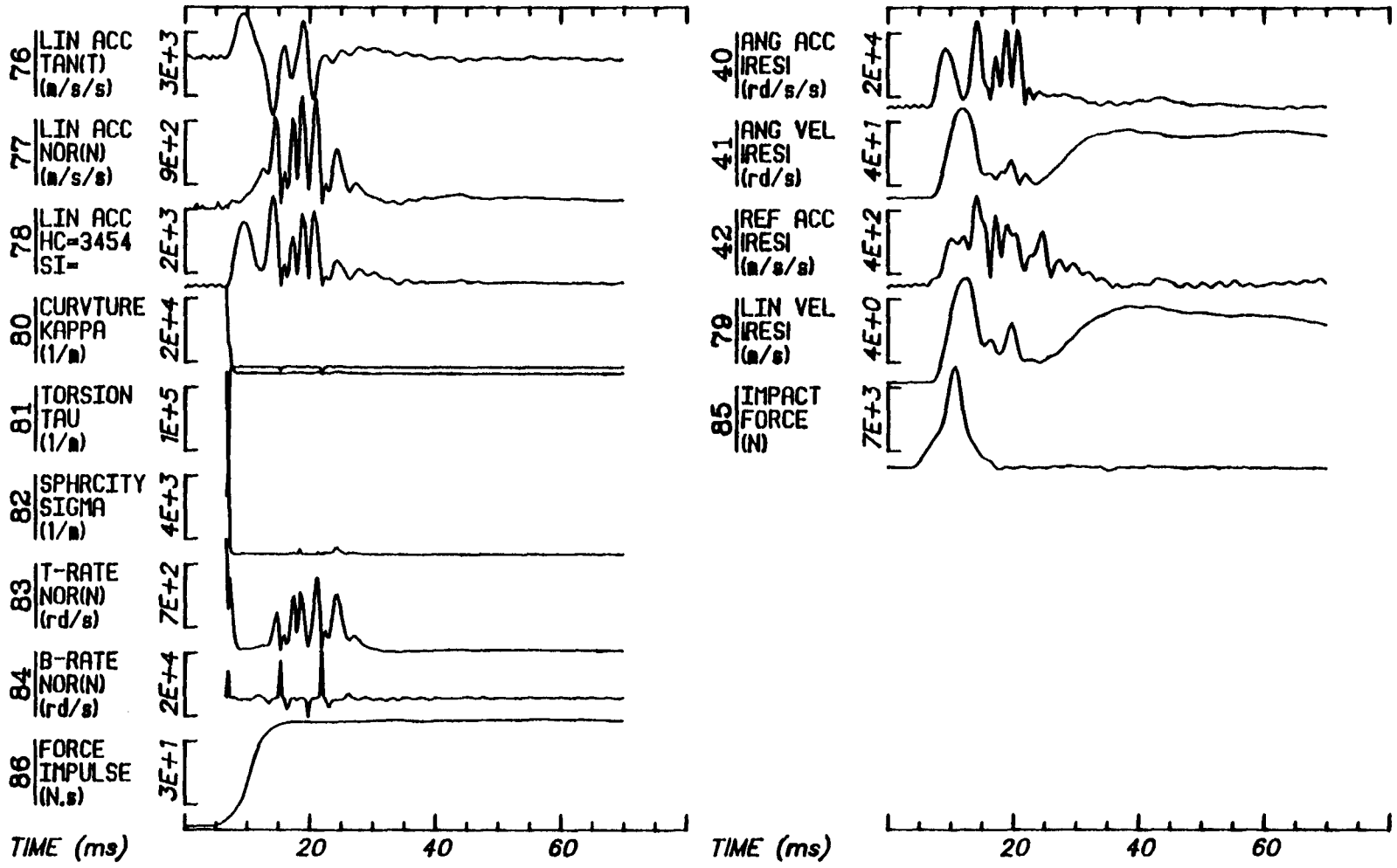

Run ID: 81H402 Tape: 3D9X--RES File: 73 Date: NOV 5, 1982 Sheet: 5/5

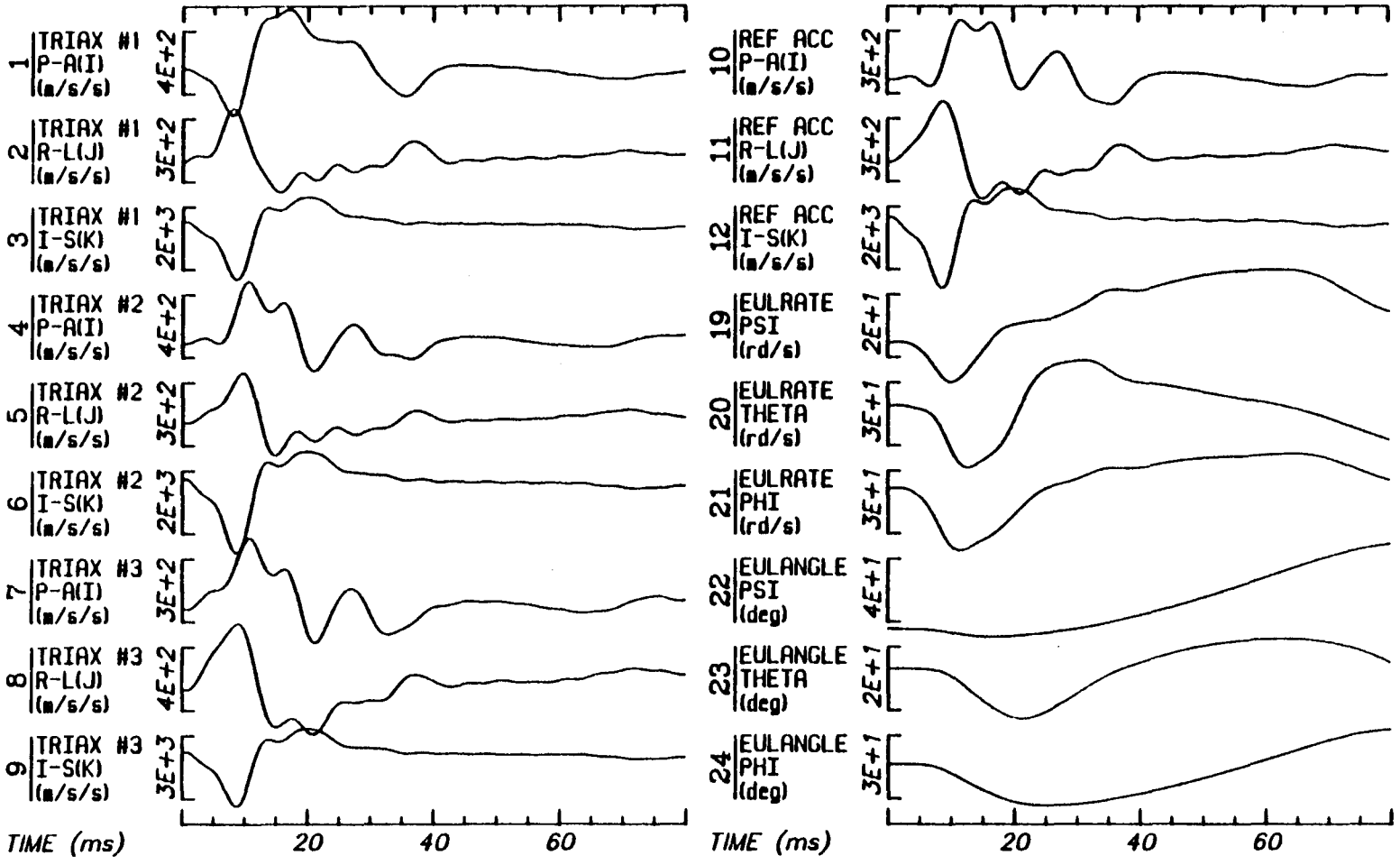

Run ID: 81H403 Tape: 3DSIMP.O File: 1 Date: MAY 4, 1981 Sheet: 1/5

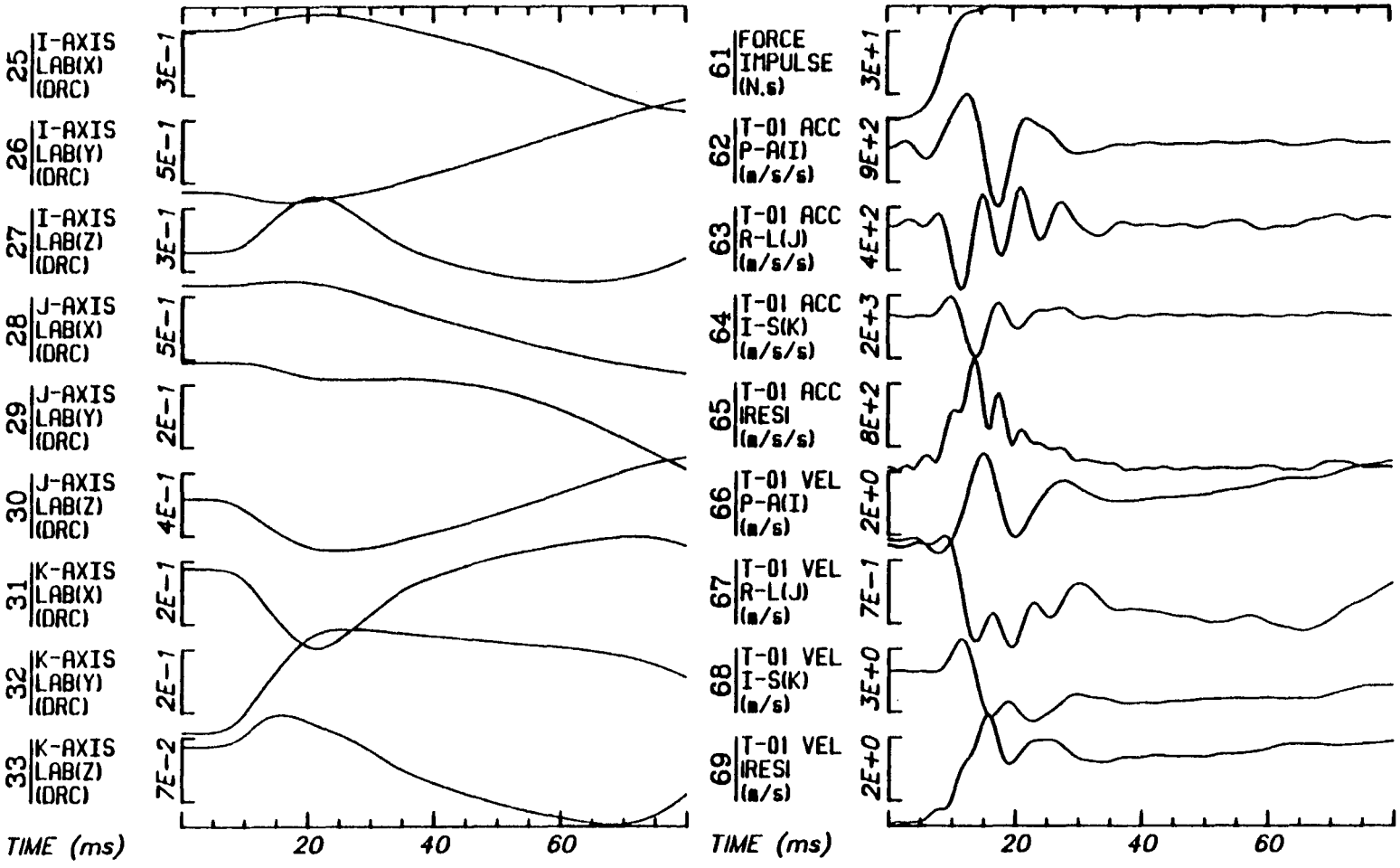

Run ID: 81H403 Tape: 3DSIMP.O File: 1 Date: MAY 4, 1981 Sheet: 2/5

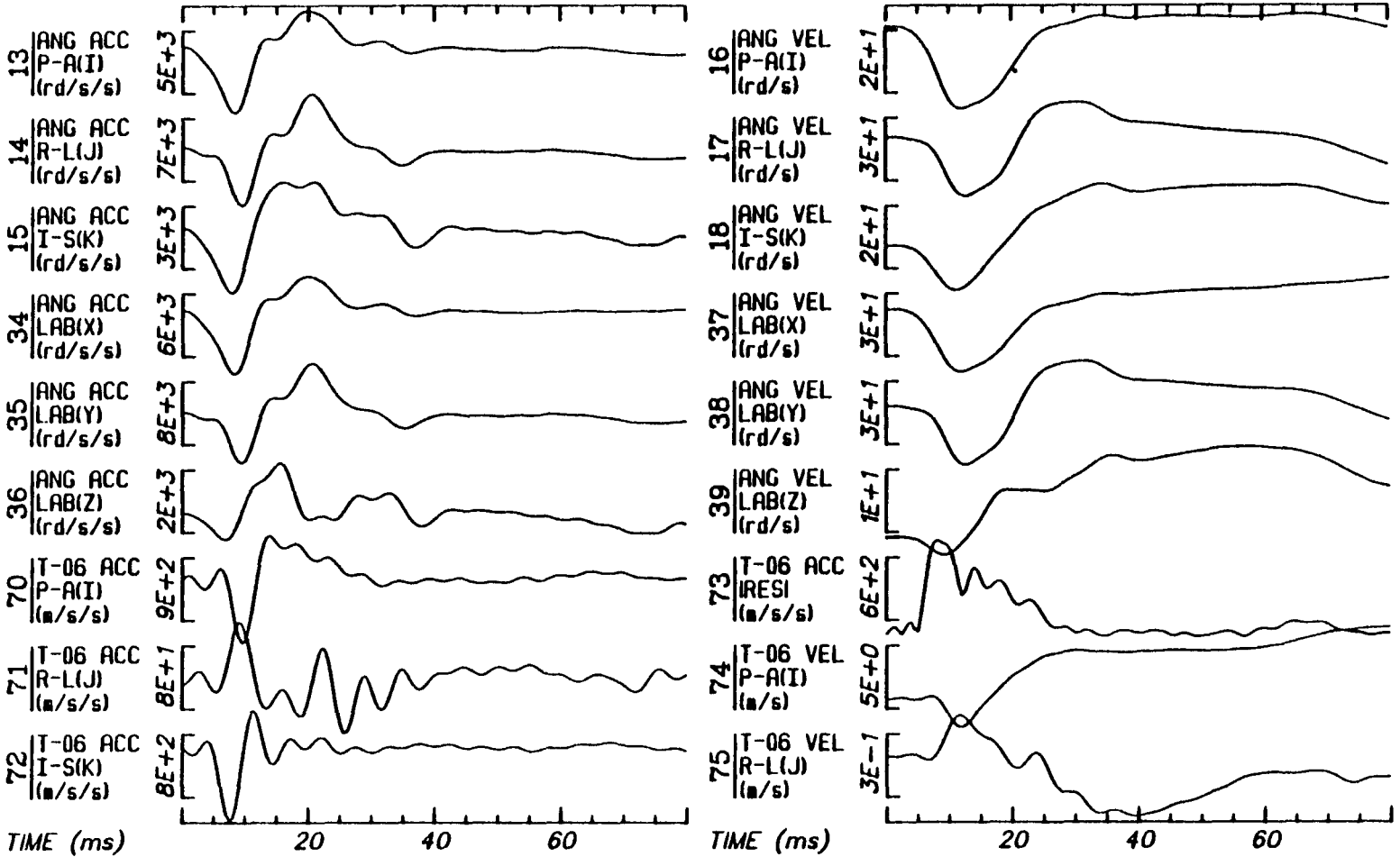

Run ID: 81H403 Tape: 3DSIMP.0 File: 1 Date: MAY 4, 1981 Sheet: 3/5

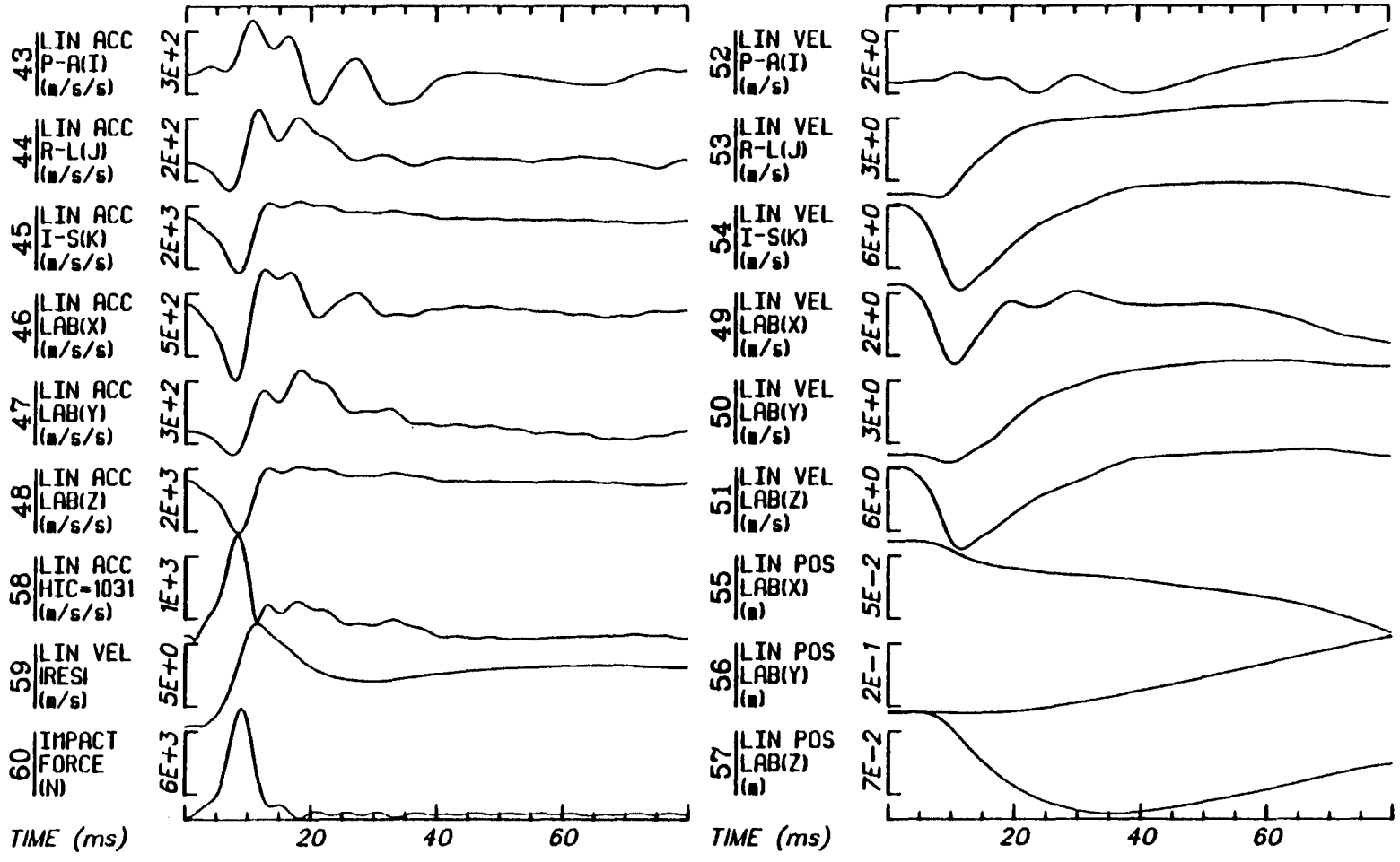

Run ID: 81H403 Tape: 3DSIMP.O File: 1 Date: MAY 4, 1981 Sheet: 4/5

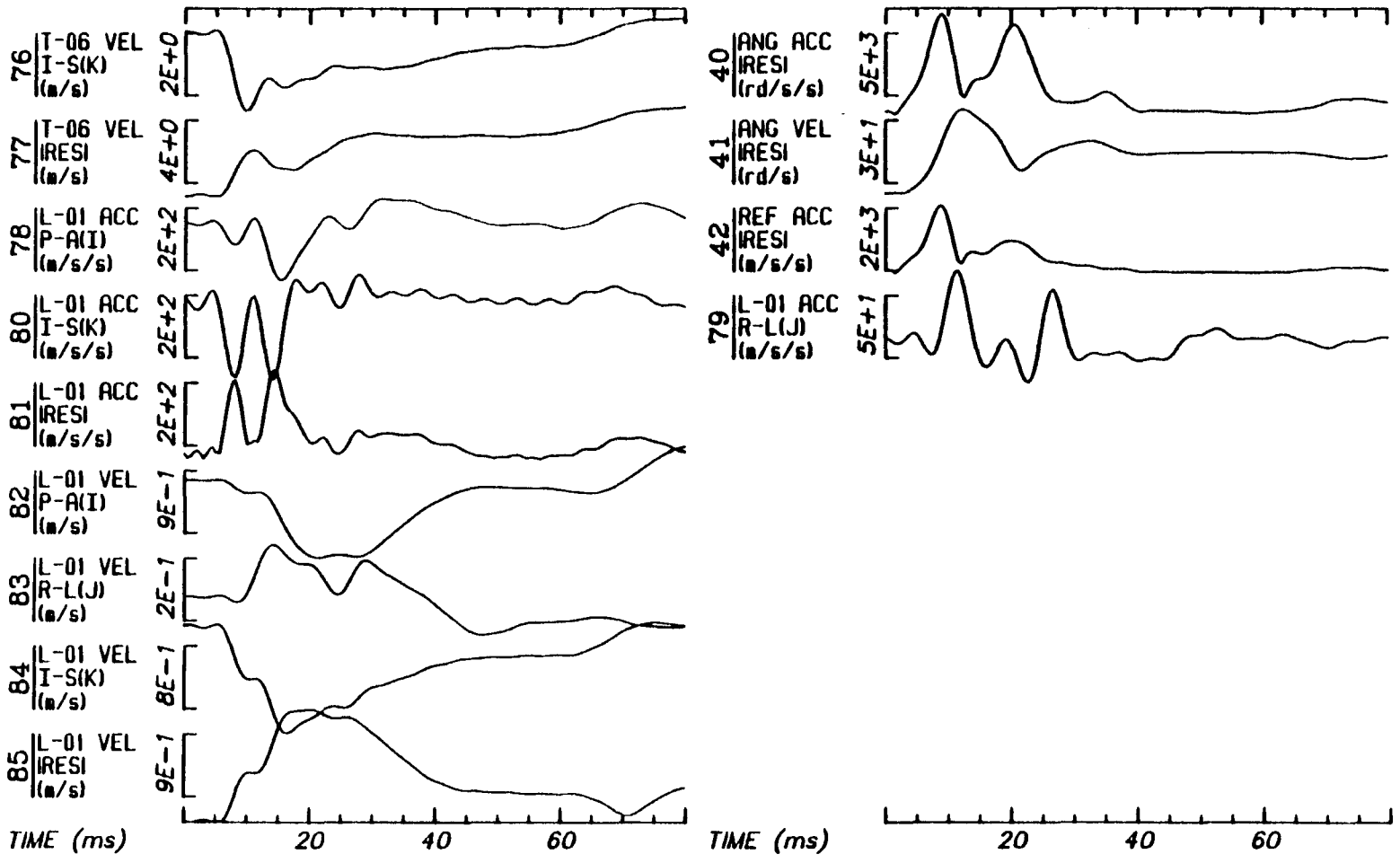

Run ID: 81H403 Tape: 3DSIMP.0 File: 1 Date: MAY 4, 1981 Sheet: 5/5

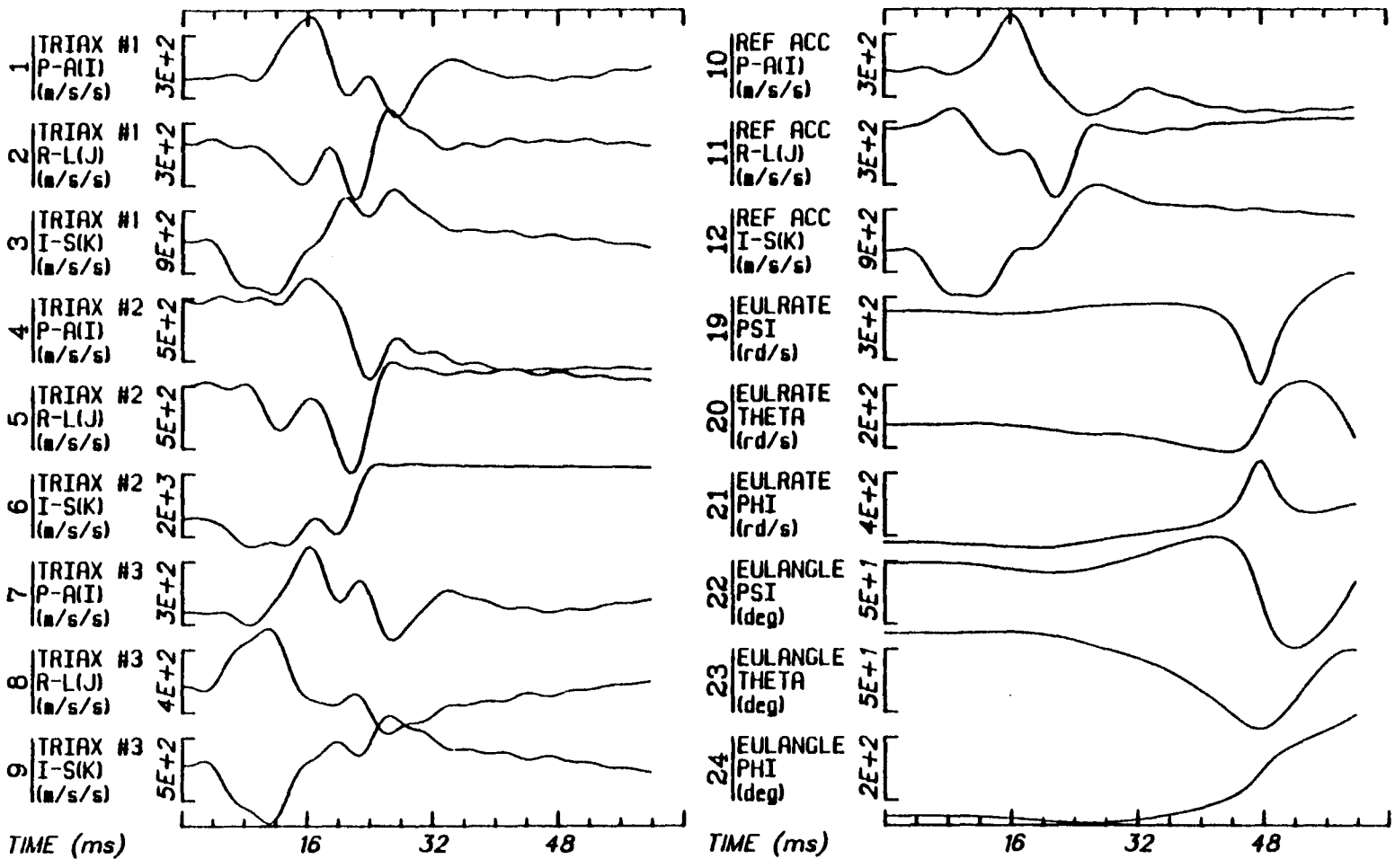

Run ID: 81H404 Tape: 3DSIMP.O File: 1 Date: MAY 15, 1981 Sheet: 1/5

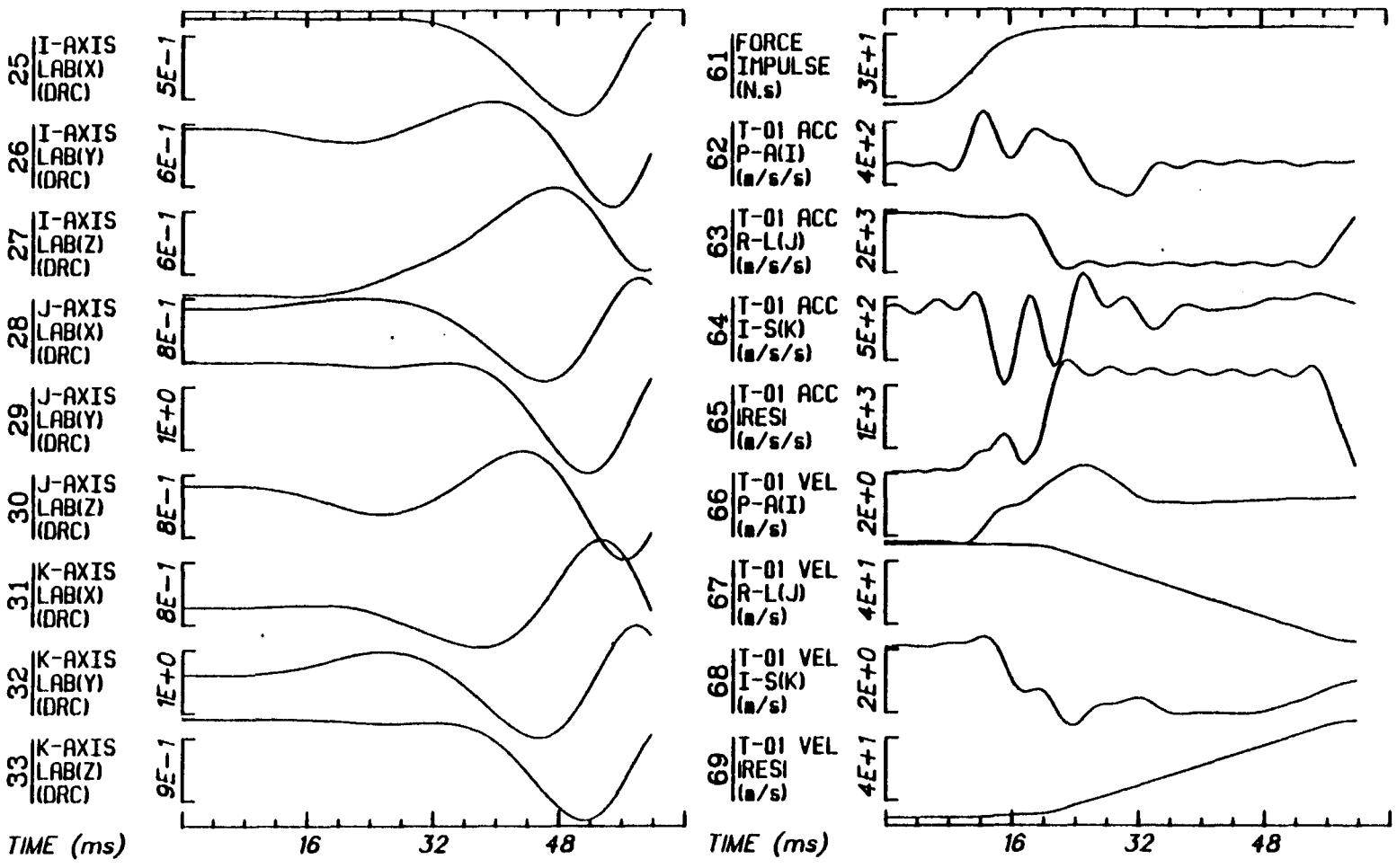

Run ID: 81H404 Tape: 3DSIMP.0 File: 1 Date: MAY 15, 1981 Sheet: 2/5

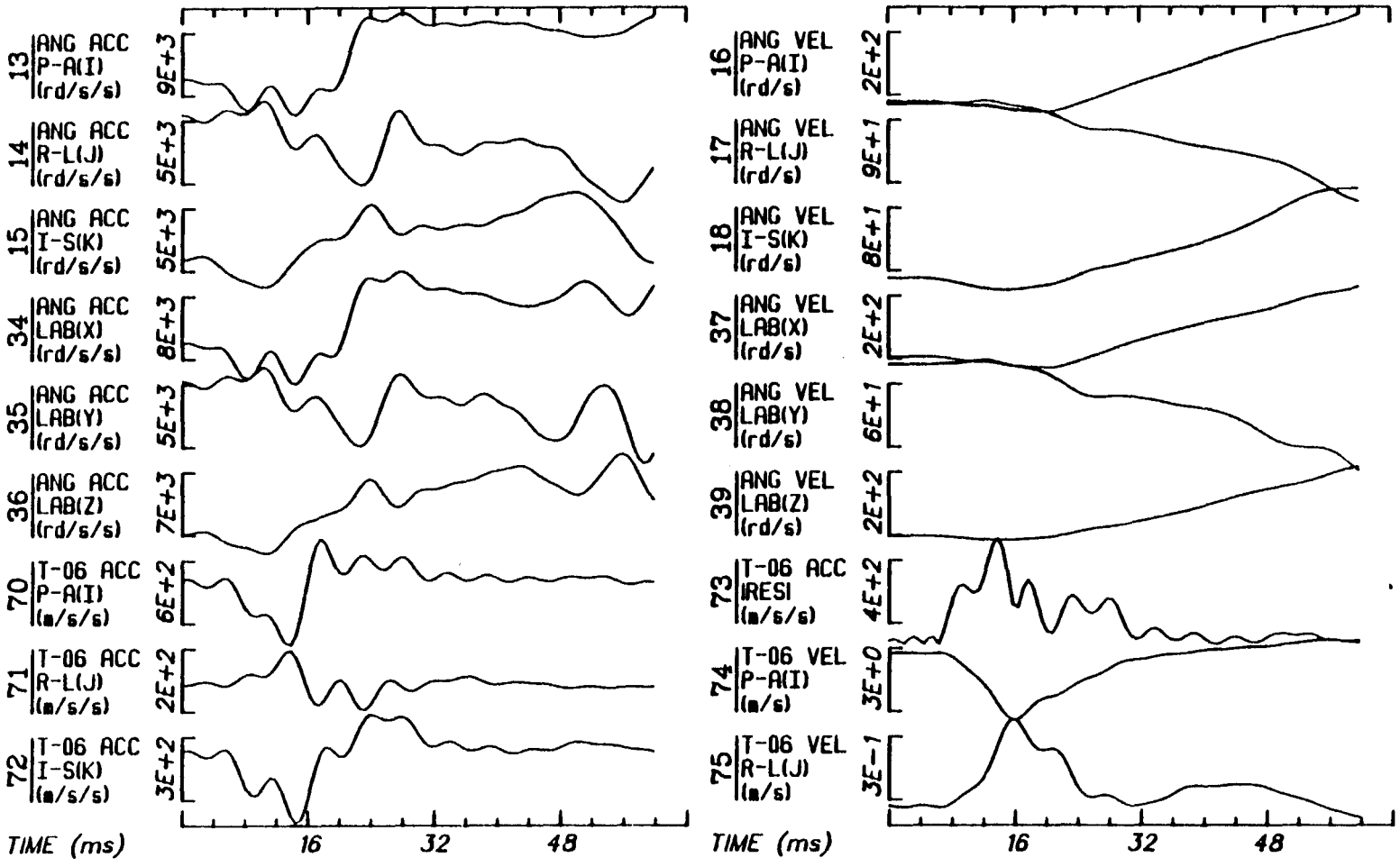

Run ID: 81H404 Tape: 3DSIMP.0 File: 1 Date: MAY 15, 1981 Sheet: 3/5

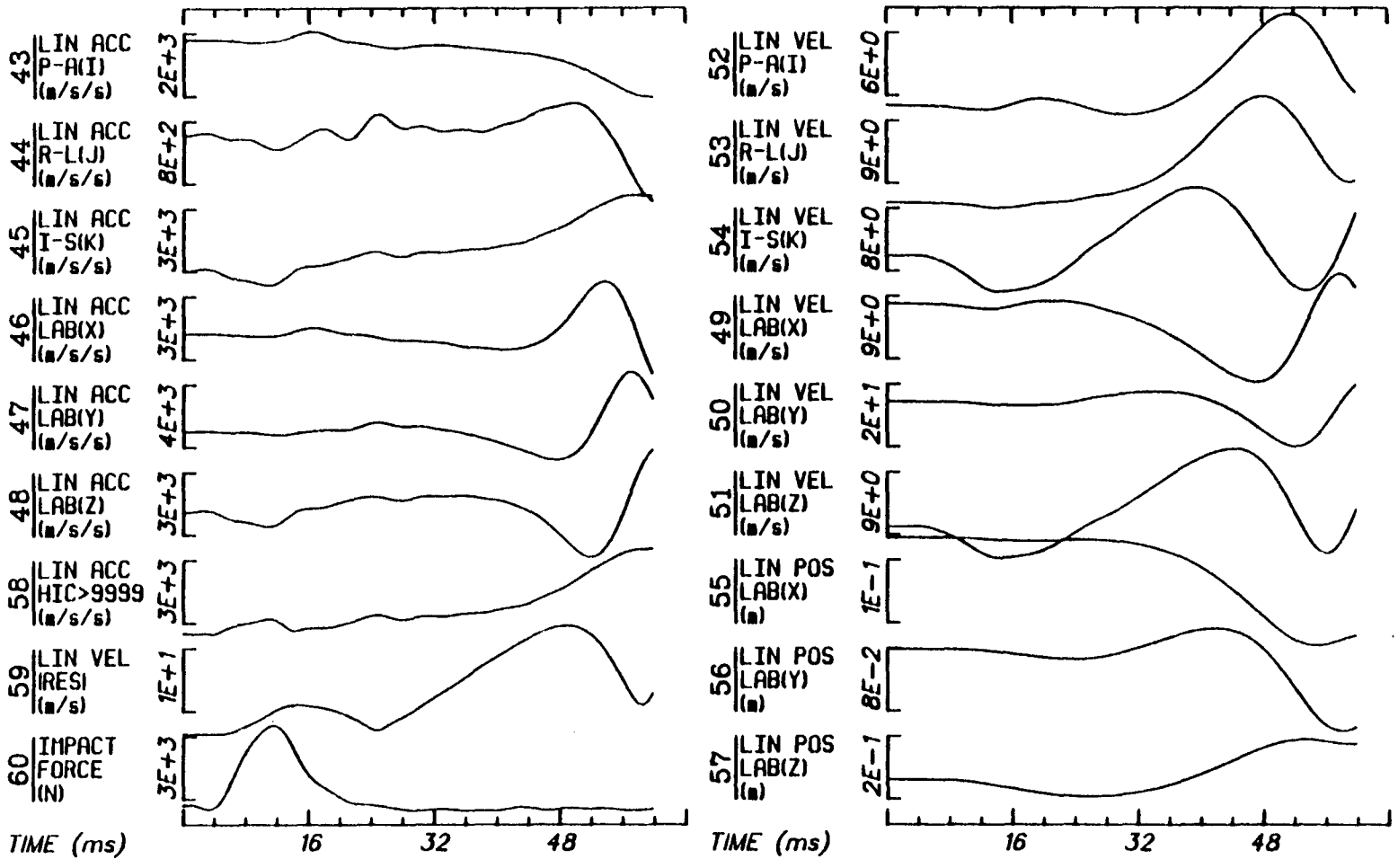

Run ID: 81H404 Tape: 3DSIMP.O File: 1 Date: MAY 15, 1981 Sheet: 4/5

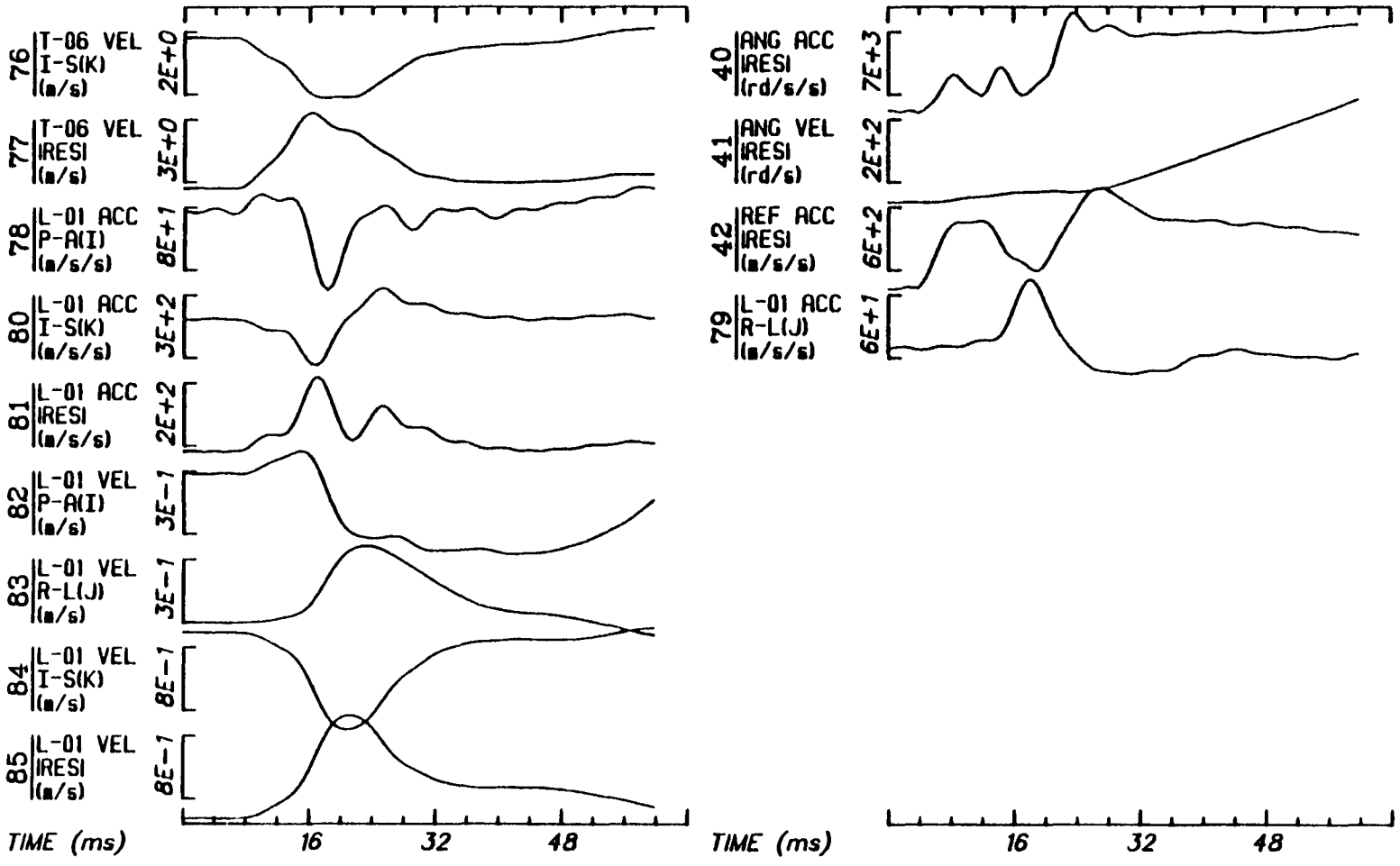

Run ID: 81H404 Tape: 3DSIMP.0 File: 1 Date: MAY 15, 1981 Sheet: 5/5

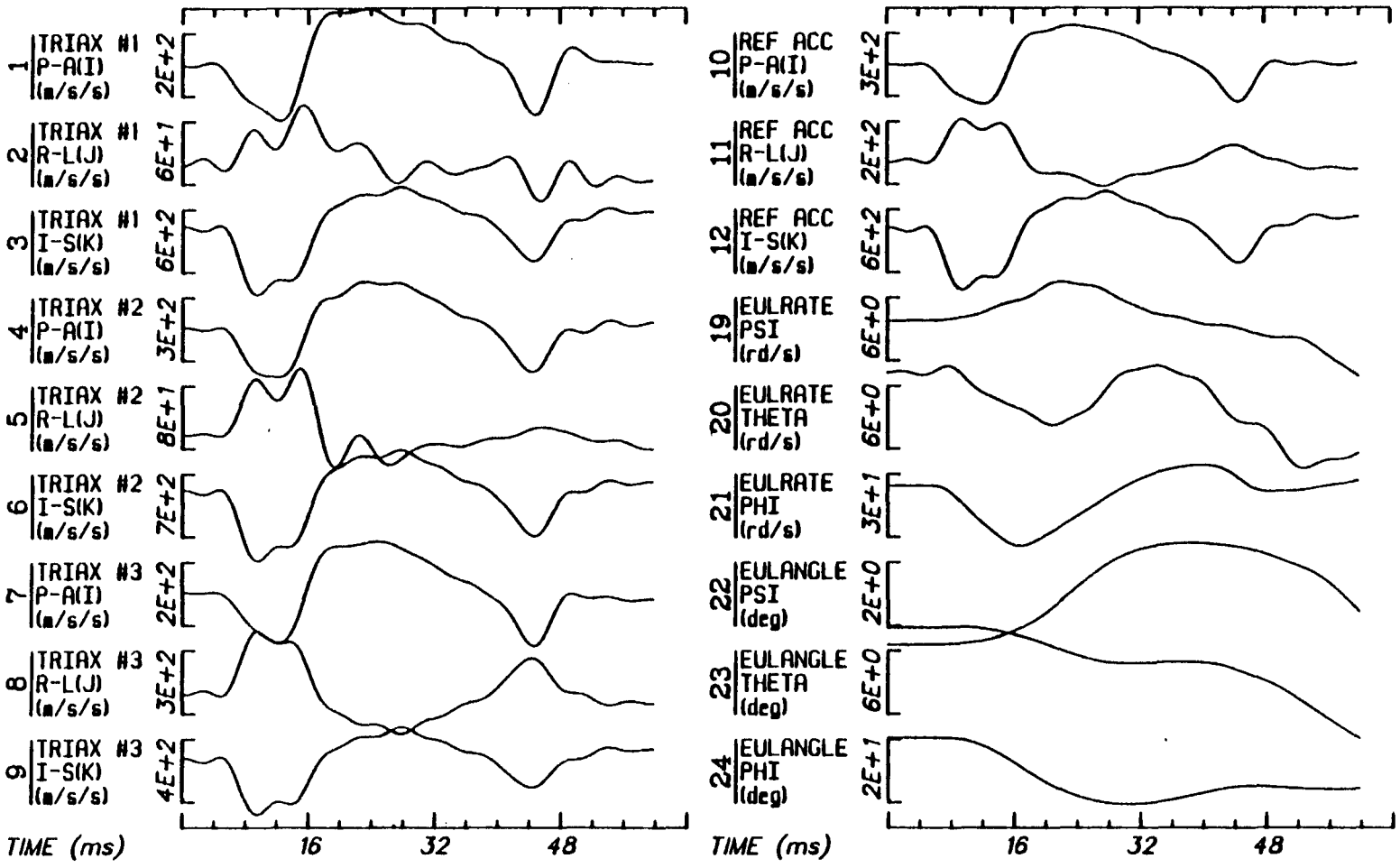

Run ID: 81H405 Tape: 3DSIMP.0 File: 2 Date: MAY 15, 1981 Sheet: 1/5

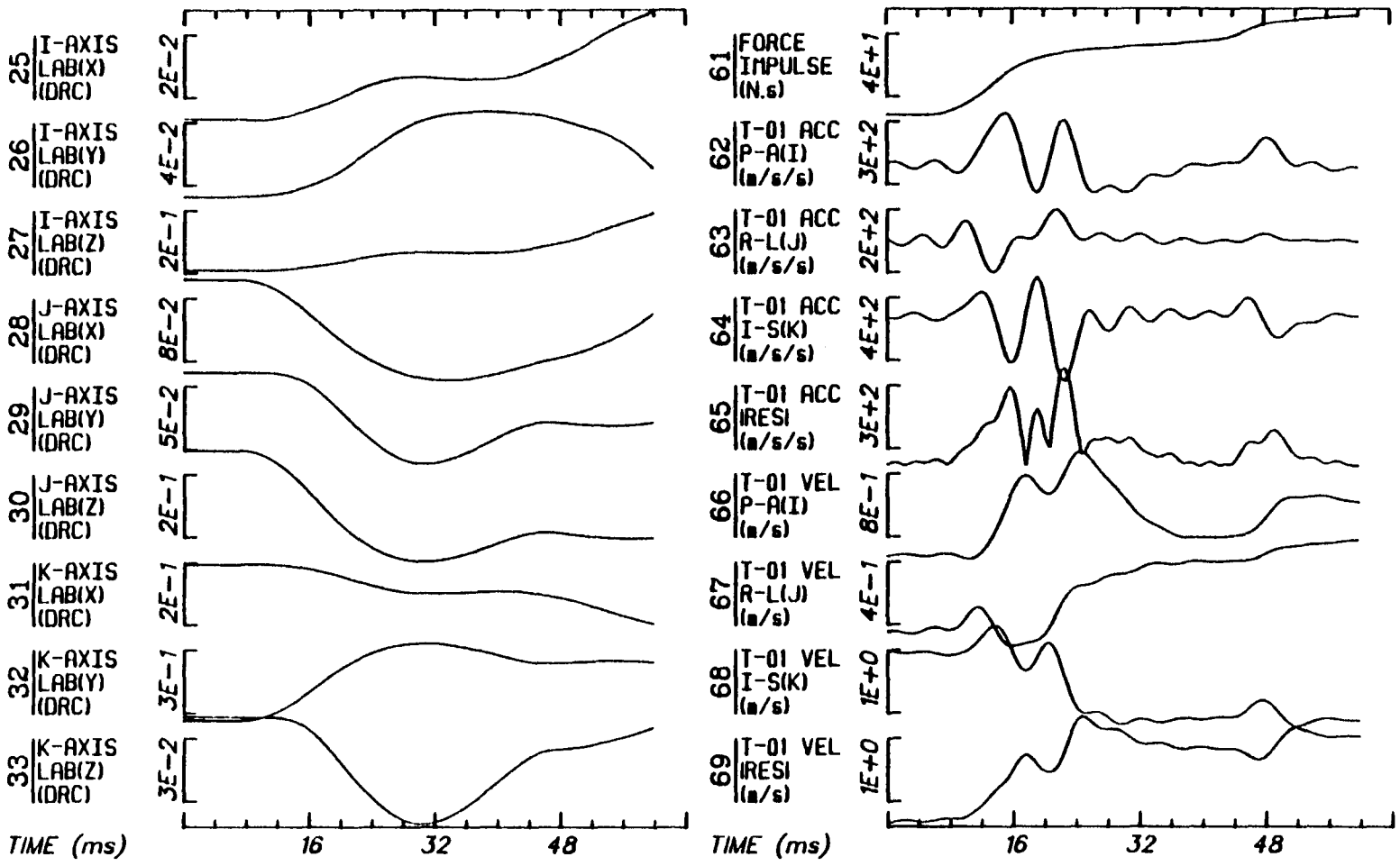

Run ID: 81H405 Tape: 3DSIMP.0 File: 2 Date: MAY 15, 1981 Sheet: 2/5

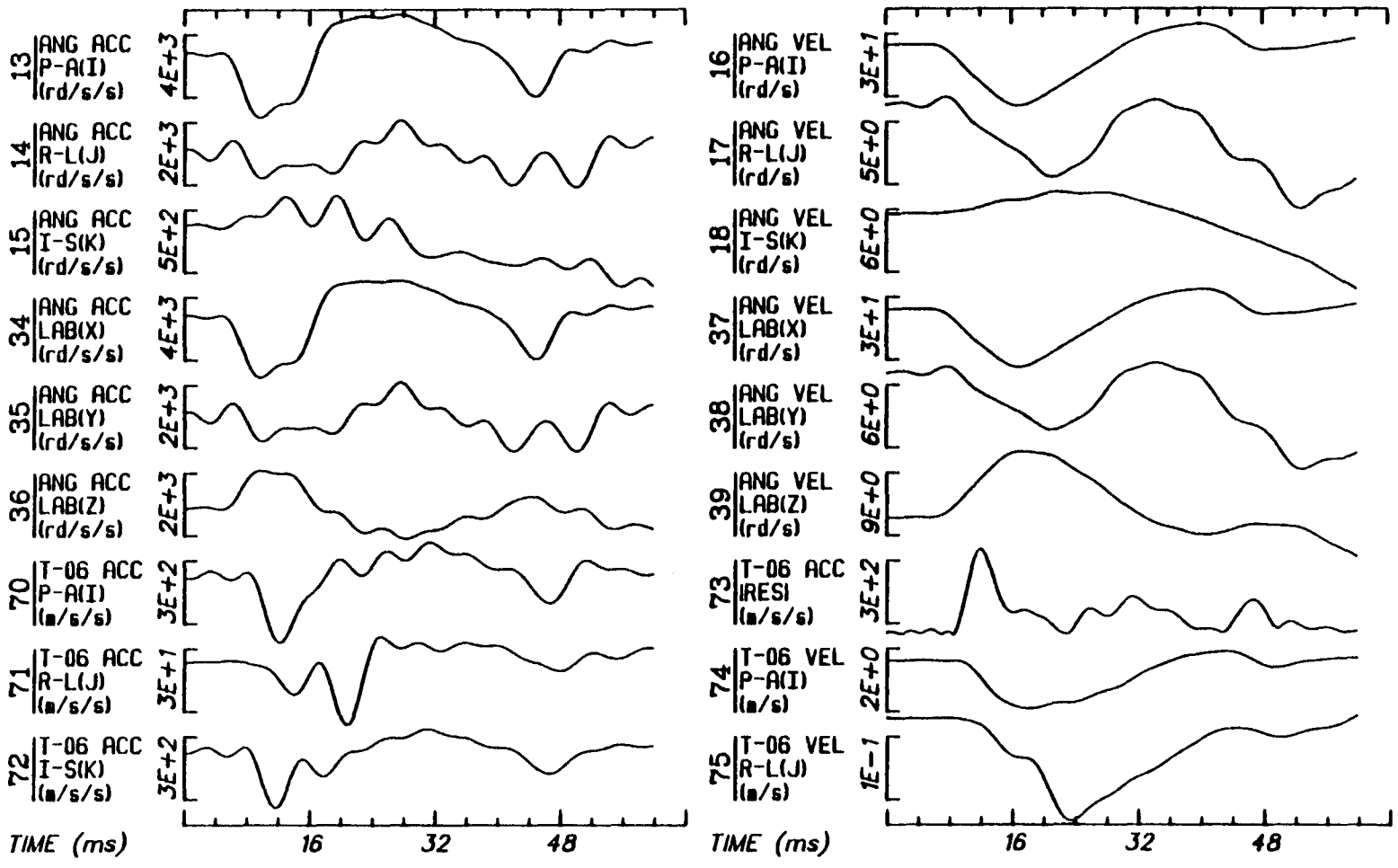

Run ID: 81H405 Tape: 3DSIMP.O File: 2 Date: MAY 15, 1981 Sheet: 3/5

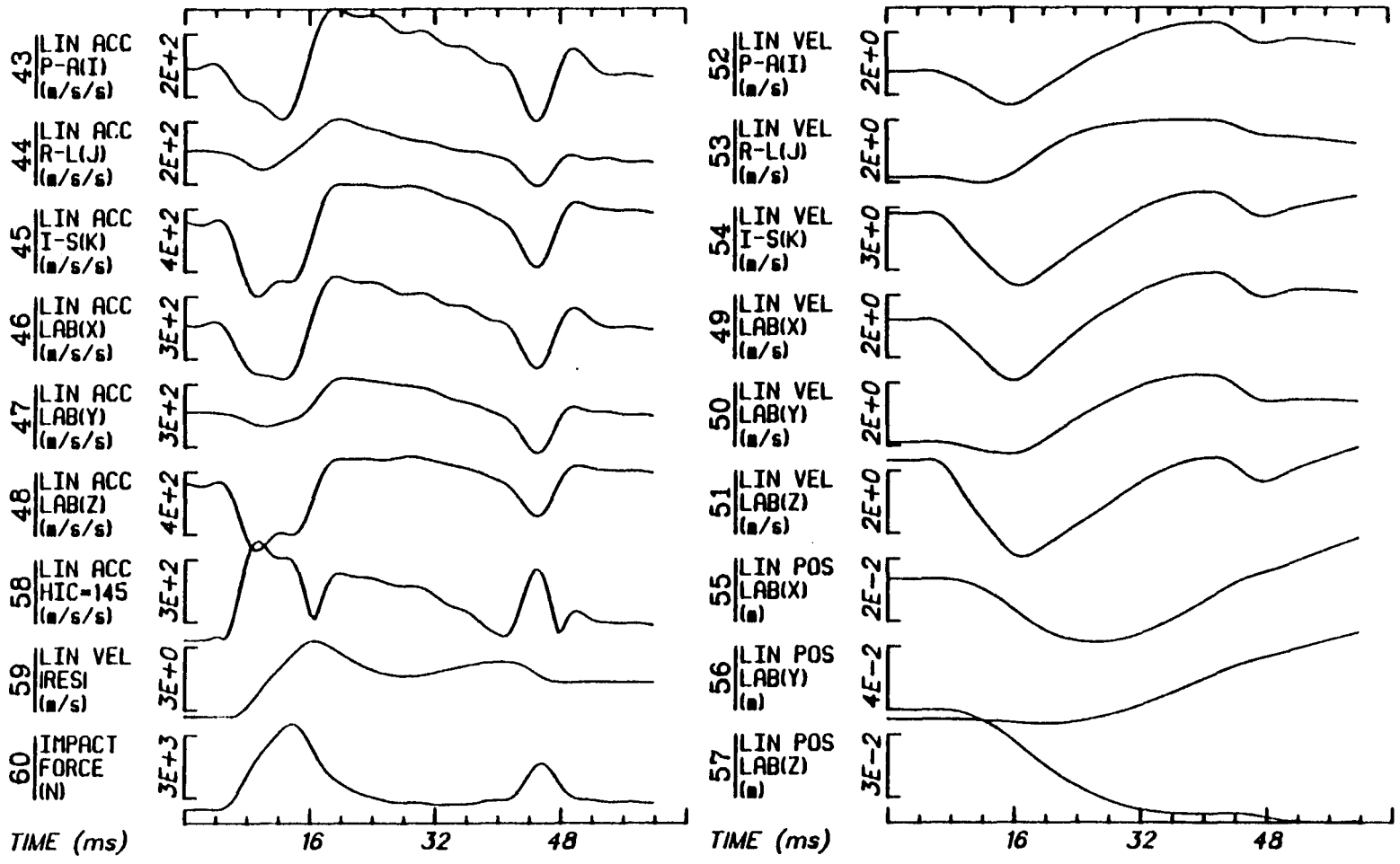

Run ID: 81H405 Tape: 3DSIMP.O File: 2 Date: MAY 15, 1981 Sheet: 4/5

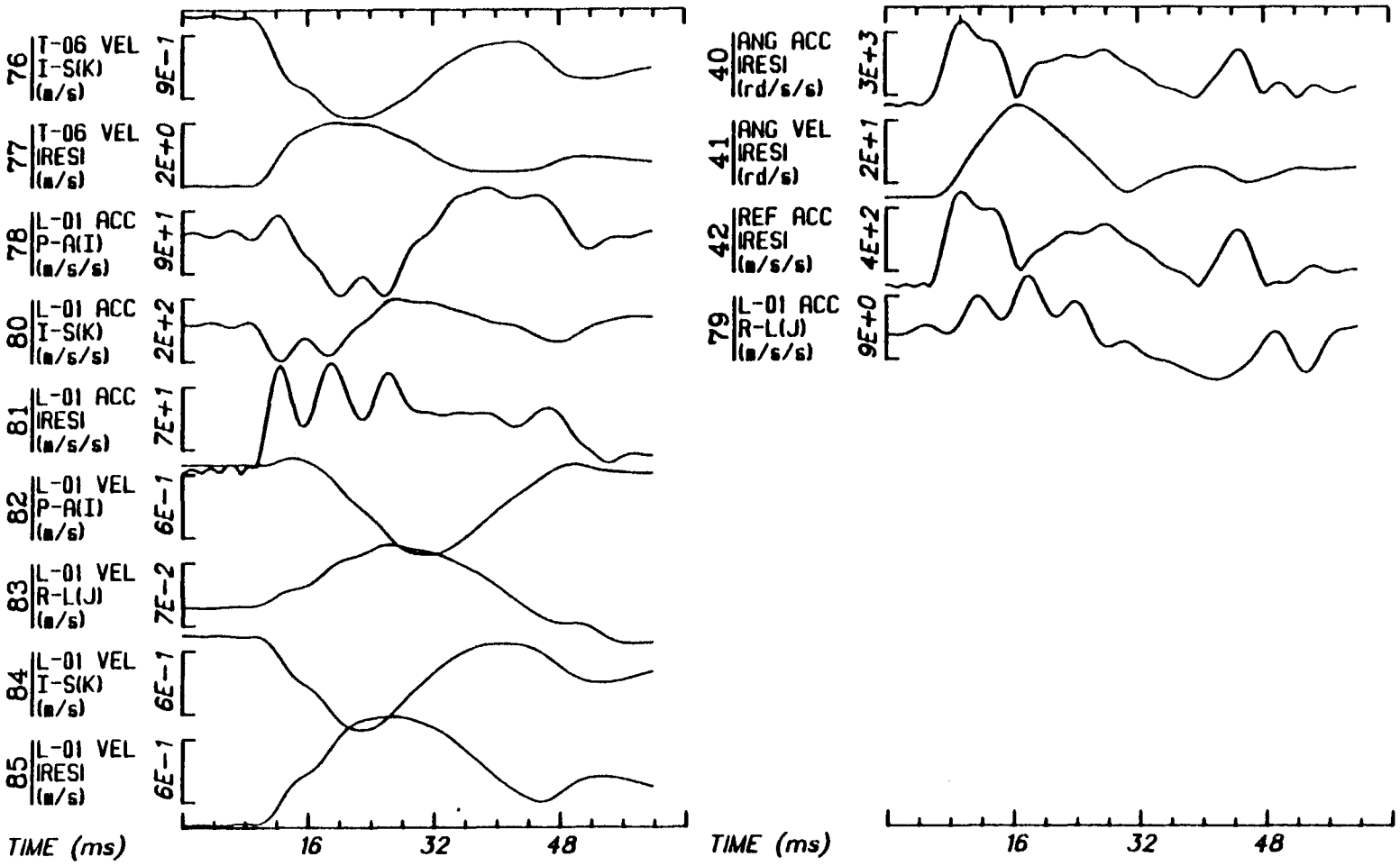

Run ID: 81H405 Tape: 3DSIMP.0 File: 2 Date: MAY 15, 1981 Sheet: 5/5

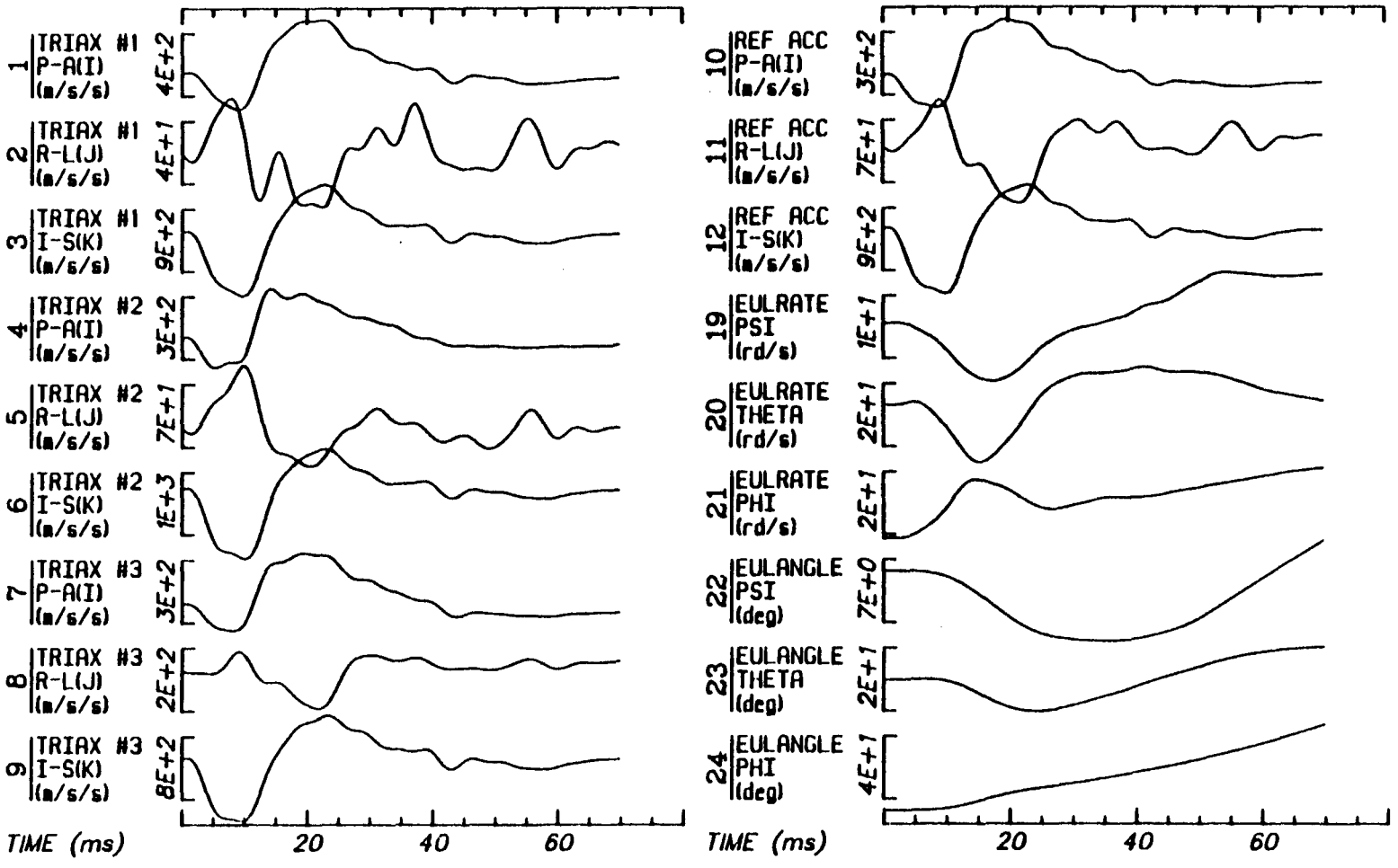

Run ID: 81H406 Tape: 3DSIMP.. File: 1 Date: JUN 4, 1981 Sheet: 1/5

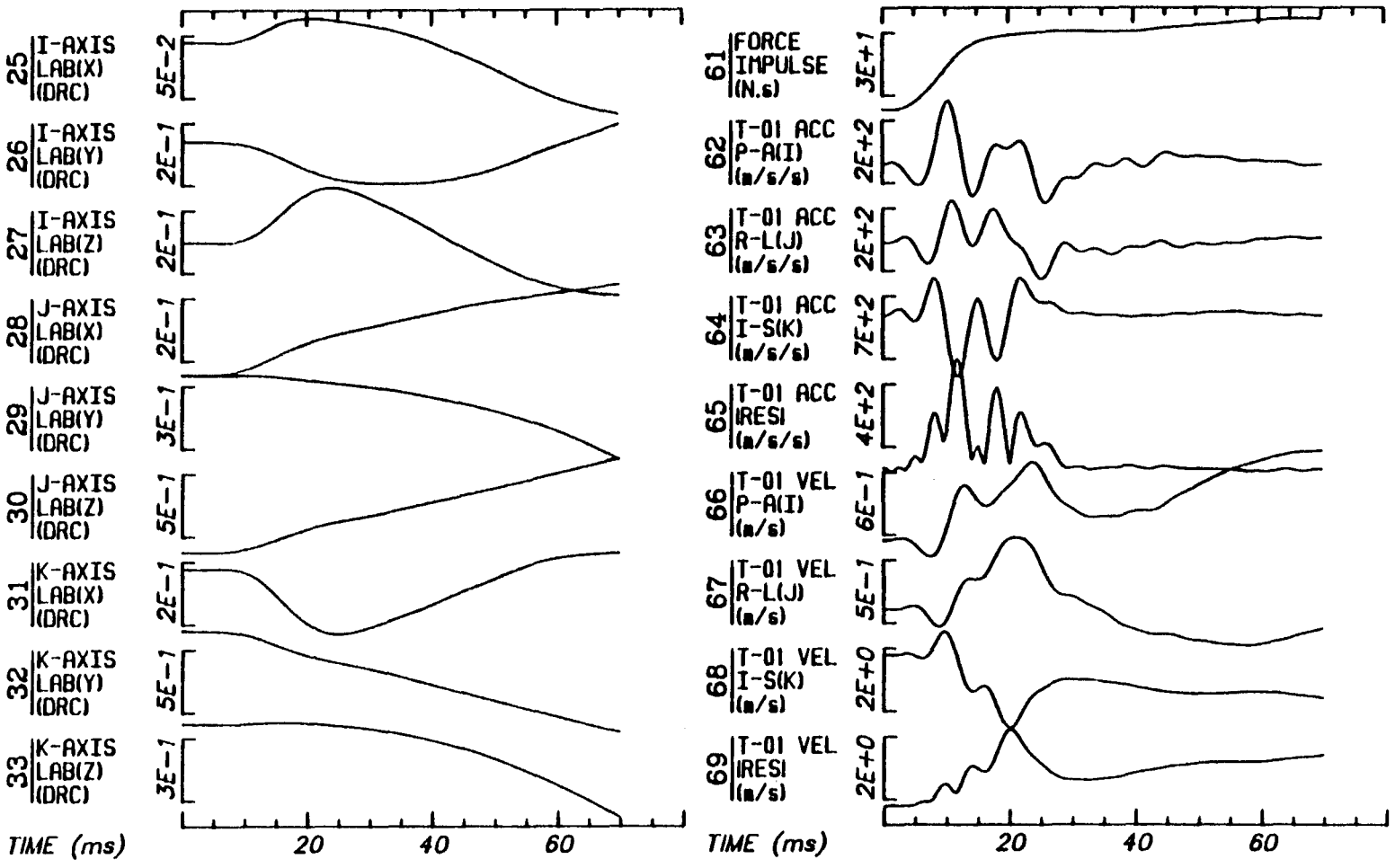

Run ID: 81H406 Tape: 3DSIMP.. File: 1 Date: JUN 4, 1981 Sheet: 2/5

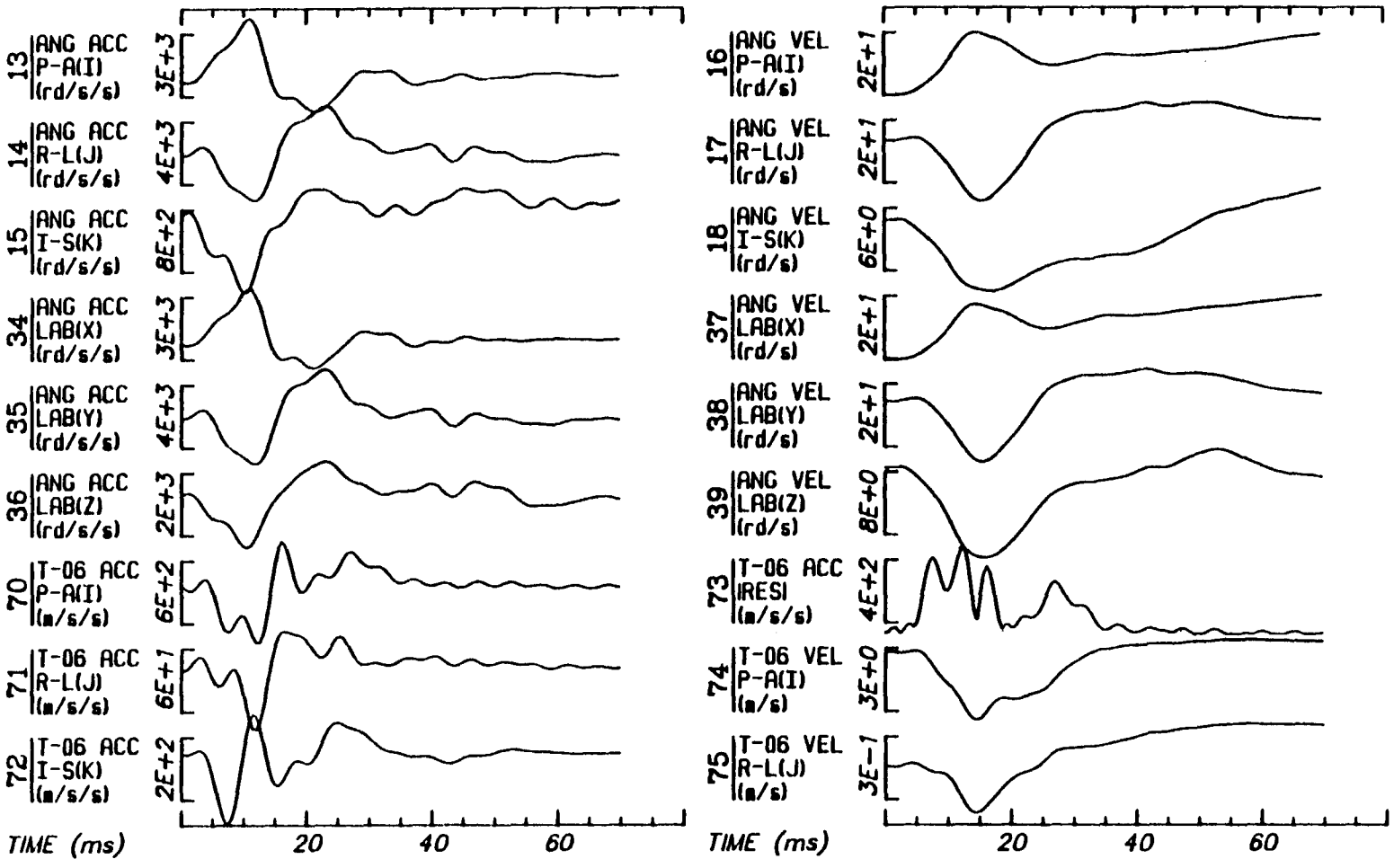

Run ID: 81H406 Tape: 3DSIMP.. File: 1 Date: JUN 4, 1981 Sheet: 3/5

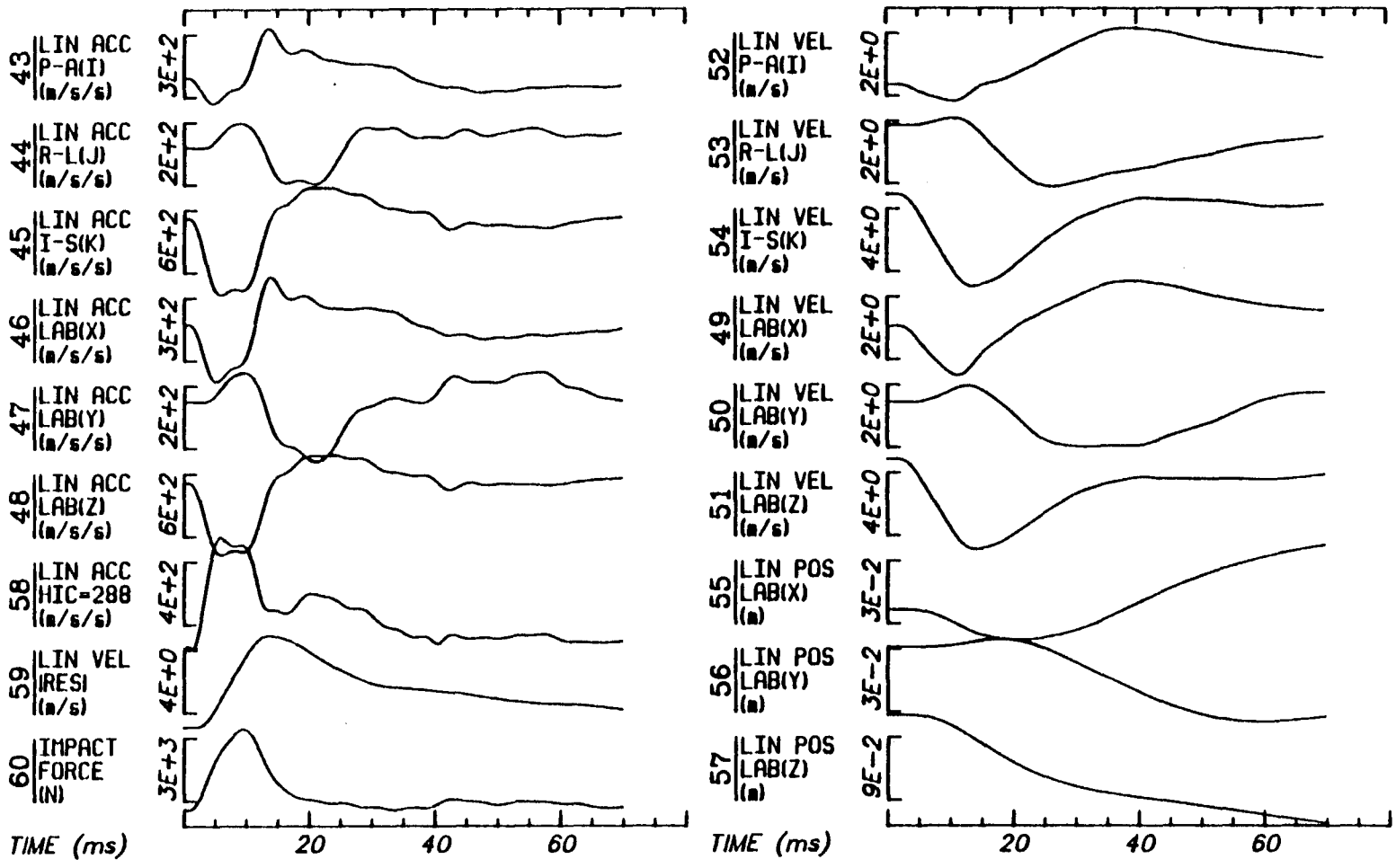

Run ID: 81H406 Tape: 3DSIMP.. File: 1 Date: JUN 4, 1981 Sheet: 4/5

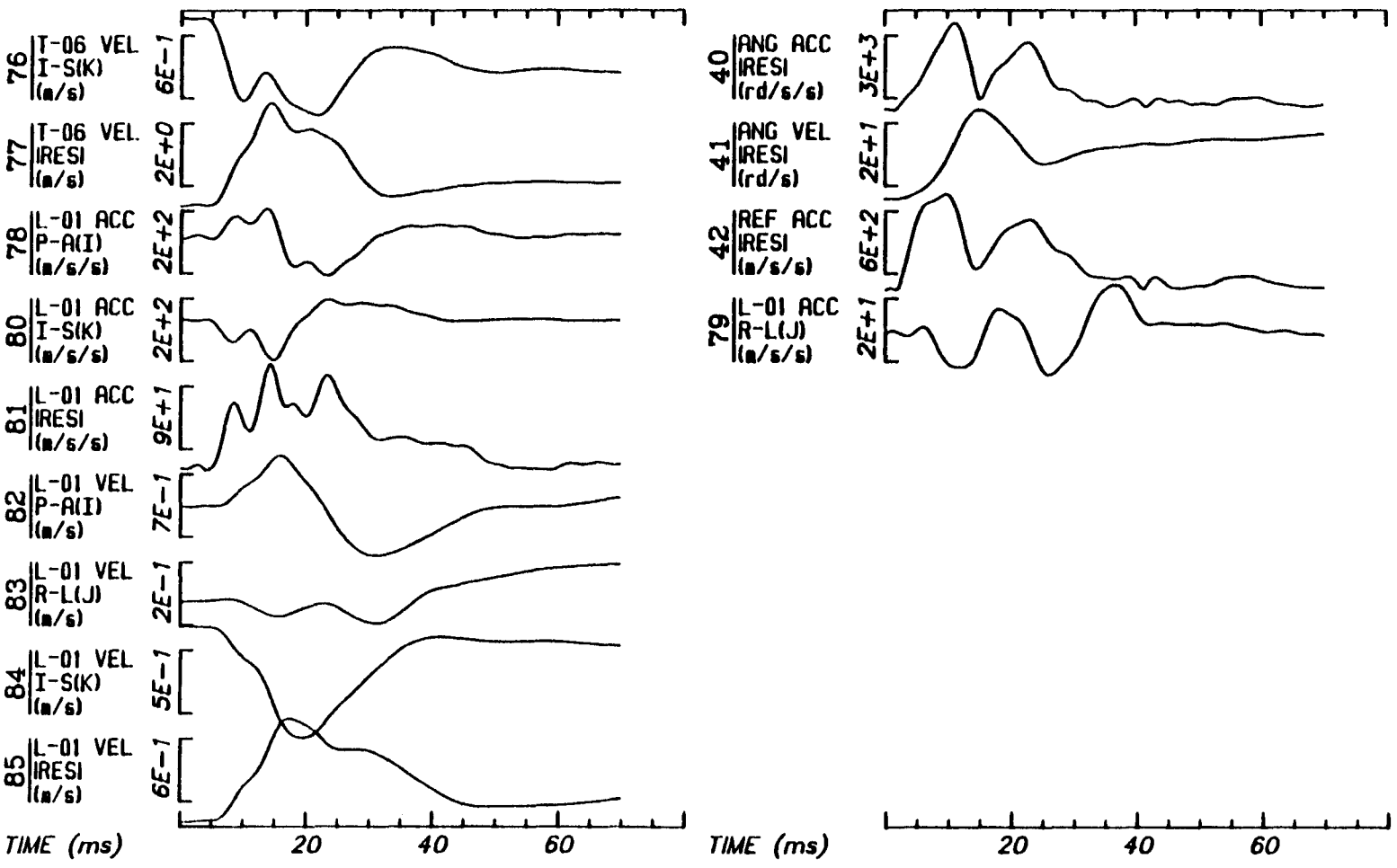

Run ID: 81H406 Tape: 3DSIMP.. File: 1 Date: JUN 4, 1981 Sheet: 5/5

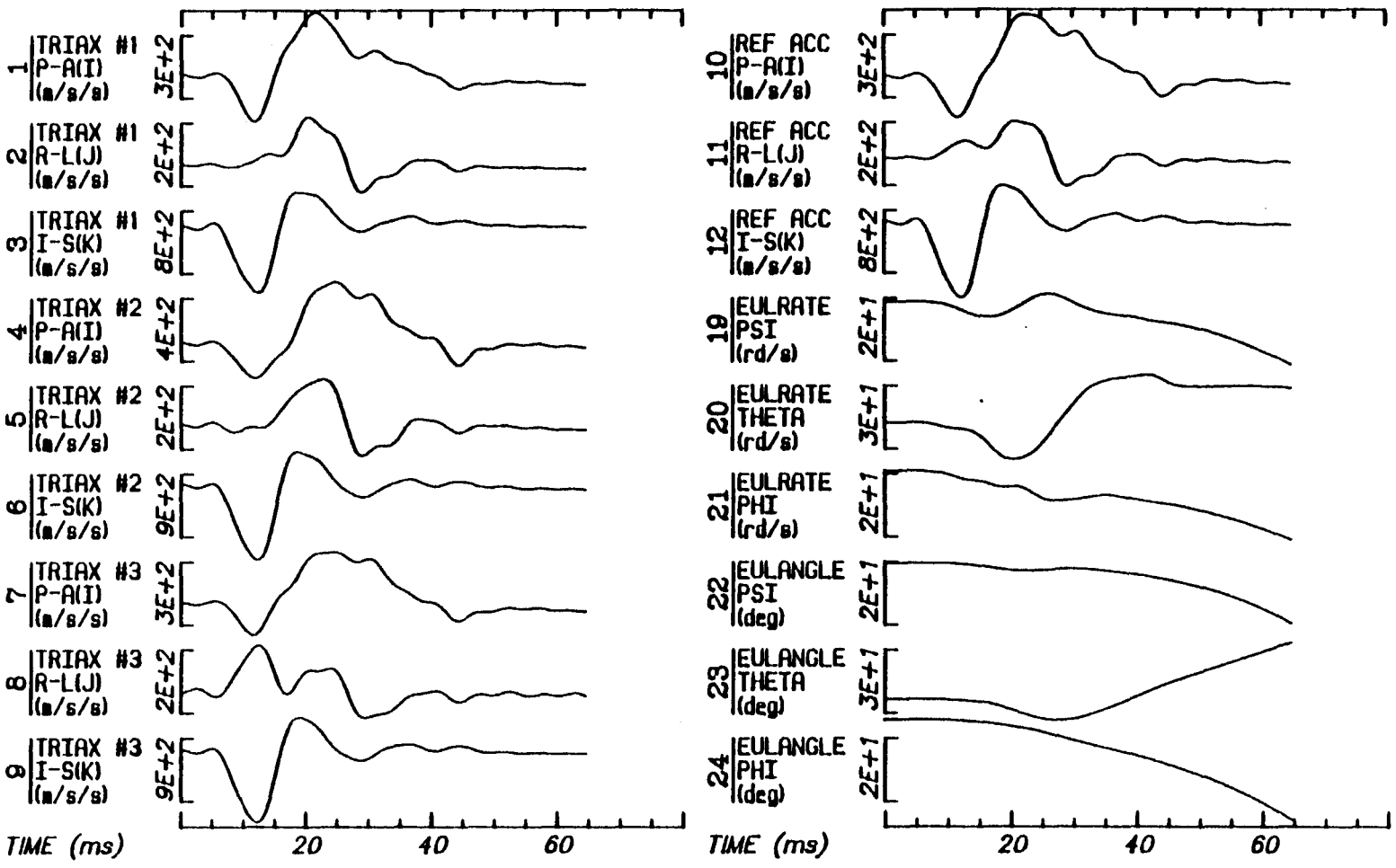

Run ID: 81H407 Tape: 3DSIMP.0 File: 1 Date: JUL 7, 1981 Sheet: 1/5

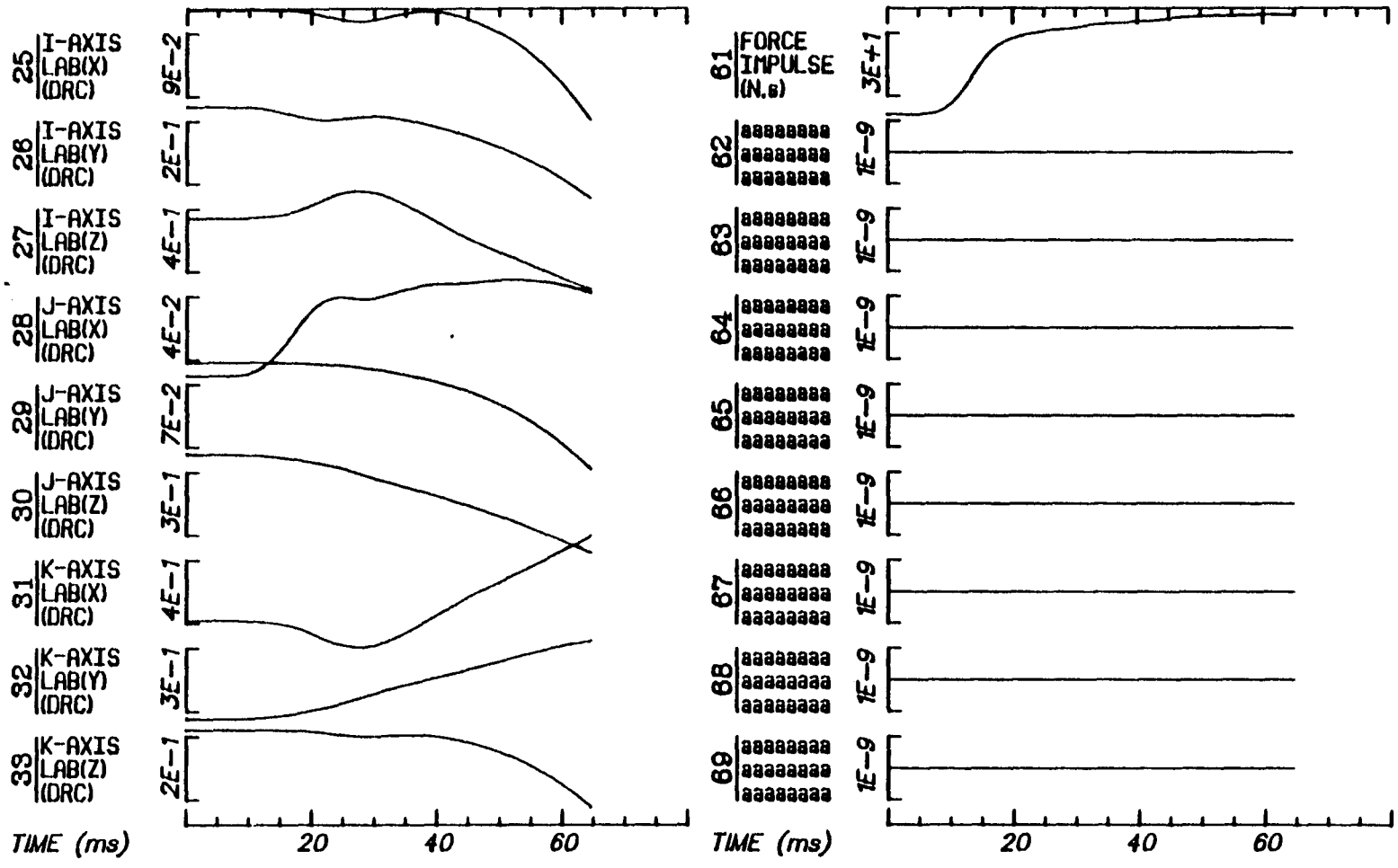

Run ID: 81H407 Tape: 3DSIMP.O File: 1 Date: JUL 7, 1981 Sheet: 2/5

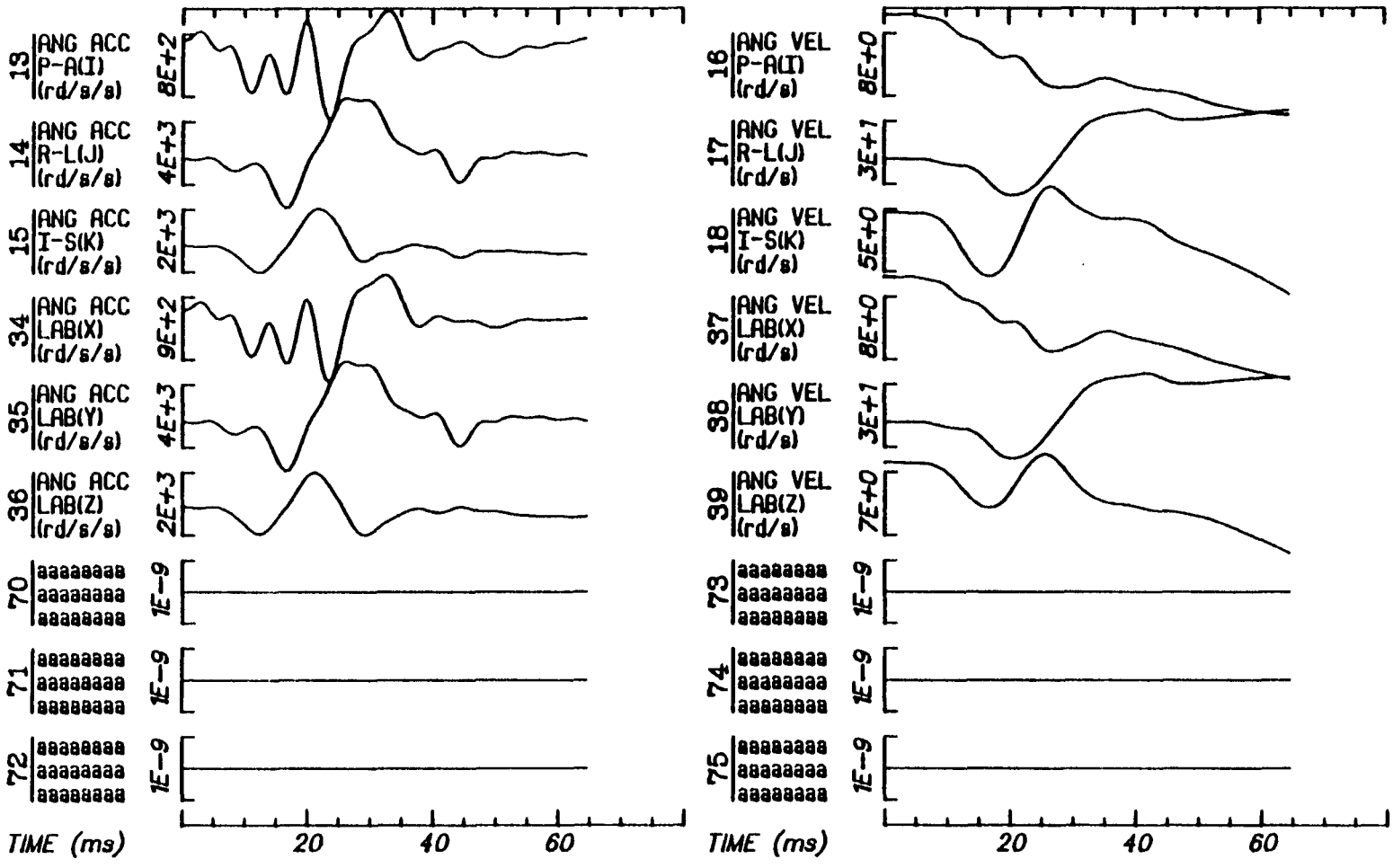

Run ID: 81H407 Tape: 3DSIMP.O File: 1 Date: JUL 7, 1981 Sheet: 3/5

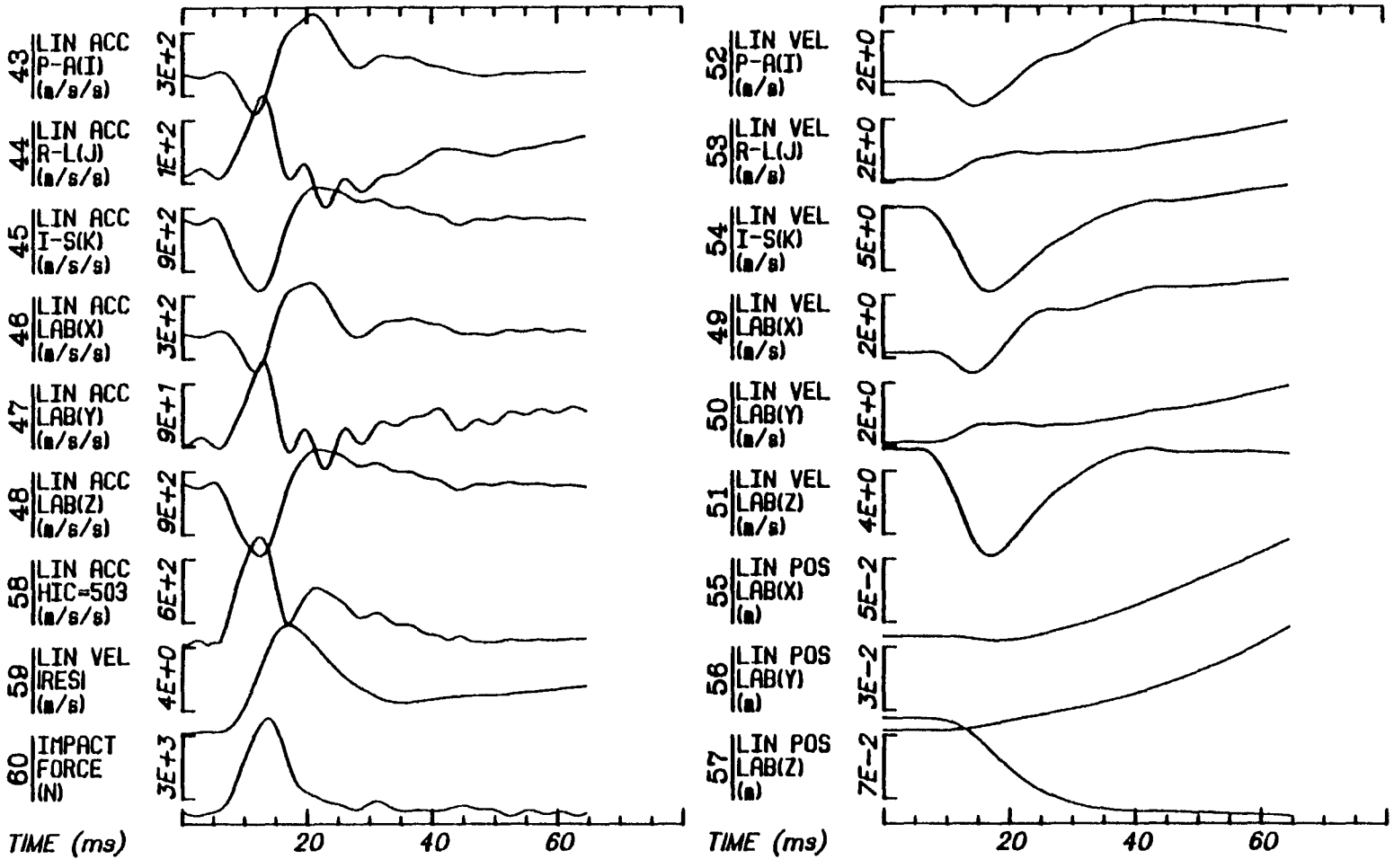

Run ID: 81H407 Tape: 3DSIMP.O File: 1 Date: JUL 7, 1981 Sheet: 4/5

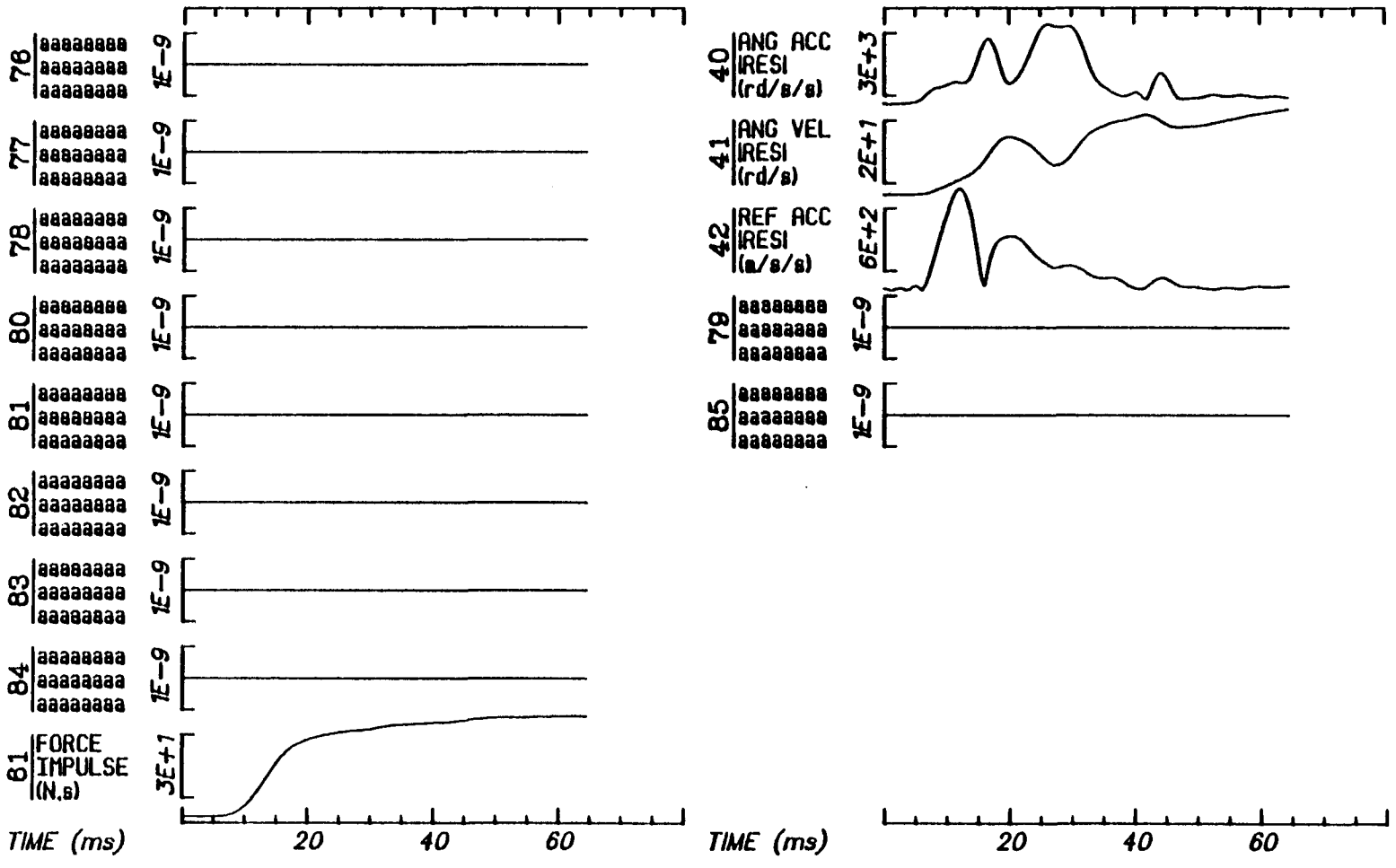

Run ID: 81H407 Tape: 3DSIMP.0 File: 1 Date: JUL 7, 1981 Sheet: 5/5

Tape: 3DSIMP File: 1 Run ID: 81H407

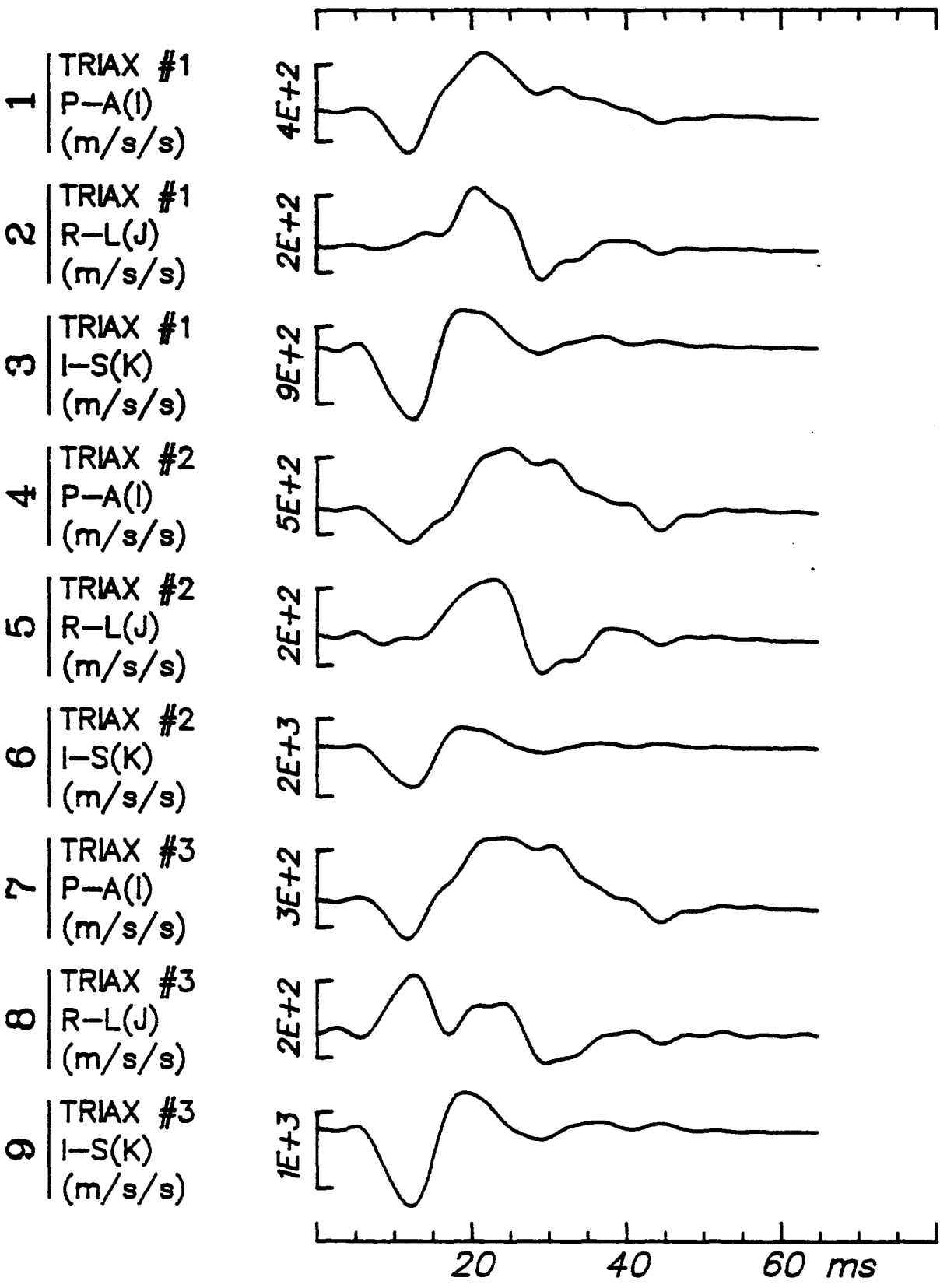

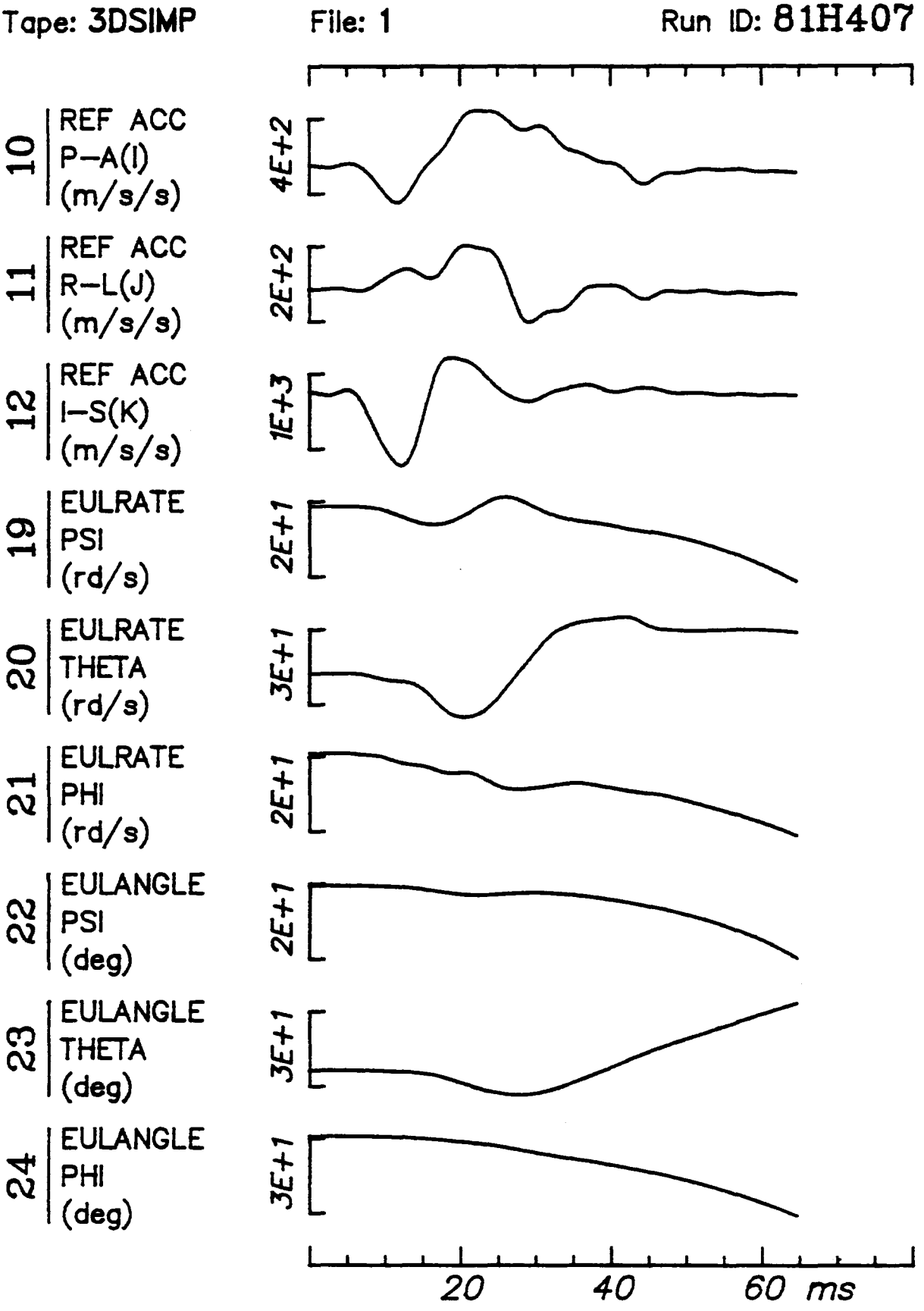
Tape: 3DSIMP
File: 1
Run ID: 81H407
10
REF ACC
P–A(I)
(m/s/s)
4E+2
11
REF ACC
R–L(J)
(m/s/s)
2E+2
12
REF ACC
I–S(K)
(m/s/s)
1E+3
19
EULRATE
PSI
(rd/s)
2E+1
20
EULRATE
THETA
(rd/s)
3E+1
21
EULRATE
PHI
(rd/s)
2E+1
22
EULANGLE
PSI
(deg)
2E+1
23
EULANGLE
THETA
(deg)
3E+1
24
EULANGLE
PHI
(deg)
3E+1
20
40
60 ms

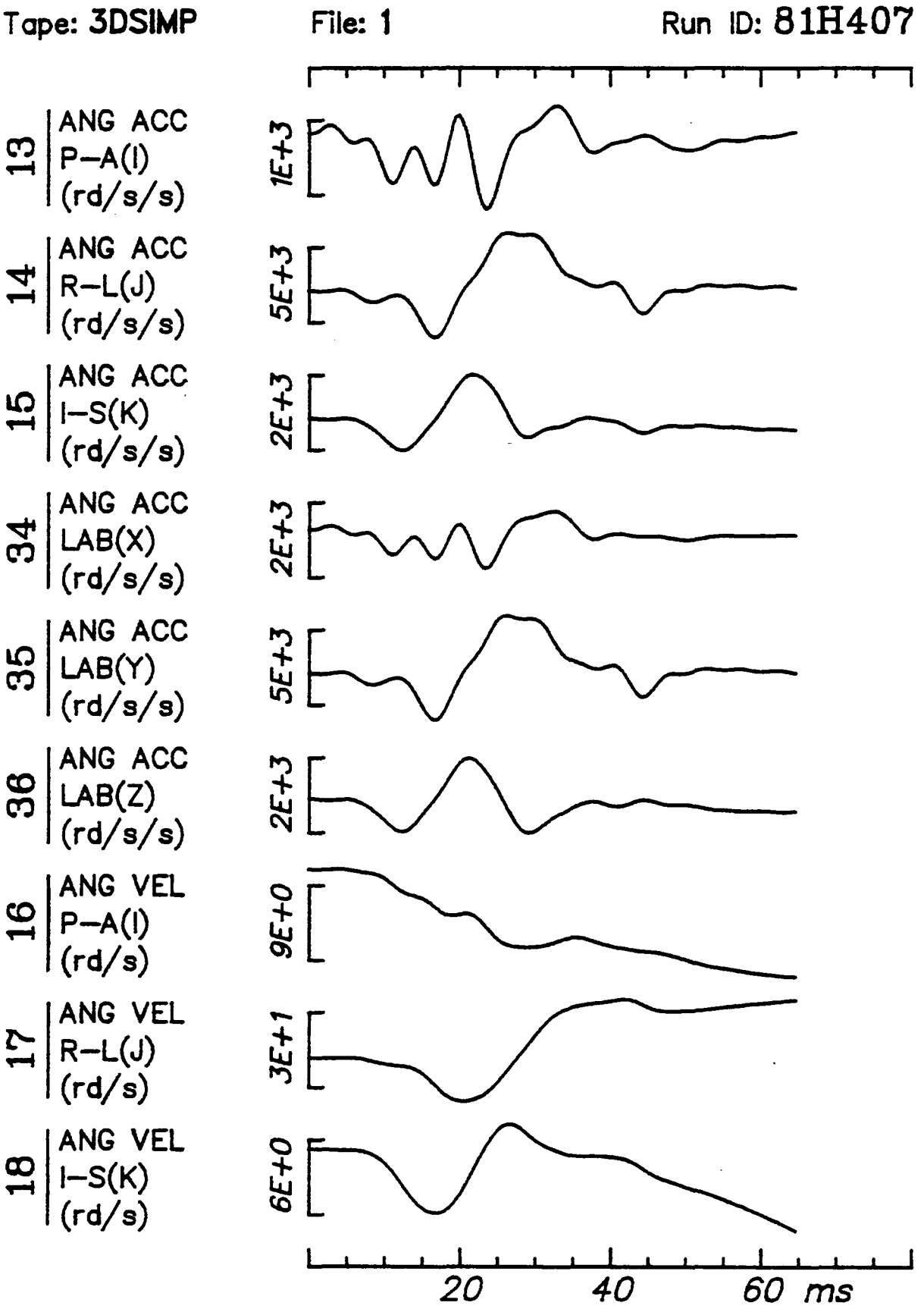
Tape: 3DSIMP
File: 1
Run ID: 81H407
13
ANG ACC
P–A(I)
(rd/s/s)
1E+3
14
ANG ACC
R–L(J)
(rd/s/s)
5E+3
15
ANG ACC
I–S(K)
(rd/s/s)
2E+3
34
ANG ACC
LAB(X)
(rd/s/s)
2E+3
35
ANG ACC
LAB(Y)
(rd/s/s)
5E+3
36
ANG ACC
LAB(Z)
(rd/s/s)
2E+3
16
ANG VEL
P–A(I)
(rd/s)
9E+0
17
ANG VEL
R–L(J)
(rd/s)
3E+1
18
ANG VEL
I–S(K)
(rd/s)
6E+0
20
40
60 ms

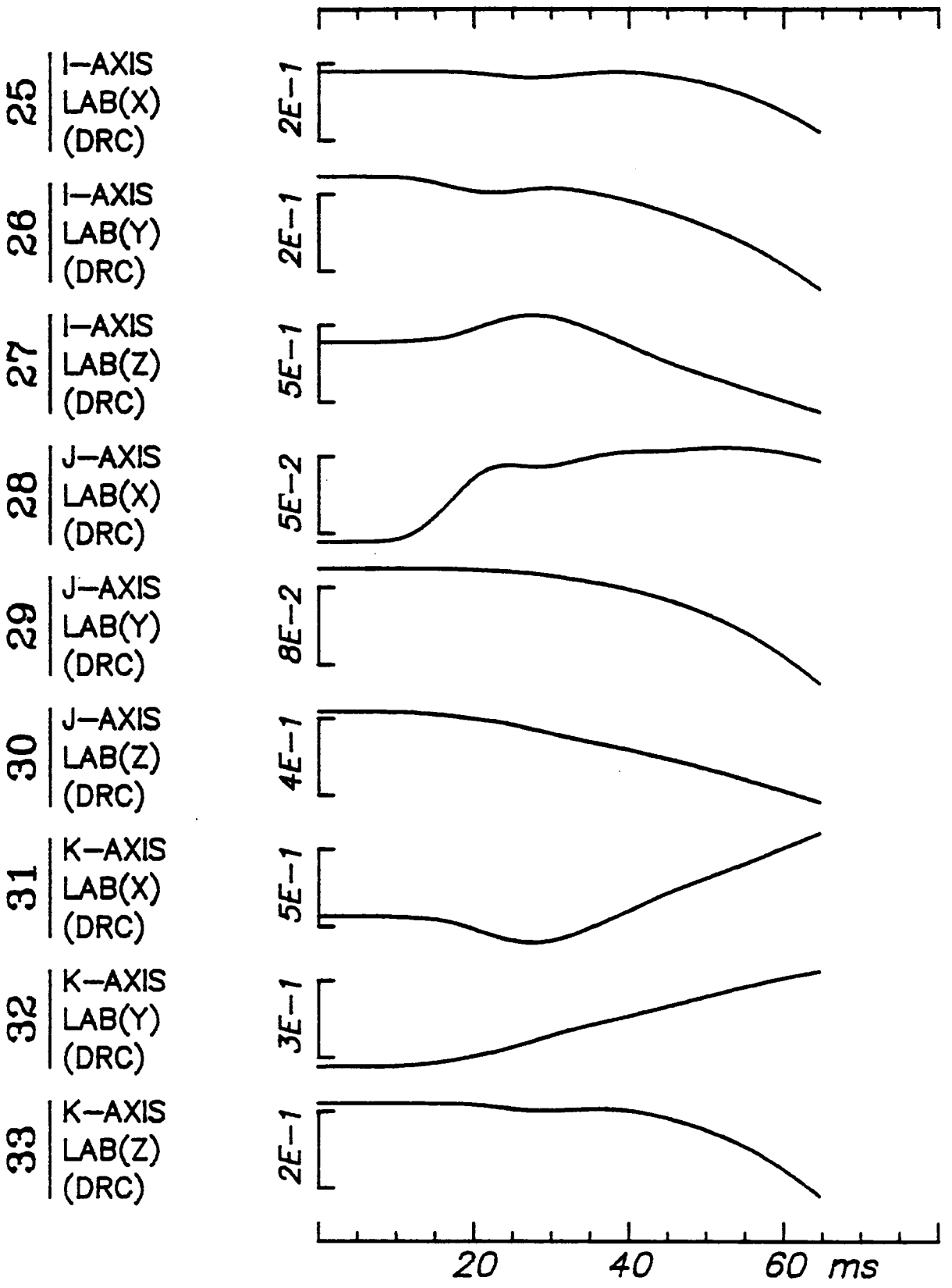
Tape: 3DSIMP
File: 1
Run ID: 81H407
25 I–AXIS LAB(X) (DRC)
26 I–AXIS LAB(Y) (DRC)
27 I–AXIS LAB(Z) (DRC)
28 J–AXIS LAB(X) (DRC)
29 J–AXIS LAB(Y) (DRC)
30 J–AXIS LAB(Z) (DRC)
31 K–AXIS LAB(X) (DRC)
32 K–AXIS LAB(Y) (DRC)
33 K–AXIS LAB(Z) (DRC)
2E-1
2E-1
5E-1
5E-2
8E-2
4E-1
5E-1
3E-1
2E-1
20
40
60 ms

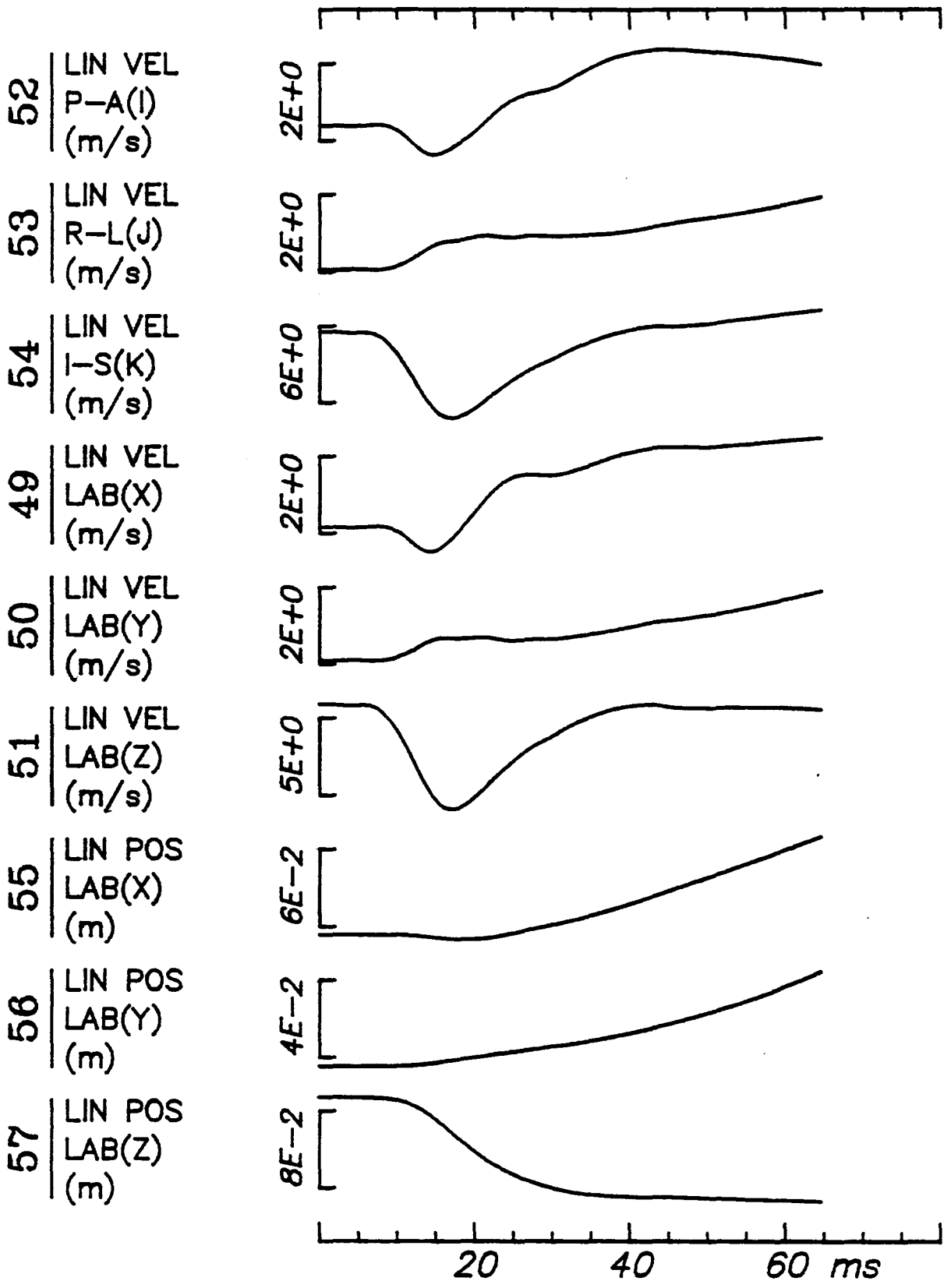
Tape: 3DSIMP
File: 1
Run ID: 81H407
52 LIN VEL P-A(I) (m/s)
2E+0
53 LIN VEL R-L(J) (m/s)
2E+0
54 LIN VEL I-S(K) (m/s)
6E+0
49 LIN VEL LAB(X) (m/s)
2E+0
50 LIN VEL LAB(Y) (m/s)
2E+0
51 LIN VEL LAB(Z) (m/s)
5E+0
55 LIN POS LAB(X) (m)
6E-2
56 LIN POS LAB(Y) (m)
4E-2
57 LIN POS LAB(Z) (m)
8E-2
20
40
60 ms

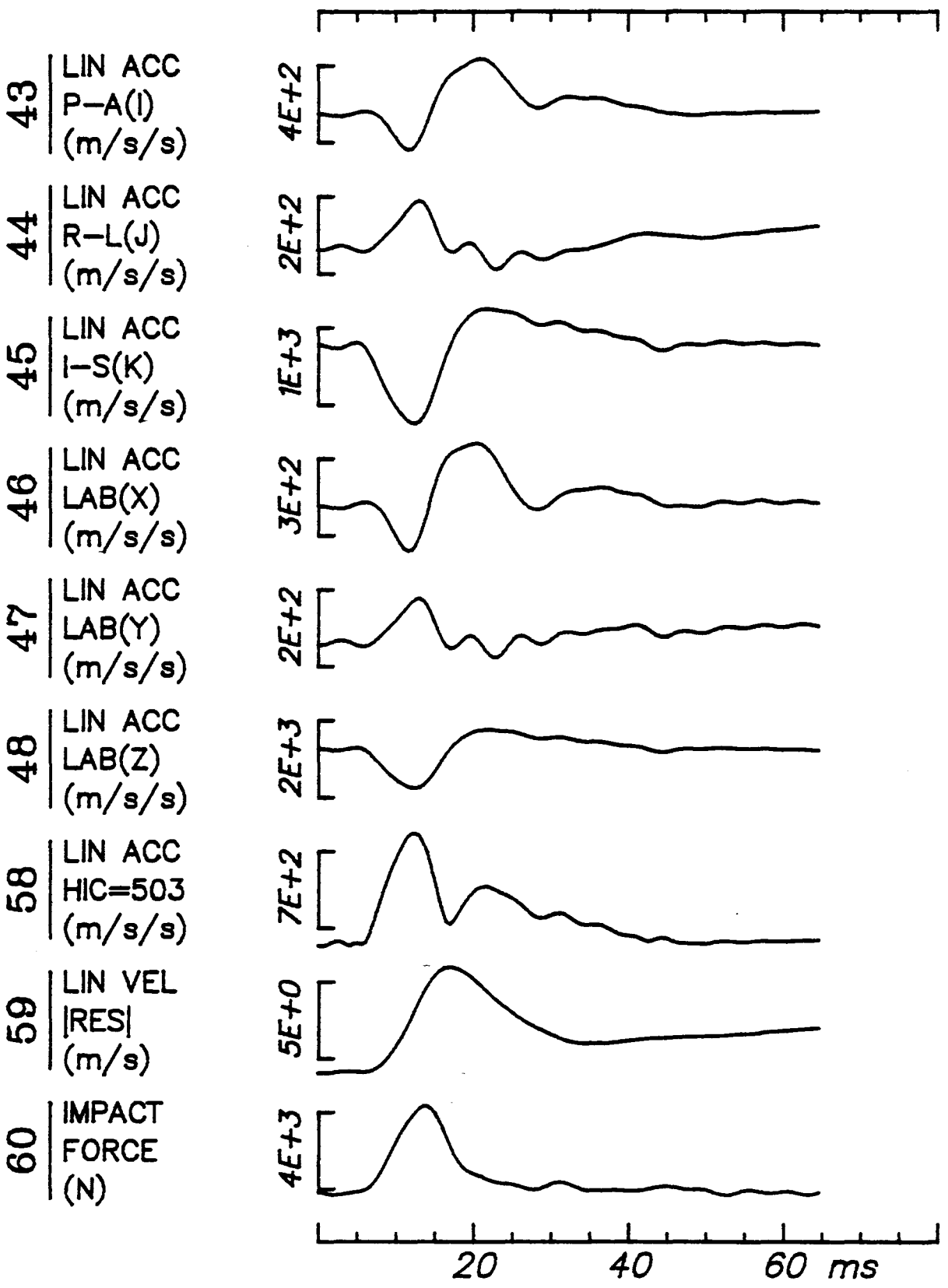
Tape: 3DSIMP
File: 1
Run ID: 81H407
43
LIN ACC
P–A(I)
(m/s/s)
4E+2
44
LIN ACC
R–L(J)
(m/s/s)
2E+2
45
LIN ACC
I–S(K)
(m/s/s)
1E+3
46
LIN ACC
LAB(X)
(m/s/s)
3E+2
47
LIN ACC
LAB(Y)
(m/s/s)
2E+2
48
LIN ACC
LAB(Z)
(m/s/s)
2E+3
58
LIN ACC
HIC=503
(m/s/s)
7E+2
59
LIN VEL
|RES|
(m/s)
5E+0
60
IMPACT
FORCE
(N)
4E+3
20
40
60 ms

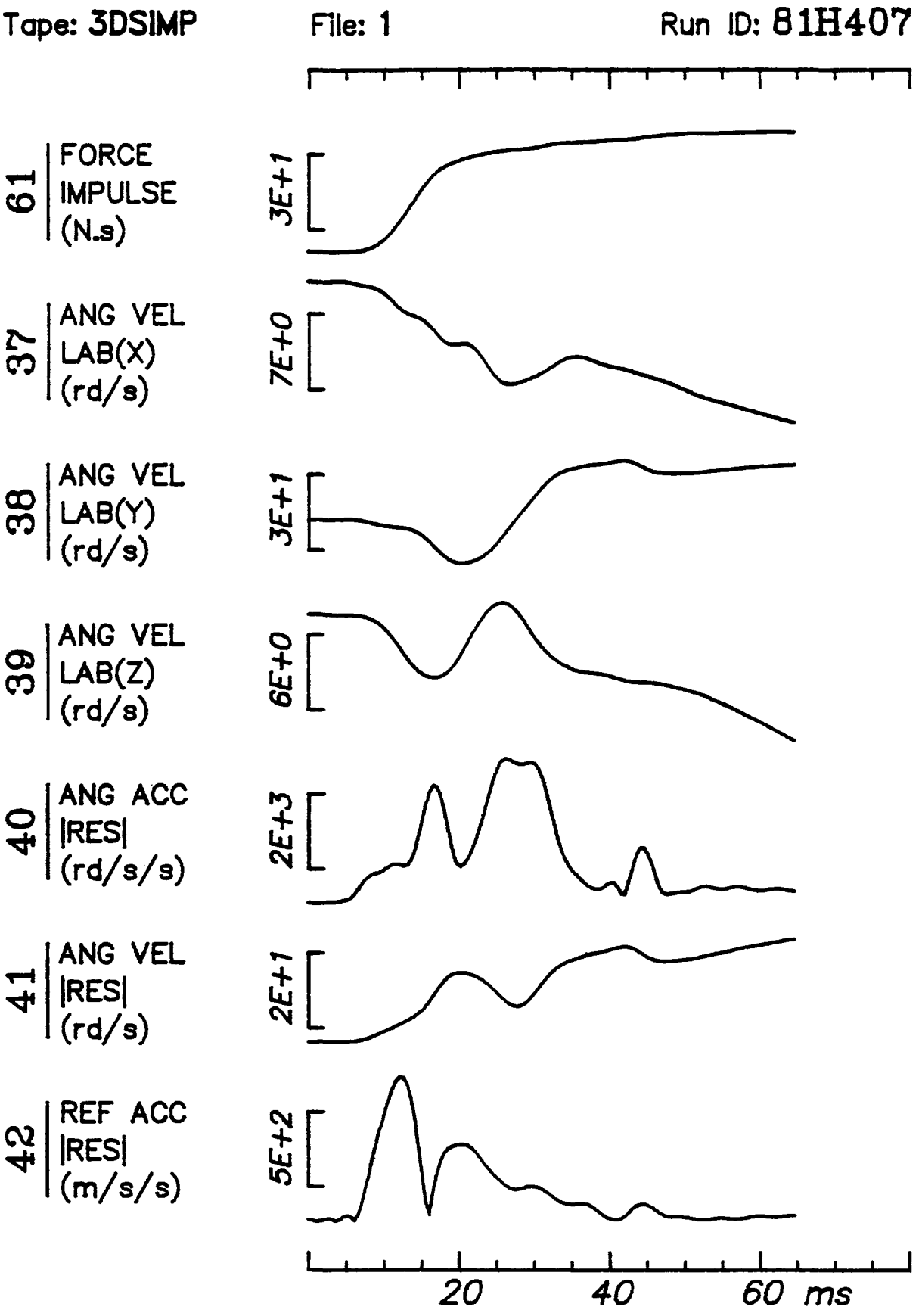
Tape: 3DSIMP
File: 1
Run ID: 81H407
61
FORCE IMPULSE (N.s)
3E+1
37
ANG VEL LAB(X) (rd/s)
7E+0
38
ANG VEL LAB(Y) (rd/s)
3E+1
39
ANG VEL LAB(Z) (rd/s)
6E+0
40
ANG ACC |RES| (rd/s/s)
2E+3
41
ANG VEL |RES| (rd/s)
2E+1
42
REF ACC |RES| (m/s/s)
5E+2
20
40
60 ms

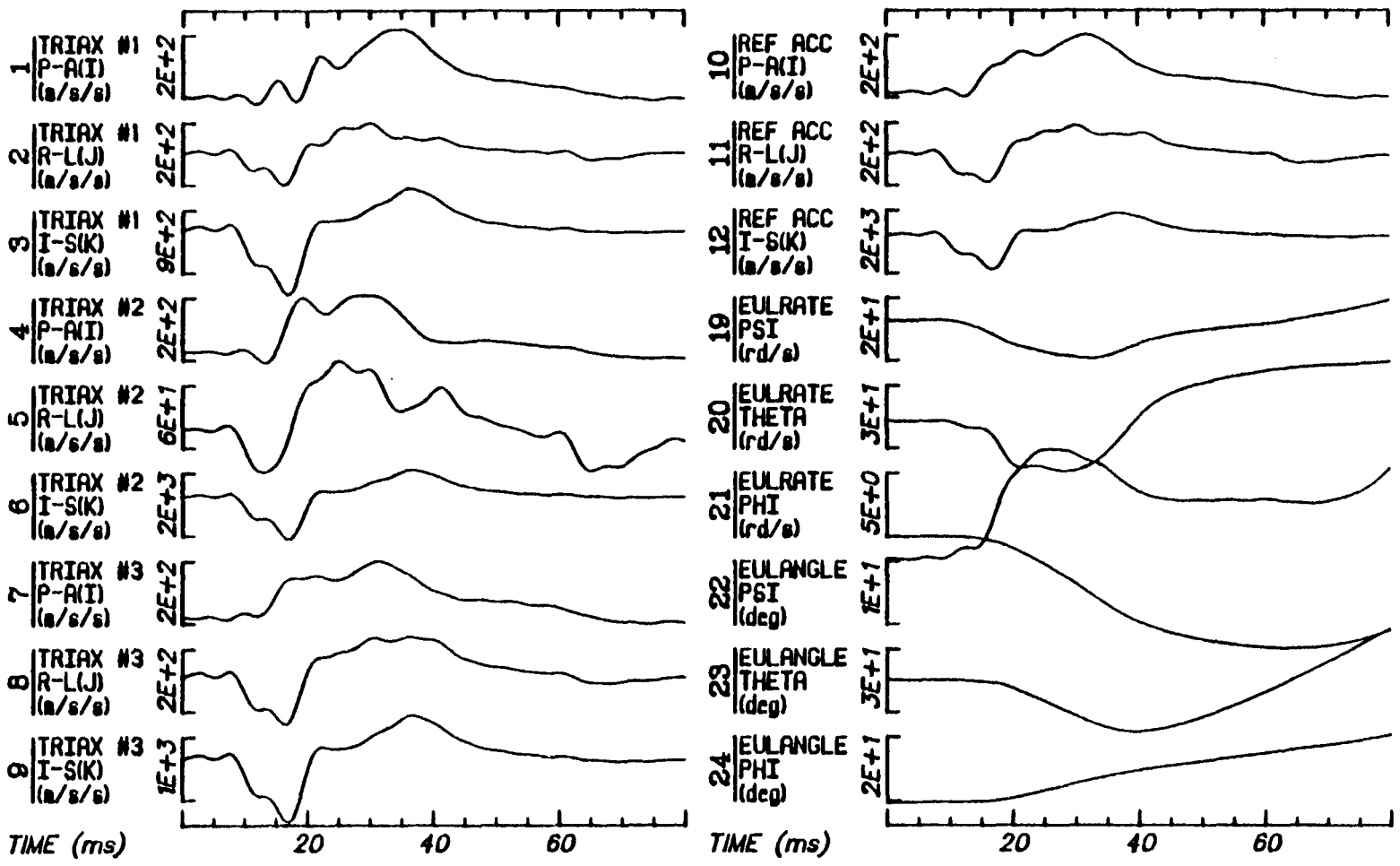

Run ID: 81H408 Tape: 3DSIMP.0 File: 3 Date: JUL 15, 1981 Sheet: 1/5

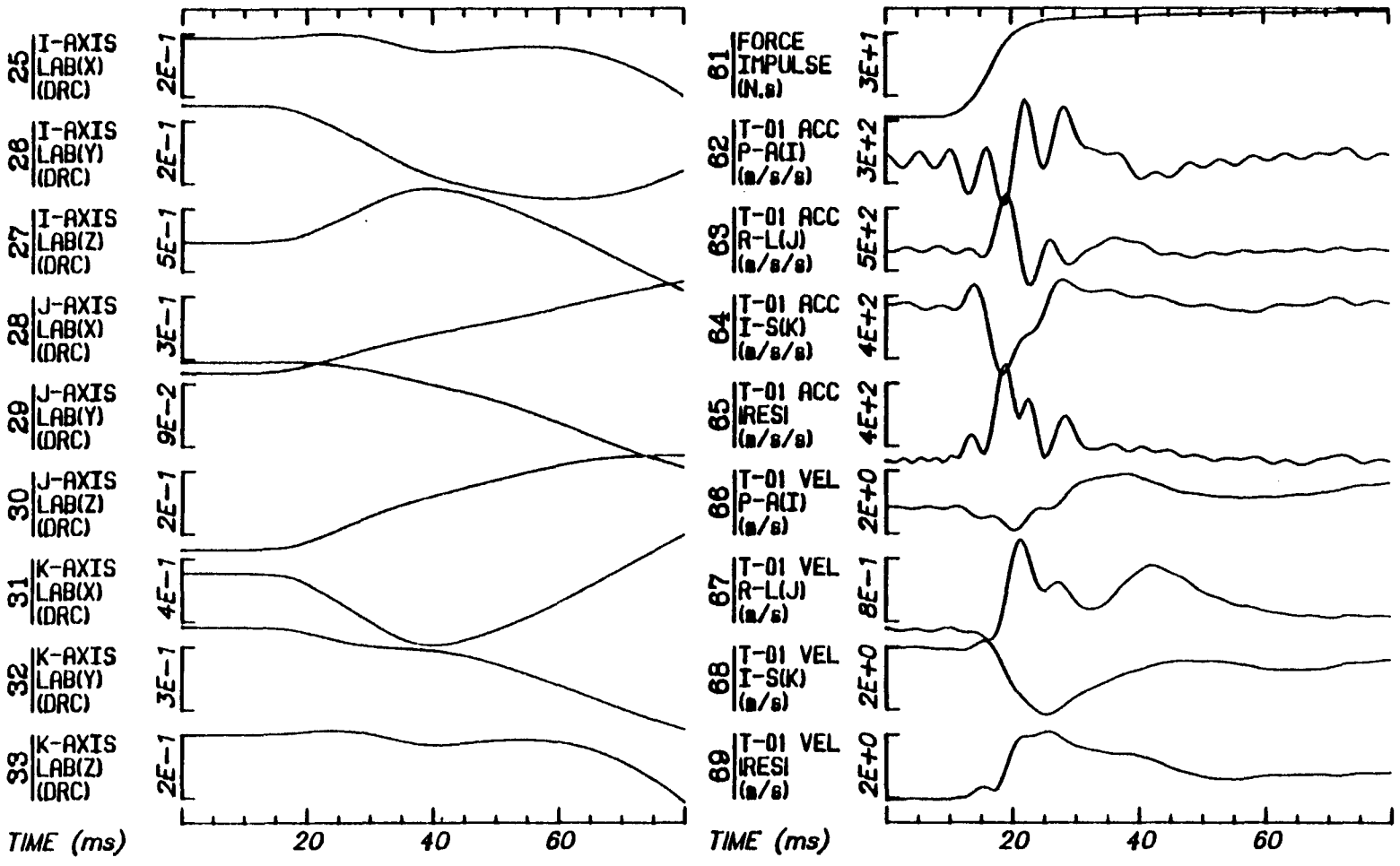

Run ID: 81H408 Tape: 3DSIMP.0 File: 3 Date: JUL 15, 1981 Sheet: 2/5

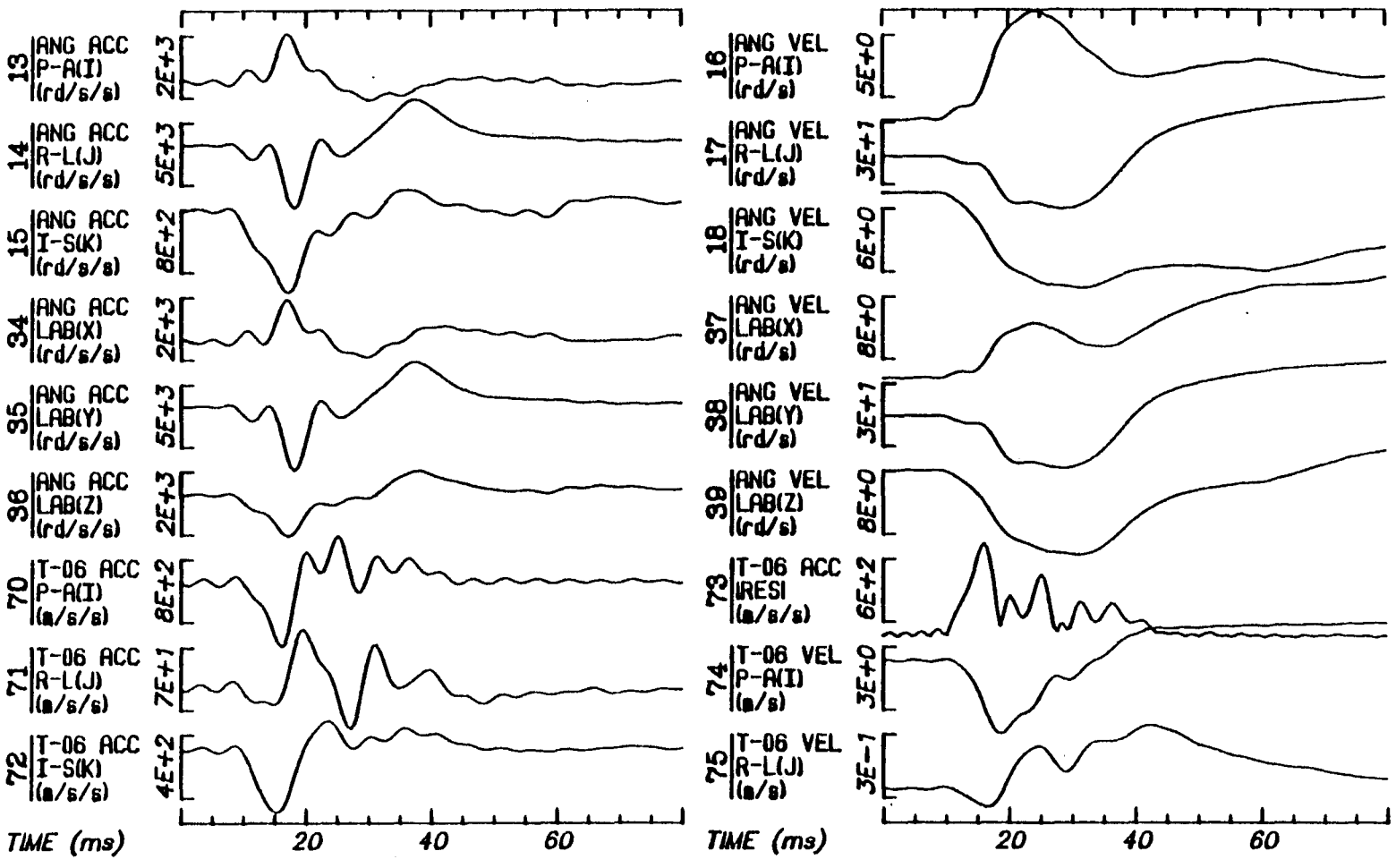

Run ID: 81H408 Tape: 3DSIMP.0 File: 3 Date: JUL 15, 1981 Sheet: 3/5

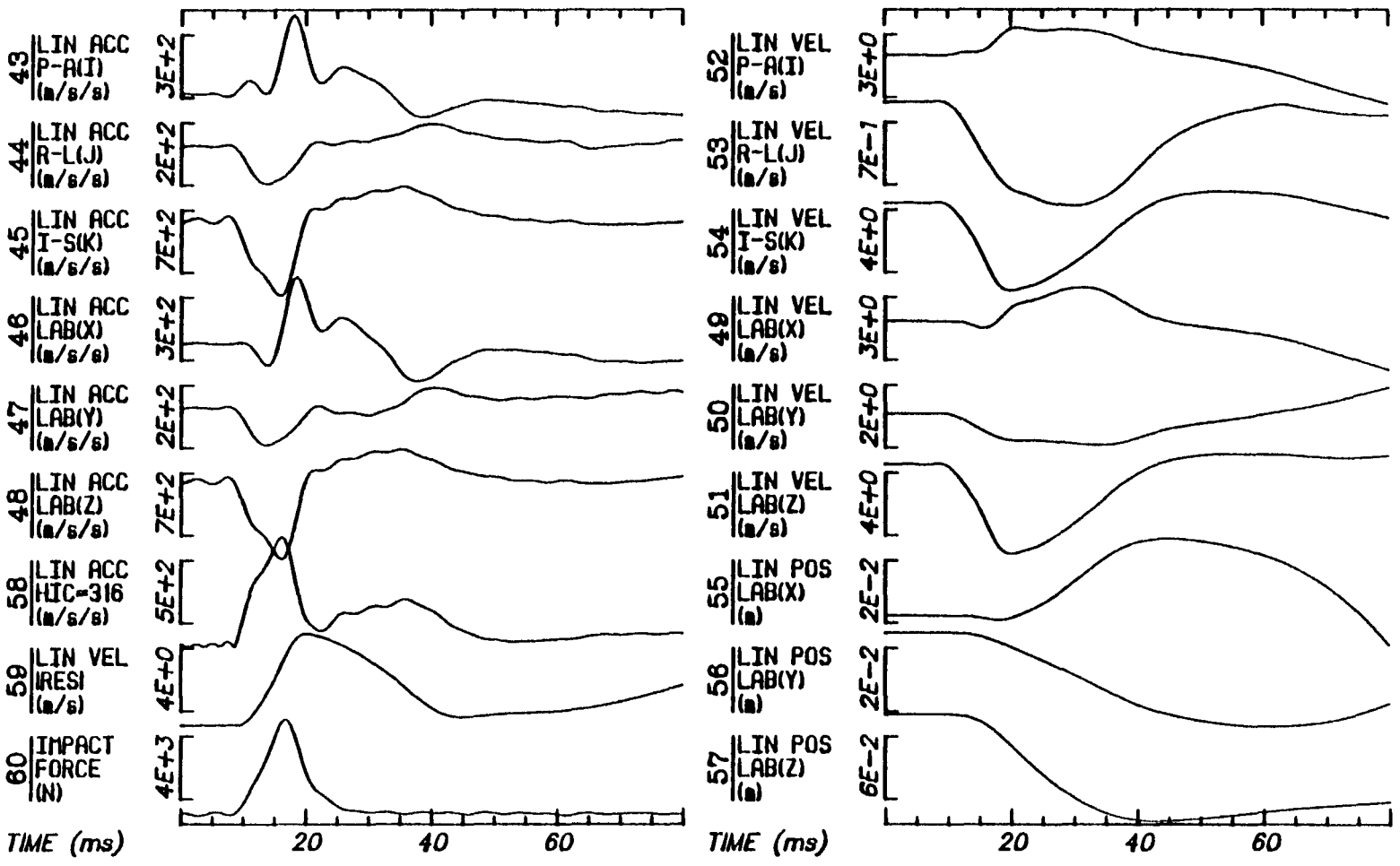

Run ID: 81H408 Tape: 3DSIMP.0 File: 3 Date: JUL 15, 1981 Sheet: 4/5

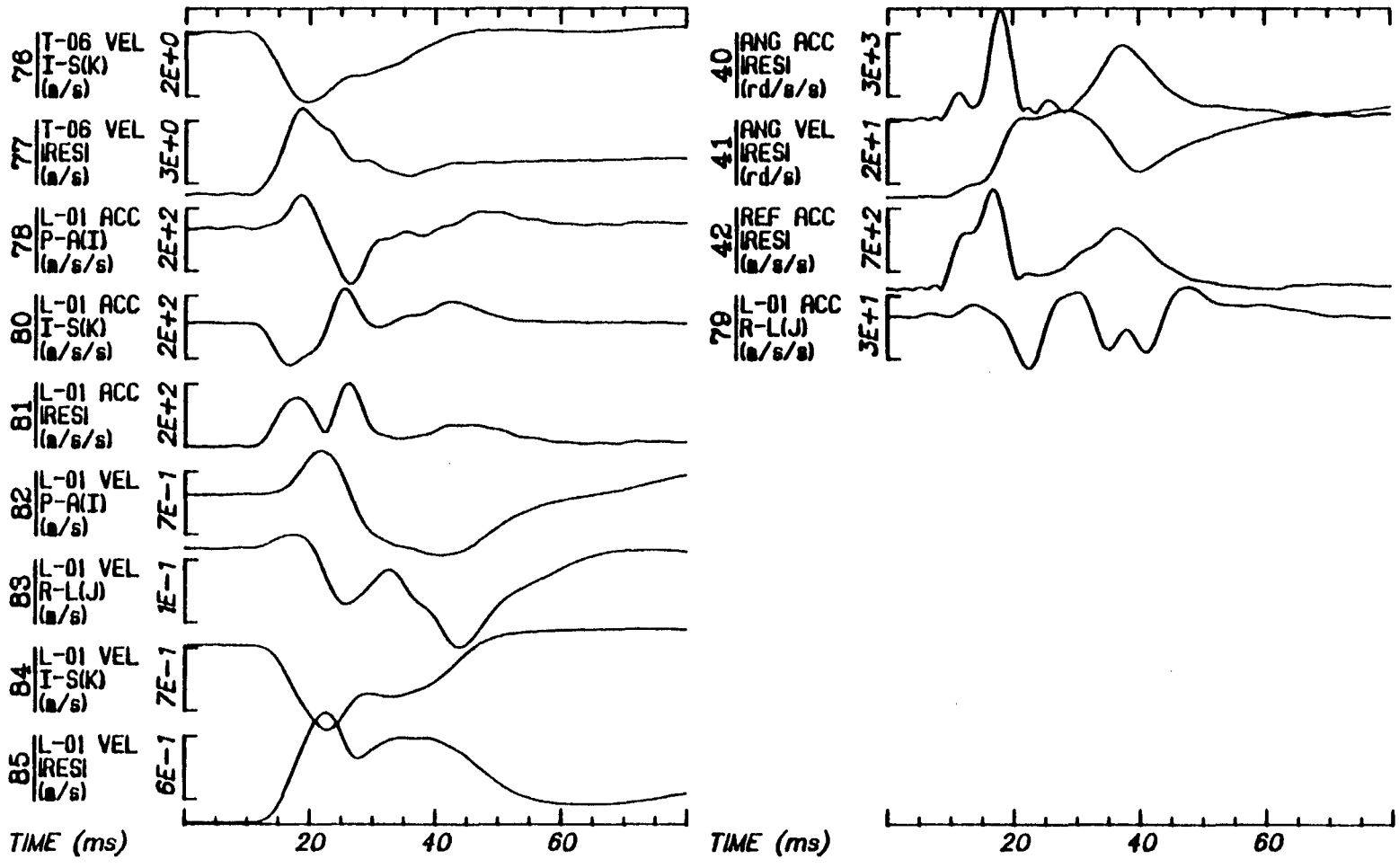

Run ID: 81H408 Tape: 3DSIMP.0 File: 3 Date: JUL 15, 1981 Sheet: 5/5

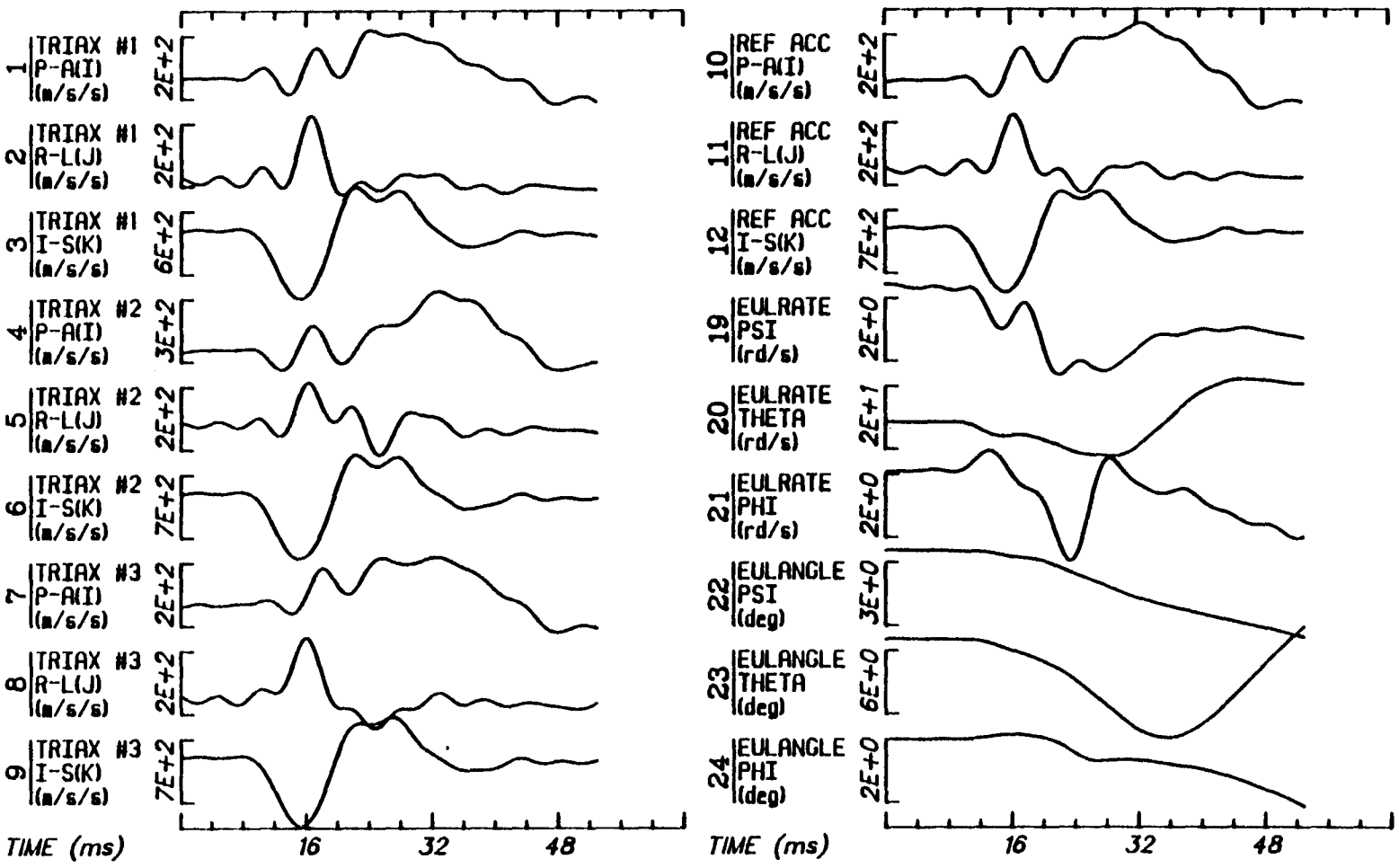

Run ID: 81H410 Tape: 3D9X-RES File: 59 Date: JUN 9, 1982 Sheet: 1/5

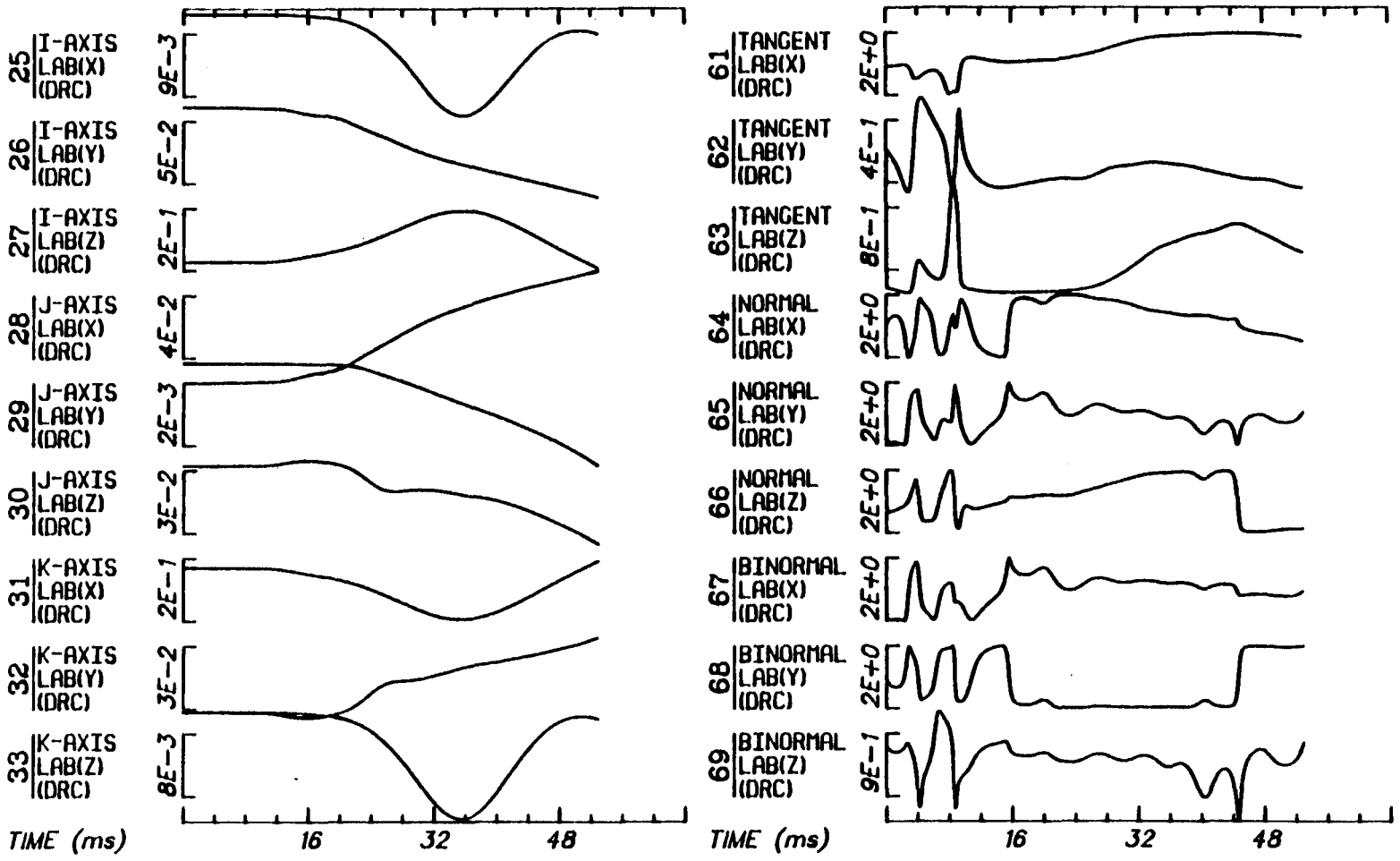

Run ID: 81H410 Tape: 3D9X-RES File: 59 Date: JUN 9, 1982 Sheet: 2/5

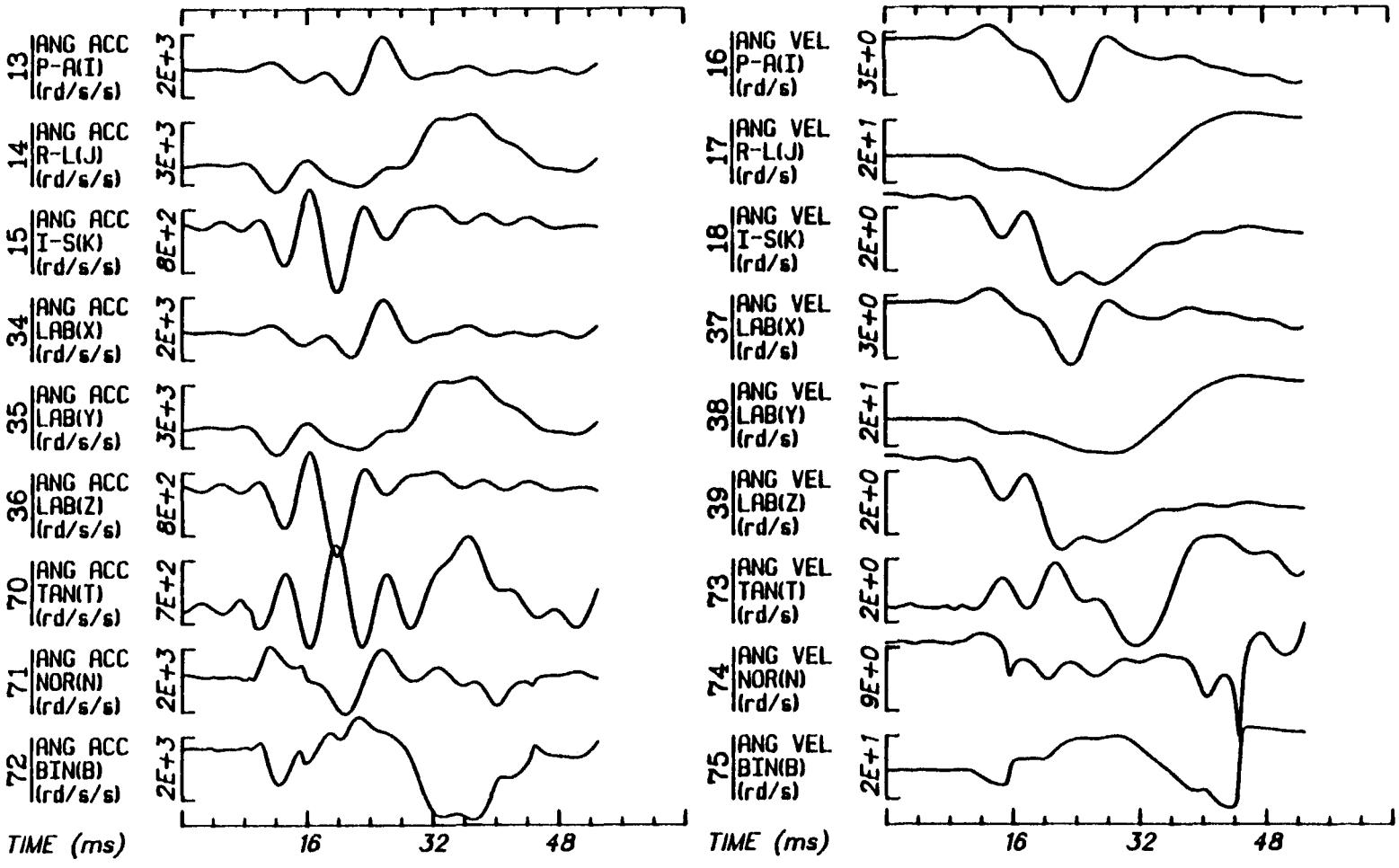

Run ID: 81H410 Tape: 3D9X-RES File: 59 Date: JUN 9, 1982 Sheet: 3/5

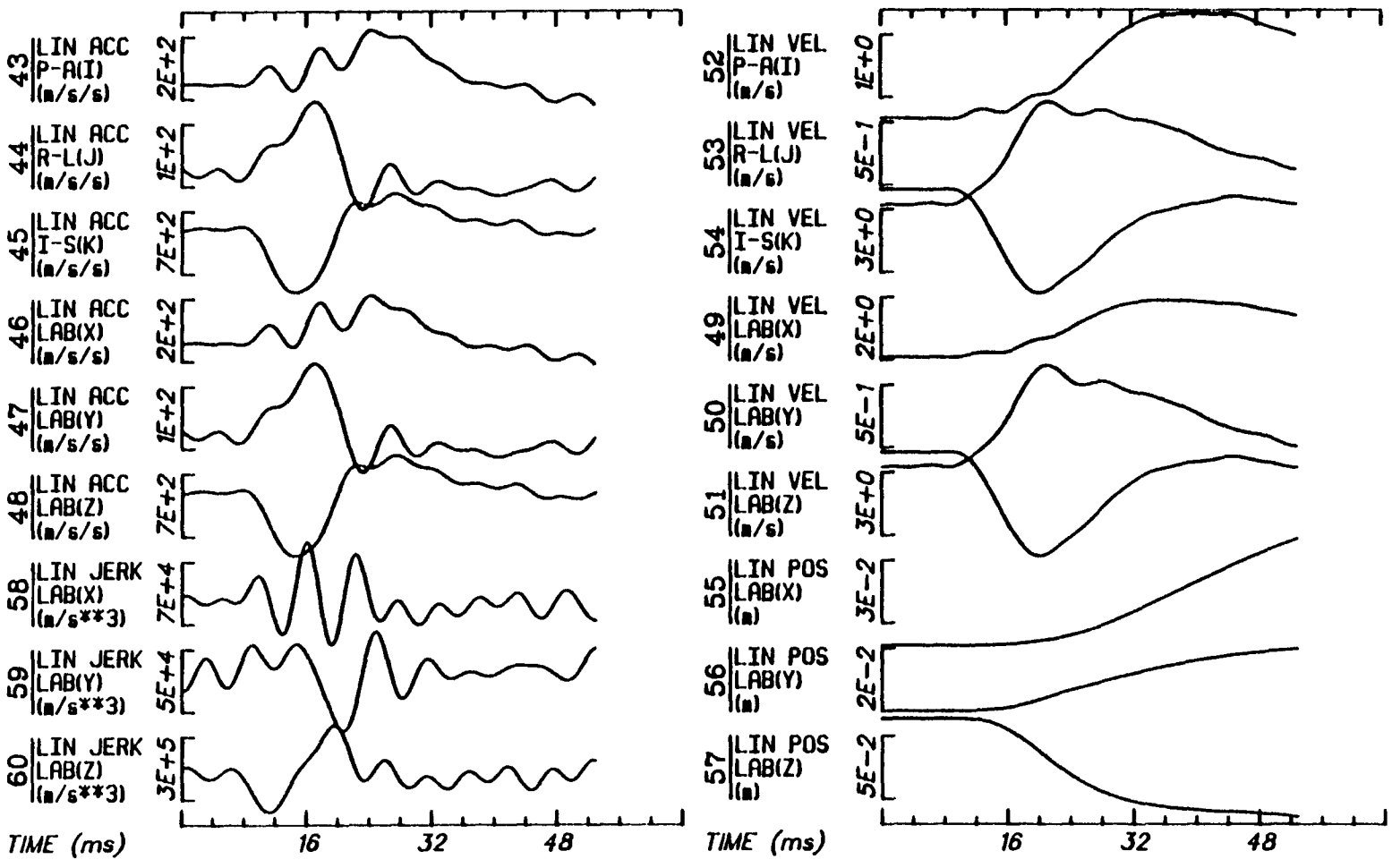

Run ID: 81H410 Tape: 3D9X-RES File: 59 Date: JUN 9, 1982 Sheet: 4/5

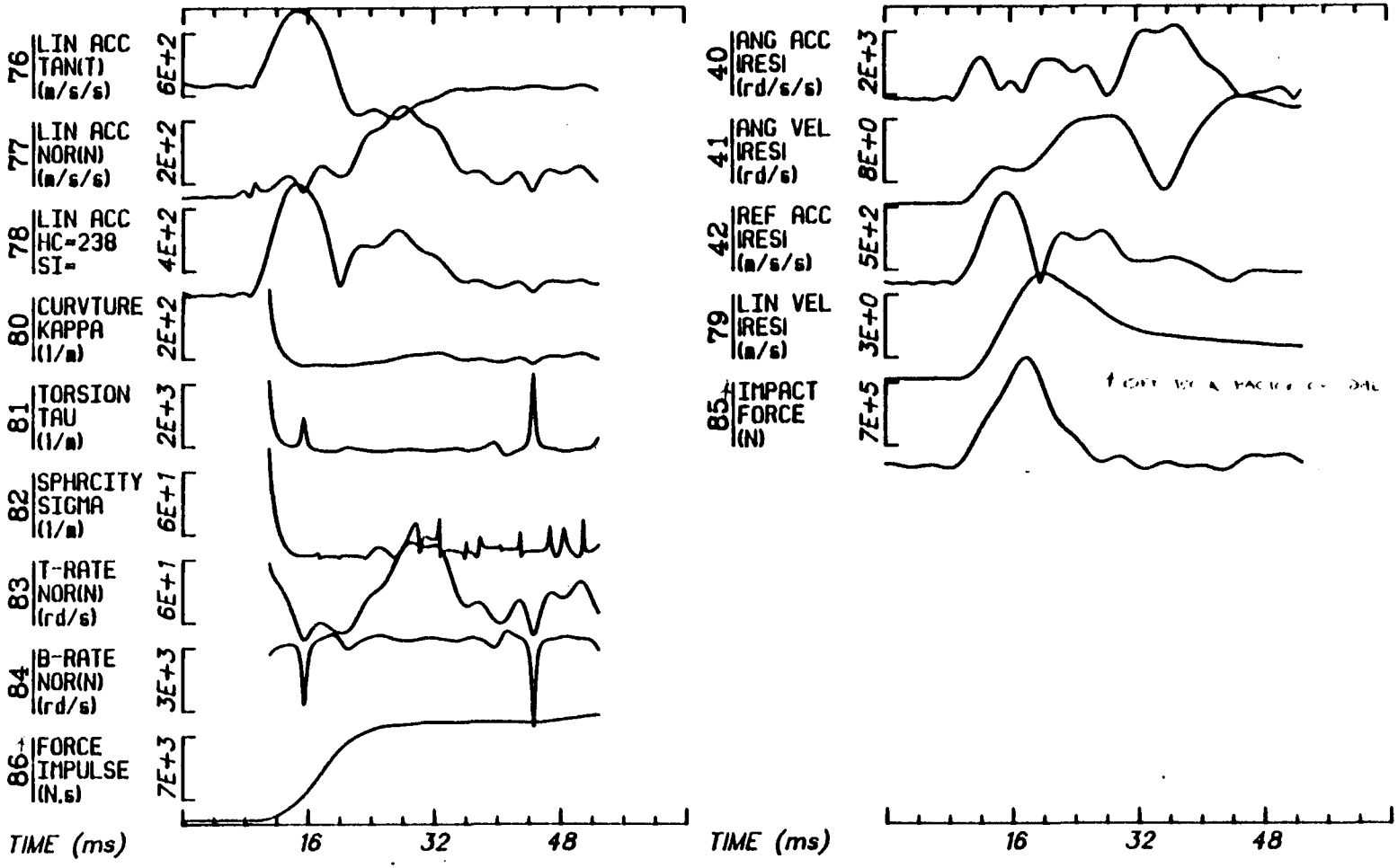

Run ID: 81H410 Tape: 3D9X-RES File: 59 Date: JUN 9, 1982 Sheet: 5/5

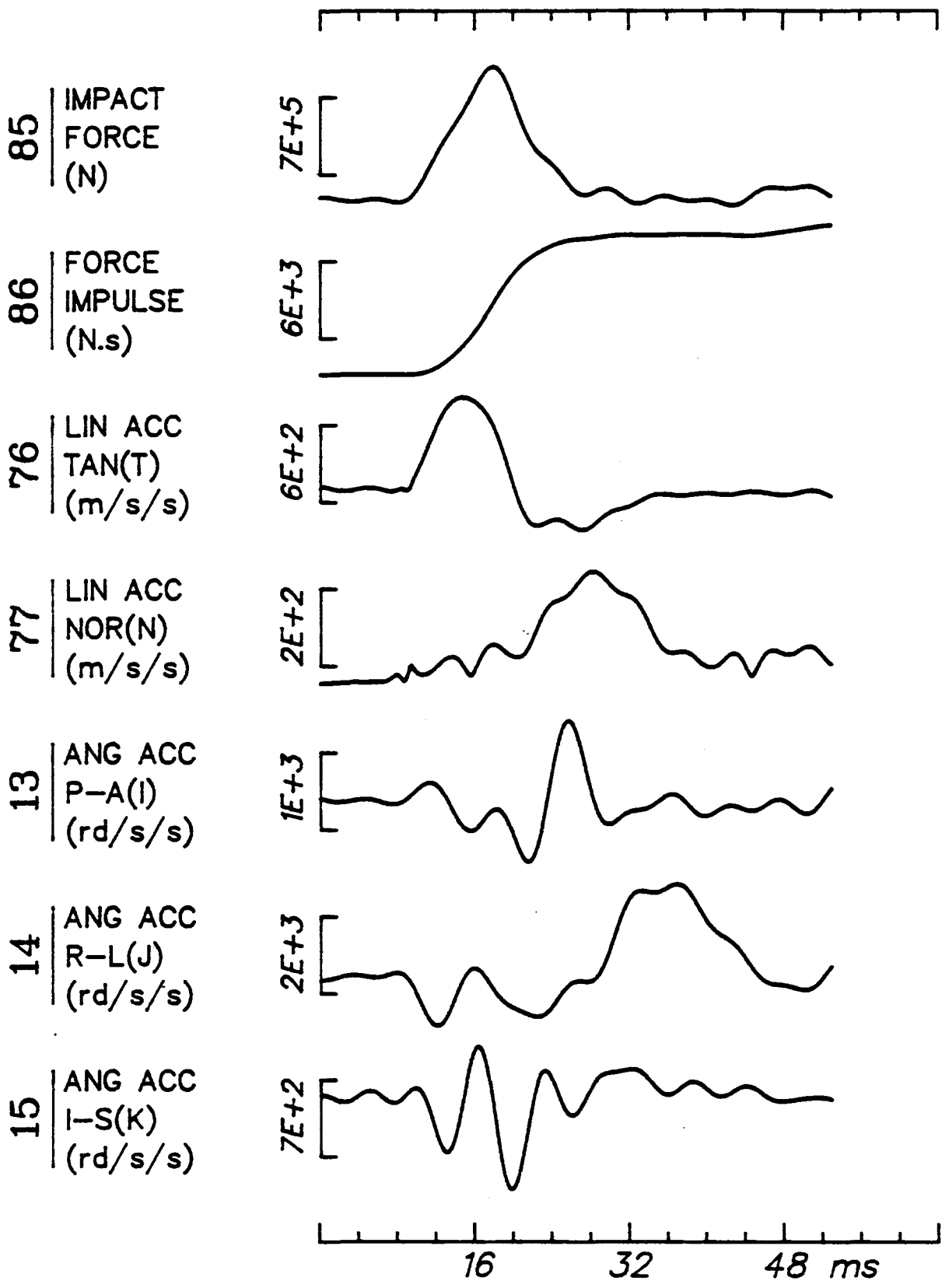
Tape: 3D9X-R
File: 59
Run ID: 81H410
85
IMPACT
FORCE
(N)
7E+5
86
FORCE
IMPULSE
(N.s)
6E+3
76
LIN ACC
TAN(T)
(m/s/s)
6E+2
77
LIN ACC
NOR(N)
(m/s/s)
2E+2
13
ANG ACC
P-A(I)
(rd/s/s)
1E+3
14
ANG ACC
R-L(J)
(rd/s/s)
2E+3
15
ANG ACC
I-S(K)
(rd/s/s)
7E+2
16
32
48 ms

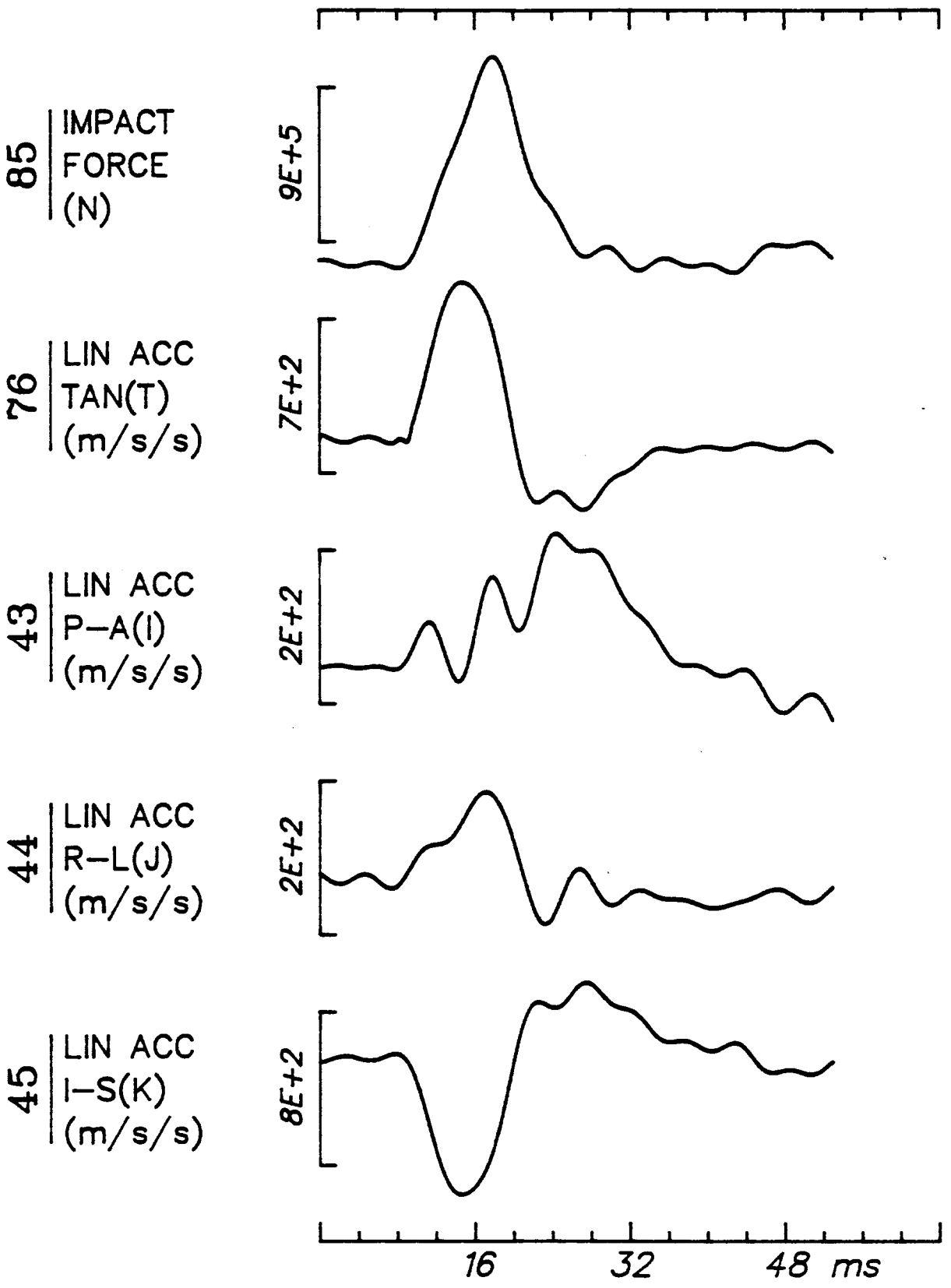
Tape: 3D9X-R
File: 59
Run ID: 81H410
85
IMPACT
FORCE
(N)
9E+5
76
LIN ACC
TAN(T)
(m/s/s)
7E+2
43
LIN ACC
P-A(I)
(m/s/s)
2E+2
44
LIN ACC
R-L(J)
(m/s/s)
2E+2
45
LIN ACC
I-S(K)
(m/s/s)
8E+2
16
32
48 ms

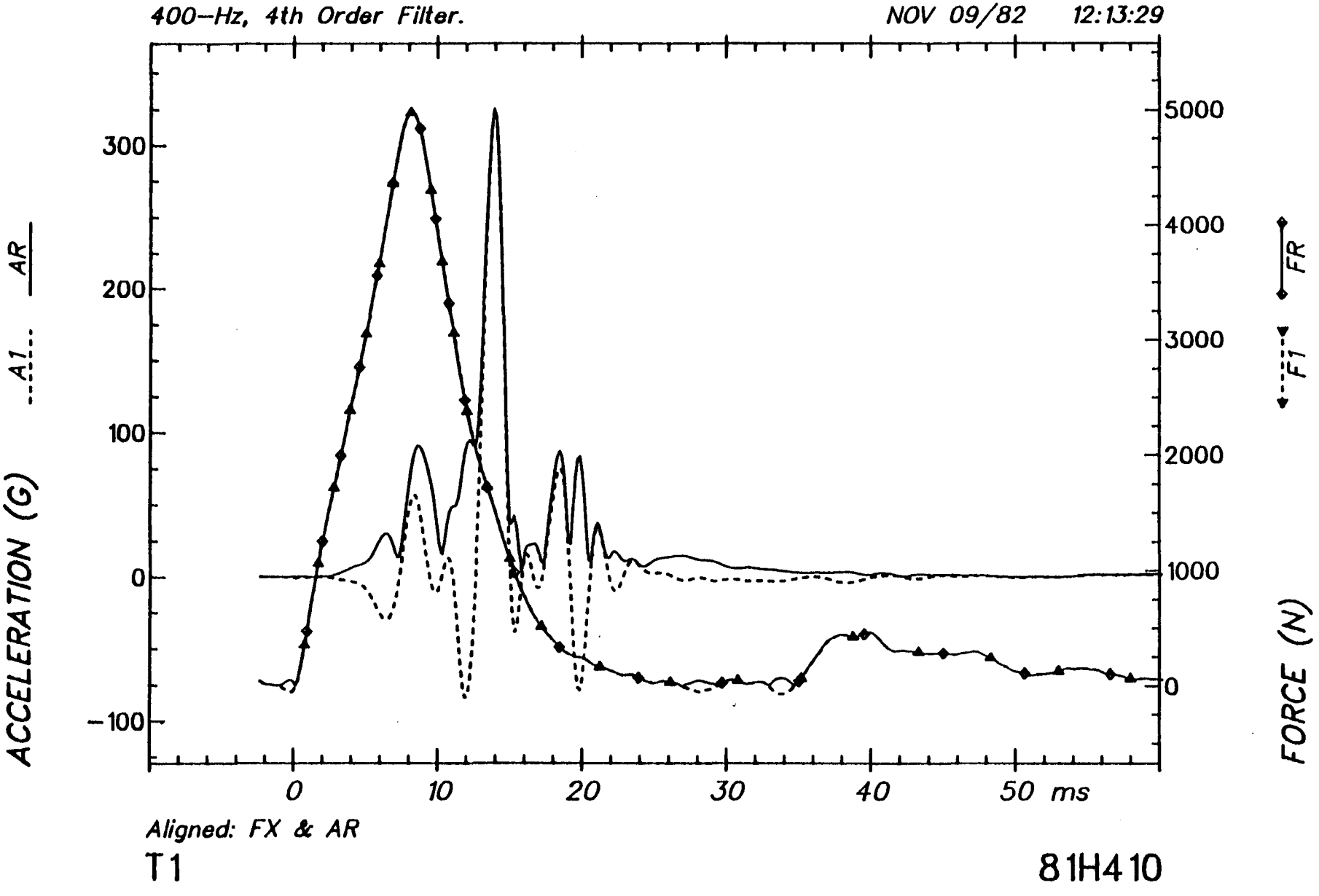
400–Hz, 4th Order Filter.
NOV 09/82 12:13:29
ACCELERATION (G)
AR
A1
300
200
100
0
–100
5000
4000
3000
2000
1000
0
FR
F1
FORCE (N)
0
10
20
30
40
50 ms
Aligned: FX & AR
T1
81H410

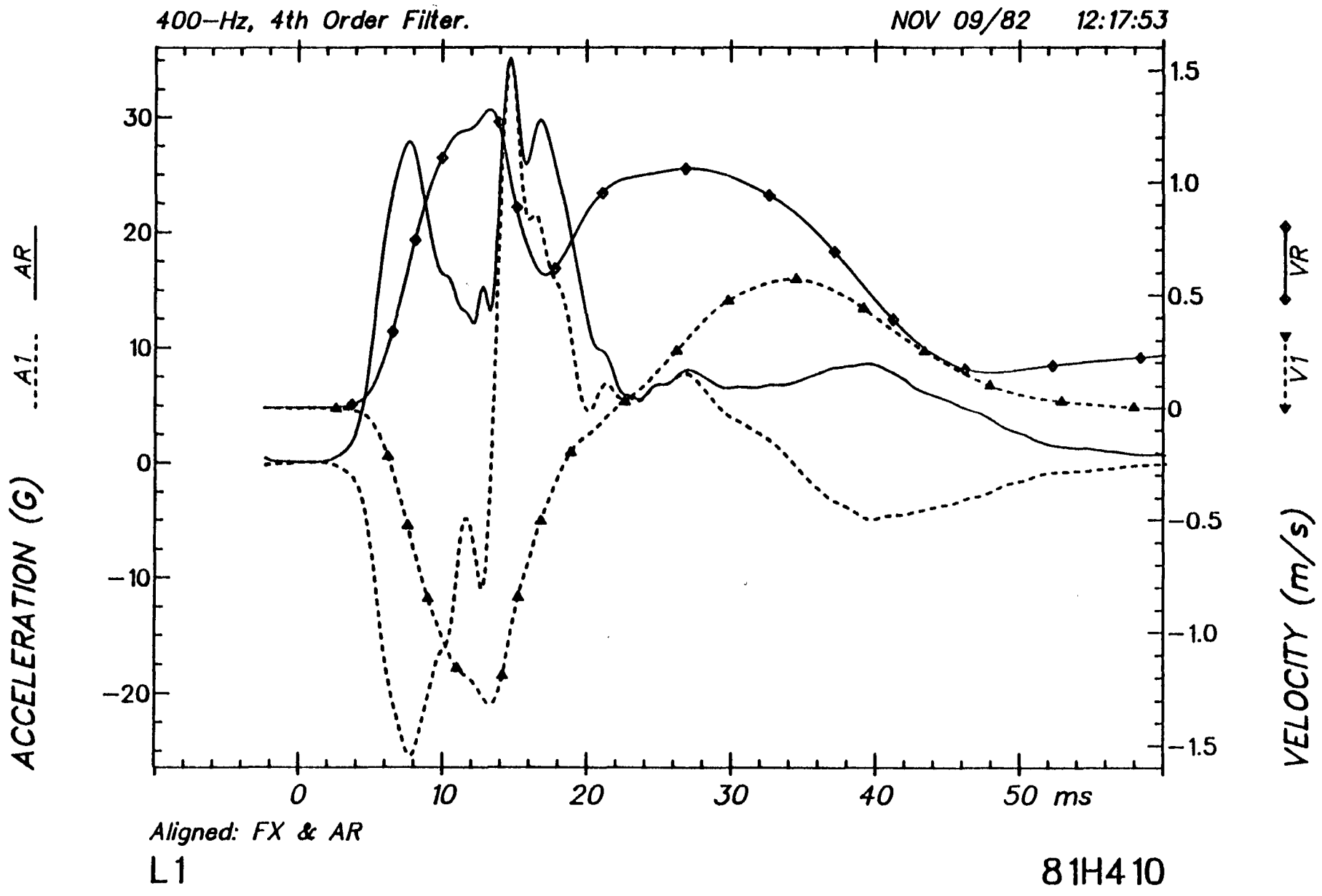
400–Hz, 4th Order Filter.
NOV 09/82 12:17:53
ACCELERATION (G)
A1
AR
VELOCITY (m/s)
VR
VI
30
20
10
0
−10
−20
1.5
1.0
0.5
0
−0.5
−1.0
−1.5
0
10
20
30
40
50 ms
Aligned: FX & AR
L1
81H410

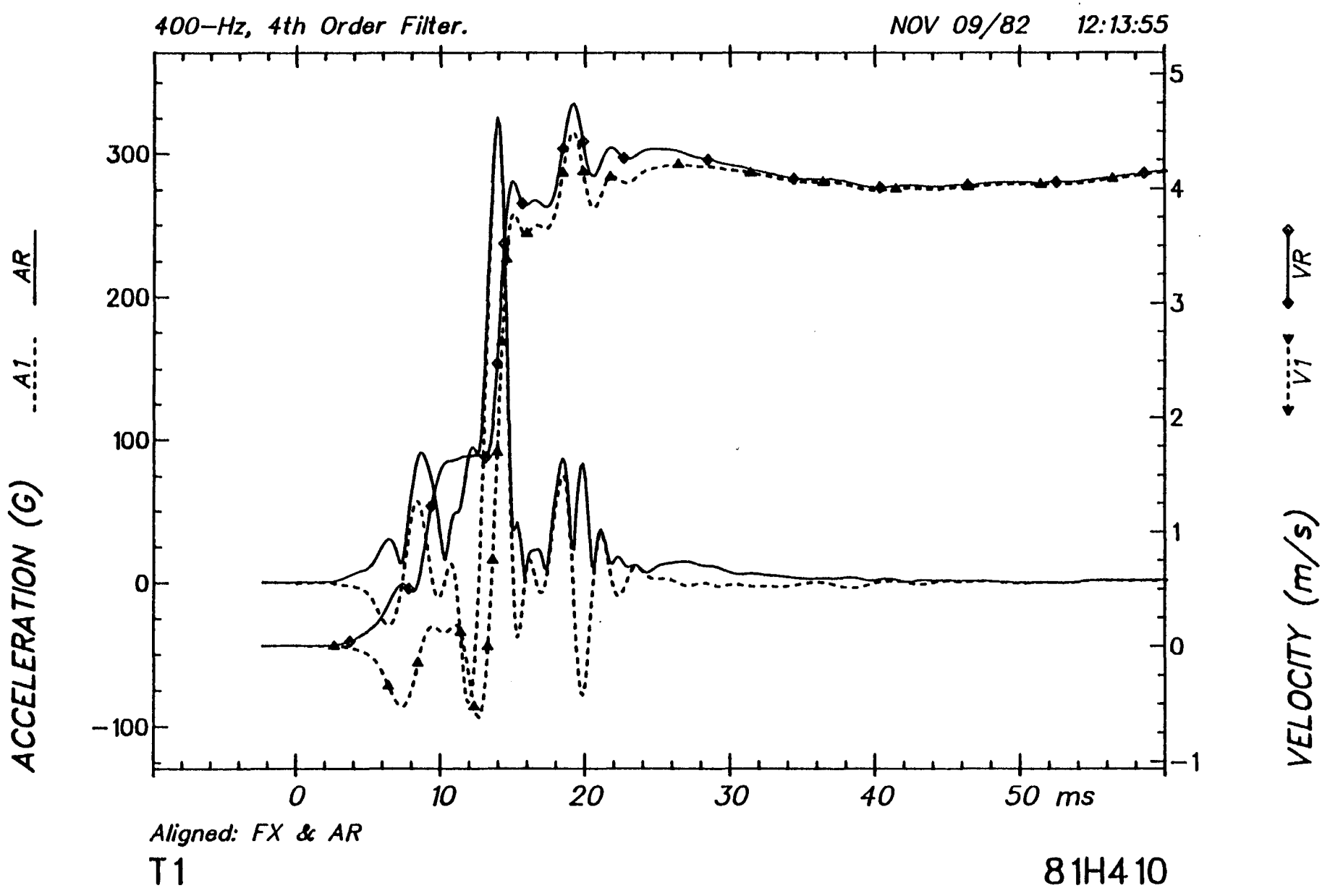
400–Hz, 4th Order Filter.
NOV 09/82 12:13:55
ACCELERATION (G)
A1
AR
VELOCITY (m/s)
V1
VR
300
200
100
0
–100
5
4
3
2
1
0
–1
0
10
20
30
40
50 ms
Aligned: FX & AR
T1
81H410

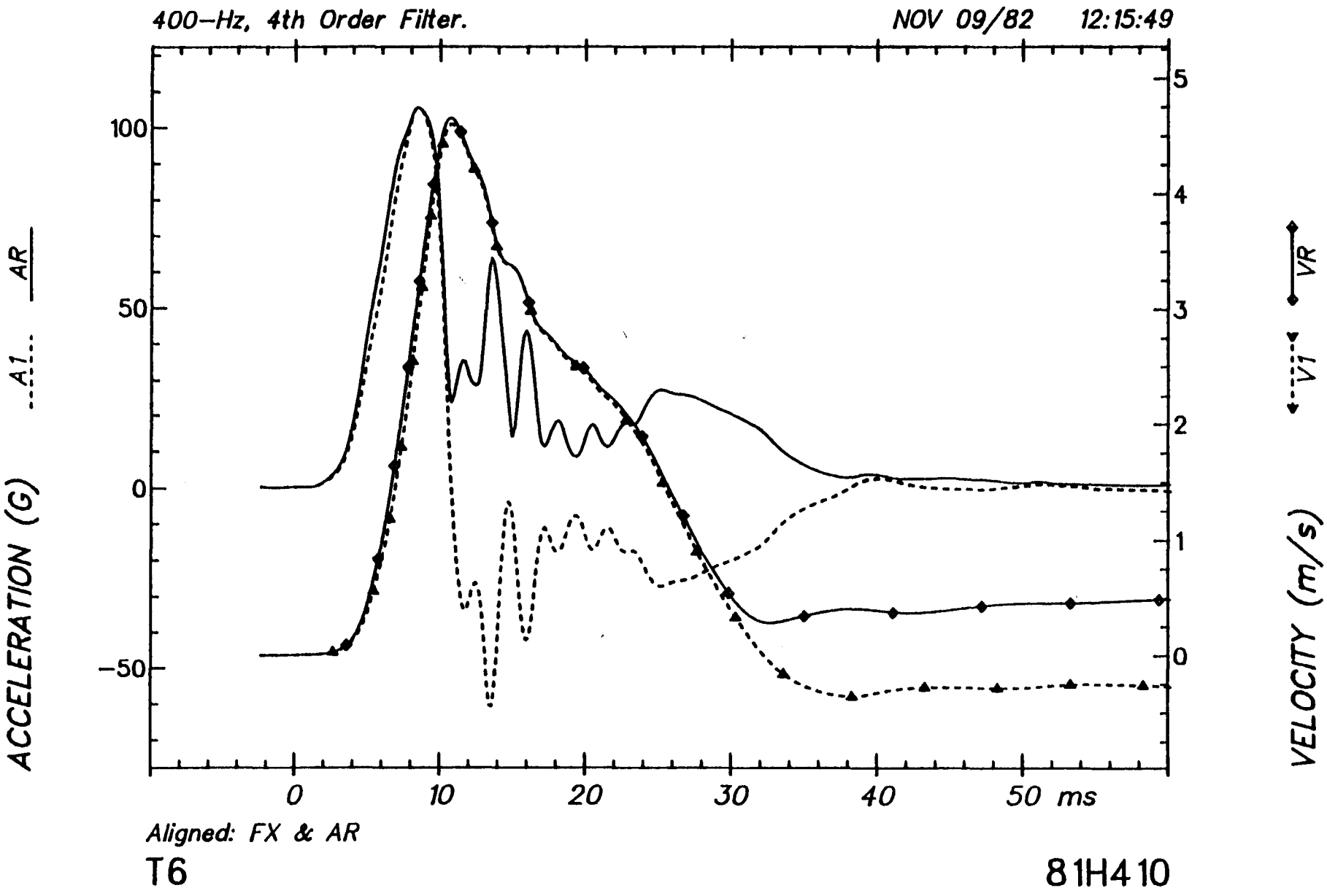
400–Hz, 4th Order Filter.
NOV 09/82 12:15:49
ACCELERATION (G)
A1
AR
VELOCITY (m/s)
V1
VR
100
50
0
-50
5
4
3
2
1
0
0
10
20
30
40
50 ms
Aligned: FX & AR
T6
81H410

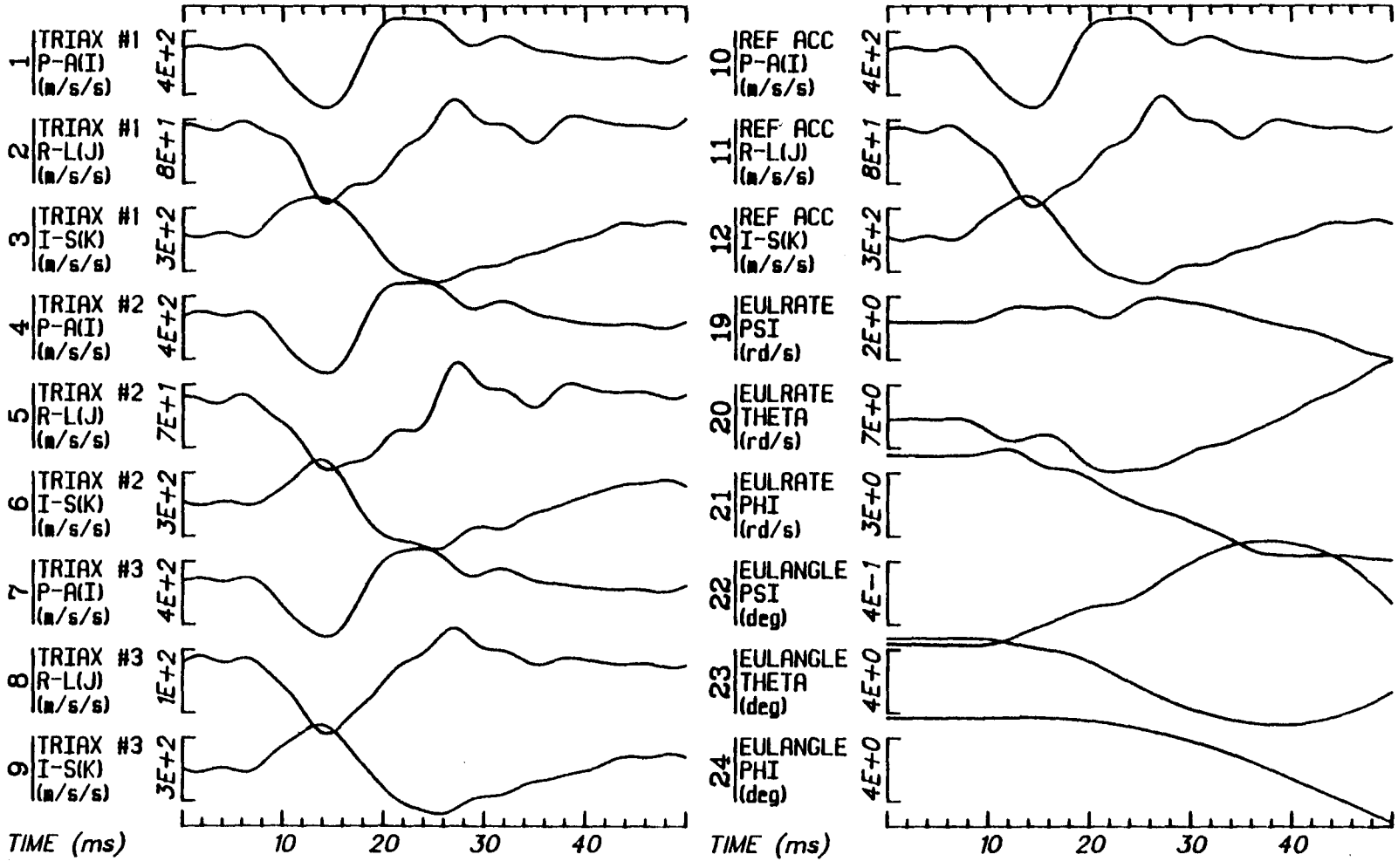

Run ID: 81H411 Tape: 3D9X-RES File: 60 Date: JUN 9, 1982 Sheet: 1/5

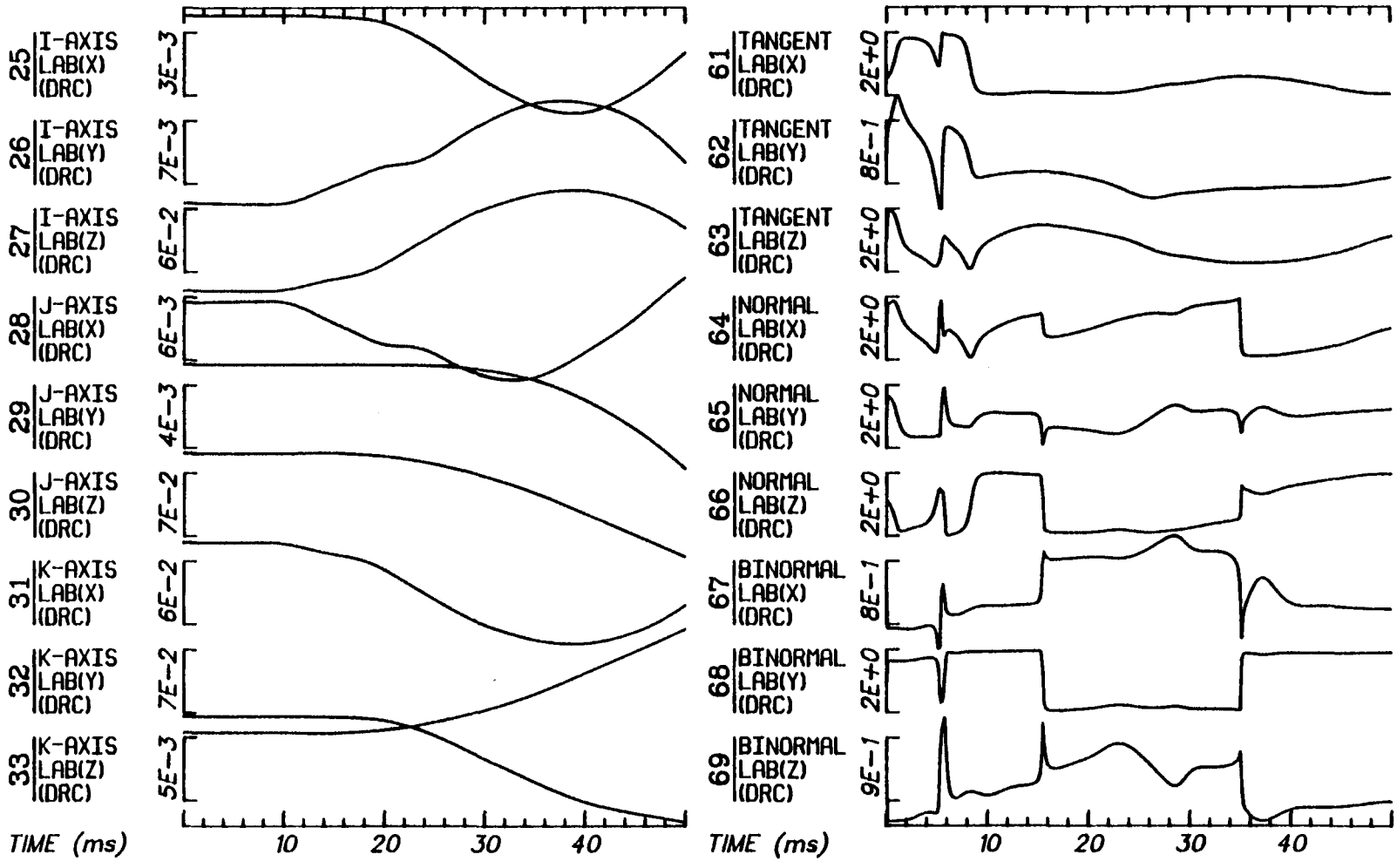

Run ID: 81H411 Tape: 3D9X-RES File: 60 Date: JUN 9, 1982 Sheet: 2/5

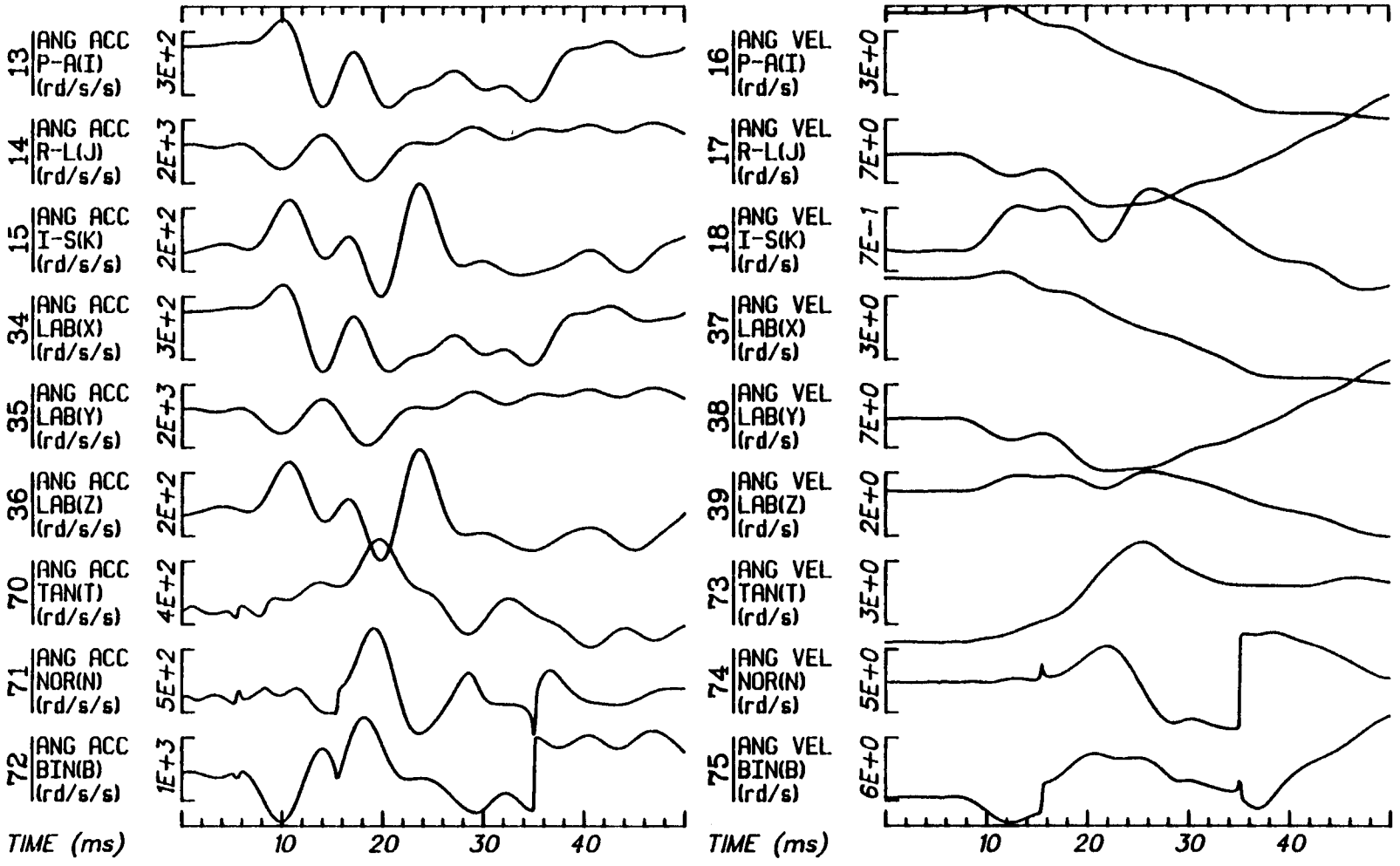

Run ID: 81H411 Tape: 3D9X-RES File: 60 Date: JUN 9, 1982 Sheet: 3/5

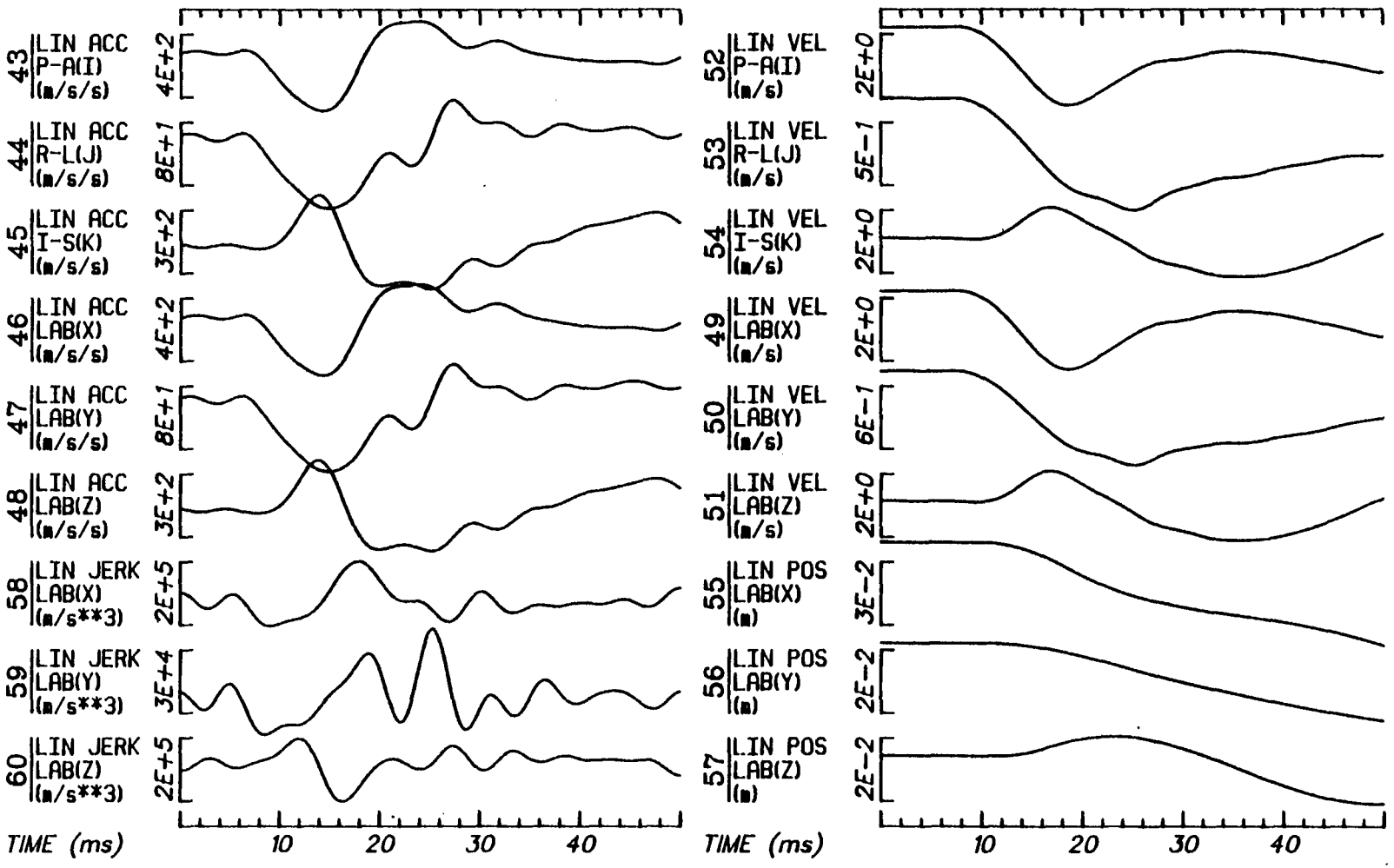

Run ID: 81H411 Tape: 3D9X-RES File: 60 Date: JUN 9, 1982 Sheet: 4/5

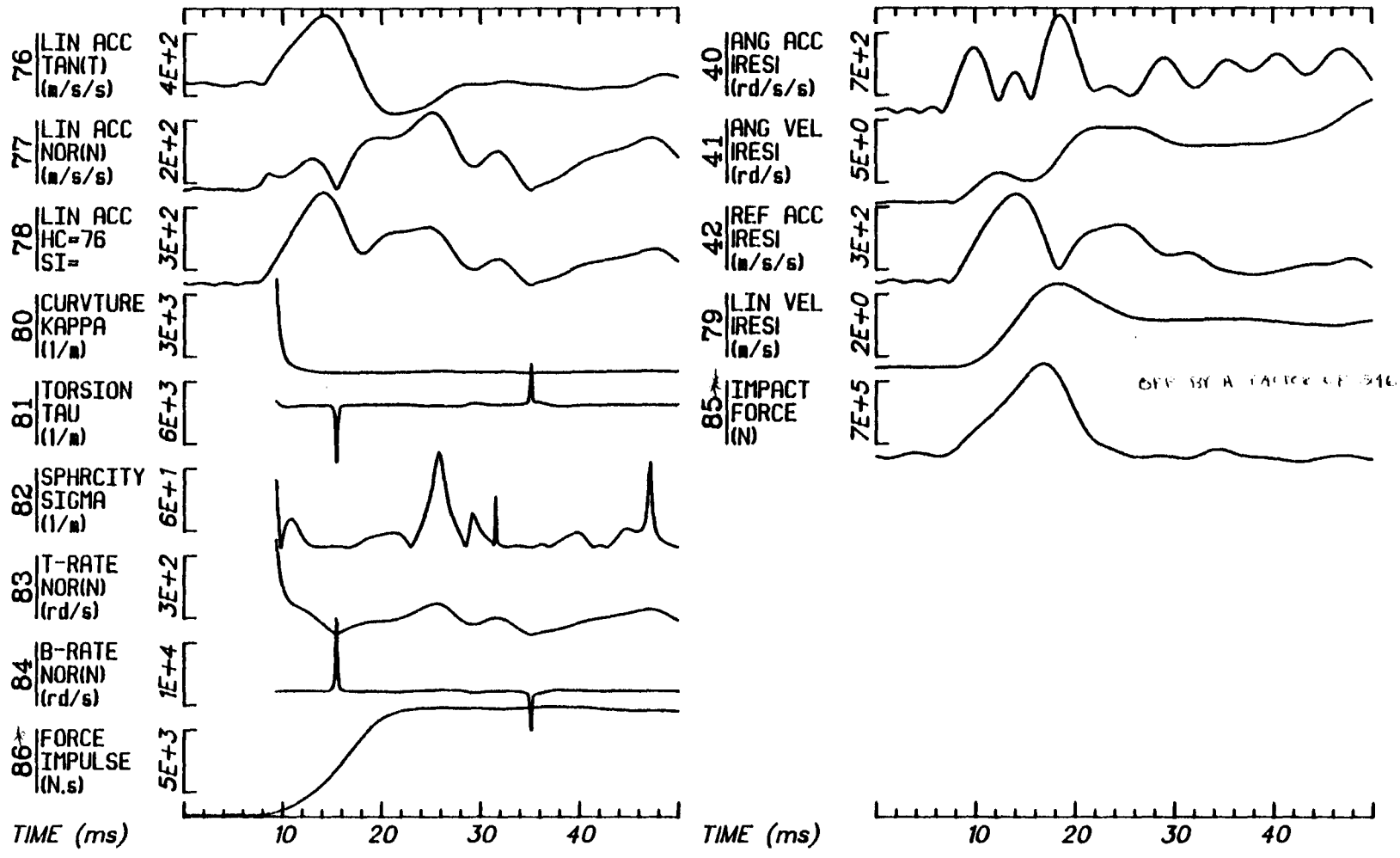

Run ID: 81H411 Tape: 3D9X-RES File: 60 Date: JUN 9, 1982 Sheet: 5/5

Tape: 3D9X-R File: 60 Run ID: 81H411

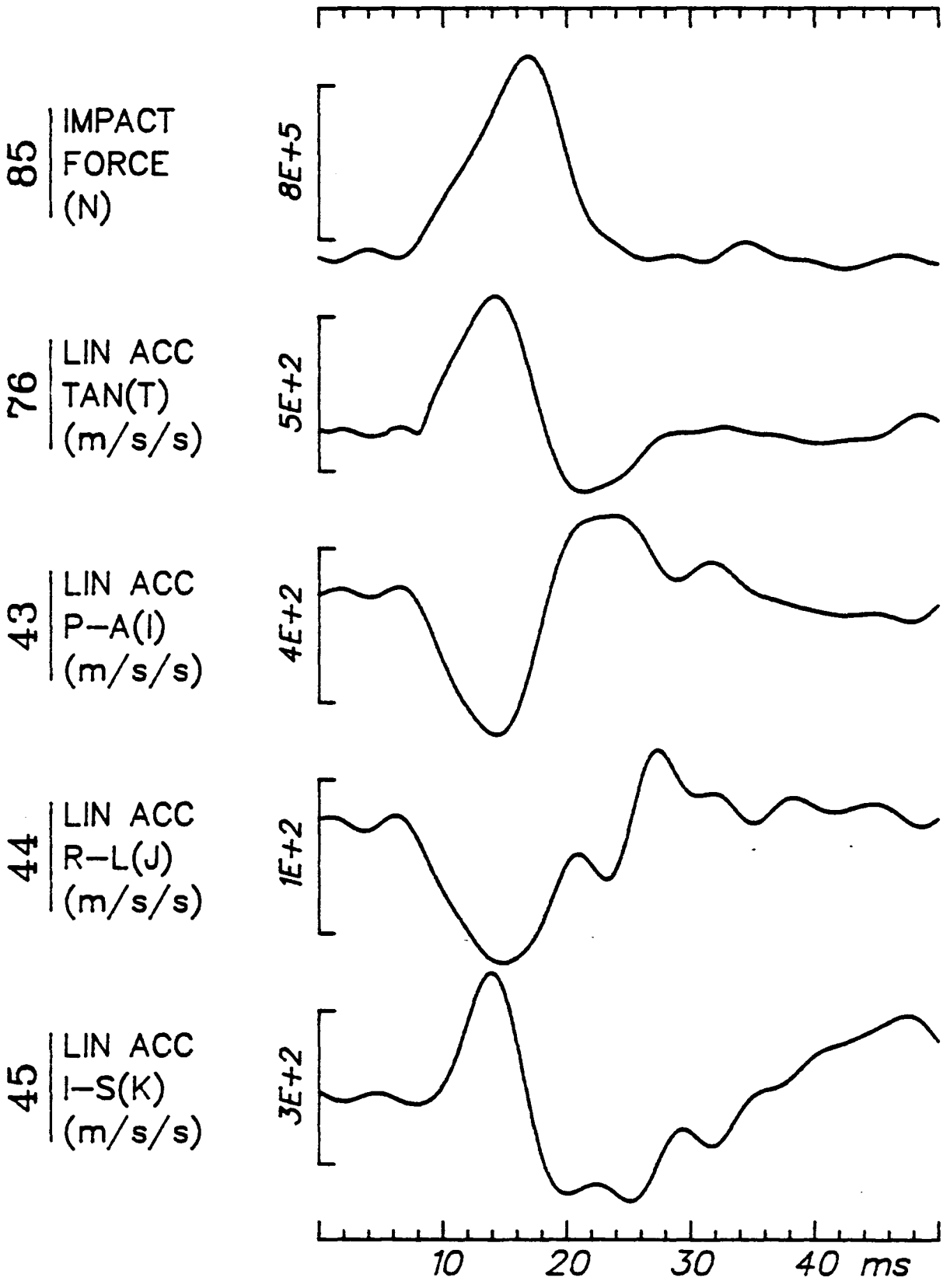

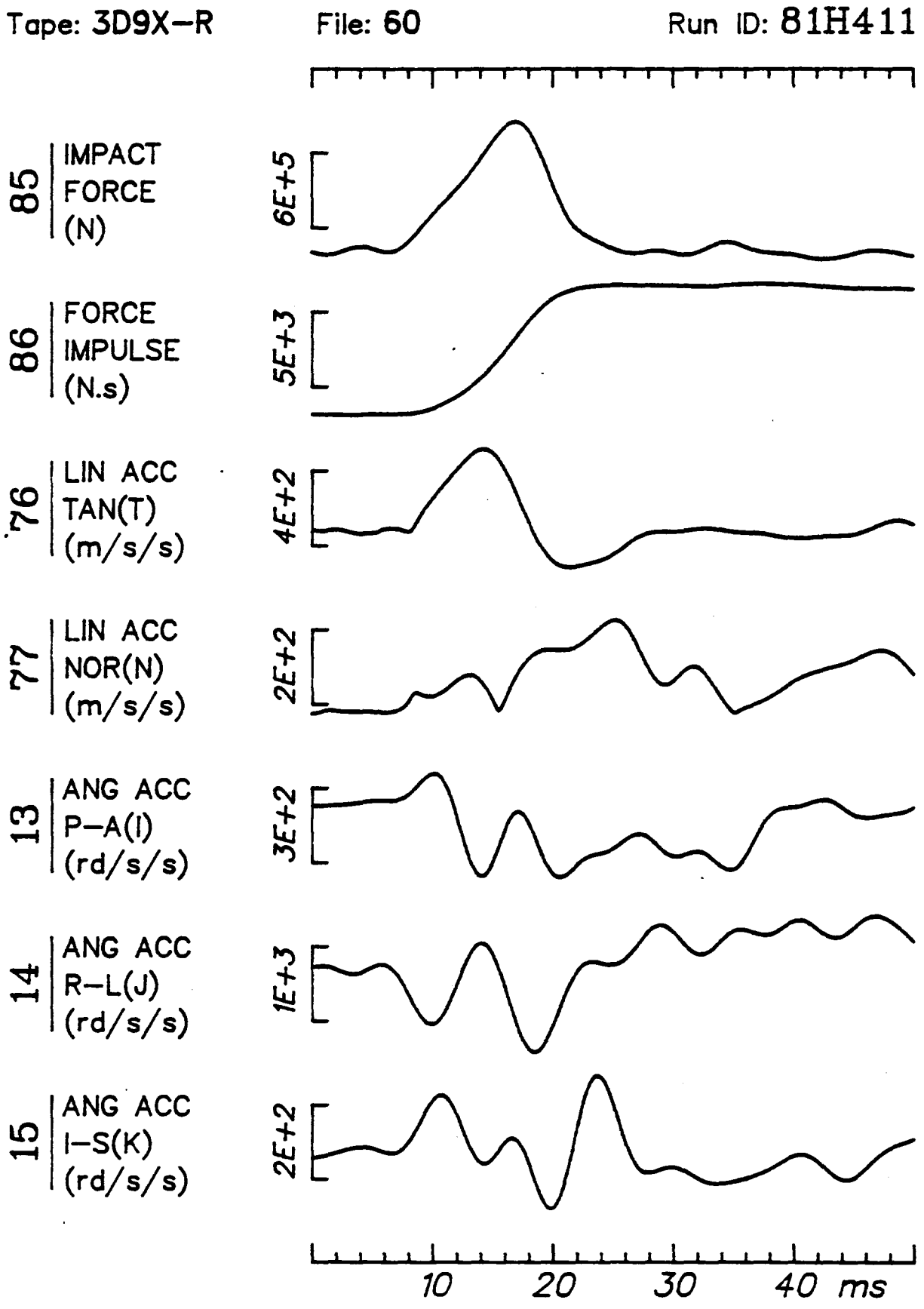
Tape: 3D9X-R
File: 60
Run ID: 81H411
85
IMPACT
FORCE
(N)
6E+5
86
FORCE
IMPULSE
(N.s)
5E+3
76
LIN ACC
TAN(T)
(m/s/s)
4E+2
77
LIN ACC
NOR(N)
(m/s/s)
2E+2
13
ANG ACC
P-A(I)
(rd/s/s)
3E+2
14
ANG ACC
R-L(J)
(rd/s/s)
1E+3
15
ANG ACC
I-S(K)
(rd/s/s)
2E+2
10
20
30
40 ms

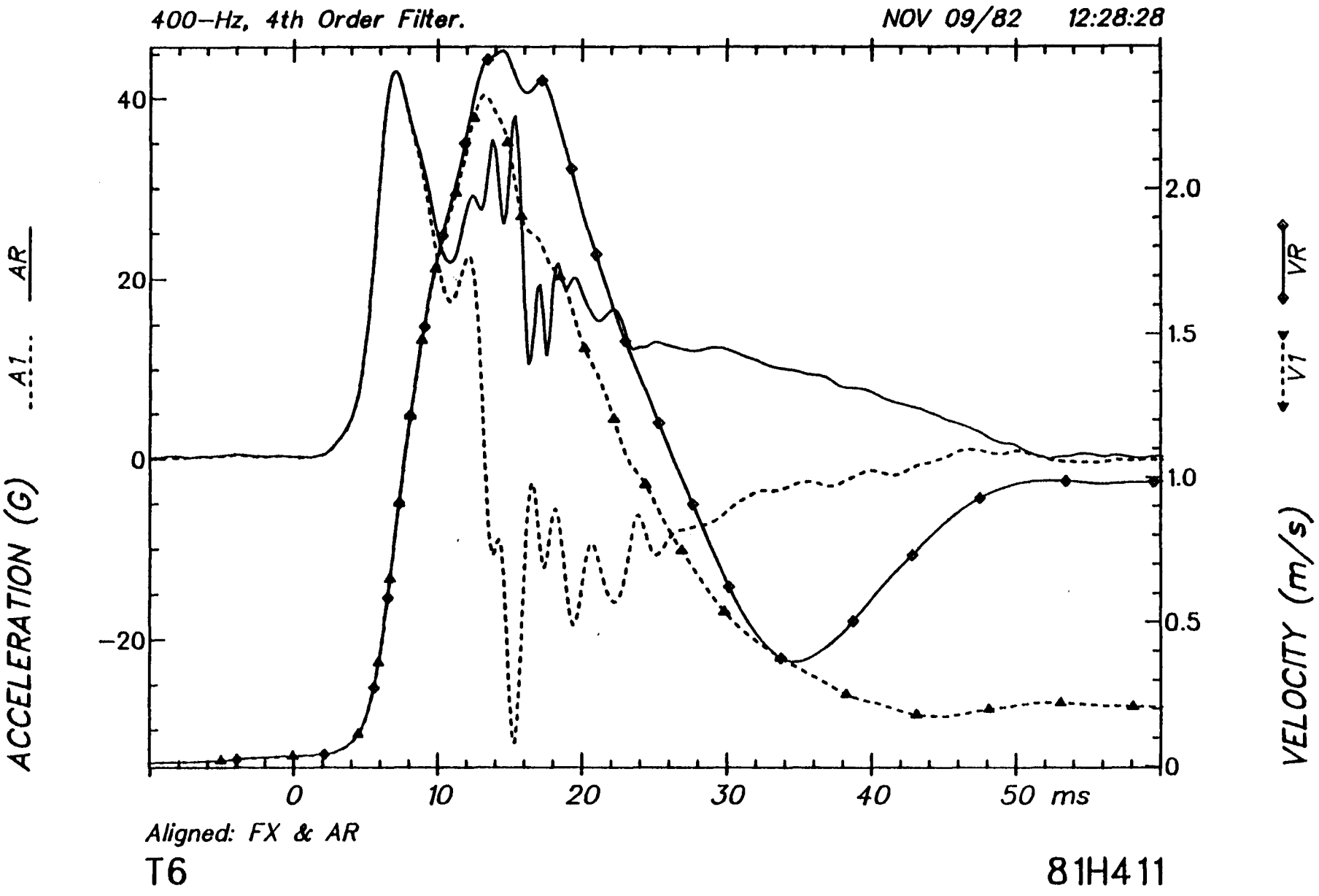
400–Hz, 4th Order Filter.
NOV 09/82 12:28:28
ACCELERATION (G)
A1
AR
VELOCITY (m/s)
V1
VR
40
20
0
-20
2.0
1.5
1.0
0.5
0
0
10
20
30
40
50 ms
Aligned: FX & AR
T6
81H411

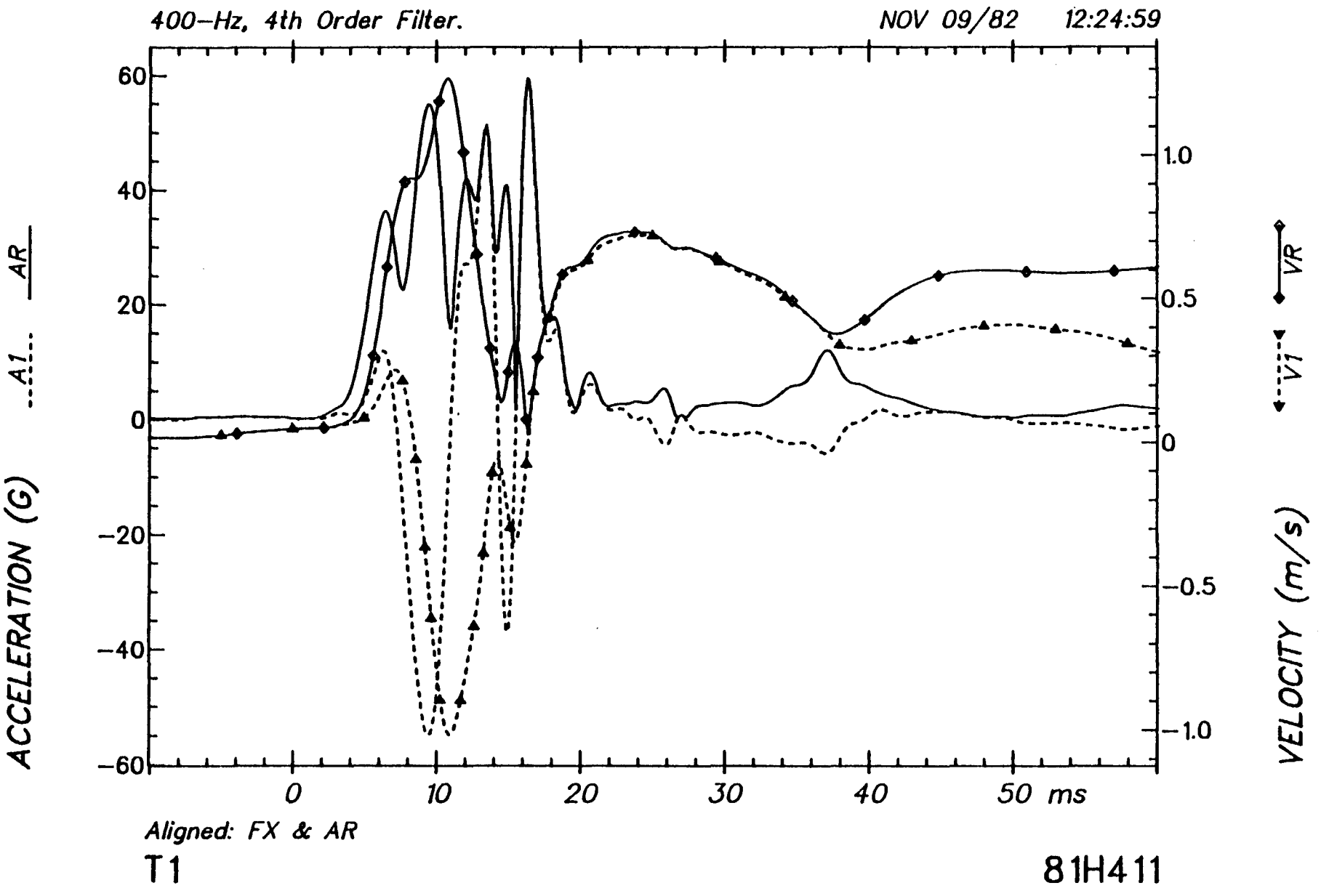
400–Hz, 4th Order Filter.
NOV 09/82 12:24:59
ACCELERATION (G)
A1
AR
VELOCITY (m/s)
VR
V1
60
40
20
0
−20
−40
−60
1.0
0.5
0
−0.5
−1.0
0
10
20
30
40
50 ms
Aligned: FX & AR
T1
81H411

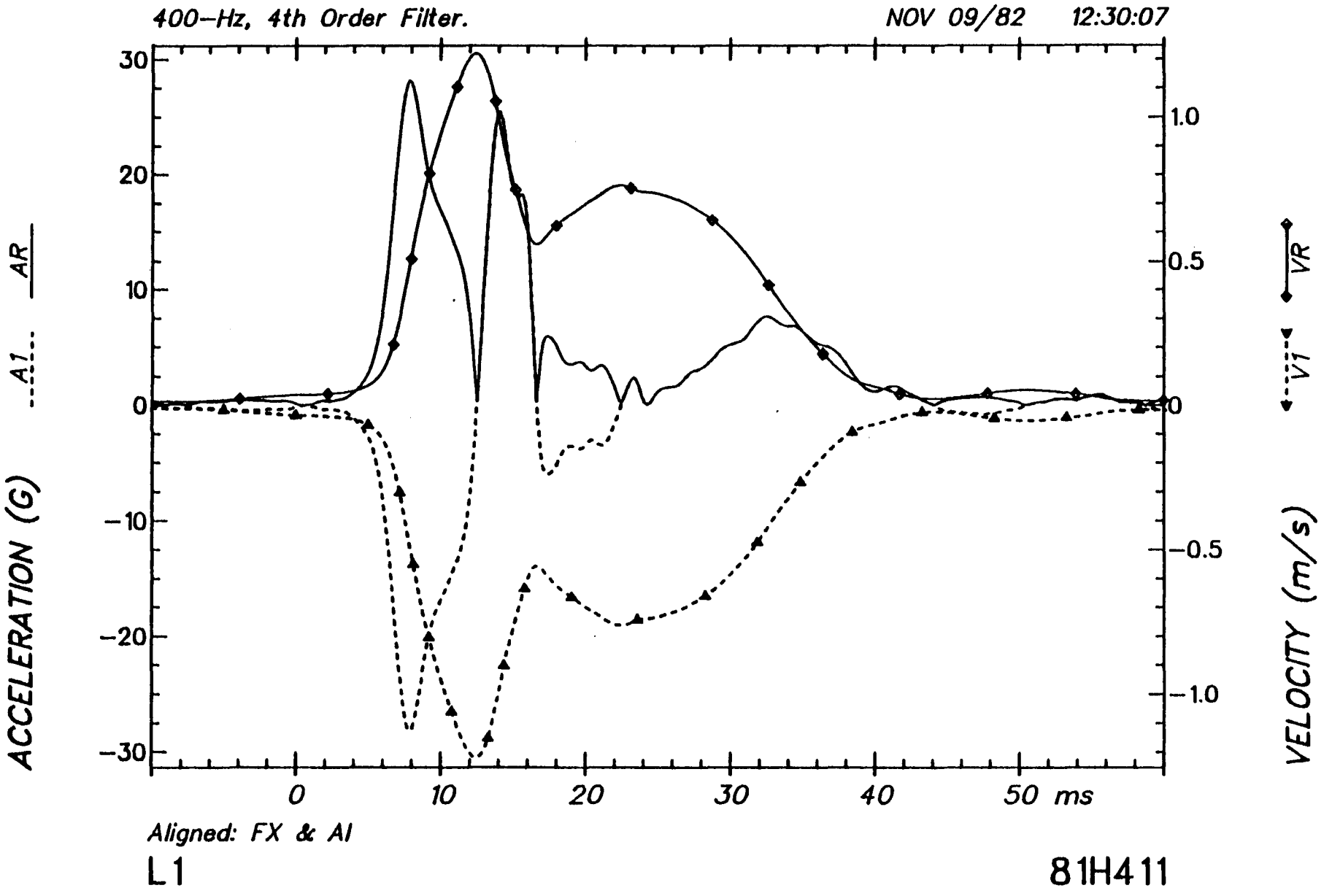
400–Hz, 4th Order Filter.
NOV 09/82 12:30:07
ACCELERATION (G)
A1
AR
VELOCITY (m/s)
V1
VR
30
20
10
0
-10
-20
-30
1.0
0.5
0
-0.5
-1.0
0
10
20
30
40
50 ms
Aligned: FX & AI
L1
81H411

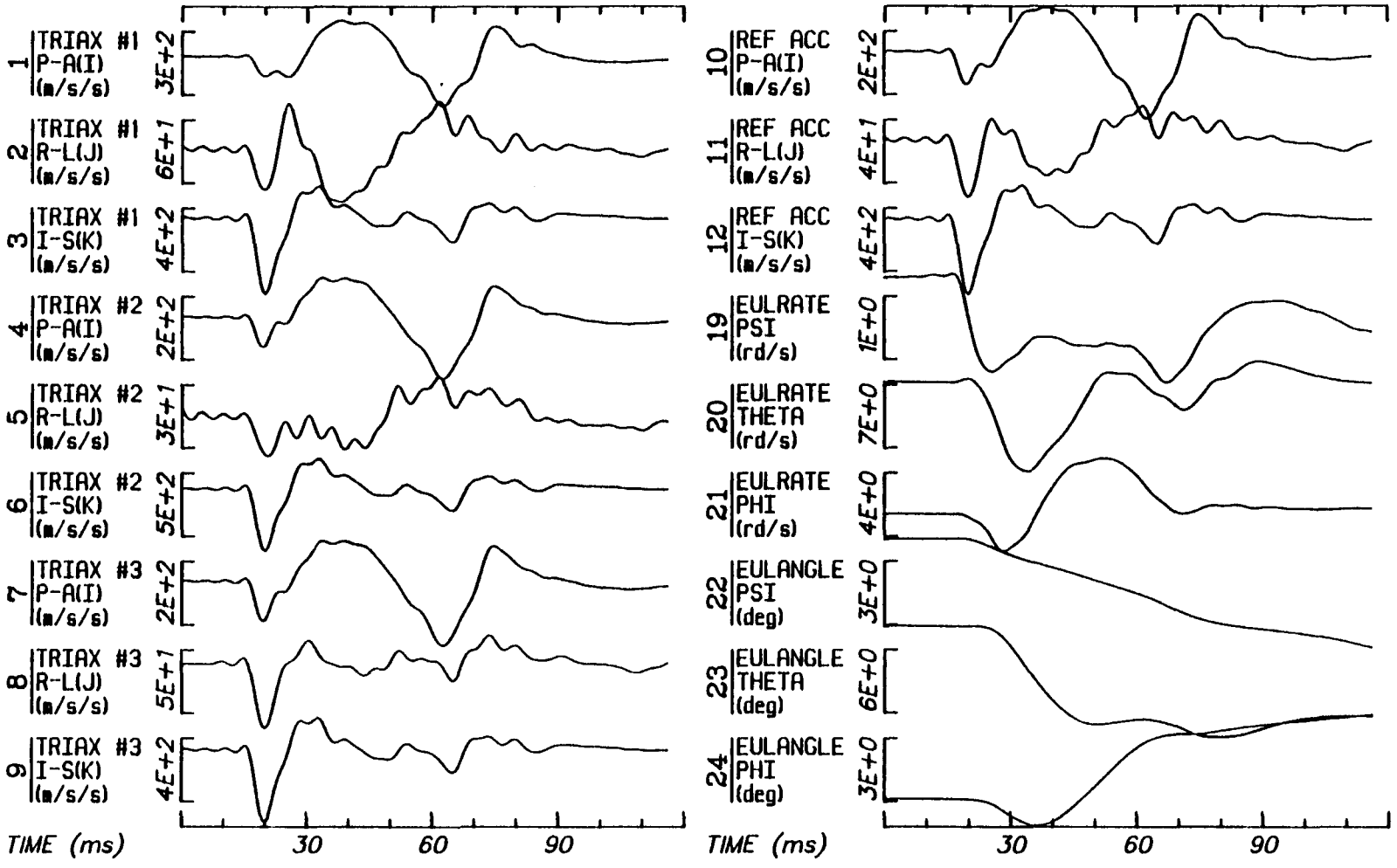

Run ID: 81H412 Tape: 3D9X-RES File: 61 Date: JUN 9, 1982 Sheet: 1/5

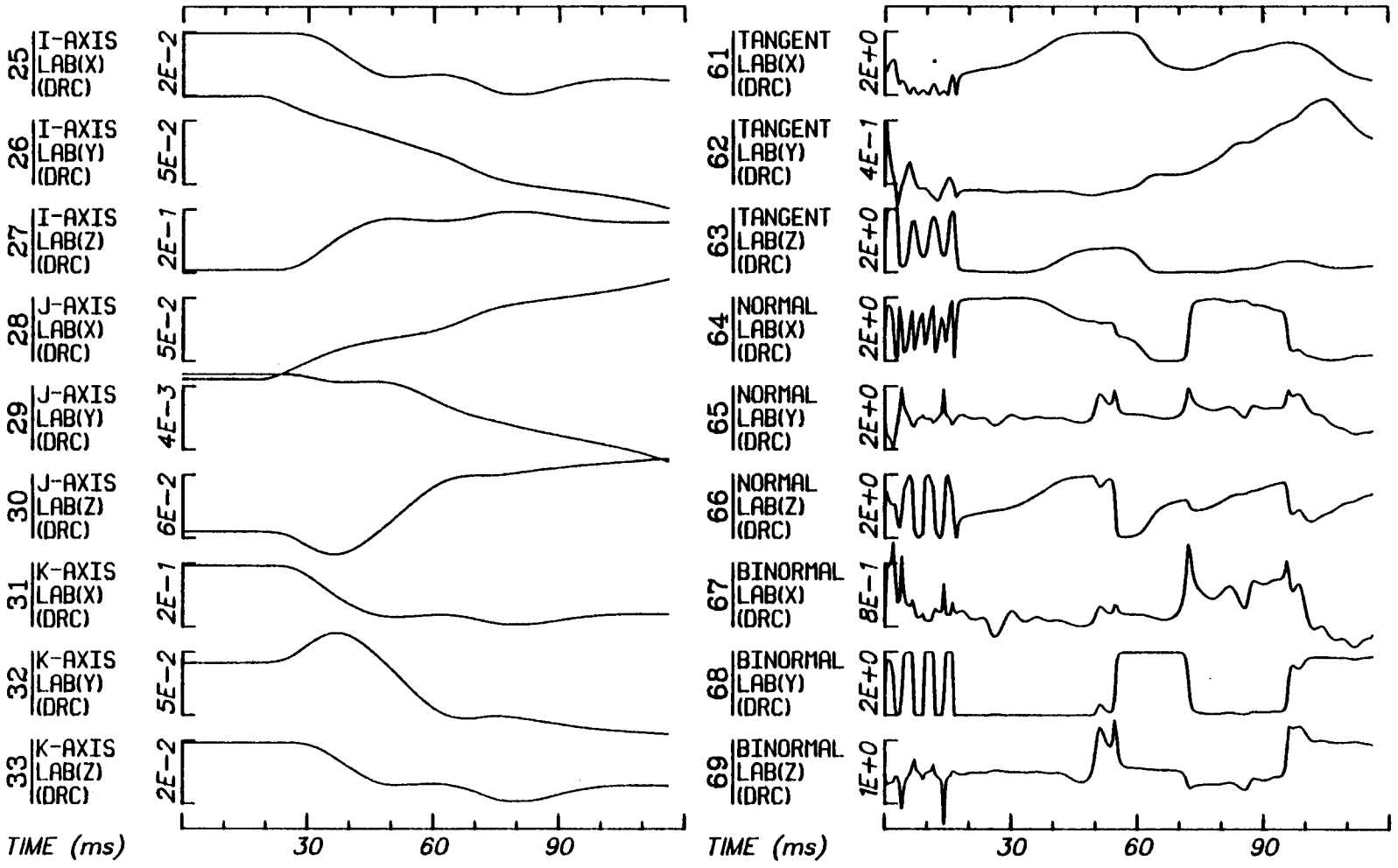

Run ID: 81H412 Tape: 3D9X-RES File: 61 Date: JUN 9, 1982 Sheet: 2/5

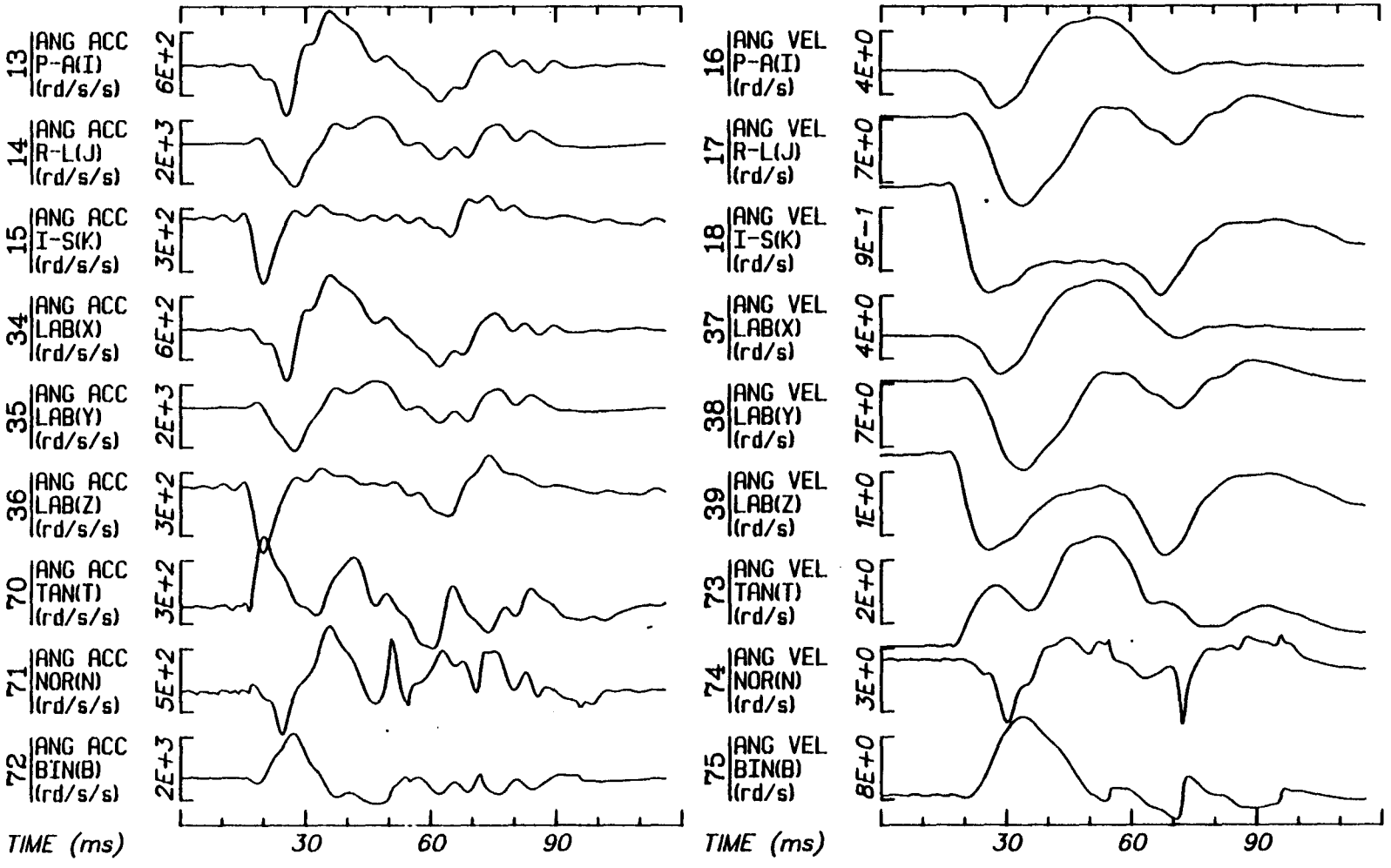

Run ID: 81H412 Tape: 3D9X-RES File: 61 Date: JUN 9, 1982 Sheet: 3/5

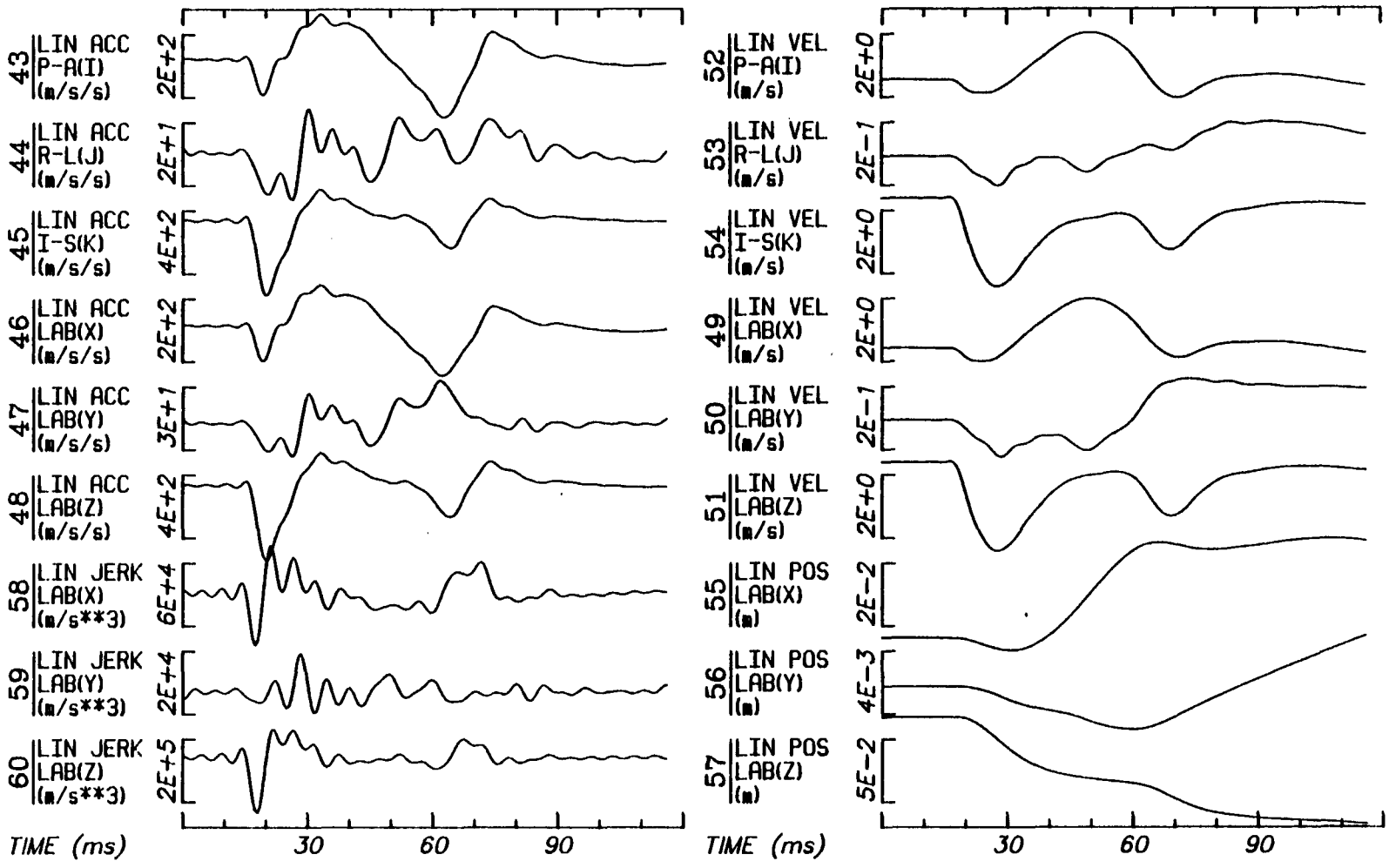

Run ID: 81H412 Tape: 3D9X-RES File: 61 Date: JUN 9, 1982 Sheet: 4/5

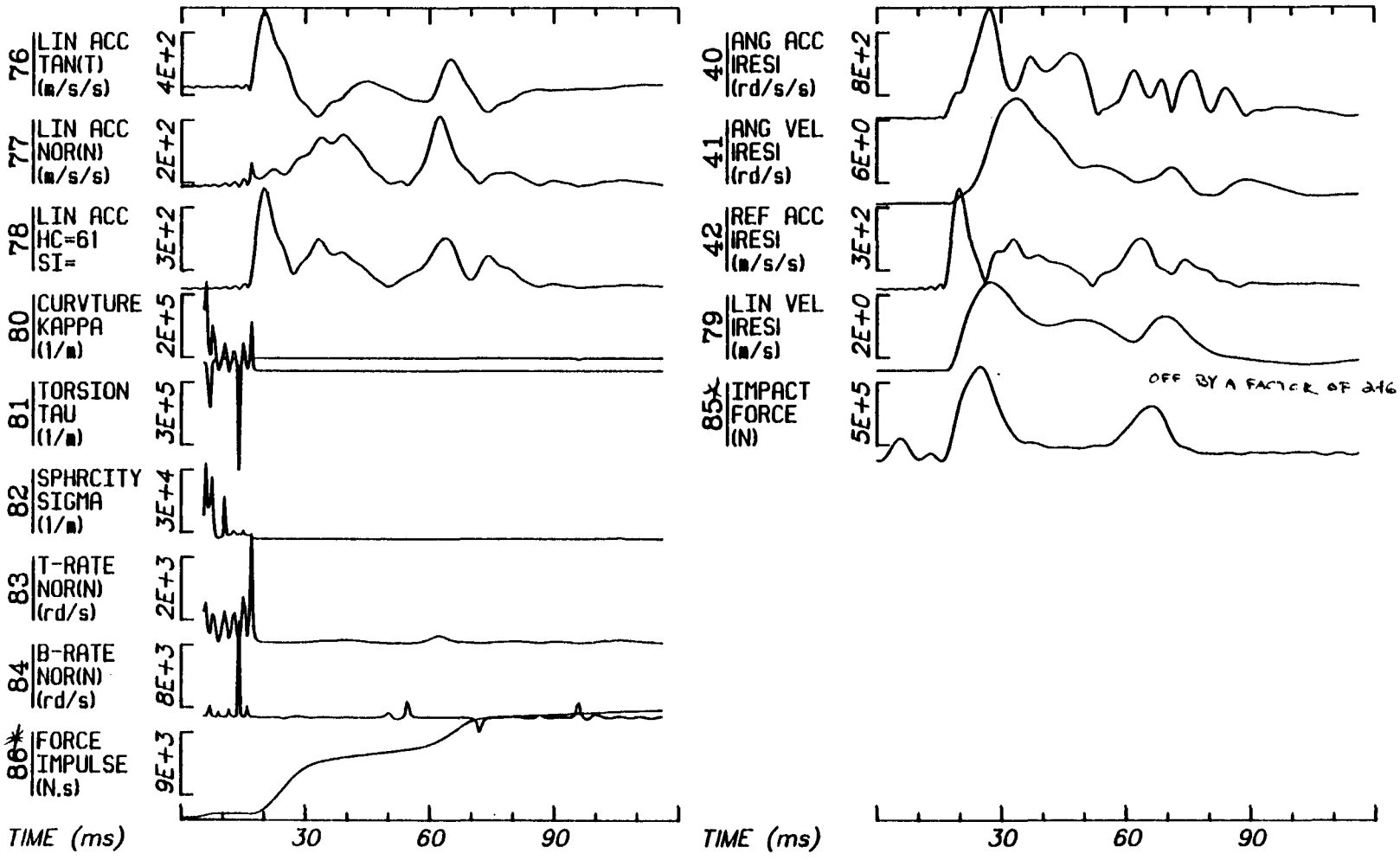

Run ID: 81H412 Tape: 3D9X-RES File: 61 Date: JUN 9, 1982 Sheet: 5/5

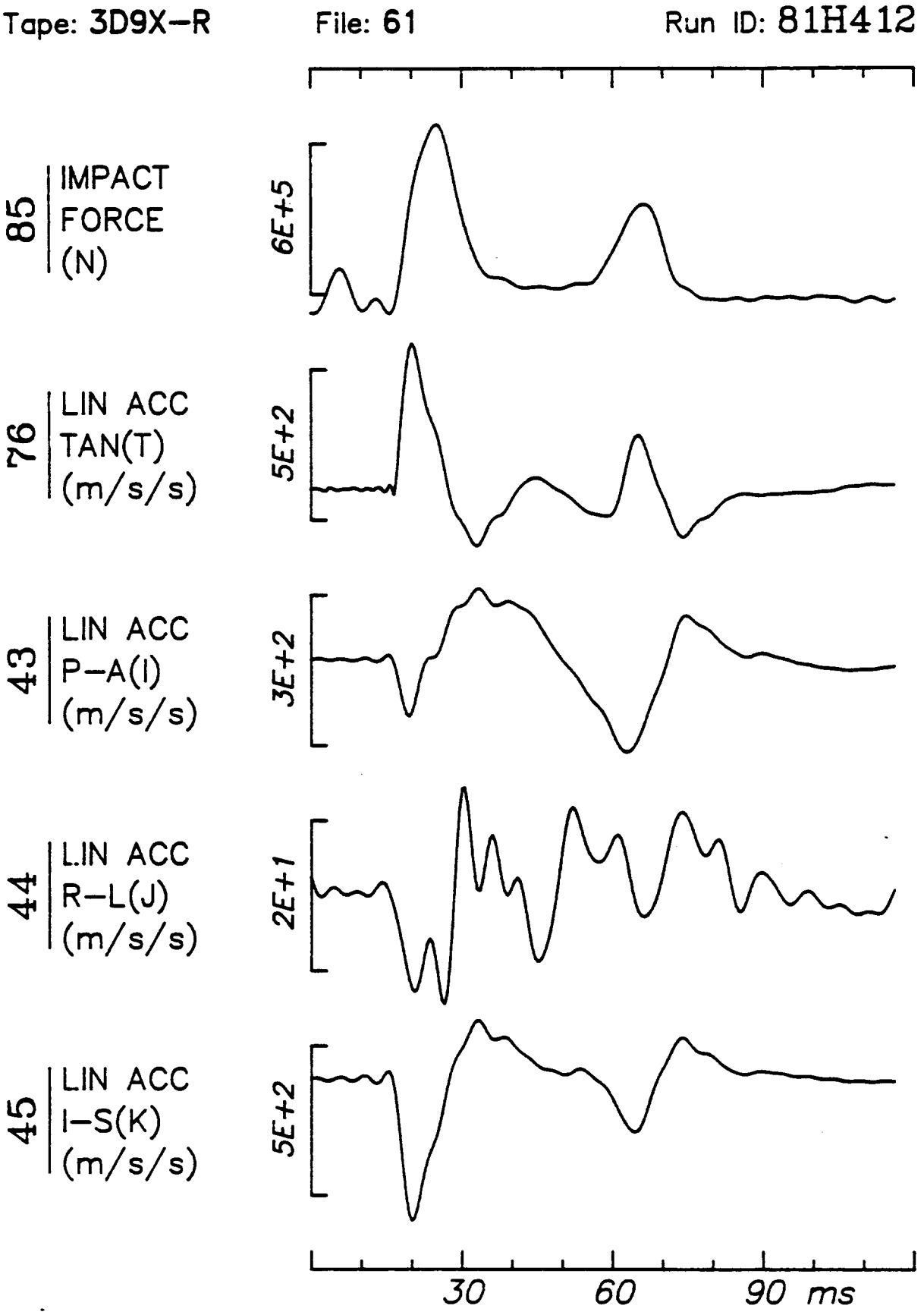
Tape: 3D9X-R
File: 61
Run ID: 81H412
85
IMPACT
FORCE
(N)
6E+5
76
LIN ACC
TAN(T)
(m/s/s)
5E+2
43
LIN ACC
P-A(I)
(m/s/s)
3E+2
44
LIN ACC
R-L(J)
(m/s/s)
2E+1
45
LIN ACC
I-S(K)
(m/s/s)
5E+2
30
60
90 ms

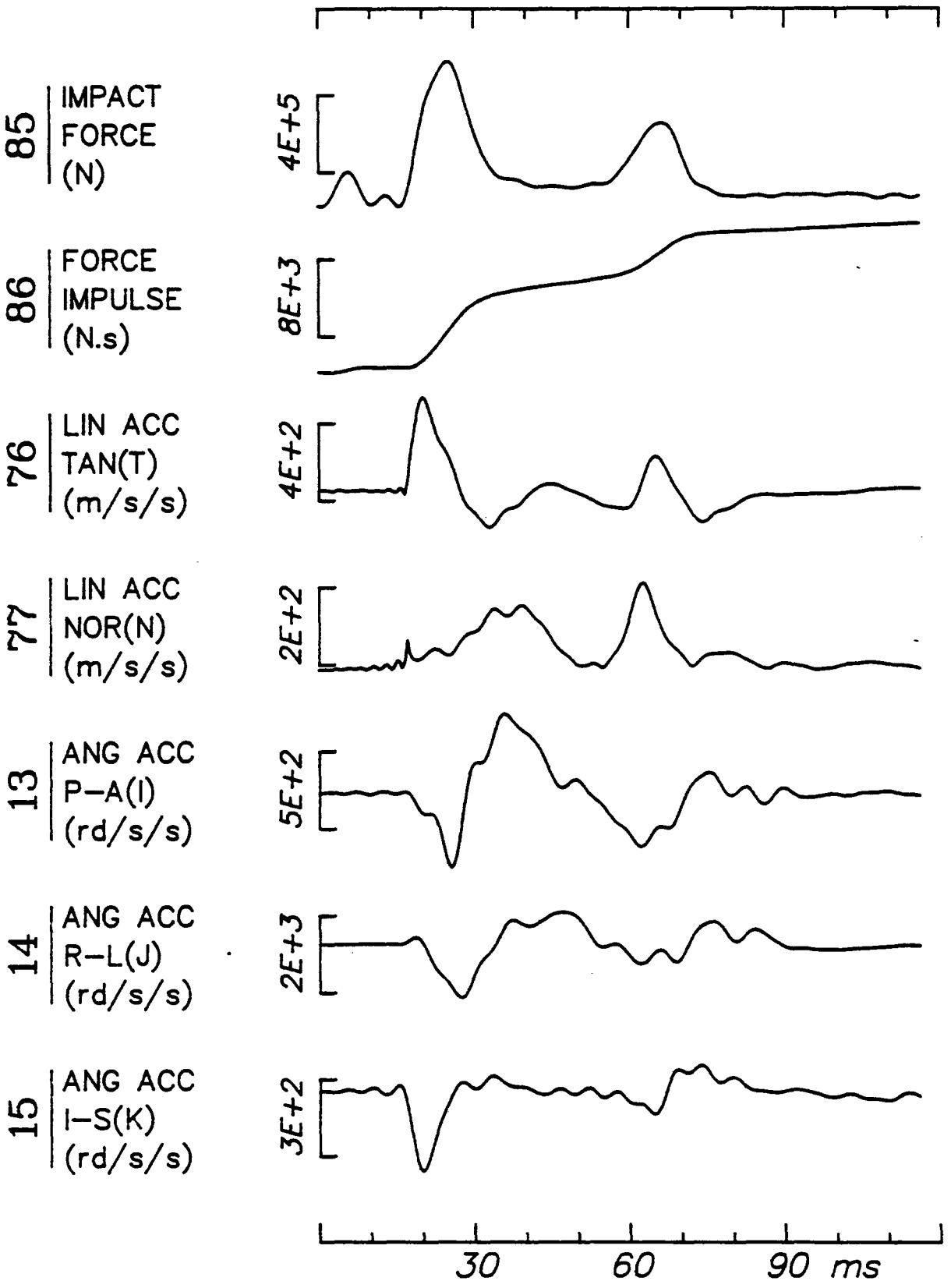
Tape: 3D9X-R
File: 61
Run ID: 81H412
85
IMPACT
FORCE
(N)
4E+5
86
FORCE
IMPULSE
(N.s)
8E+3
76
LIN ACC
TAN(T)
(m/s/s)
4E+2
77
LIN ACC
NOR(N)
(m/s/s)
2E+2
13
ANG ACC
P-A(I)
(rd/s/s)
5E+2
14
ANG ACC
R-L(J)
(rd/s/s)
2E+3
15
ANG ACC
I-S(K)
(rd/s/s)
3E+2
30
60
90 ms

APPENDIX C

KINEMATIC RESPONSE: TRANSFER FUNCTIONS

Unorthodox techniques are used in this project to obtain the mechanical impedance of the system as a function of frequencies. The method assumes that the system is time-invariant and linear, so that the principle of superposition may be applied. The method further assumes that the initial conditions of the system are all zero, allowing one to conclude that the magnitude of response at any given frequency is the result of an excitation of the same frequency.

Armed with these reasonable assumptions, and with the understanding that any irregular function of time (e.g., impact force, acceleration response) may be considered as one period of a periodic function, each of the input and output quantities were transformed to the frequency domain, resulting in a frequency spectrum at discrete frequencies ranging from the fundamental to the Nyquist rate. The fundamental is equal to the inverse of the signal duration, while the Nyquist rate is equal to half of the sampling rate. However, because of rounding errors of the Fast Fourier Transform (FFT), and since magnitudes of components in the upper frequency range are small and approach the rounding error, output/input ratio is noisy and should not be considered highly reliable.

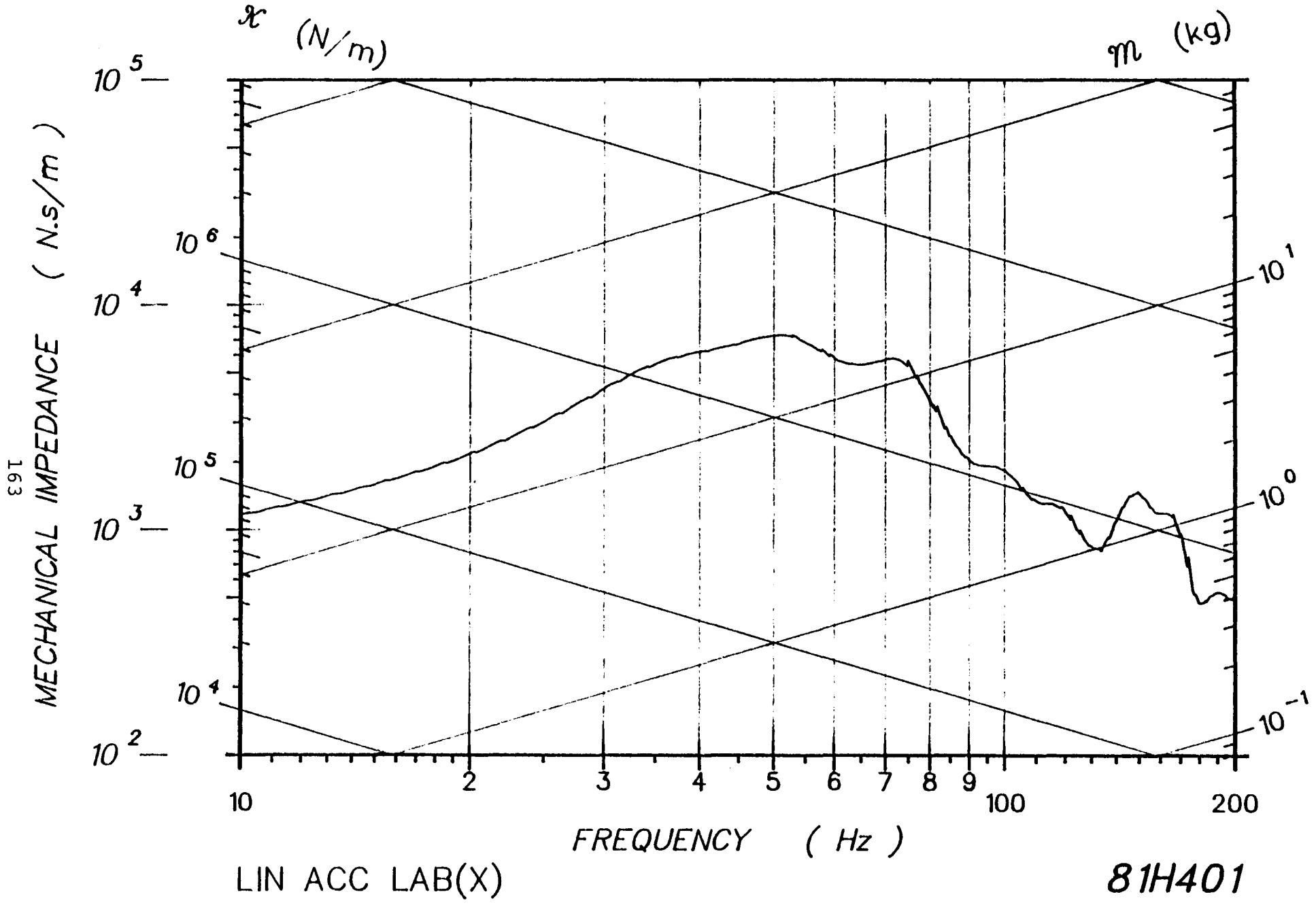
$\mathcal{K}$ (N/m)
$\mathcal{M}$ (kg)
10^5
10^4
10^3
10^2
10^6
10^5
10^4
10^1
10^0
10^{-1}
MECHANICAL IMPEDANCE (N.s/m)
10
2
3
4
5
6
7
8
9
100
200
FREQUENCY (Hz)
LIN ACC LAB(X)
81H401

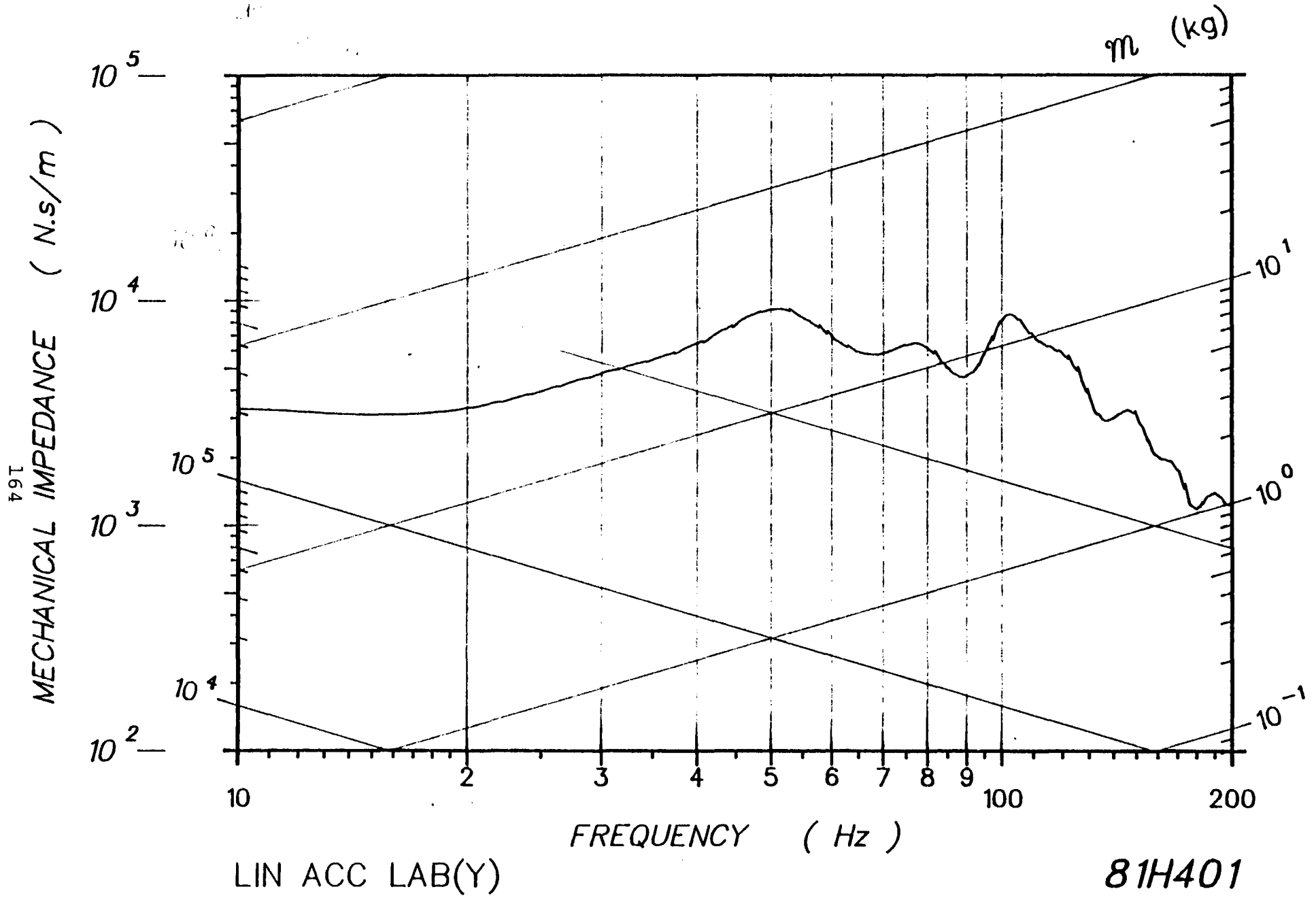
m (kg)
MECHANICAL IMPEDANCE (N.s/m)
10^5
10^4
10^3
10^2
10^5
10^4
10^1
10^0
10^{-1}
10
2
3
4
5
6
7
8
9
100
200
FREQUENCY (Hz)
LIN ACC LAB(Y)
81H401

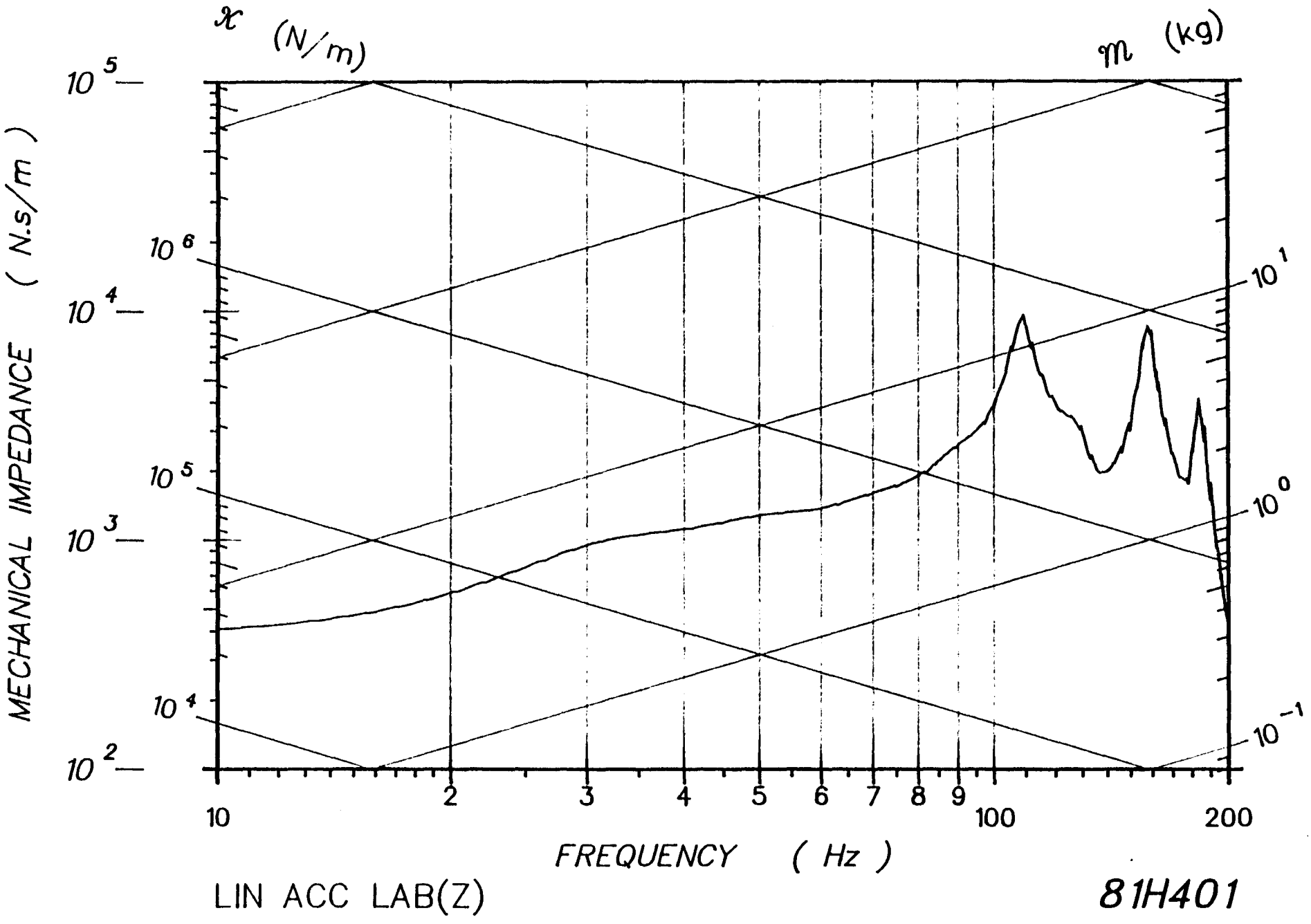
x (N/m)
m (kg)
MECHANICAL IMPEDANCE (N.s/m)
10 5
10 4
10 3
10 2
10 6
10 5
10 4
10 1
10 0
10 -1
10
2
3
4
5
6
7
8
9
100
200
FREQUENCY (Hz)
LIN ACC LAB(Z)
81H401

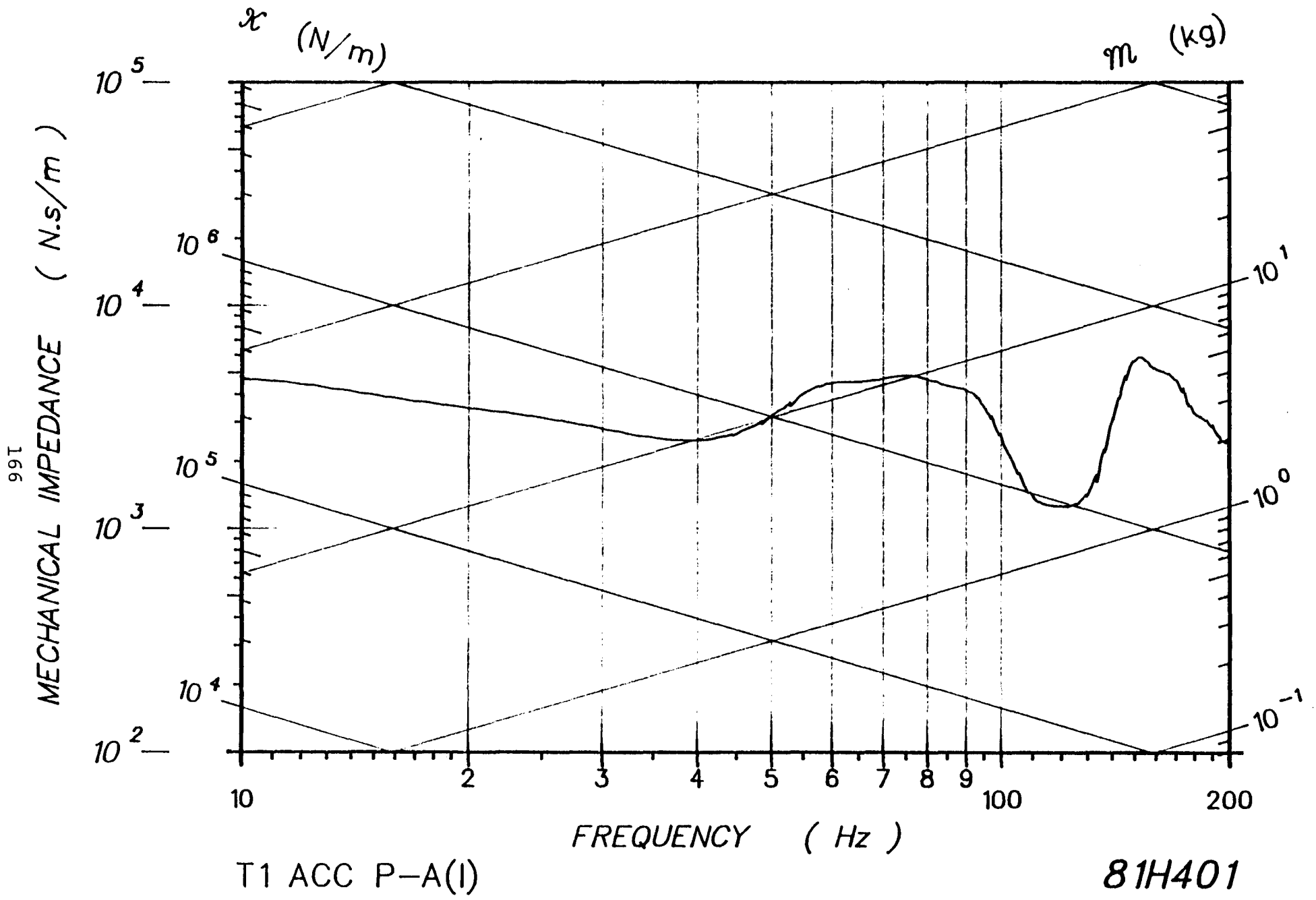
x (N/m)
m (kg)
MECHANICAL IMPEDANCE (N.s/m)
10 5
10 4
10 3
10 2
10 6
10 5
10 4
10 1
10 0
10 -1
10
2
3
4
5
6
7
8
9
100
200
FREQUENCY (Hz)
T1 ACC P-A(I)
81H401

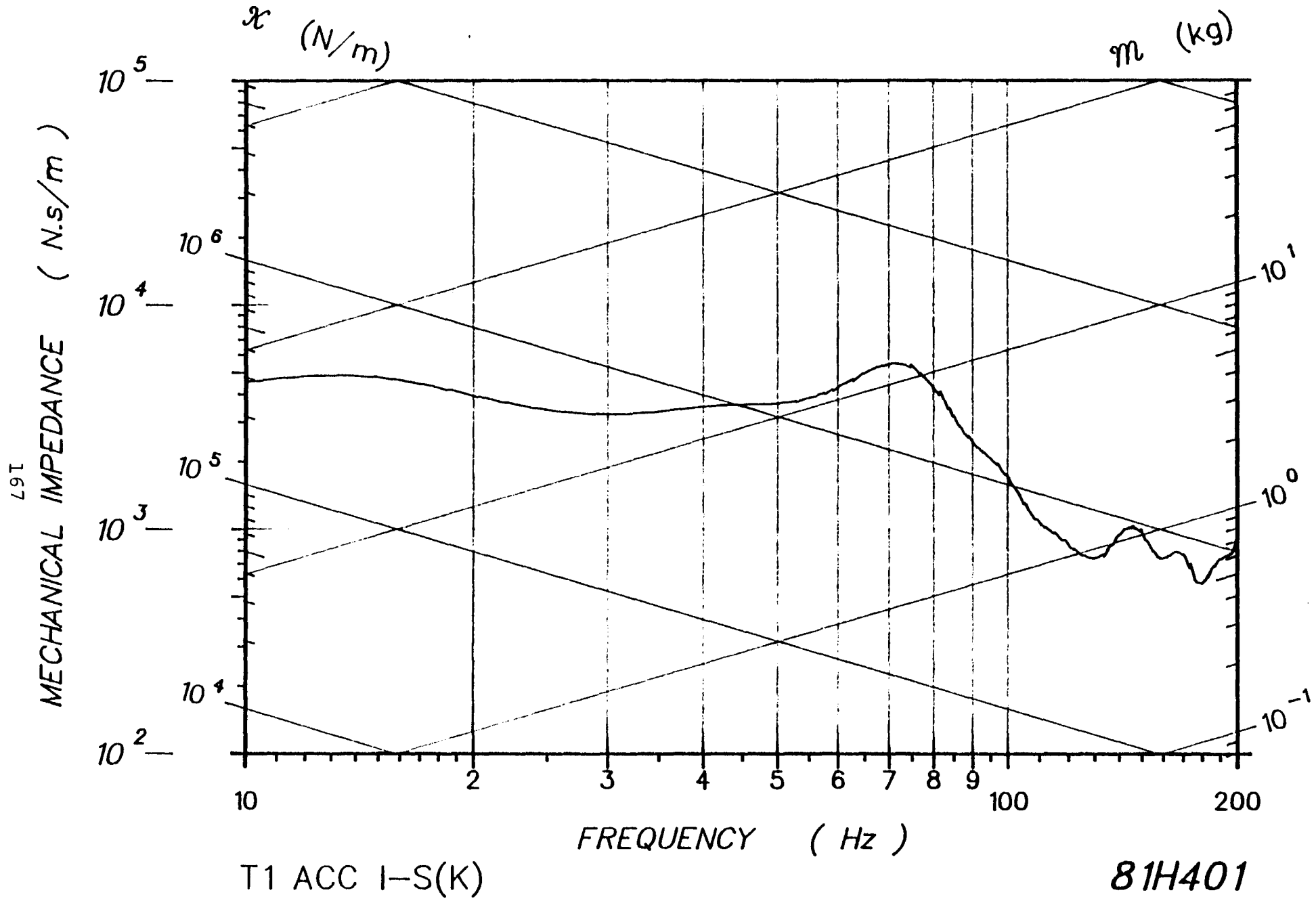

T1 ACC I–S(K)

81H401

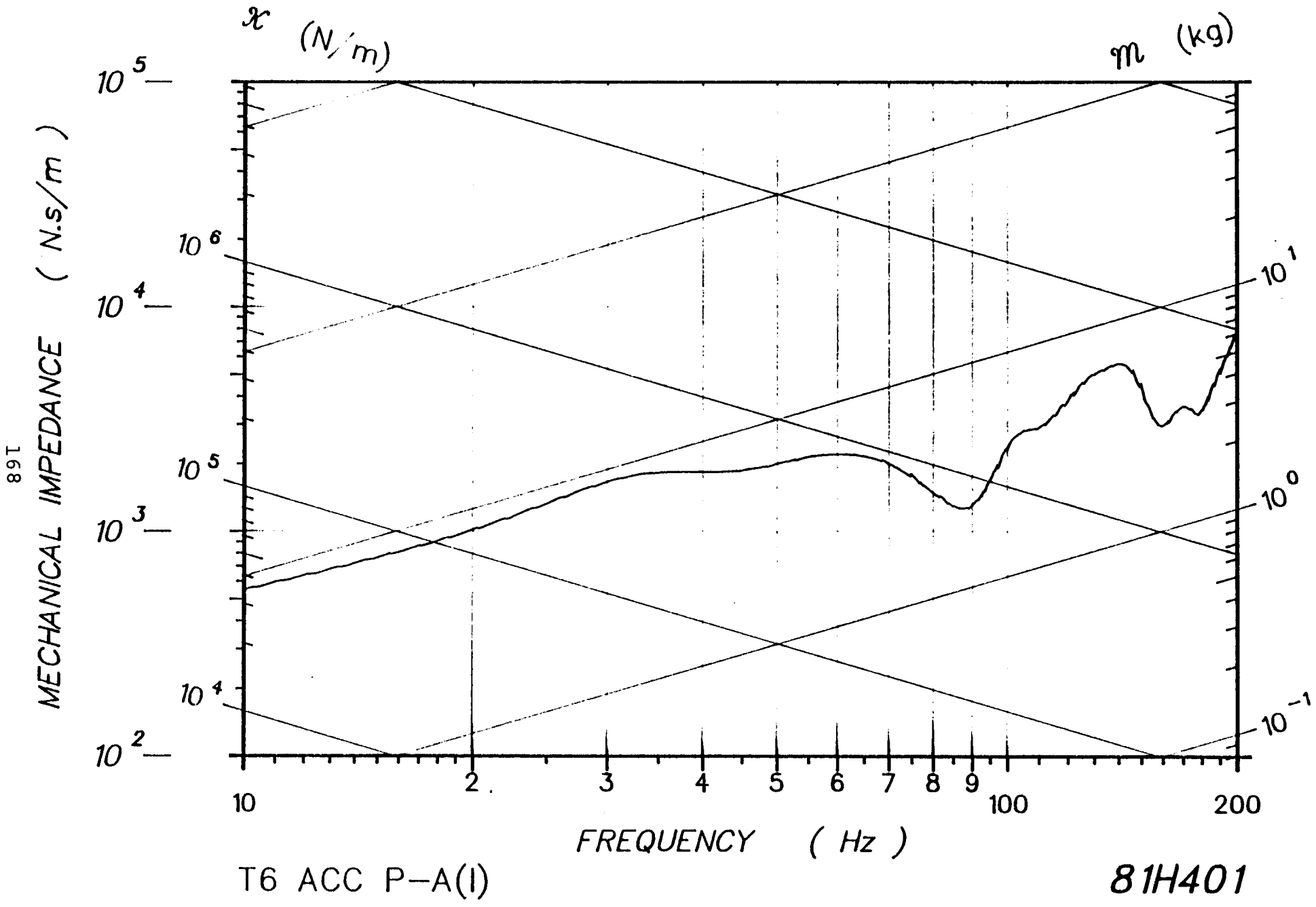
$\mathcal{K}$ (N/m)
$\mathcal{M}$ (kg)
MECHANICAL IMPEDANCE (N.s/m)
10^5
10^4
10^3
10^2
10^6
10^5
10^4
10^1
10^0
10^{-1}
10
2
3
4
5
6
7
8
9
100
200
FREQUENCY (Hz)
T6 ACC P-A(I)
81H401

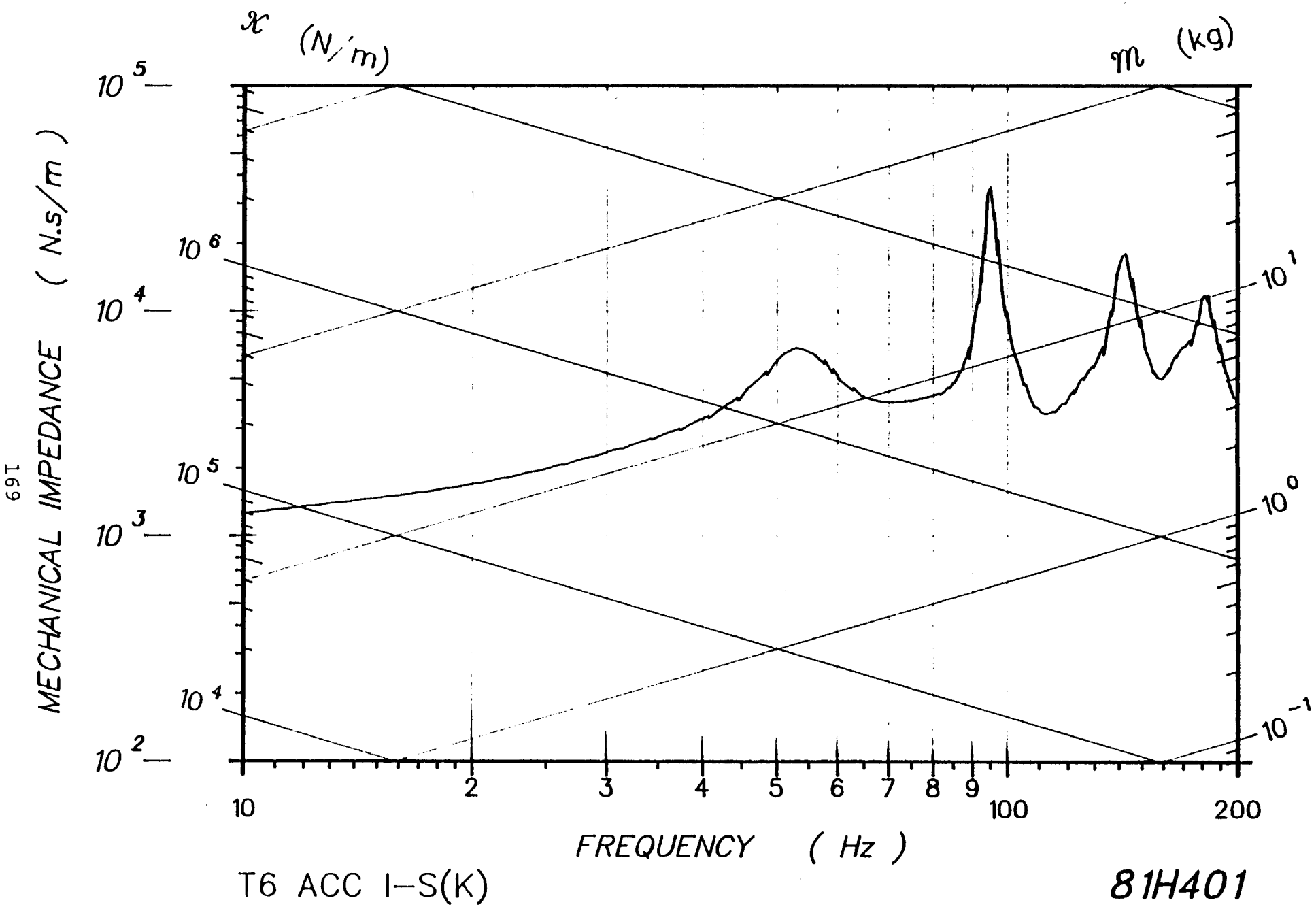
κ (N/m)
m (kg)
MECHANICAL IMPEDANCE (N.s/m)
10 5
10 4
10 3
10 2
10 6
10 5
10 4
10 1
10 0
10 −1
10
2
3
4
5
6
7
8
9
100
200
FREQUENCY (Hz)
T6 ACC I−S(K)
81H401

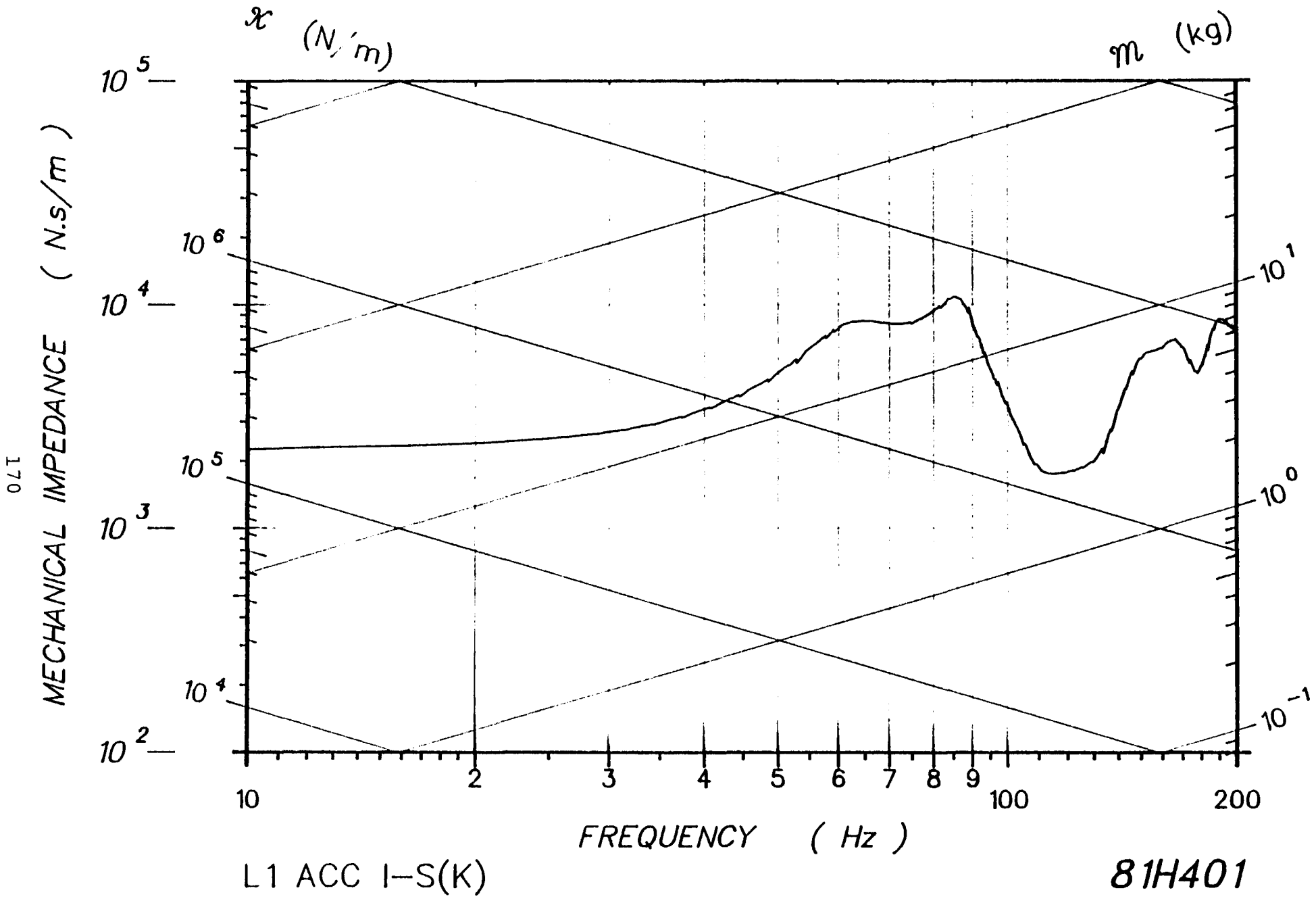
$\mathcal{K}$ (N/m)
$\mathcal{M}$ (kg)
10^5
10^4
10^3
10^2
10^6
10^5
10^4
10^1
10^0
10^{-1}
MECHANICAL IMPEDANCE (N.s/m)
10
2
3
4
5
6
7
8
9
100
200
FREQUENCY (Hz)
L1 ACC I–S(K)
81H401

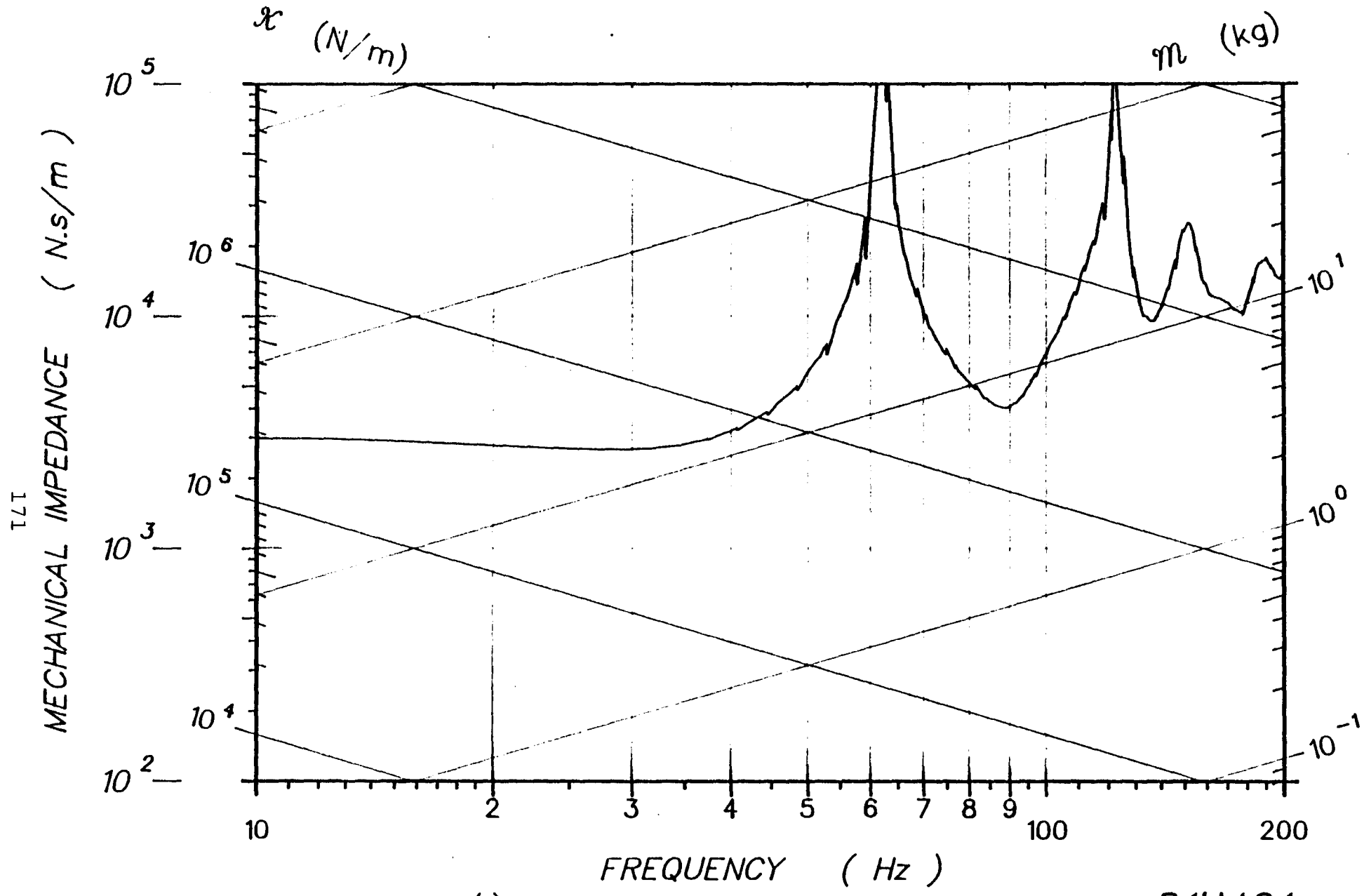

L1 ACC P–A(I)

81H401

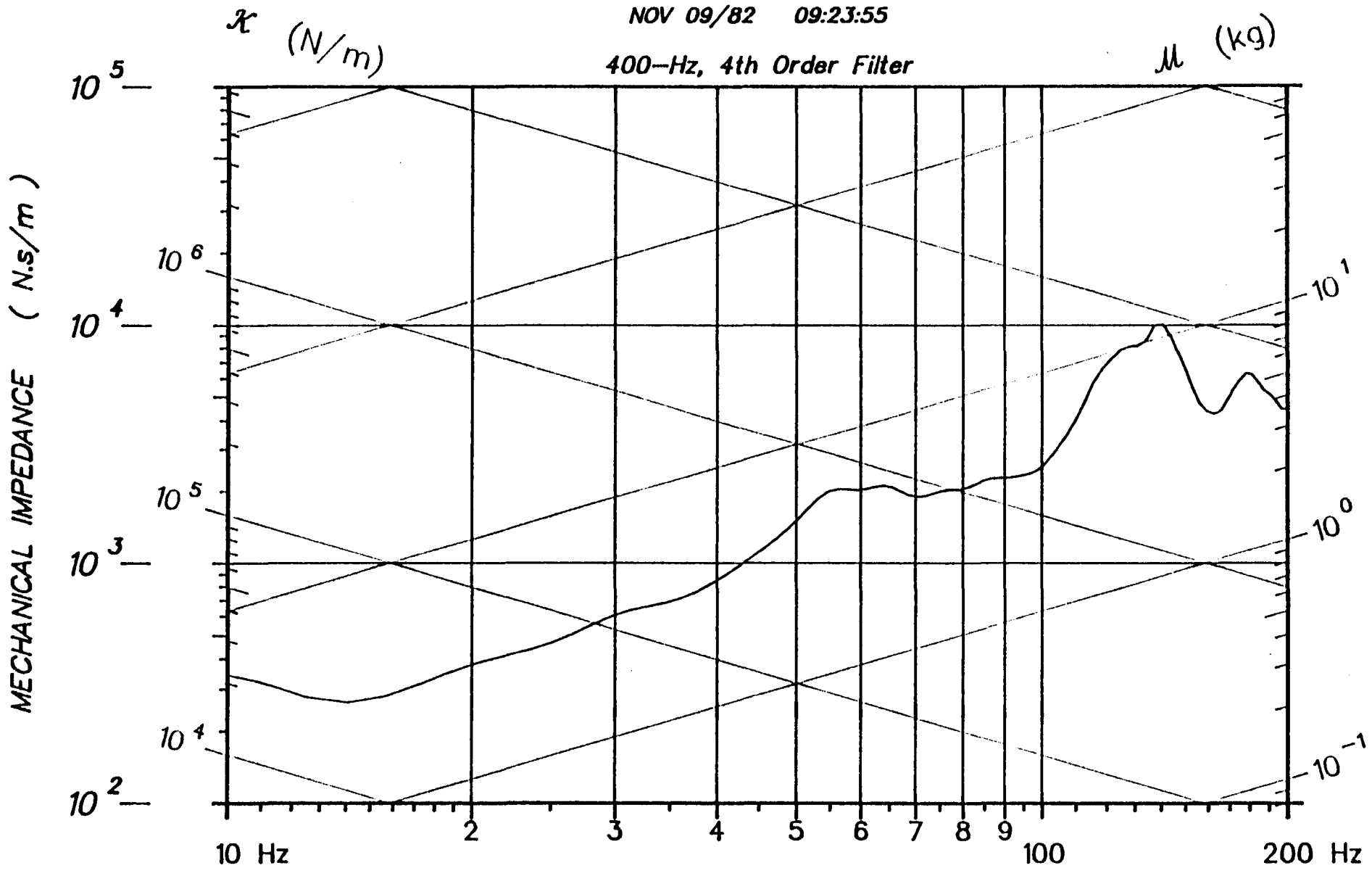

Z=F1/V1 for HEAD

81H402

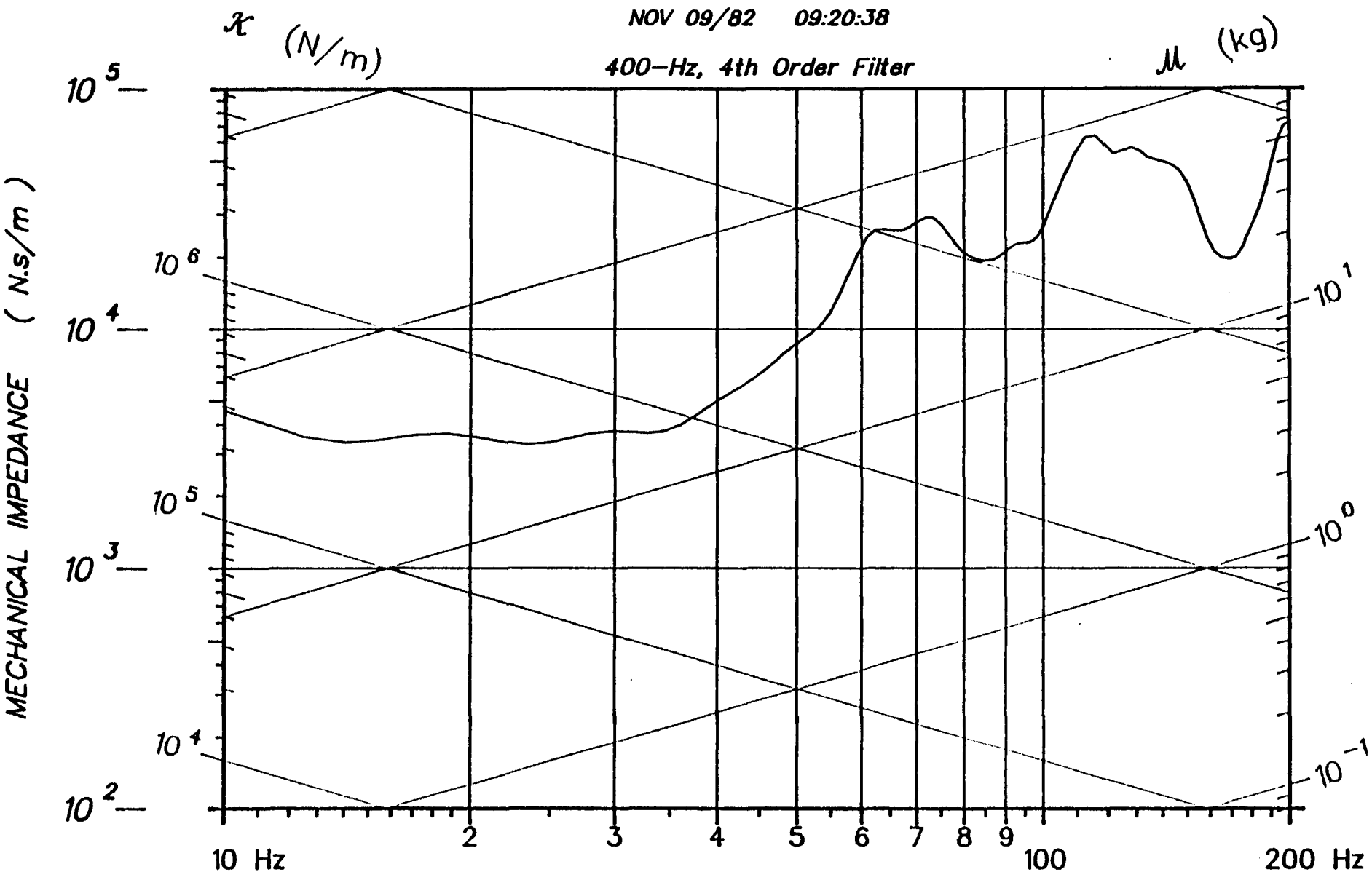
NOV 09/82 09:20:38
400-Hz, 4th Order Filter
κ (N/m)
M (kg)
MECHANICAL IMPEDANCE (N.s/m)
10 5
10 4
10 3
10 2
10 6
10 5
10 4
10 1
10 0
10 -1
10 Hz
2
3
4
5
6
7
8
9
100
200 Hz
Z=F1/V1 for L1
81H402

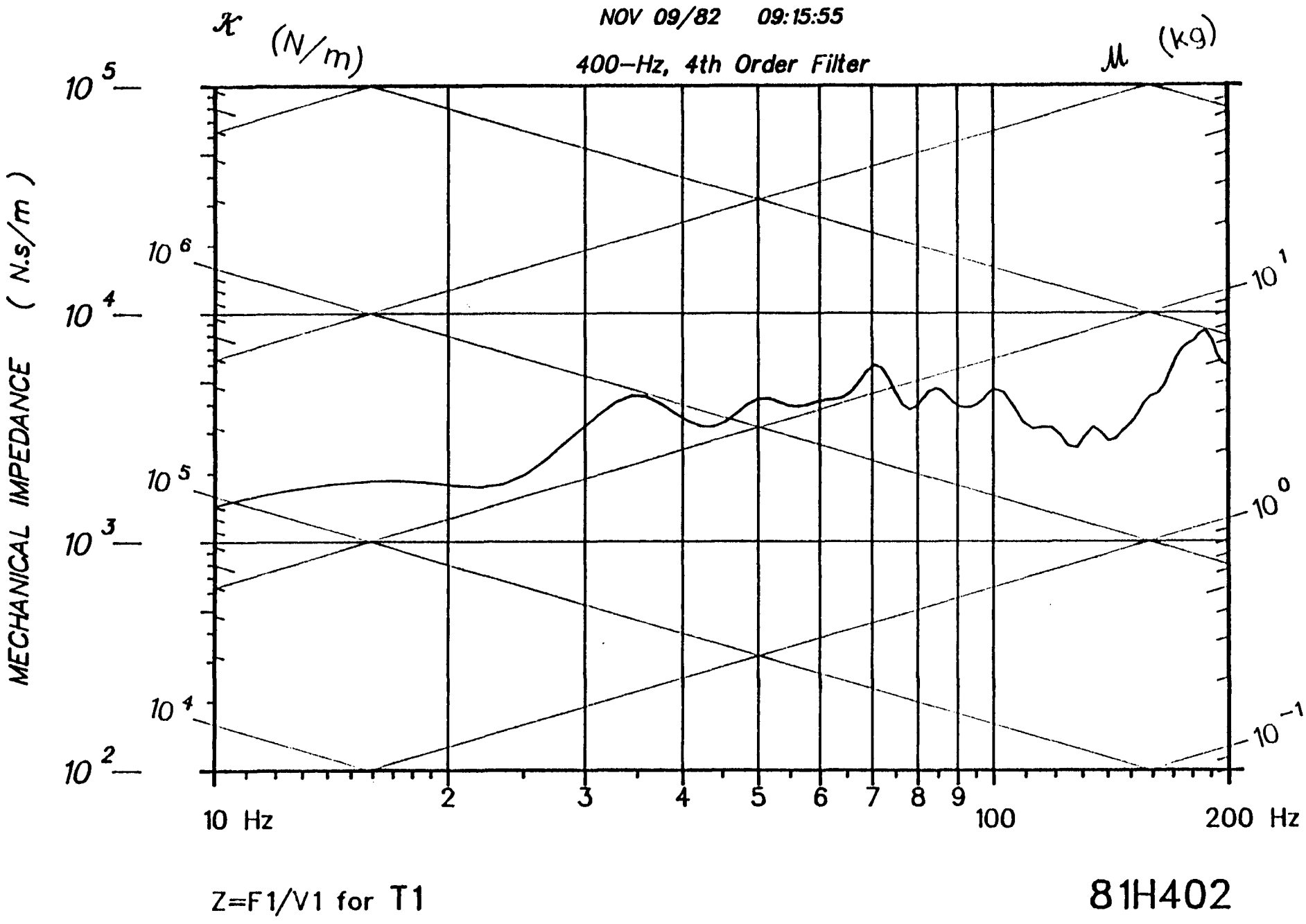
NOV 09/82 09:15:55
400-Hz, 4th Order Filter
κ (N/m)
M (kg)
MECHANICAL IMPEDANCE (N.s/m)
10 5
10 6
10 4
10 5
10 3
10 4
10 2
10 1
10 0
10 -1
10 Hz
2
3
4
5
6
7
8
9
100
200 Hz
Z=F1/V1 for T1
81H402

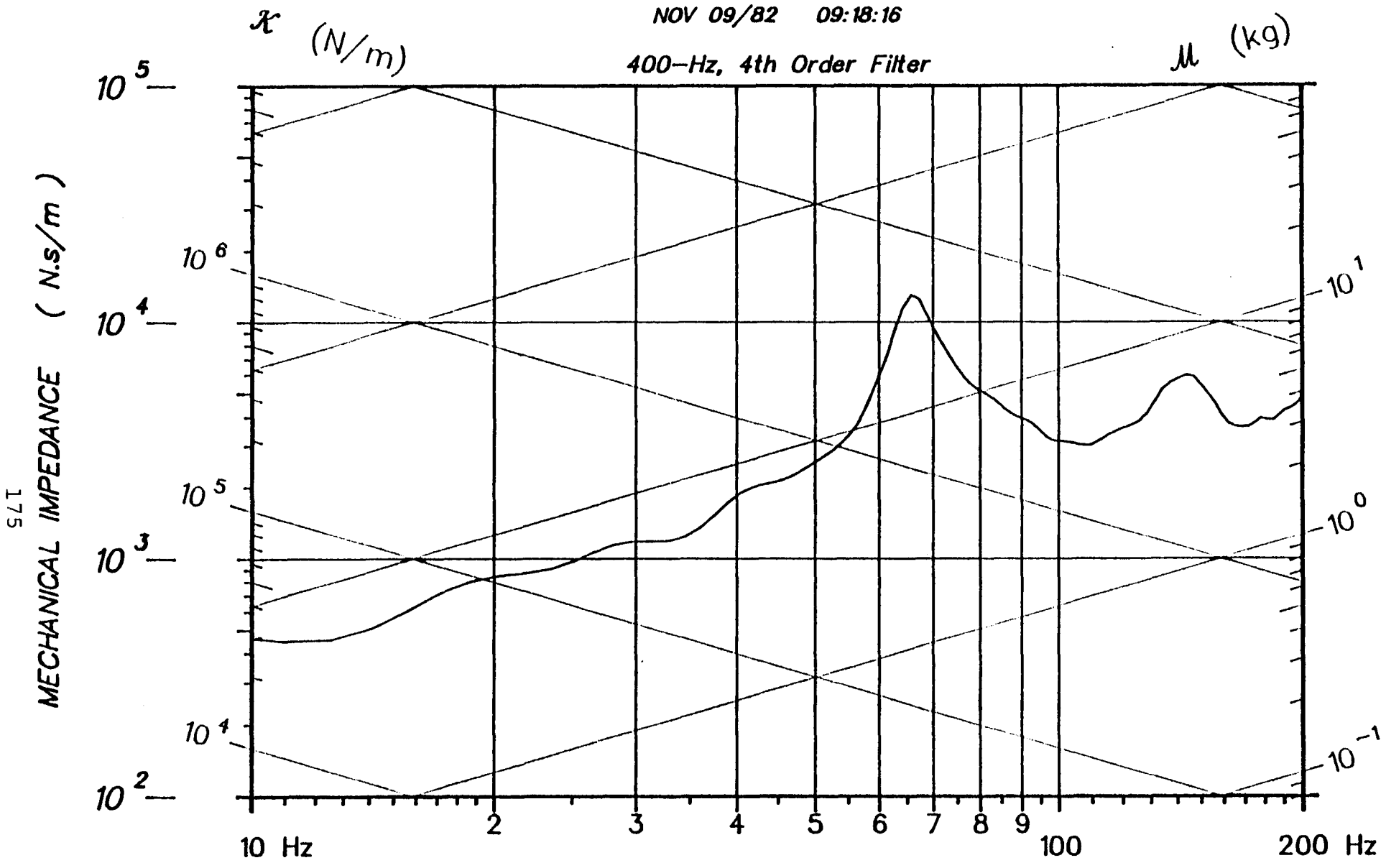

Z=F1/V1 for T6

81H402

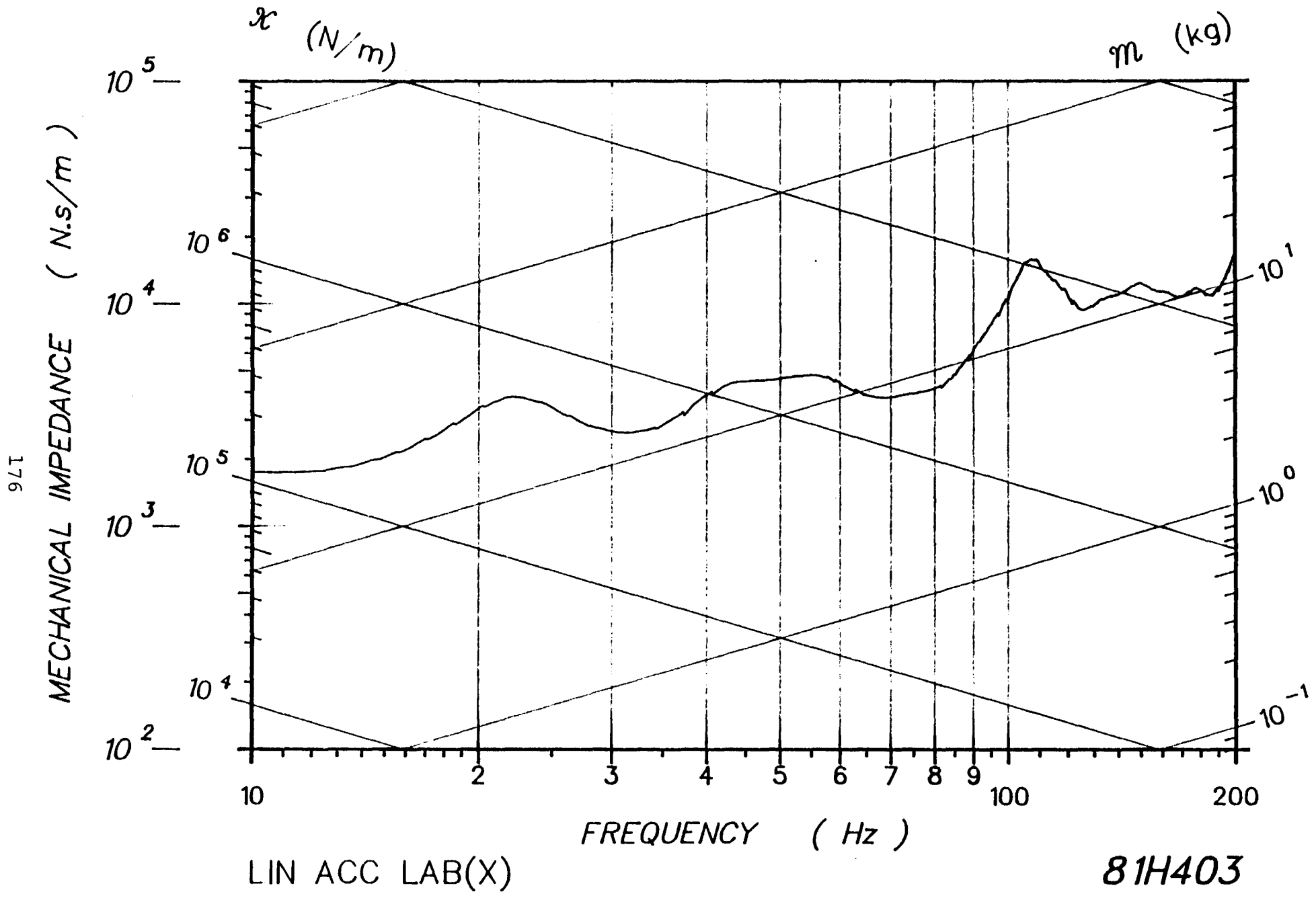
$\mathcal{K}$ (N/m)
$\mathcal{M}$ (kg)
MECHANICAL IMPEDANCE (N.s/m)
10^5
10^4
10^3
10^2
10^6
10^5
10^4
10^1
10^0
10^{-1}
10
2
3
4
5
6
7
8
9
100
200
FREQUENCY (Hz)
LIN ACC LAB(X)
81H403

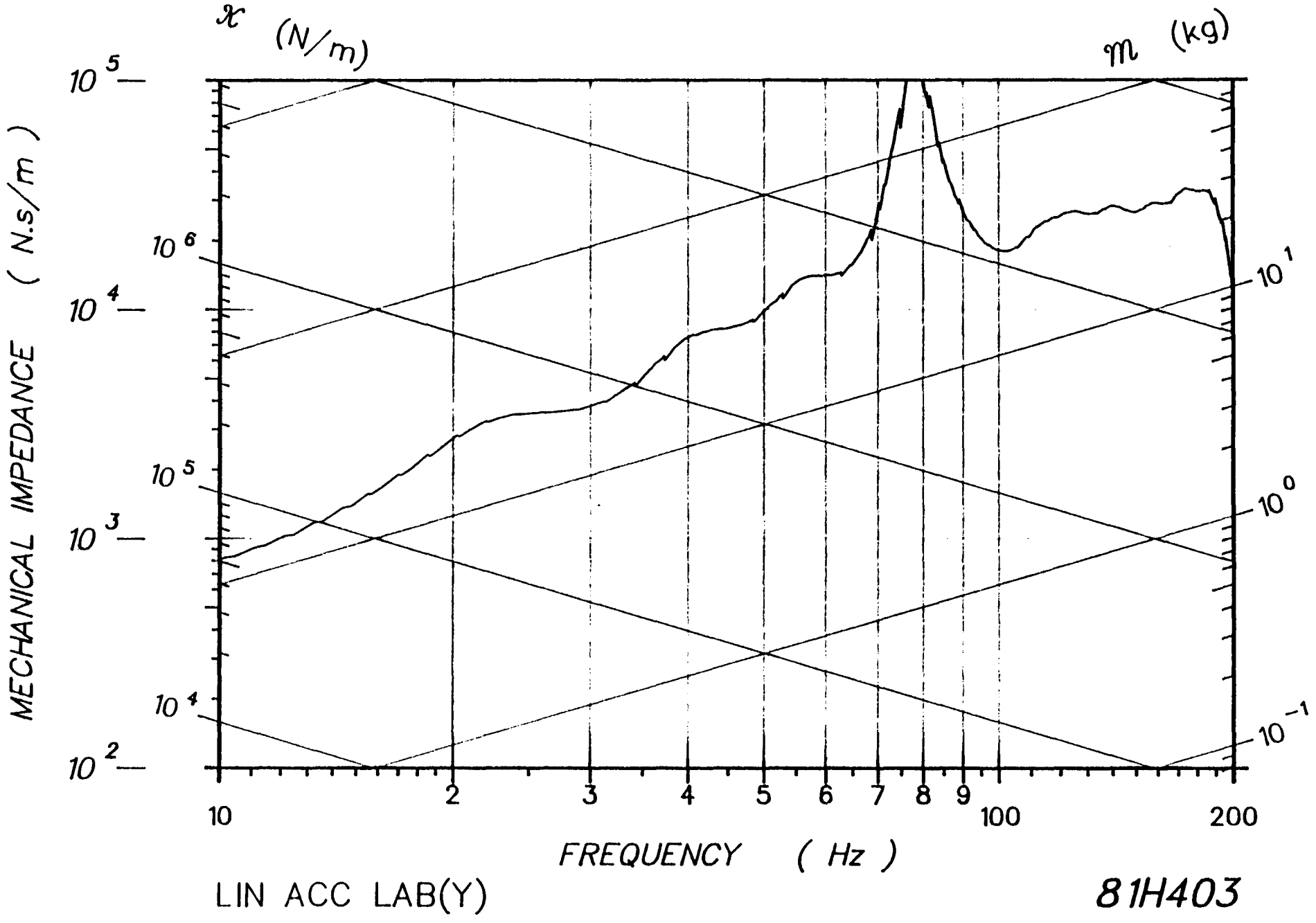
$\mathcal{K}$ (N/m)
$\mathcal{M}$ (kg)
10^5
10^4
10^3
10^2
10^6
10^5
10^4
10^1
10^0
10^{-1}
MECHANICAL IMPEDANCE (N.s/m)
10
2
3
4
5
6
7
8
9
100
200
FREQUENCY (Hz)
LIN ACC LAB(Y)
81H403

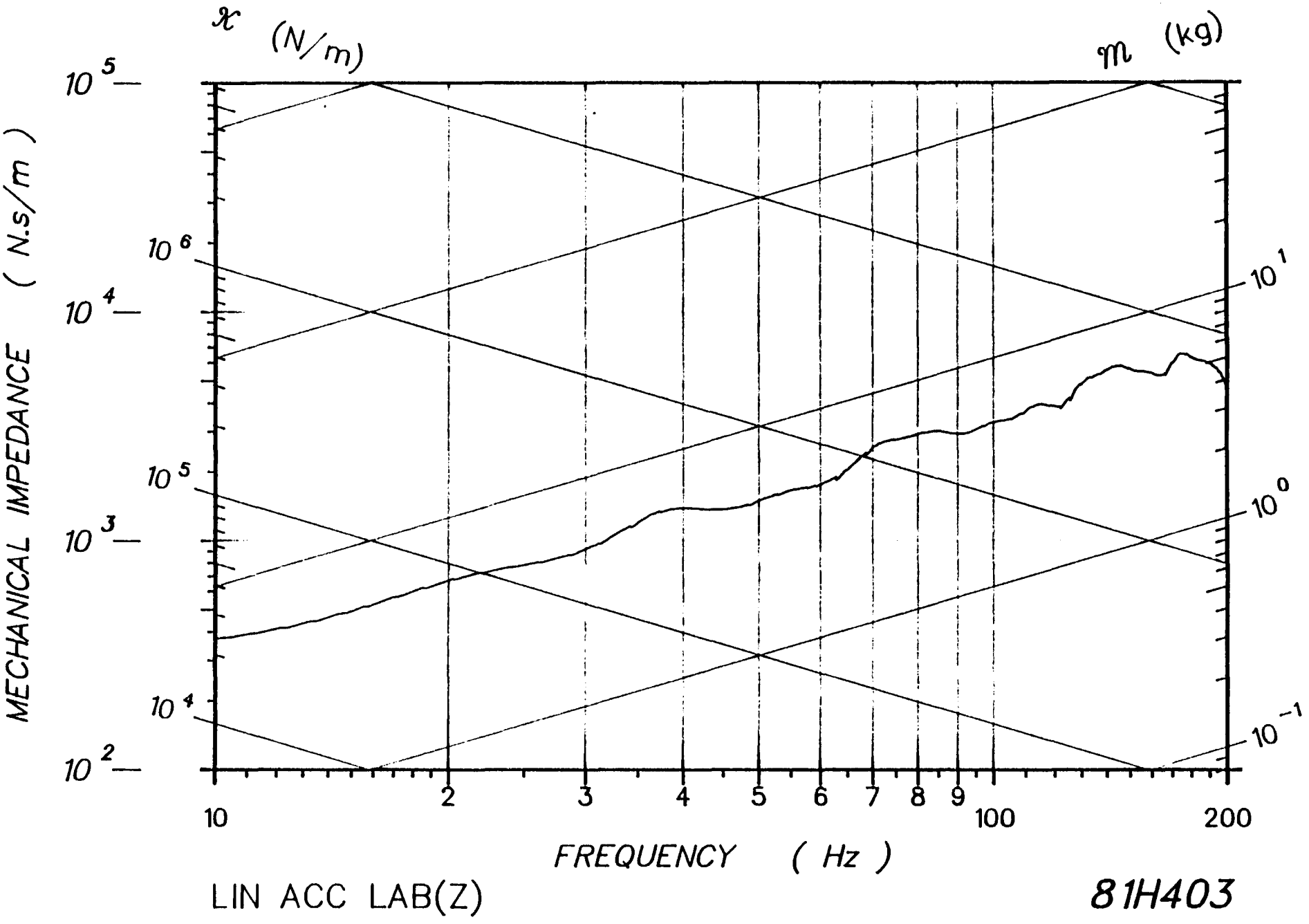
$\mathcal{K}$ (N/m)
$\mathcal{M}$ (kg)
10^5
10^4
10^3
10^2
10^6
10^5
10^4
10^1
10^0
10^{-1}
MECHANICAL IMPEDANCE (N.s/m)
10
2
3
4
5
6
7
8
9
100
200
FREQUENCY (Hz)
LIN ACC LAB(Z)
81H403

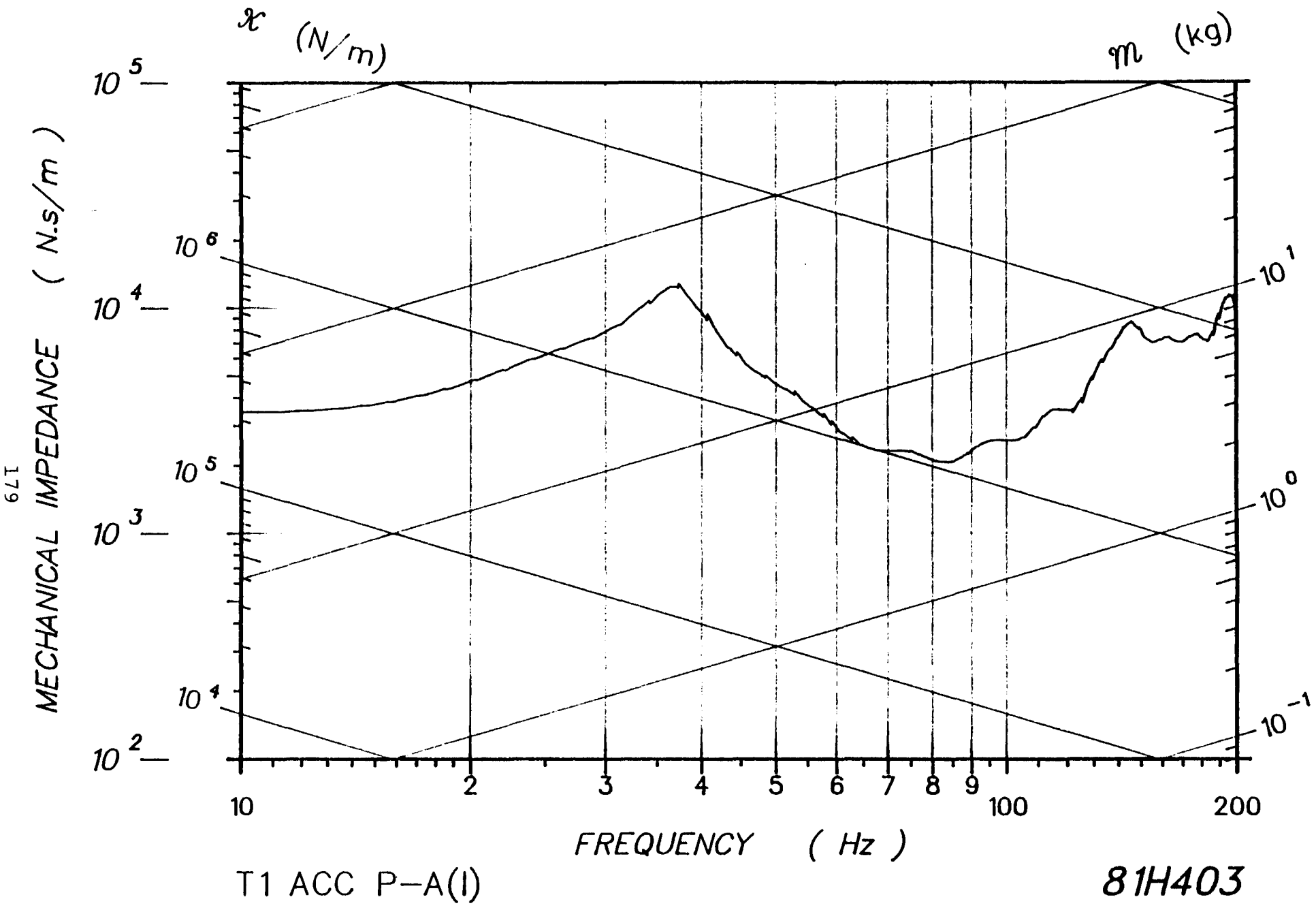

T1 ACC P–A(I)

81H403

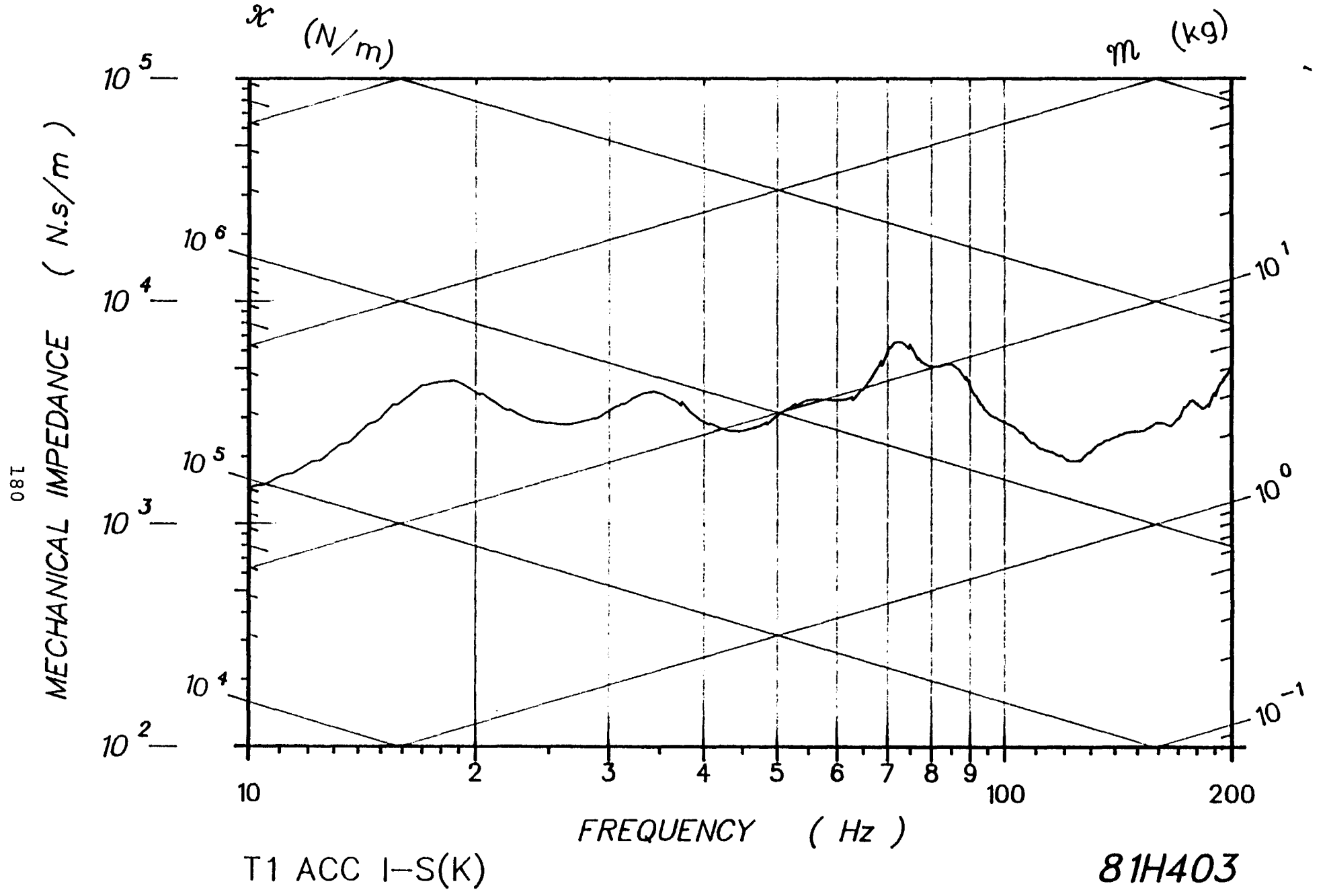
x (N/m)
m (kg)
MECHANICAL IMPEDANCE (N.s/m)
10 5
10 4
10 3
10 2
10 6
10 5
10 4
10 1
10 0
10 −1
10
2
3
4
5
6
7
8
9
100
200
FREQUENCY (Hz)
T1 ACC I−S(K)
81H403

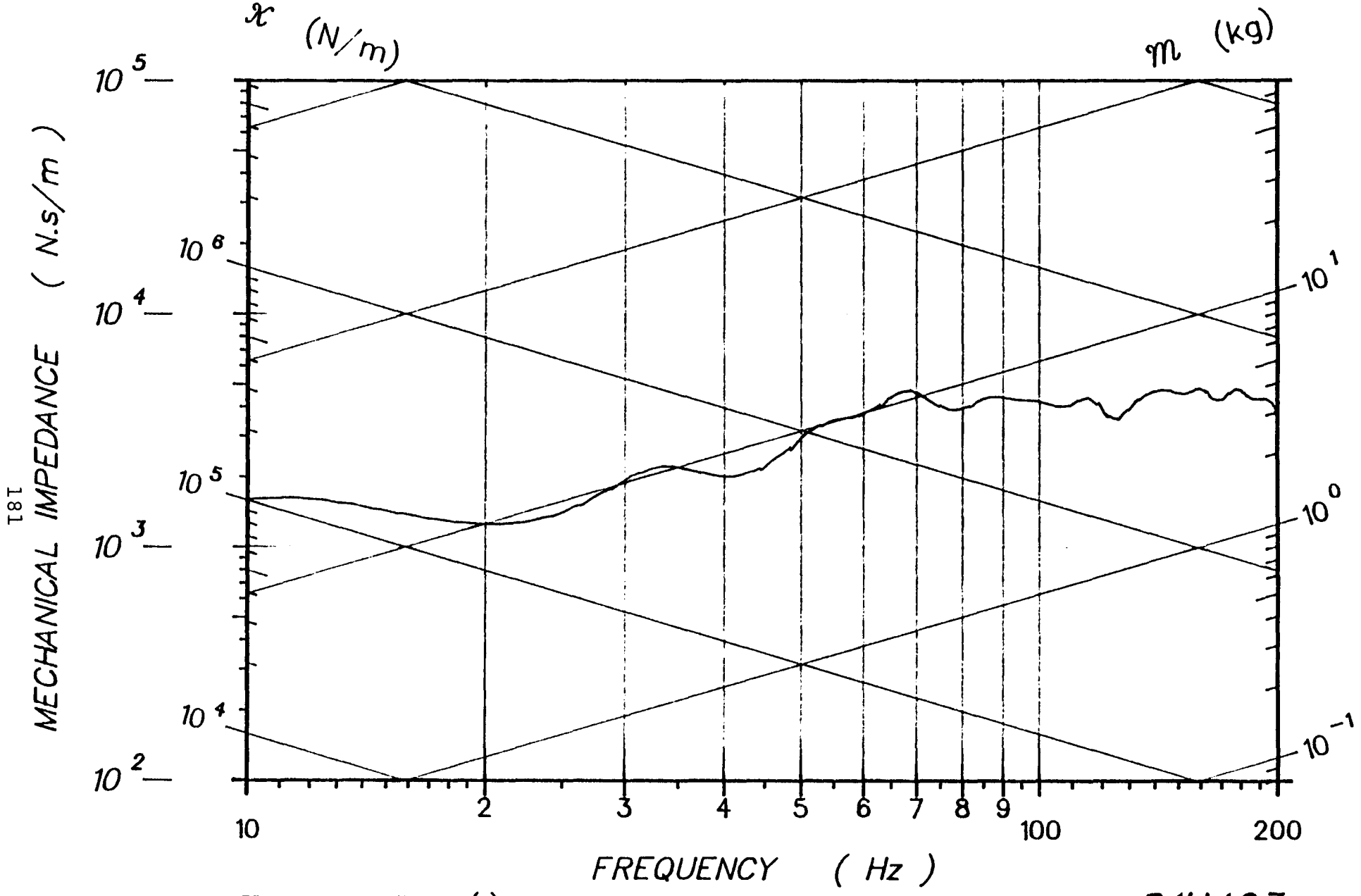

T6 ACC P–A(I)

81H403

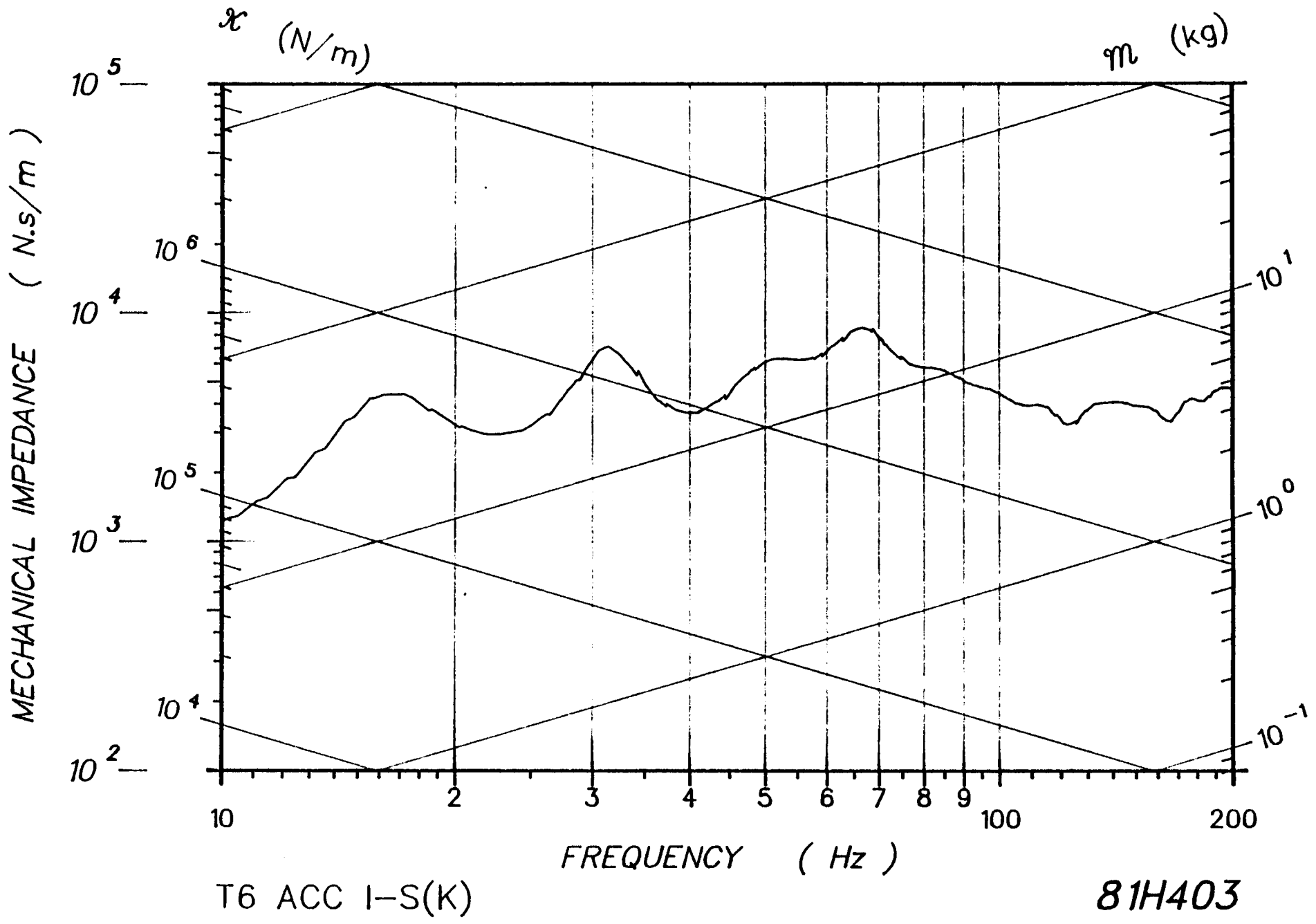
$\mathcal{K}$ (N/m)
$\mathcal{M}$ (kg)
MECHANICAL IMPEDANCE (N.s/m)
10^5
10^4
10^3
10^2
10^6
10^5
10^4
10^1
10^0
10^{-1}
10
2
3
4
5
6
7
8
9
100
200
FREQUENCY (Hz)
T6 ACC I–S(K)
81H403

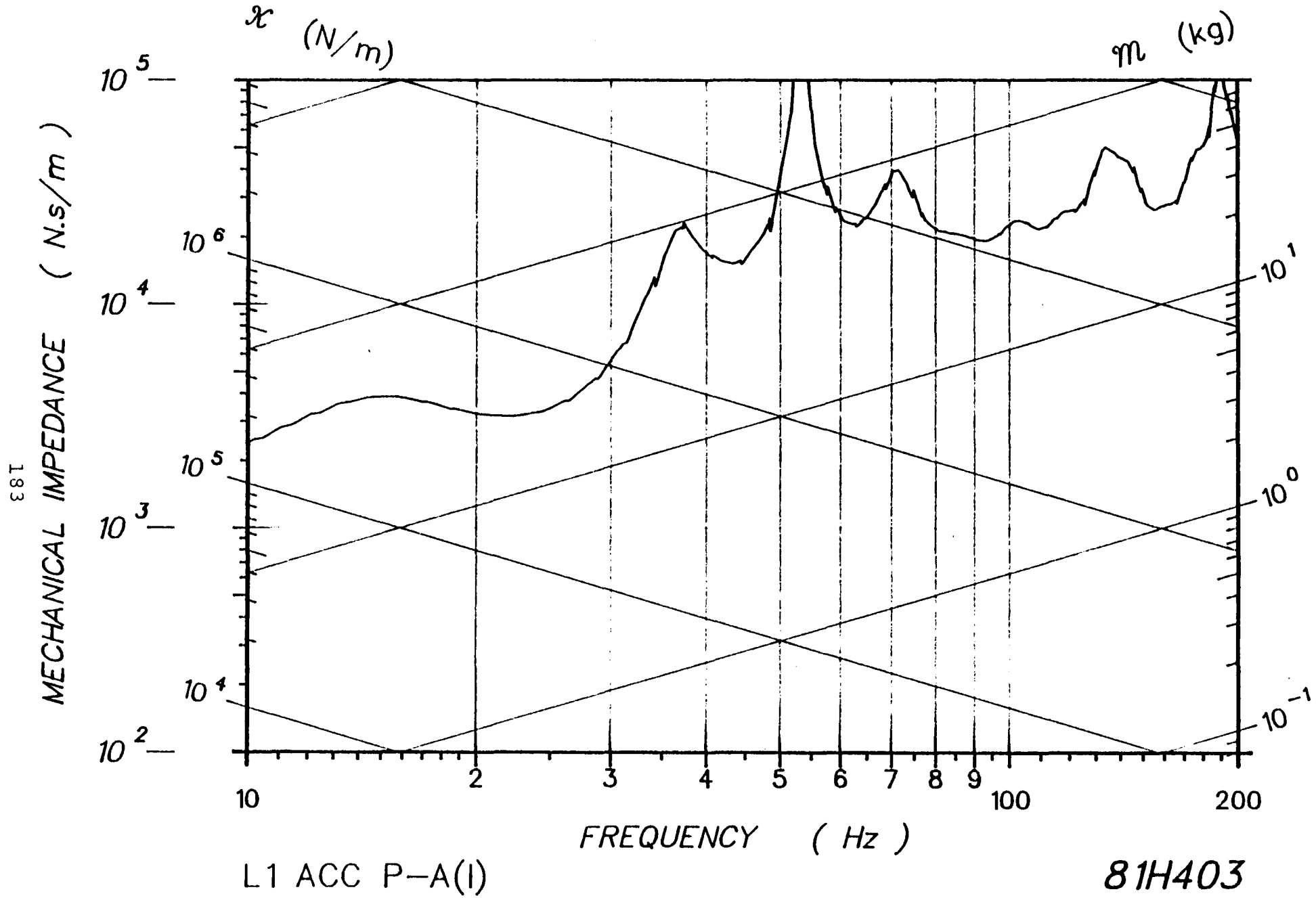

L1 ACC P–A(I)

81H403

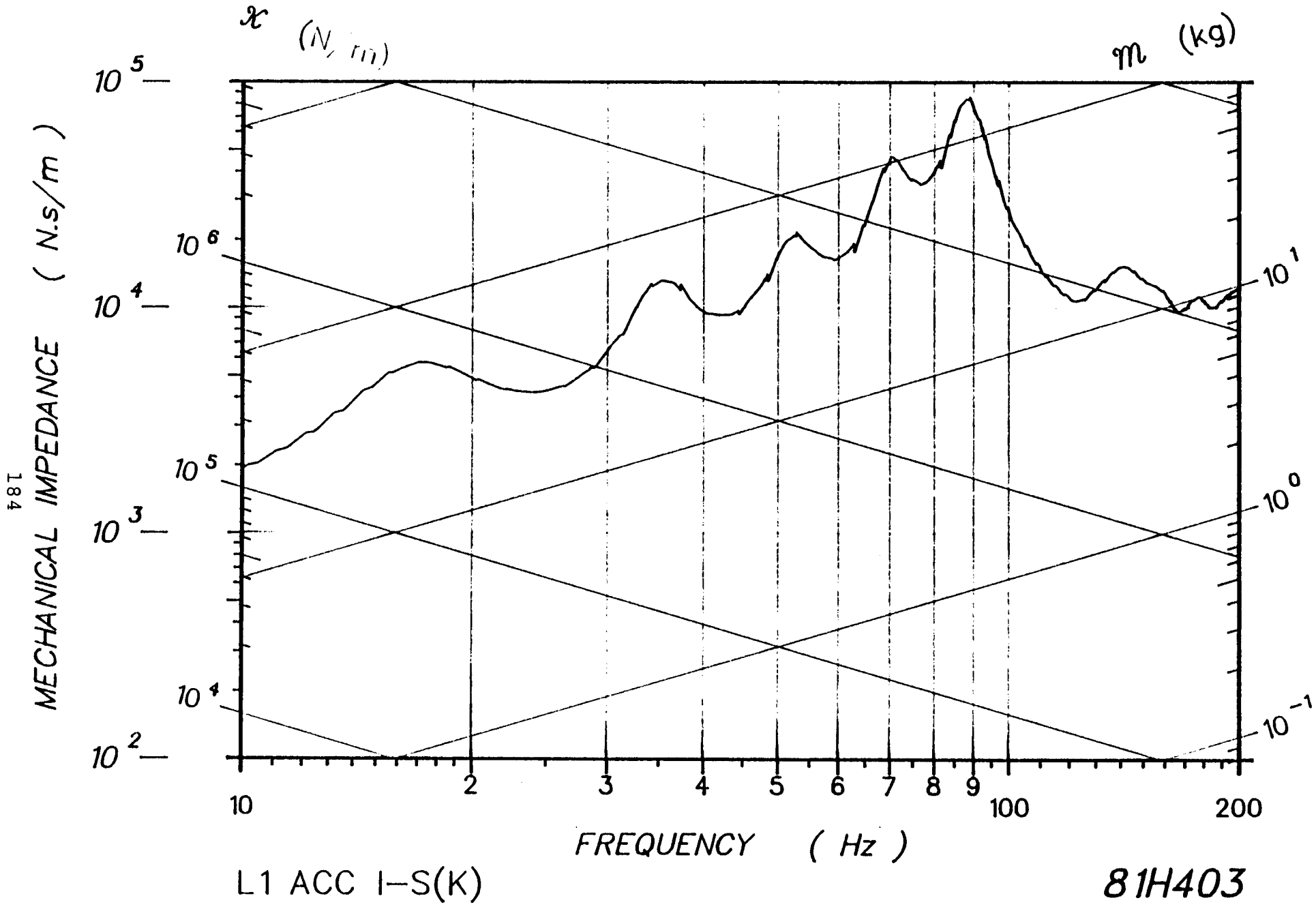
x (N/m)
m (kg)
MECHANICAL IMPEDANCE (N.s/m)
10 5
10 4
10 3
10 2
10 6
10 5
10 4
10 1
10 0
10 -1
10
2
3
4
5
6
7
8
9
100
200
FREQUENCY (Hz)
L1 ACC I-S(K)
81H403

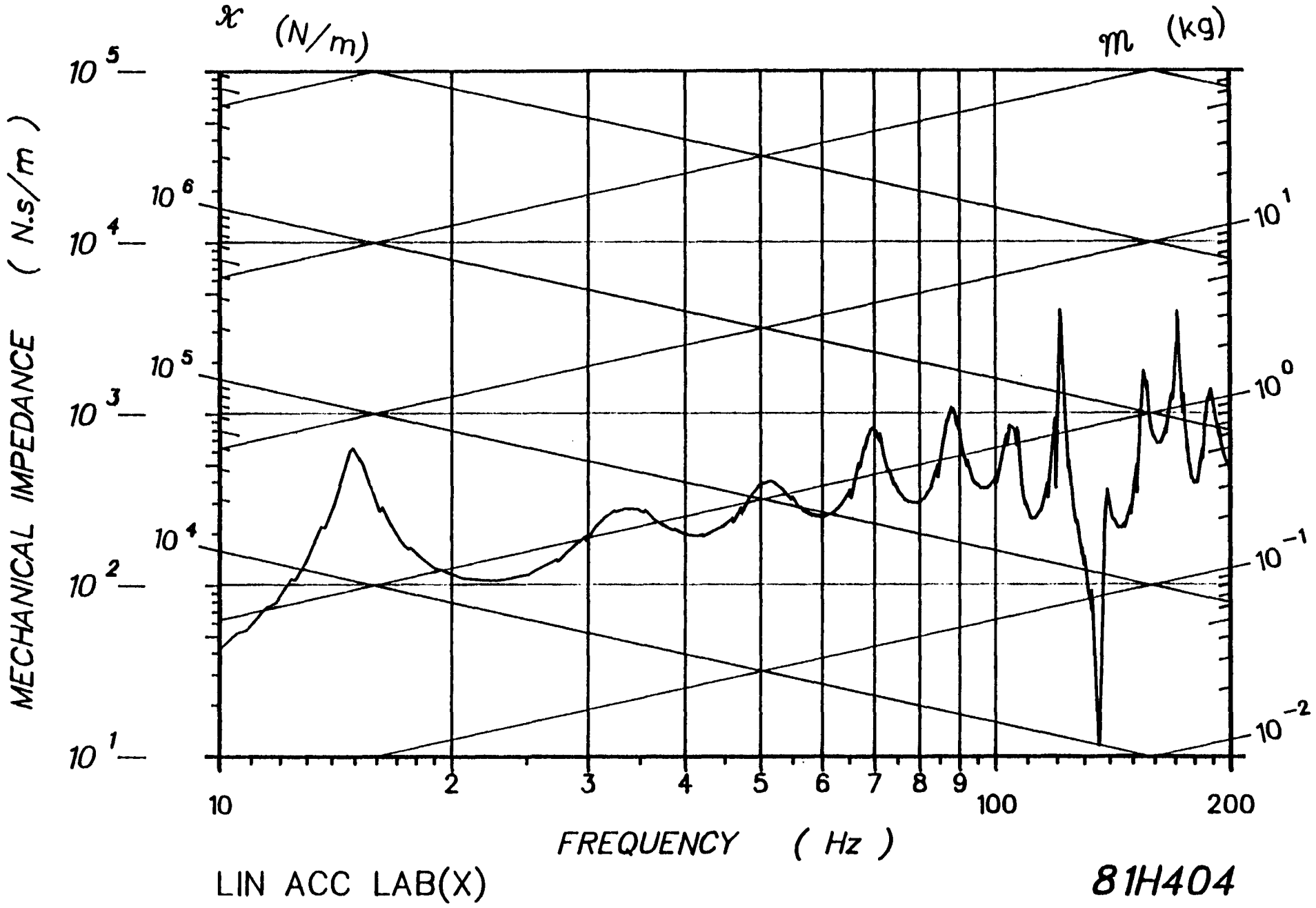
MECHANICAL IMPEDANCE (N.s/m)
$\mathcal{R}$ (N/m)
$\mathcal{M}$ (kg)
10^5
10^4
10^3
10^2
10^1
10^6
10^5
10^4
10^1
10^0
10^{-1}
10^{-2}
10
2
3
4
5
6
7
8
9
100
200
FREQUENCY (Hz)
LIN ACC LAB(X)
81H404

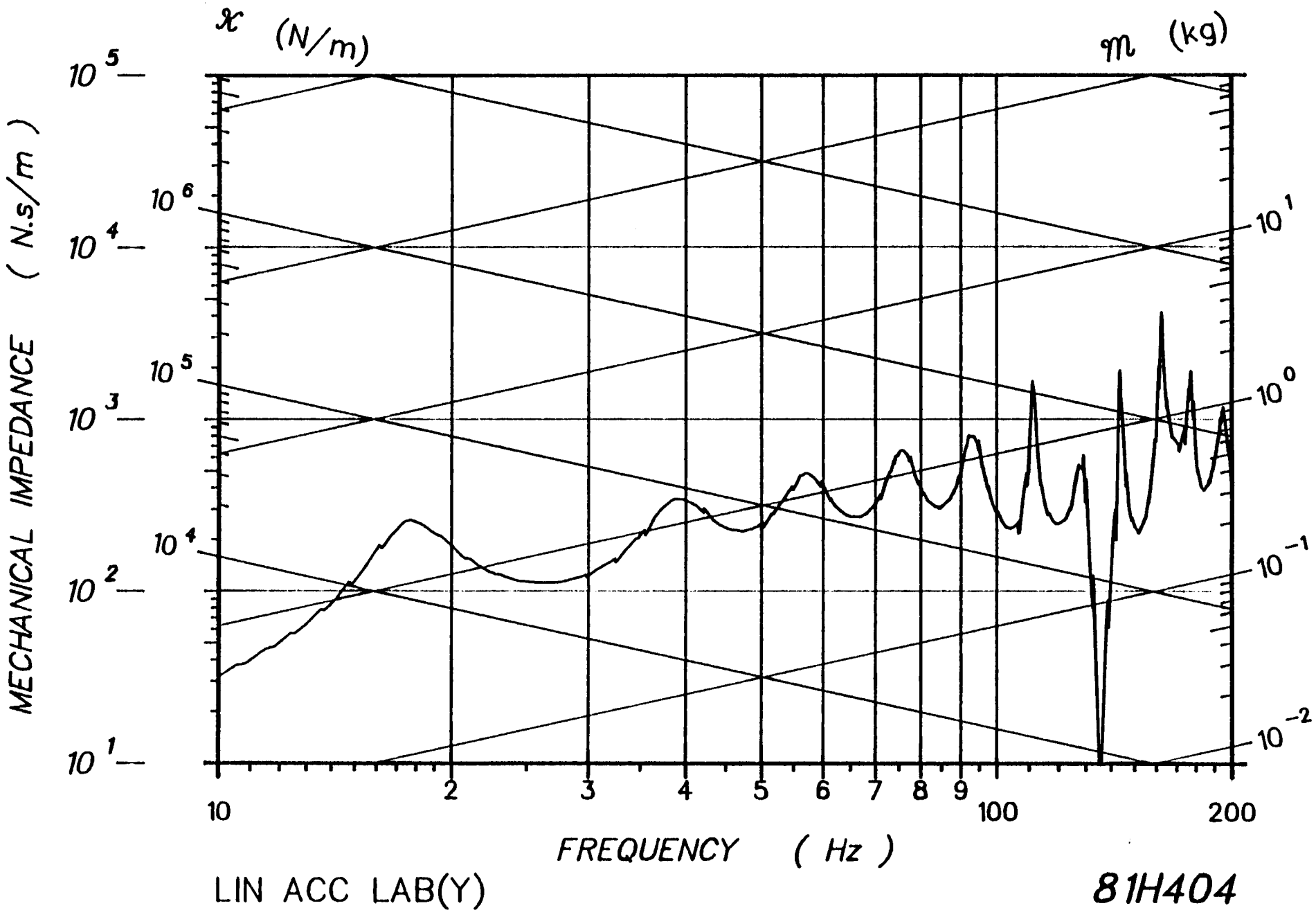
$\mathcal{K}$ (N/m)
$\mathcal{M}$ (kg)
MECHANICAL IMPEDANCE (N.s/m)
10^5
10^4
10^3
10^2
10^1
10^6
10^5
10^4
10^1
10^0
10^{-1}
10^{-2}
10
2
3
4
5
6
7
8
9
100
200
FREQUENCY (Hz)
LIN ACC LAB(Y)
81H404

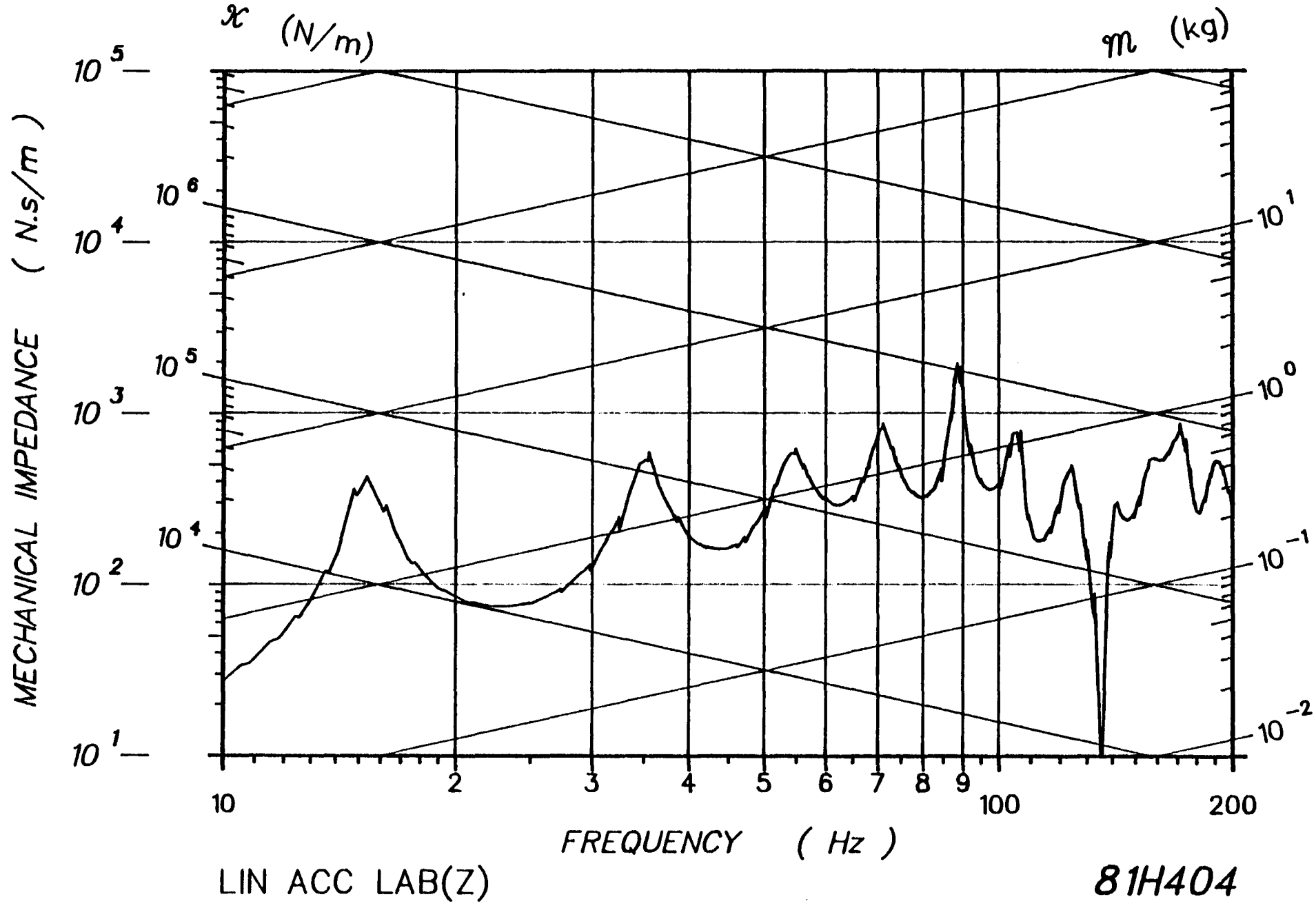
x (N/m)
m (kg)
MECHANICAL IMPEDANCE (N.s/m)
10 5
10 4
10 3
10 2
10 1
10 6
10 5
10 4
10 1
10 0
10 −1
10 −2
10
2
3
4
5
6
7
8
9
100
200
FREQUENCY (Hz)
LIN ACC LAB(Z)
81H404

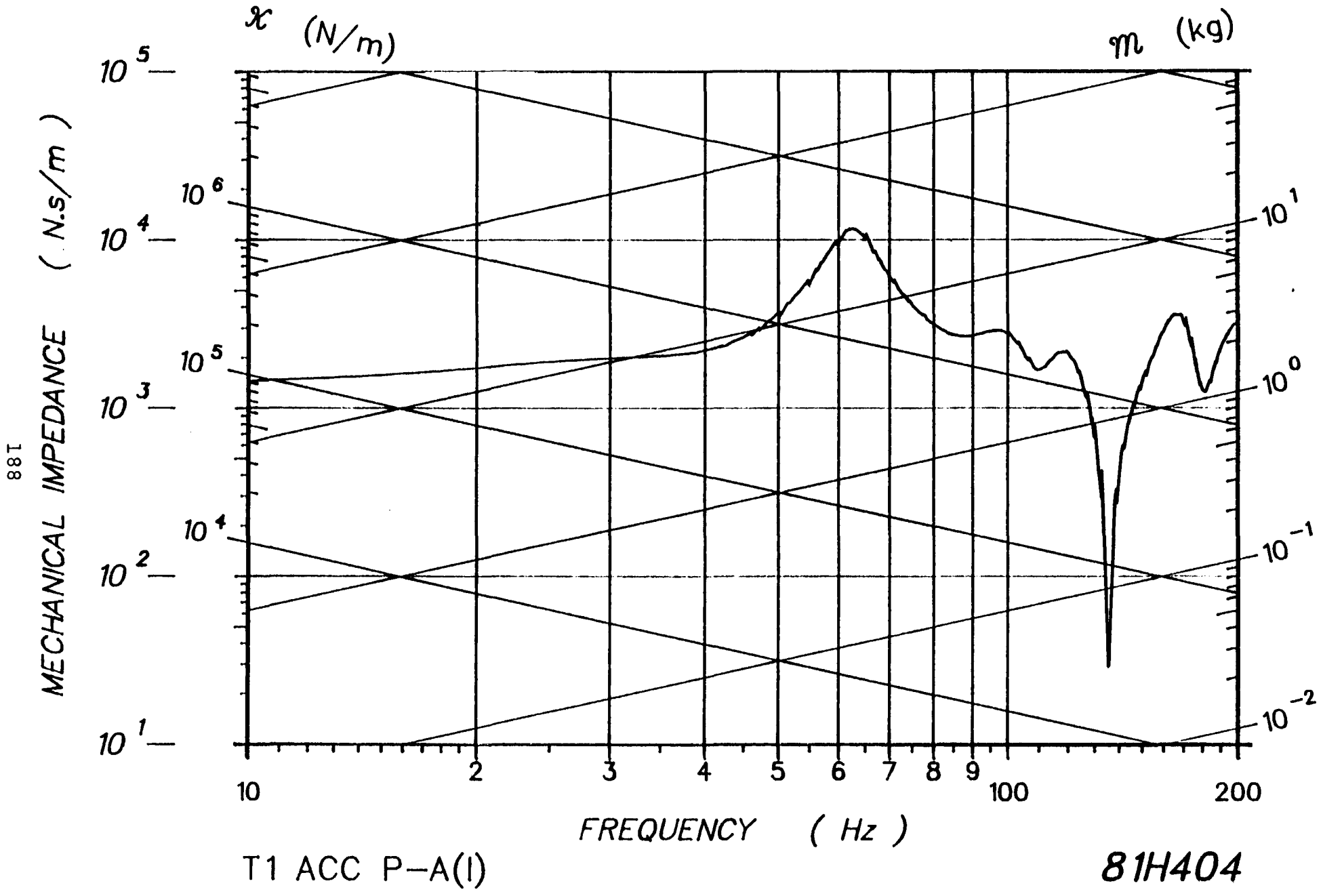
κ (N/m)
m (kg)
MECHANICAL IMPEDANCE (N.s/m)
10 5
10 4
10 3
10 2
10 1
10 6
10 5
10 4
10 1
10 0
10 −1
10 −2
10
2
3
4
5
6
7
8
9
100
200
FREQUENCY (Hz)
T1 ACC P−A(I)
81H404

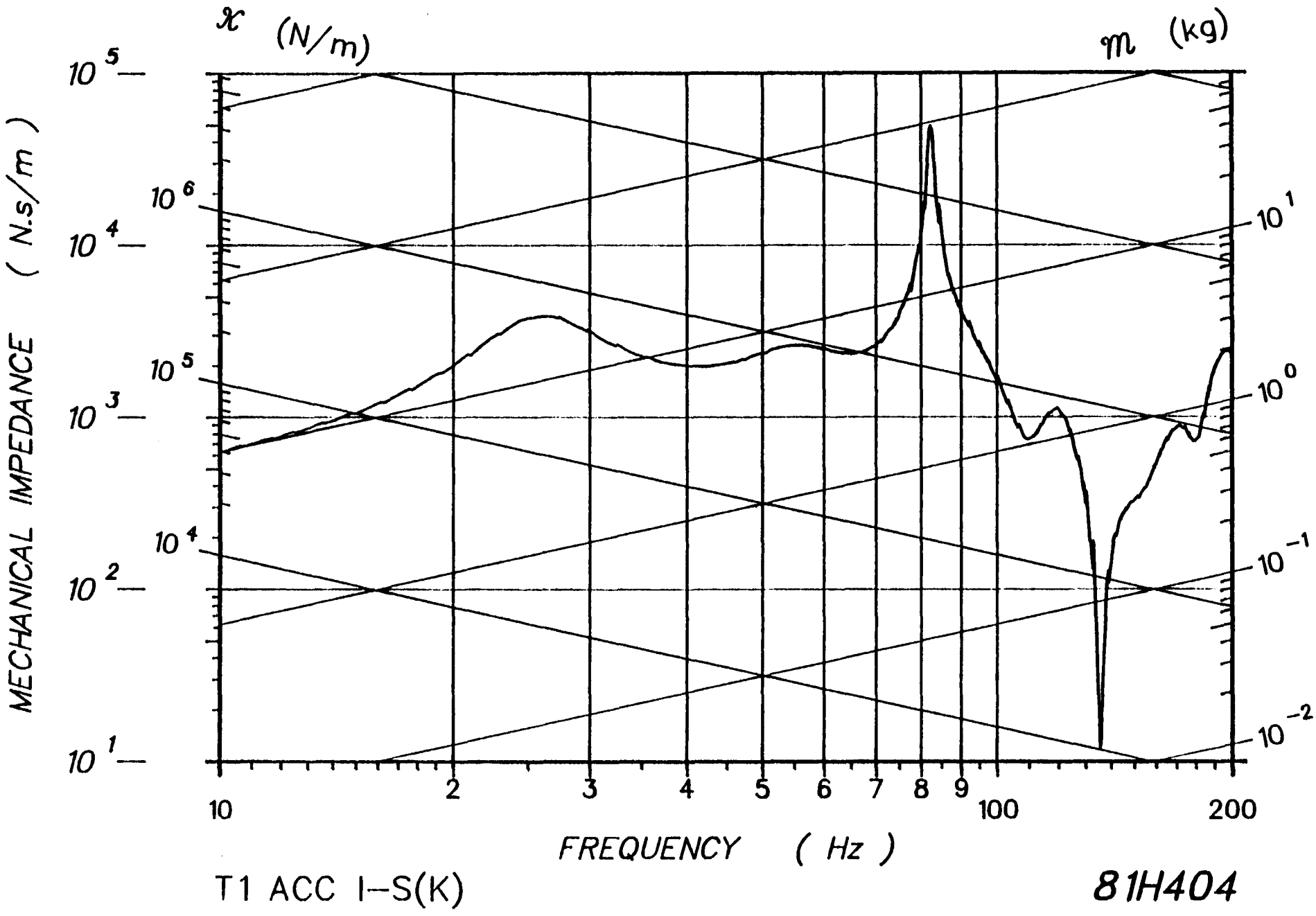
κ (N/m)
m (kg)
MECHANICAL IMPEDANCE (N.s/m)
10 5
10 4
10 3
10 2
10 1
10 6
10 5
10 4
10 1
10 0
10 −1
10 −2
10
2
3
4
5
6
7
8
9
100
200
FREQUENCY (Hz)
T1 ACC I−S(K)
81H404

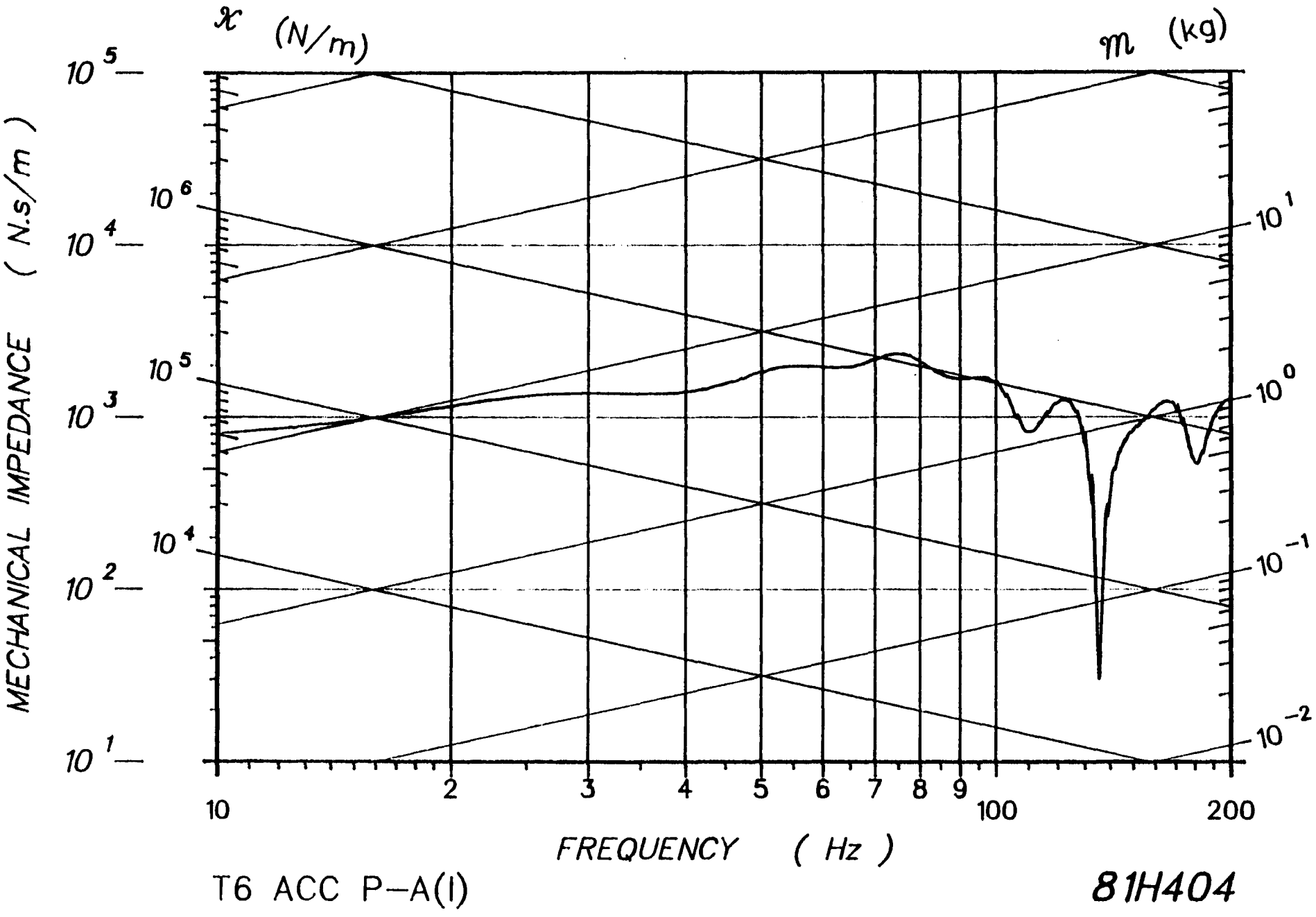

T6 ACC P–A(I)

81H404

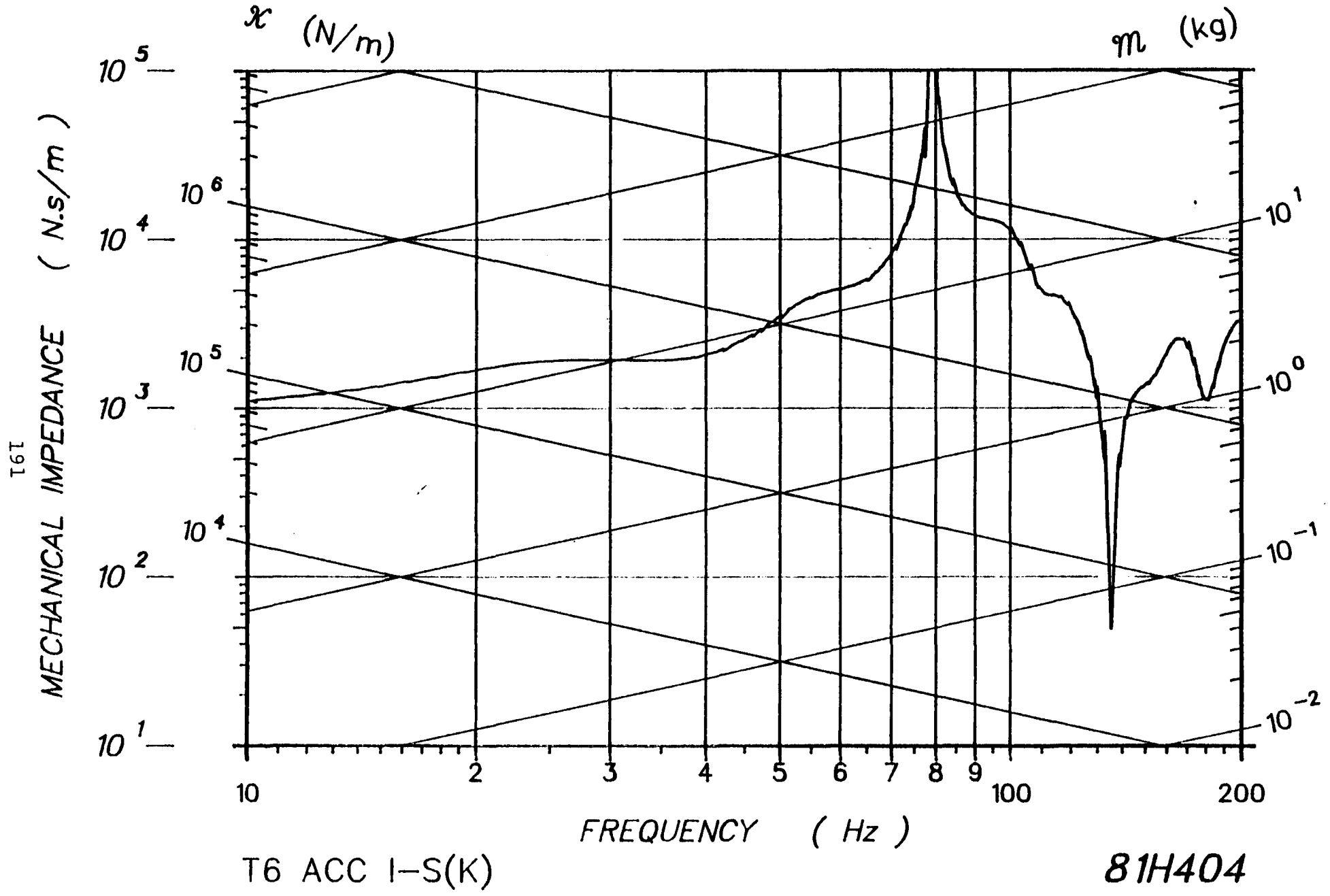

T6 ACC I–S(K)

81H404

191

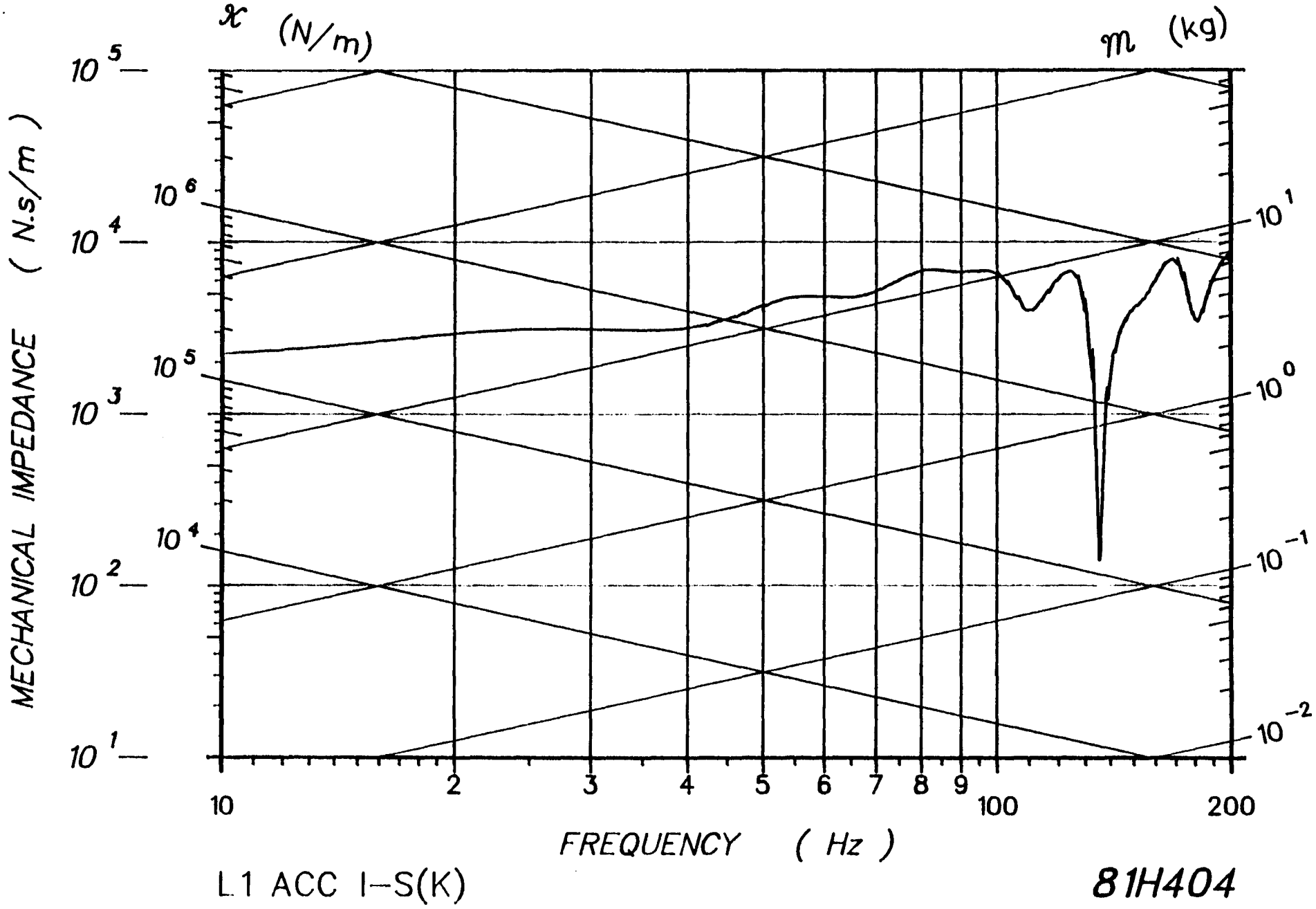

L1 ACC I–S(K)

81H404

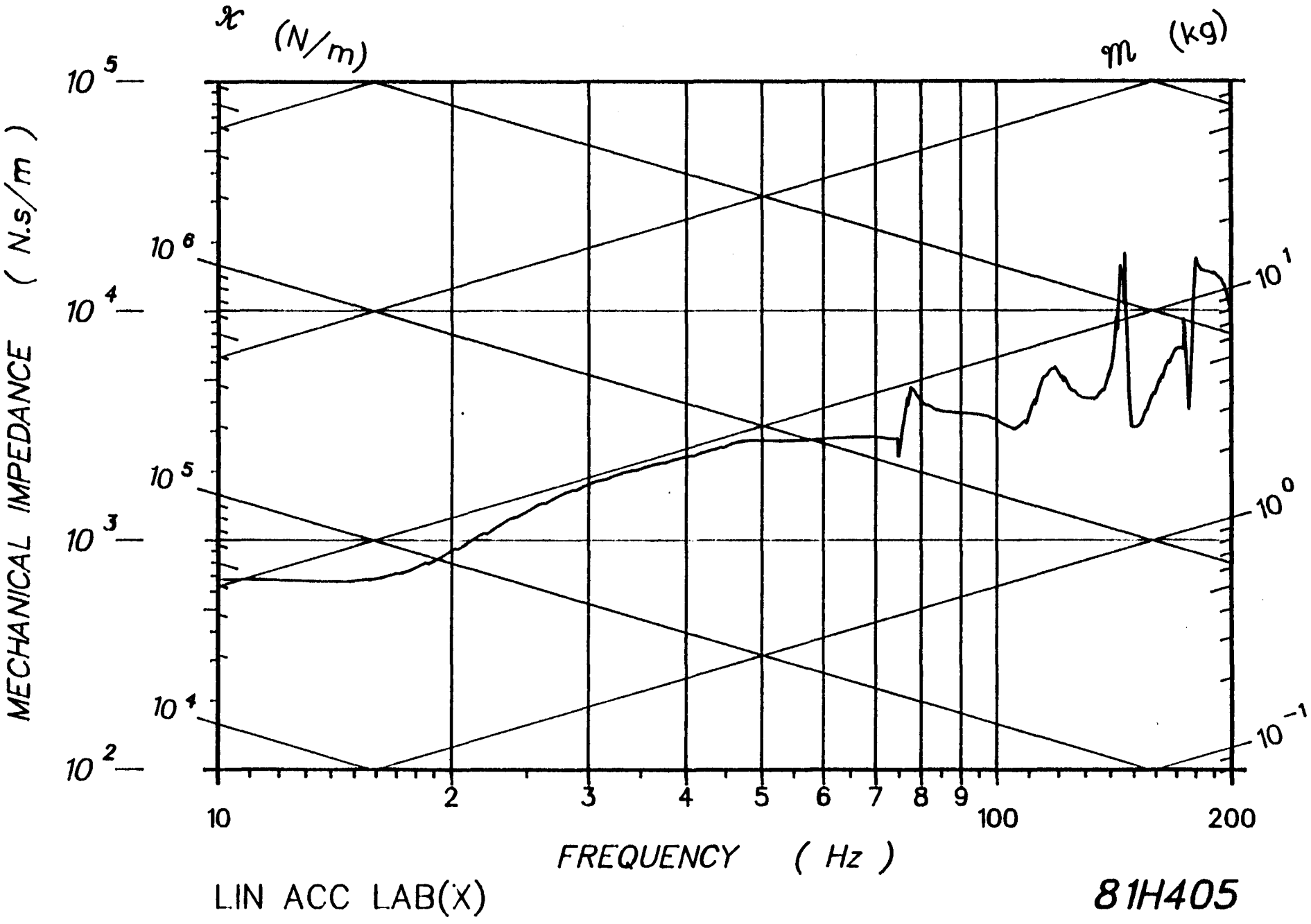
$\mathcal{K}$ (N/m)
$\mathcal{M}$ (kg)
MECHANICAL IMPEDANCE (N.s/m)
10^5
10^4
10^3
10^2
10^6
10^5
10^4
10^1
10^0
10^{-1}
10
2
3
4
5
6
7
8
9
100
200
FREQUENCY (Hz)
LIN ACC LAB(X)
81H405

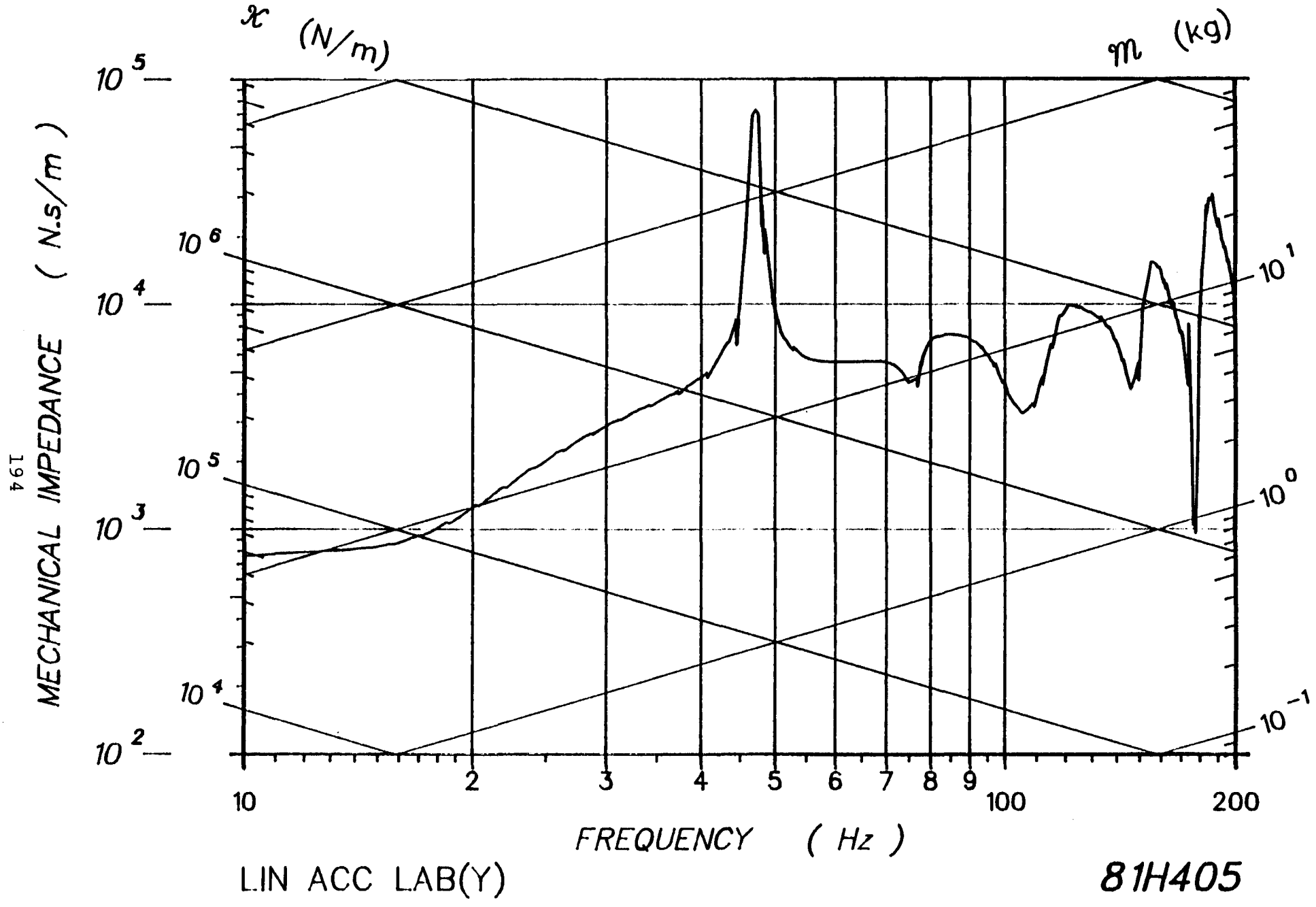
κ (N/m)
m (kg)
MECHANICAL IMPEDANCE (N.s/m)
10 5
10 4
10 3
10 2
10 6
10 5
10 4
10 1
10 0
10 -1
10
2
3
4
5
6
7
8
9
100
200
FREQUENCY (Hz)
LIN ACC LAB(Y)
81H405

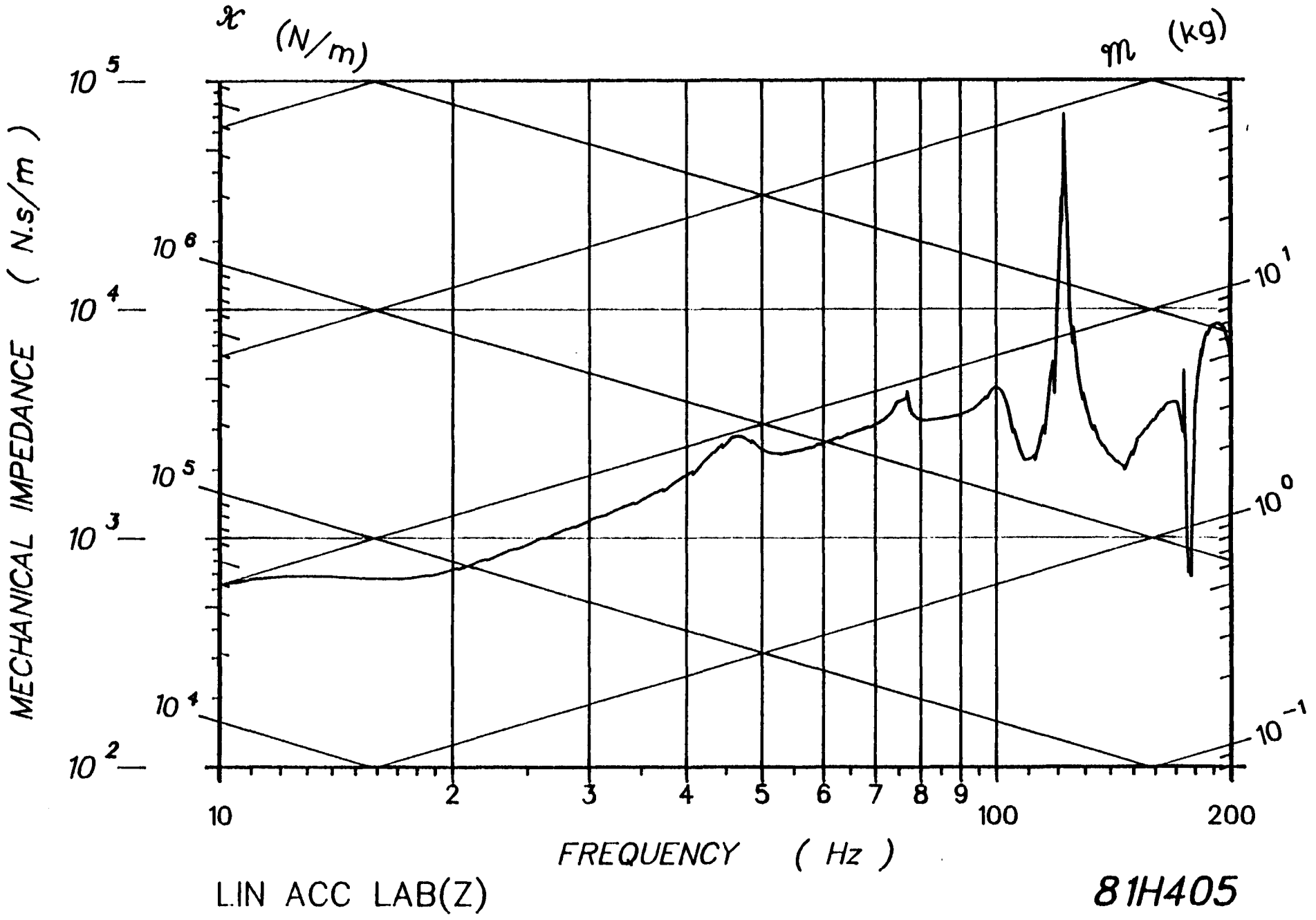
$\mathcal{K}$ (N/m)
$\mathcal{M}$ (kg)
MECHANICAL IMPEDANCE (N.s/m)
10^5
10^4
10^3
10^2
10^6
10^5
10^4
10^1
10^0
10^{-1}
10
2
3
4
5
6
7
8
9
100
200
FREQUENCY (Hz)
LIN ACC LAB(Z)
81H405

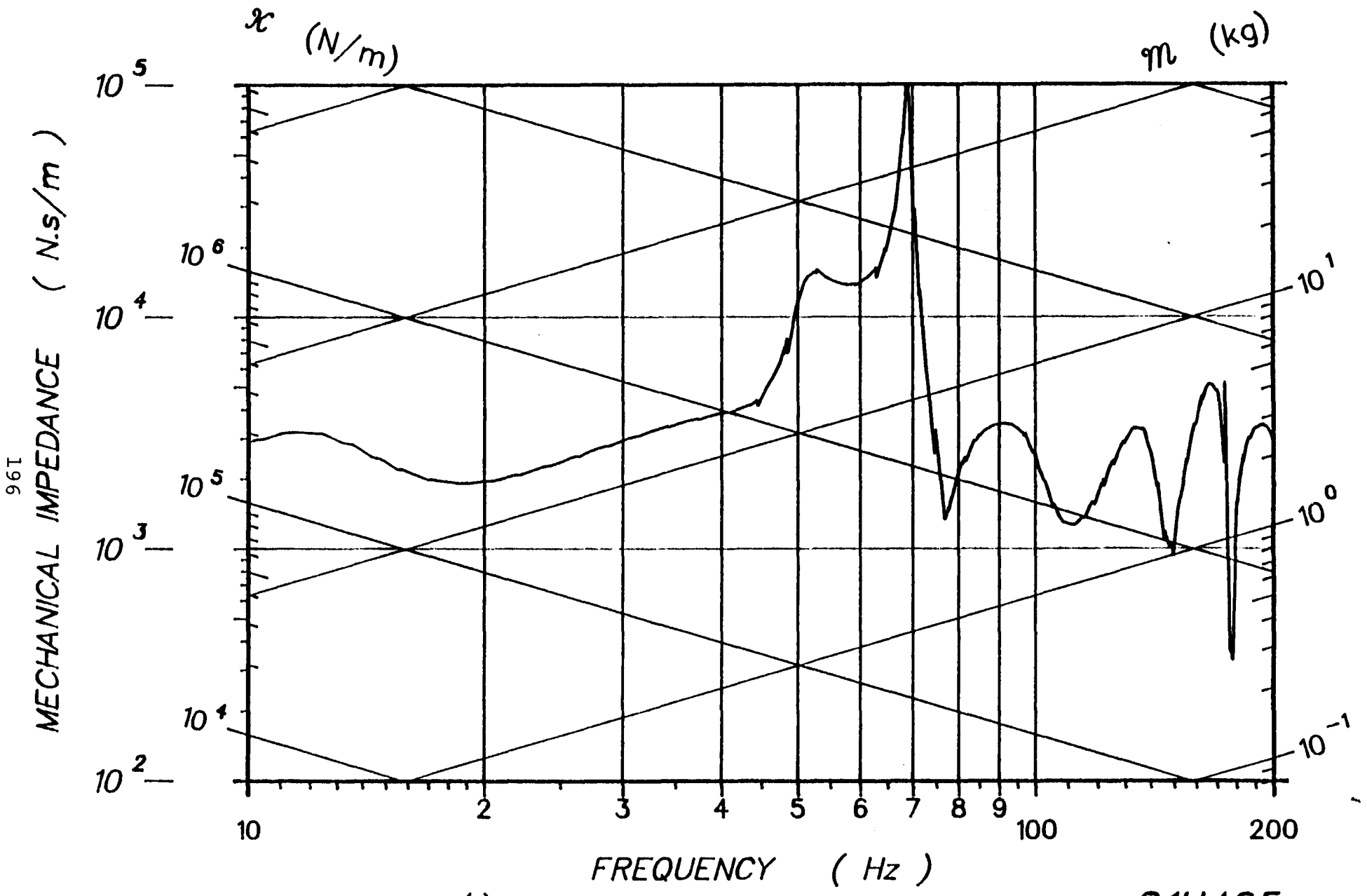
χ (N/m)
m (kg)
MECHANICAL IMPEDANCE (N.s/m)
10 5
10 4
10 3
10 2
10 6
10 5
10 4
10 1
10 0
10 -1
10
2
3
4
5
6
7
8
9
100
200
FREQUENCY (Hz)
T1 ACC P-A(I)
81H405

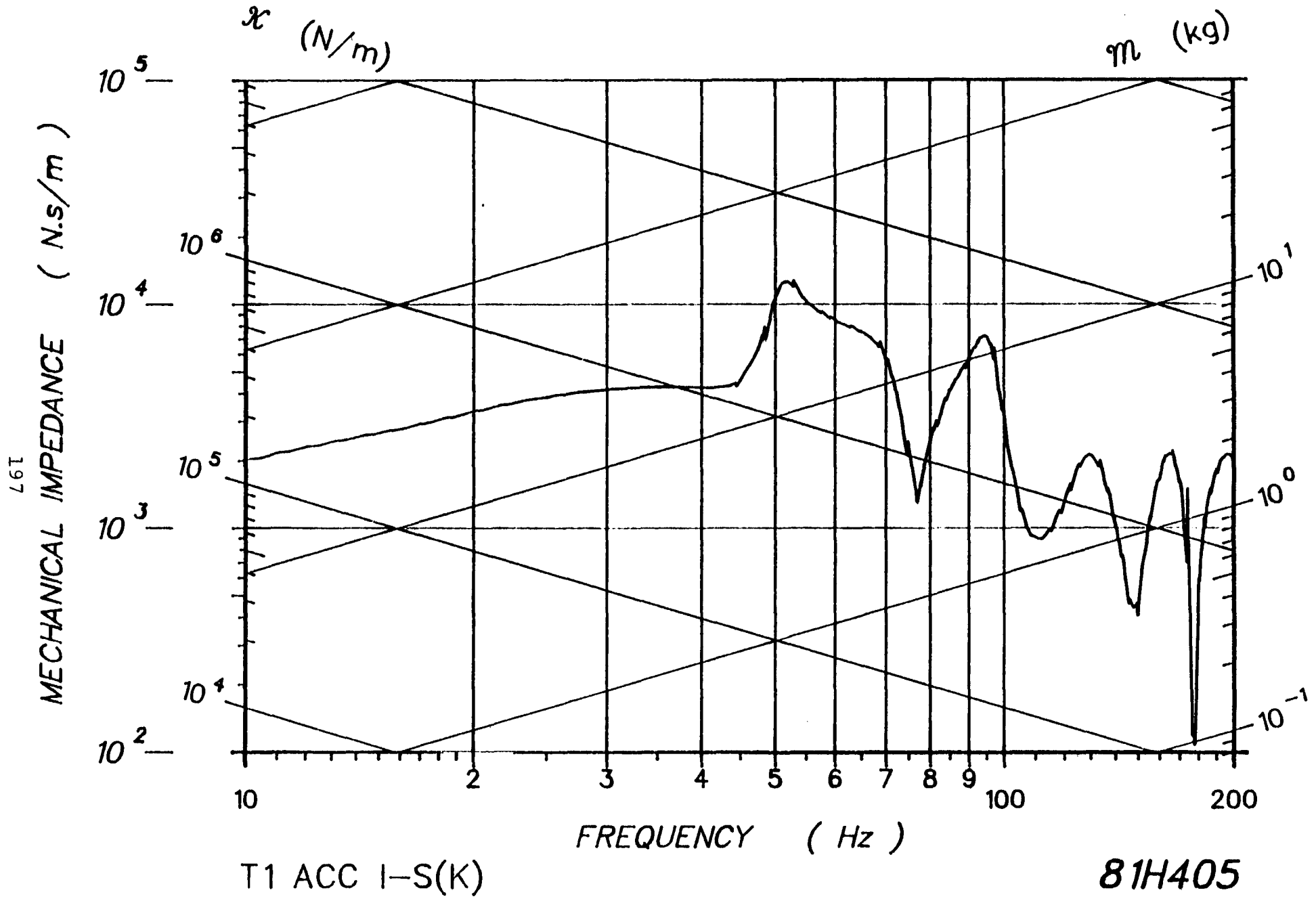
$\mathcal{K}$ (N/m)
$\mathcal{M}$ (kg)
MECHANICAL IMPEDANCE (N.s/m)
10^5
10^4
10^3
10^2
10^6
10^5
10^4
10^1
10^0
10^{-1}
10
2
3
4
5
6
7
8
9
100
200
FREQUENCY (Hz)
T1 ACC I–S(K)
81H405

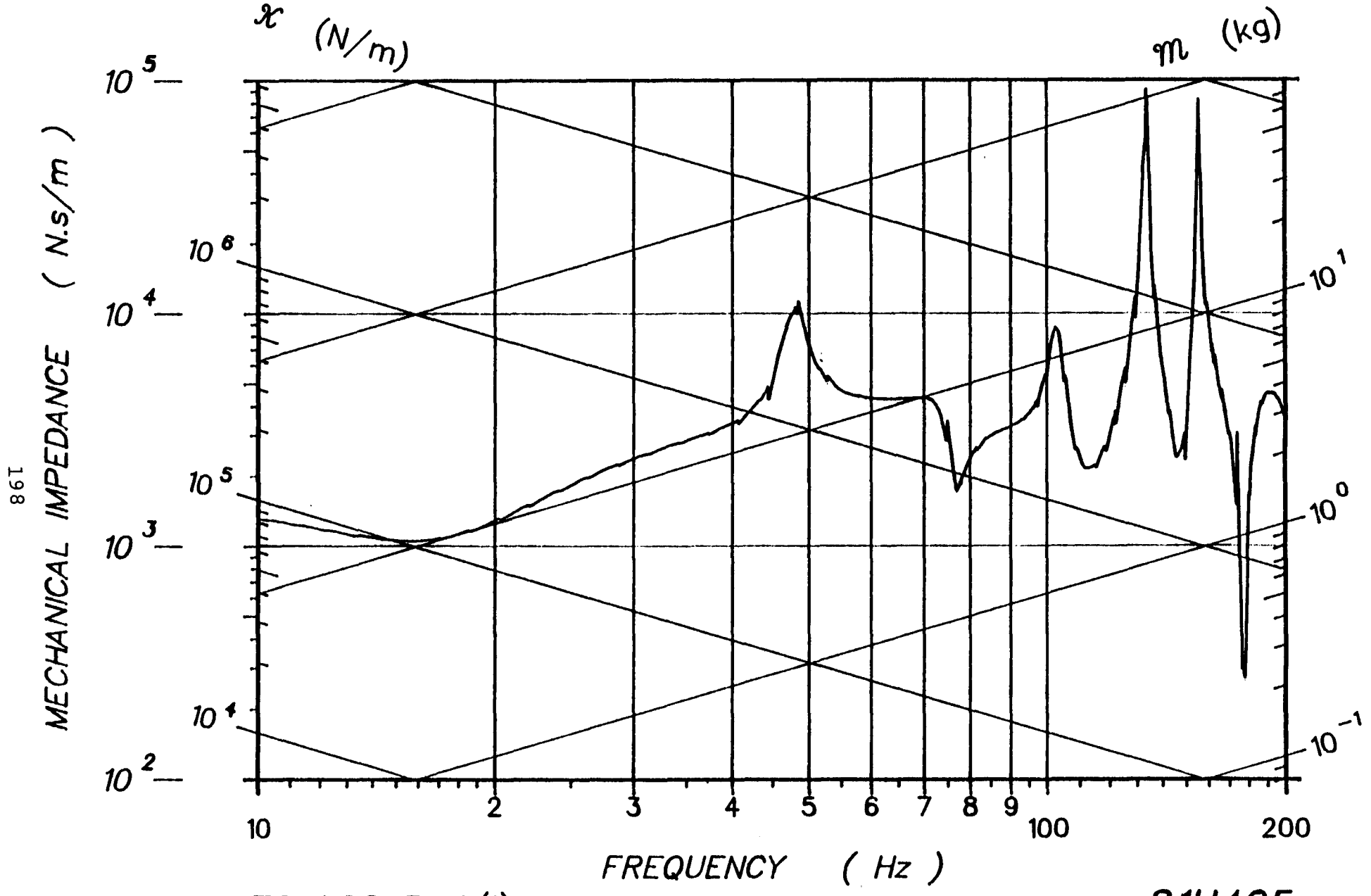
κ (N/m)
m (kg)
MECHANICAL IMPEDANCE (N.s/m)
10 5
10 4
10 3
10 2
10 6
10 5
10 4
10 1
10 0
10 -1
10
2
3
4
5
6
7
8
9
100
200
FREQUENCY (Hz)
T6 ACC P-A(I)
81H405

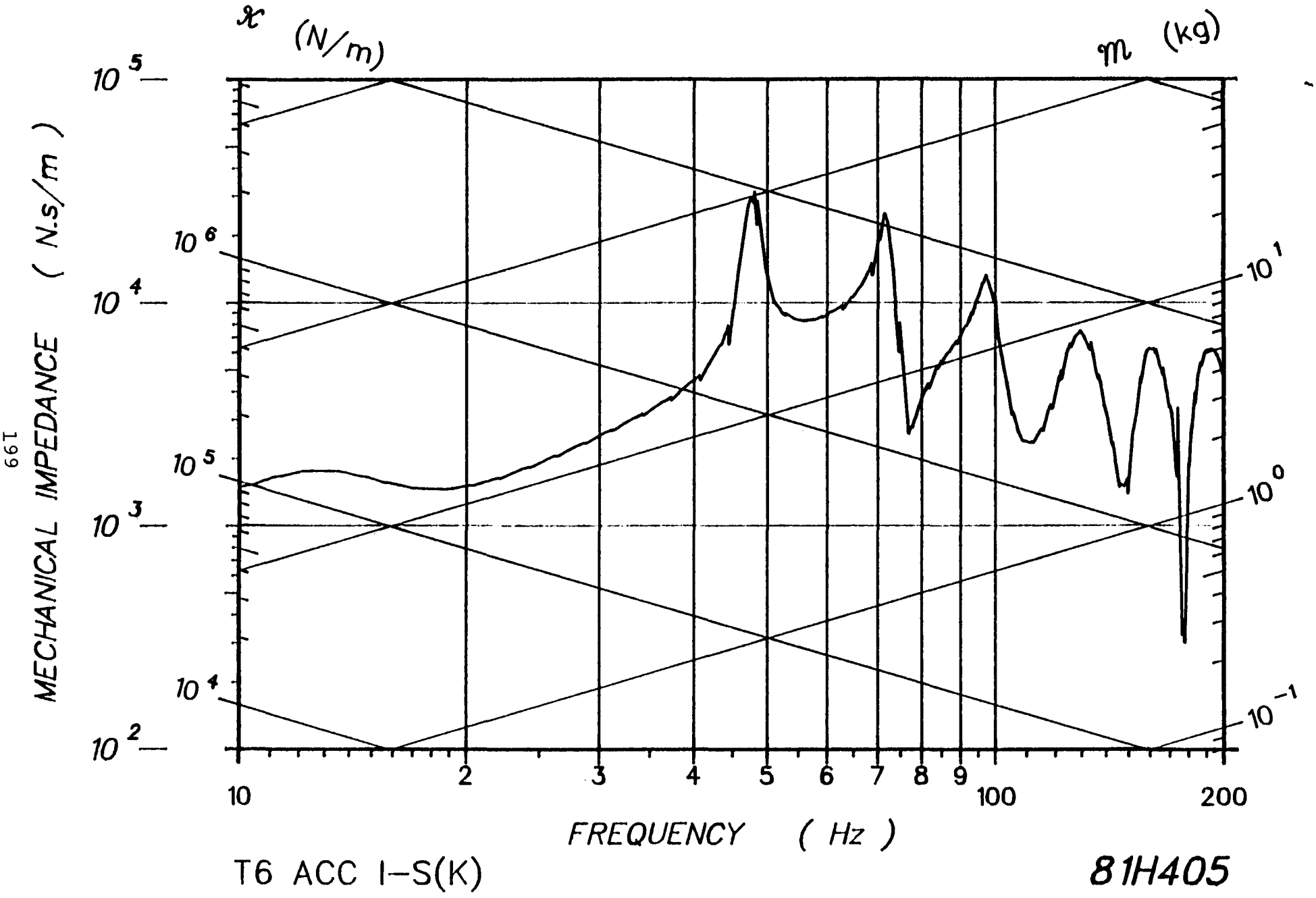

T6 ACC I–S(K)

81H405

199

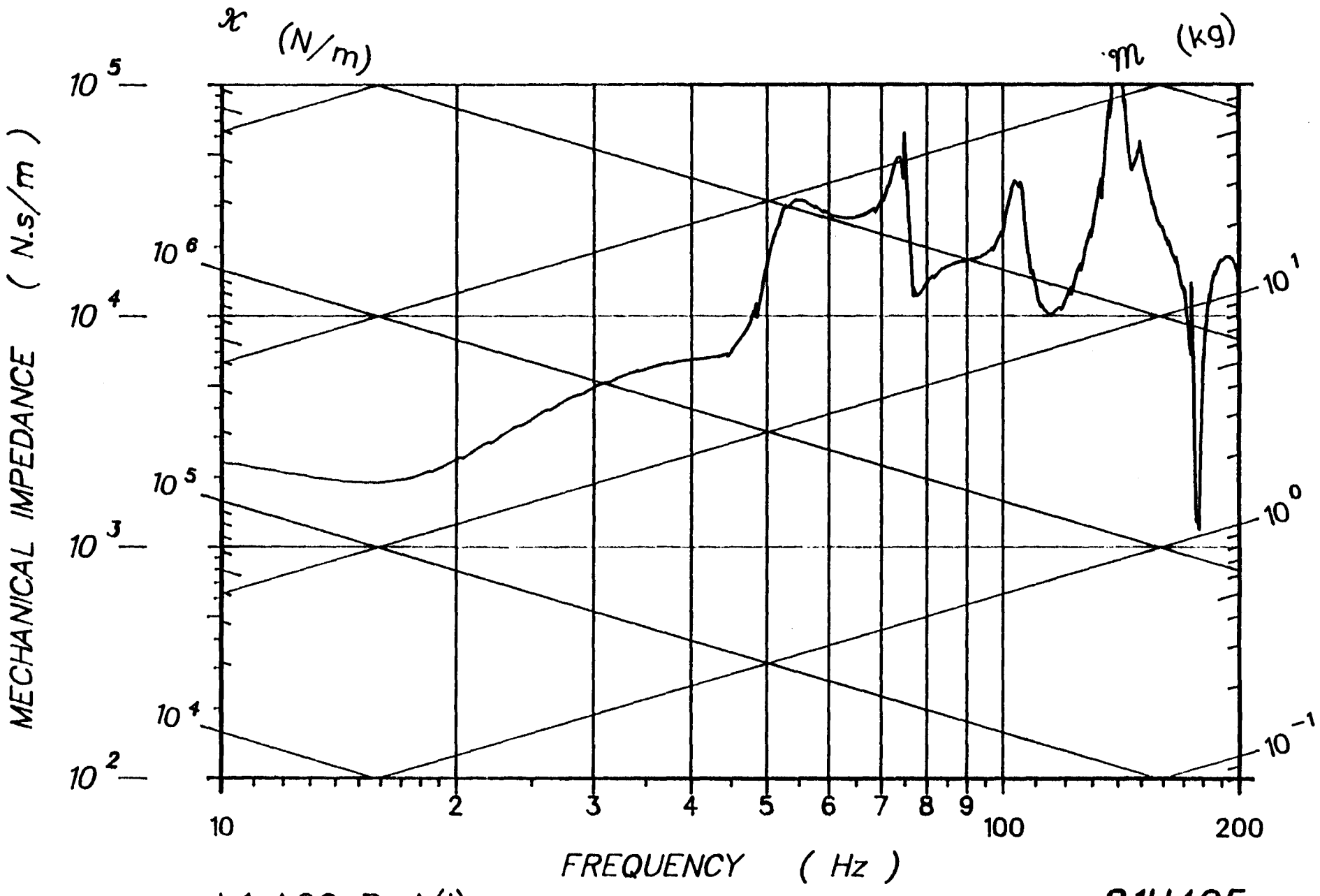

L1 ACC P–A(I)

81H405

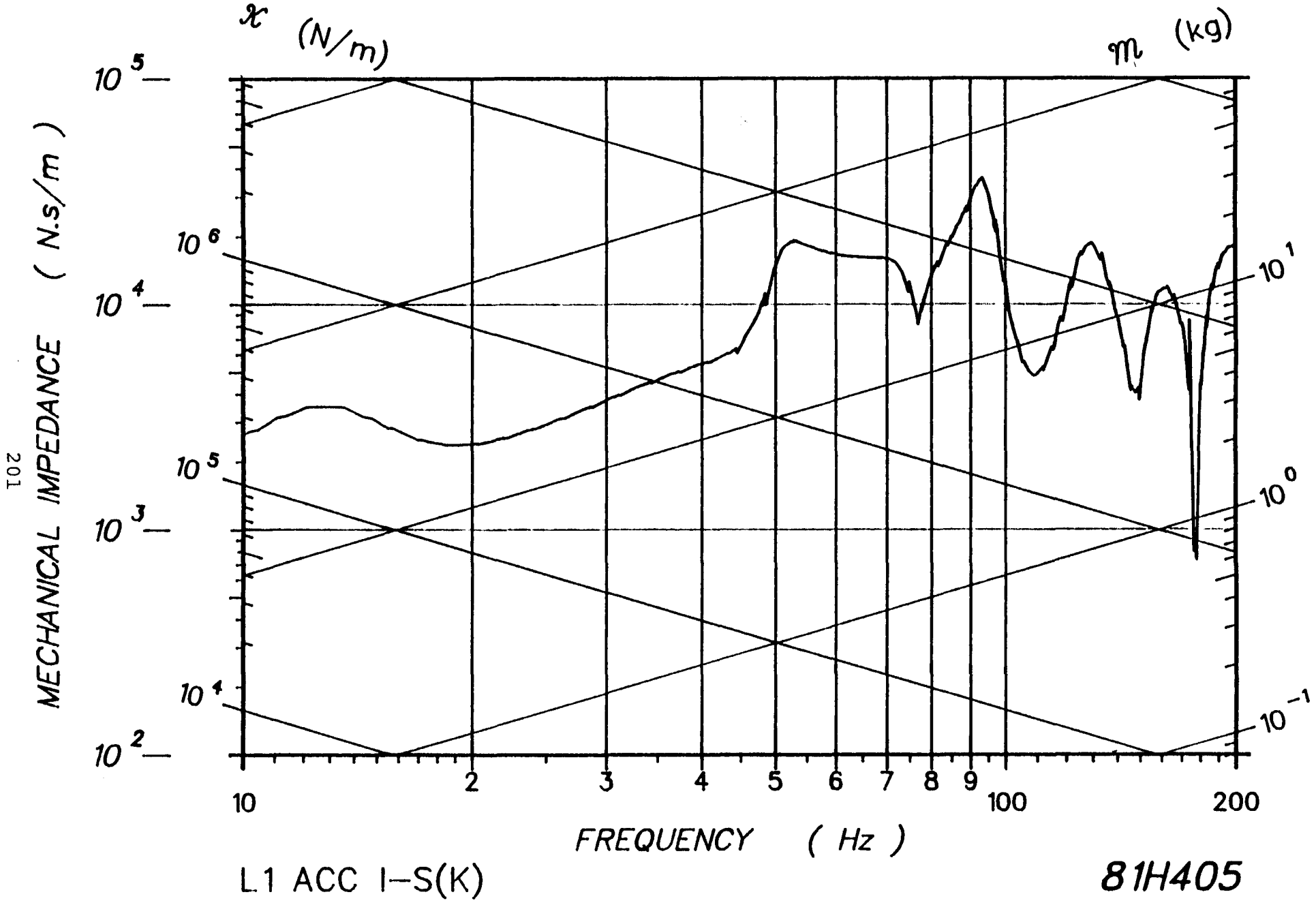
$\mathcal{K}$ (N/m)
m (kg)
10^5
10^4
10^3
10^2
10^6
10^5
10^4
10^1
10^0
10^{-1}
MECHANICAL IMPEDANCE (N.s/m)
10
2
3
4
5
6
7
8
9
100
200
FREQUENCY (Hz)
L1 ACC I–S(K)
81H405

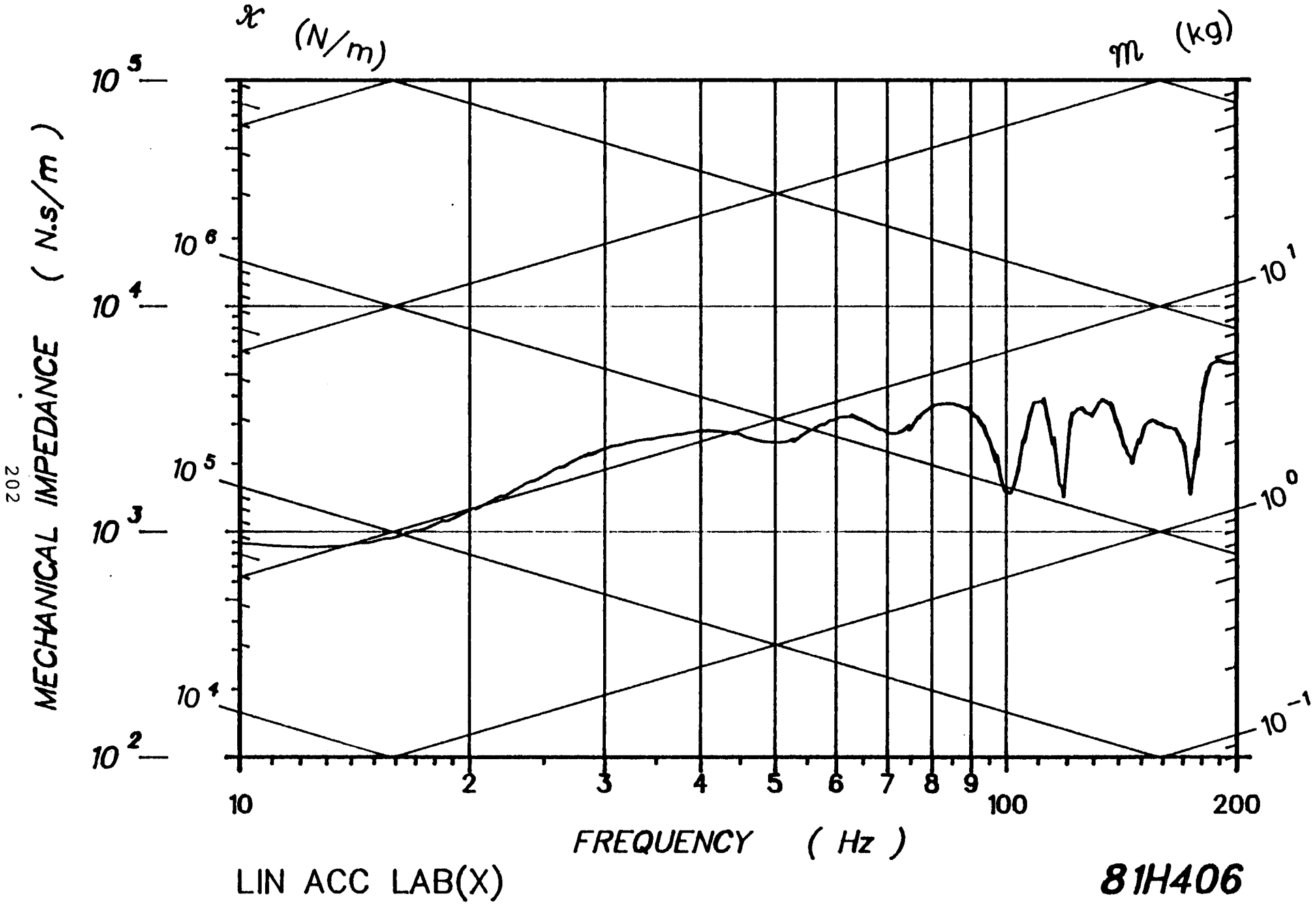

LIN ACC LAB(X)

81H406

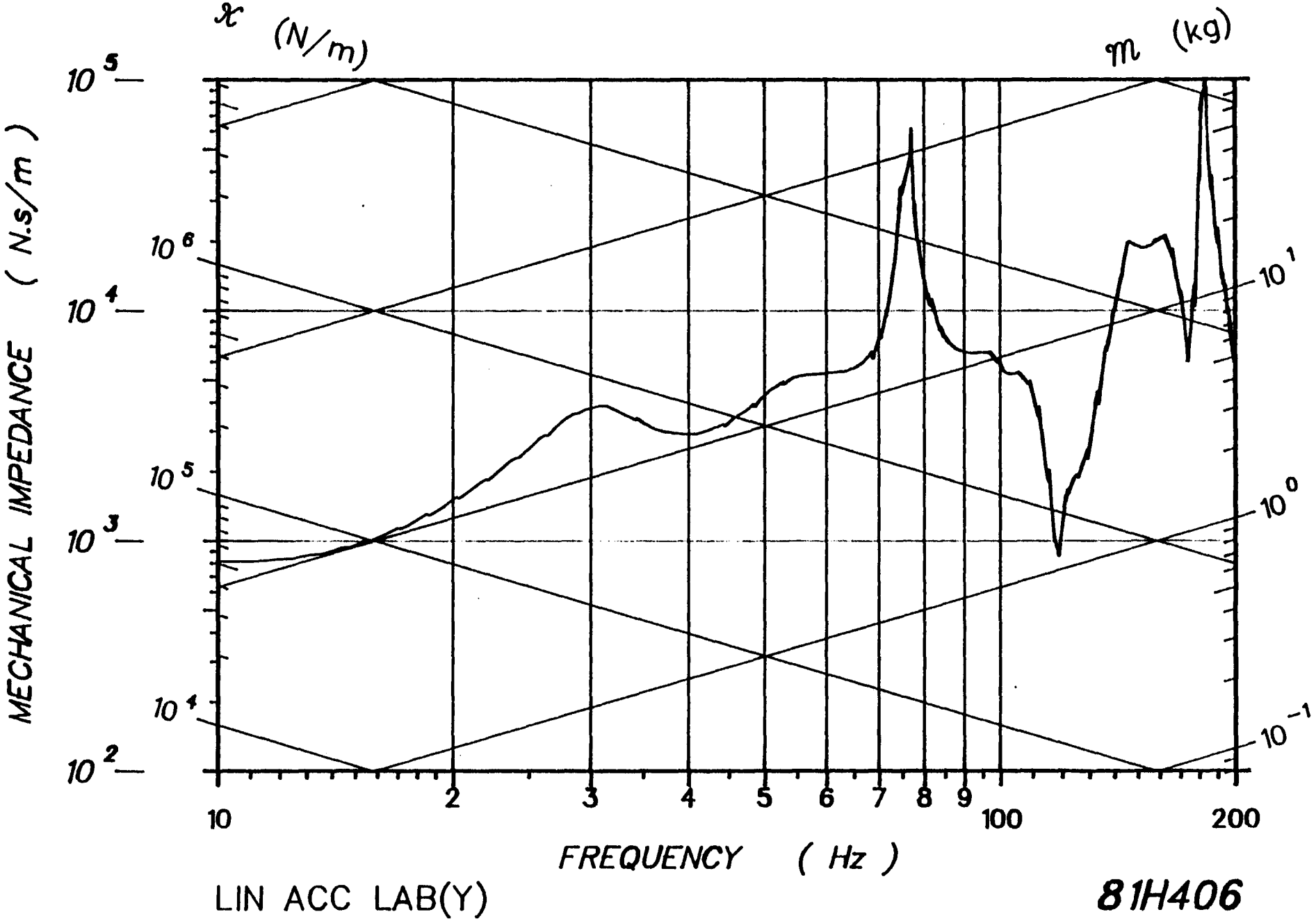
κ (N/m)
m (kg)
MECHANICAL IMPEDANCE (N.s/m)
10^5
10^4
10^3
10^2
10^6
10^5
10^4
10^1
10^0
10^-1
10
2
3
4
5
6
7
8
9
100
200
FREQUENCY (Hz)
LIN ACC LAB(Y)
81H406

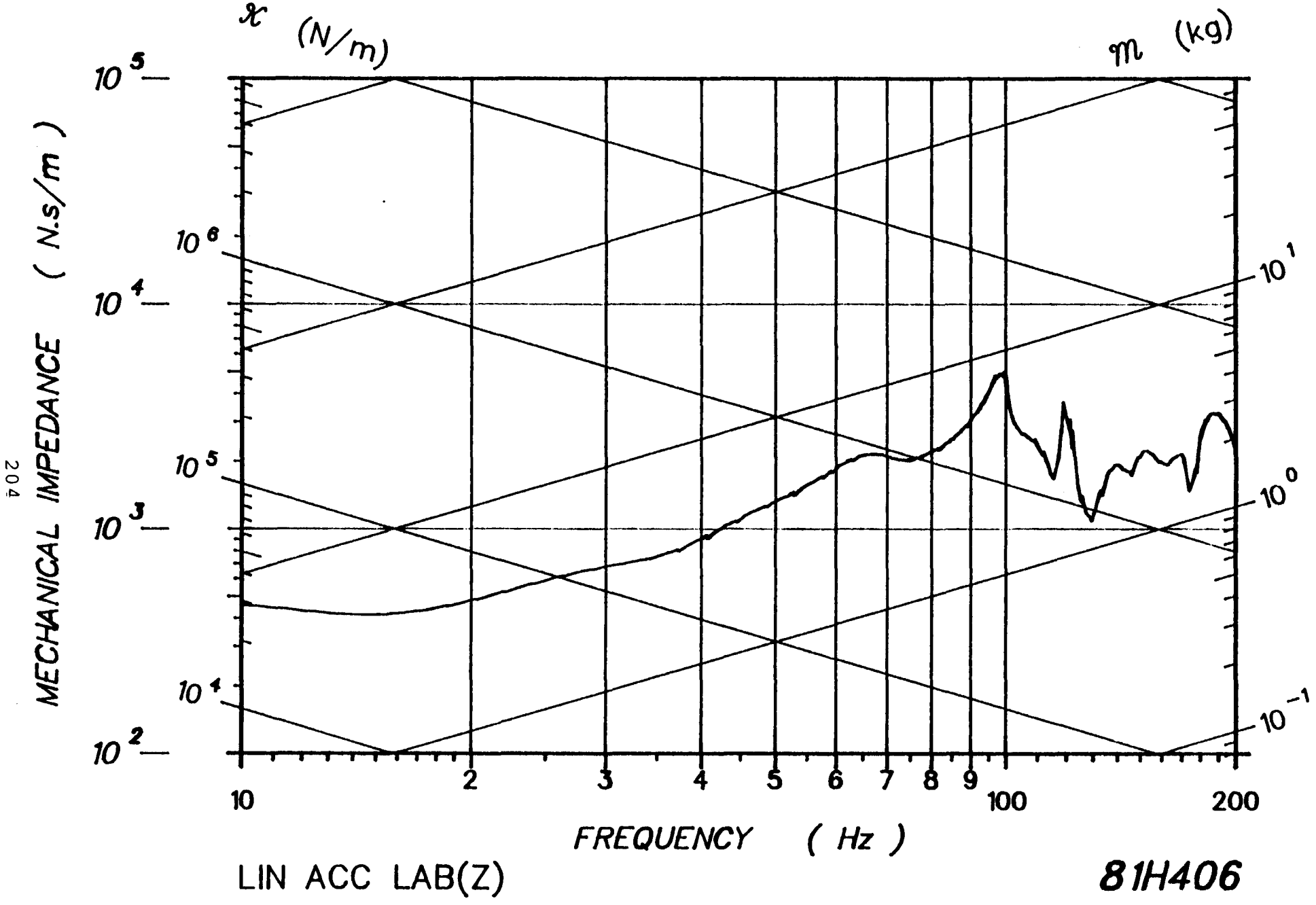
𝔎 (N/m)
𝔪 (kg)
MECHANICAL IMPEDANCE (N.s/m)
10^5
10^4
10^3
10^2
10^6
10^5
10^4
10^1
10^0
10^-1
10
2
3
4
5
6
7
8
9
100
200
FREQUENCY (Hz)
LIN ACC LAB(Z)
81H406

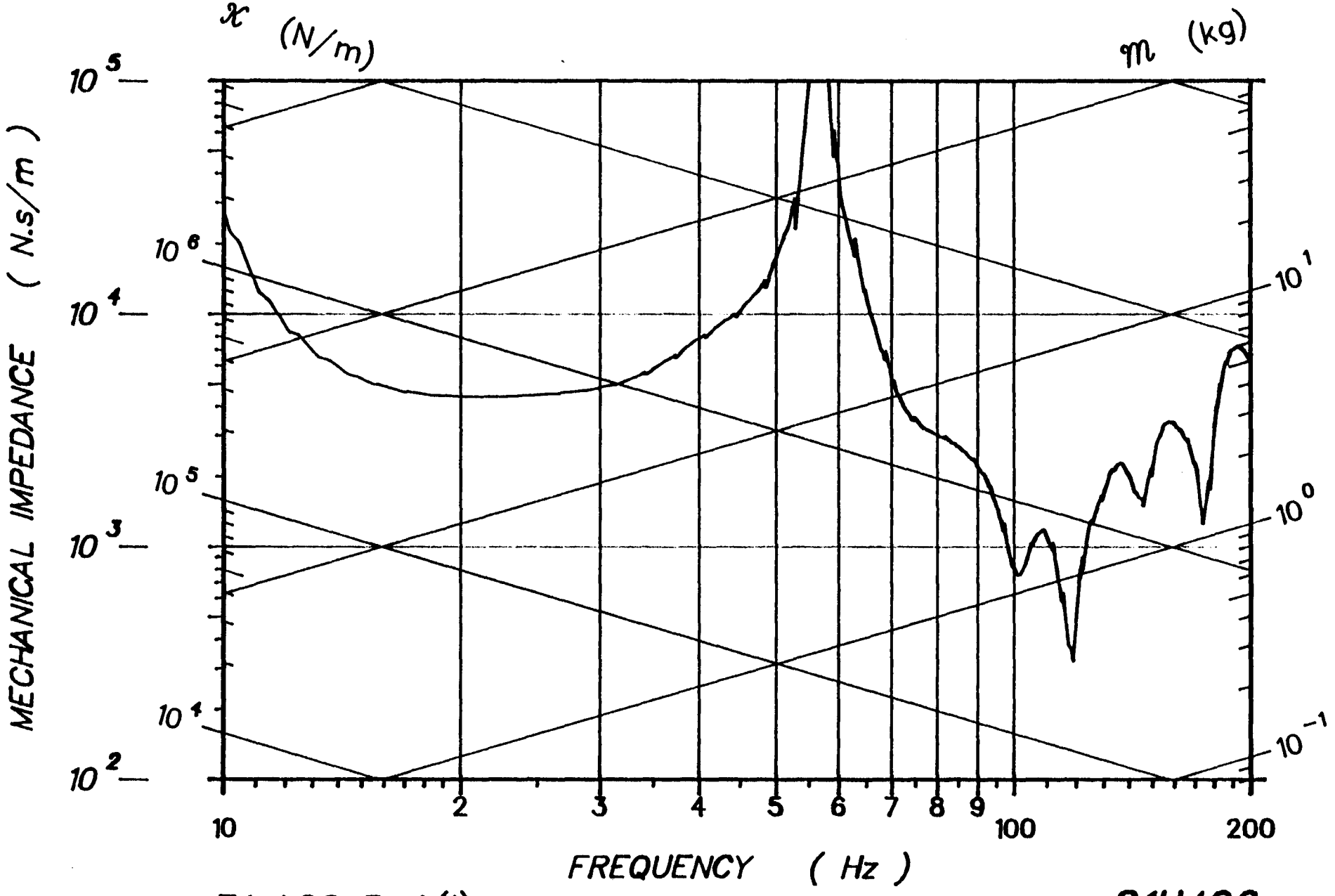

T1 ACC P--A(I)

81H406

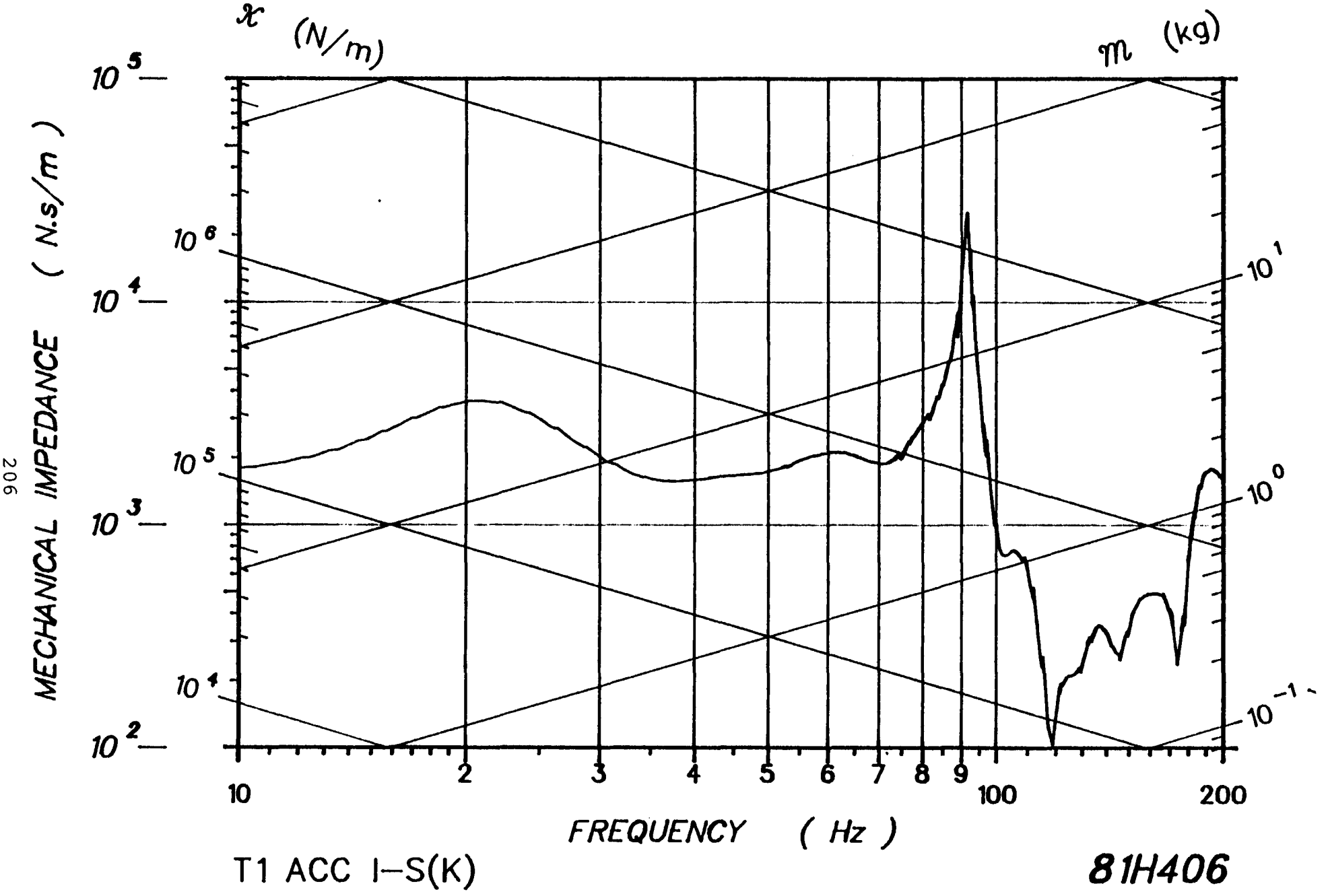
x (N/m)
m (kg)
MECHANICAL IMPEDANCE (N.s/m)
10 5
10 4
10 3
10 2
10 6
10 5
10 4
10 1
10 0
10 -1
10
2
3
4
5
6
7
8
9
100
200
FREQUENCY (Hz)
T1 ACC I-S(K)
81H406

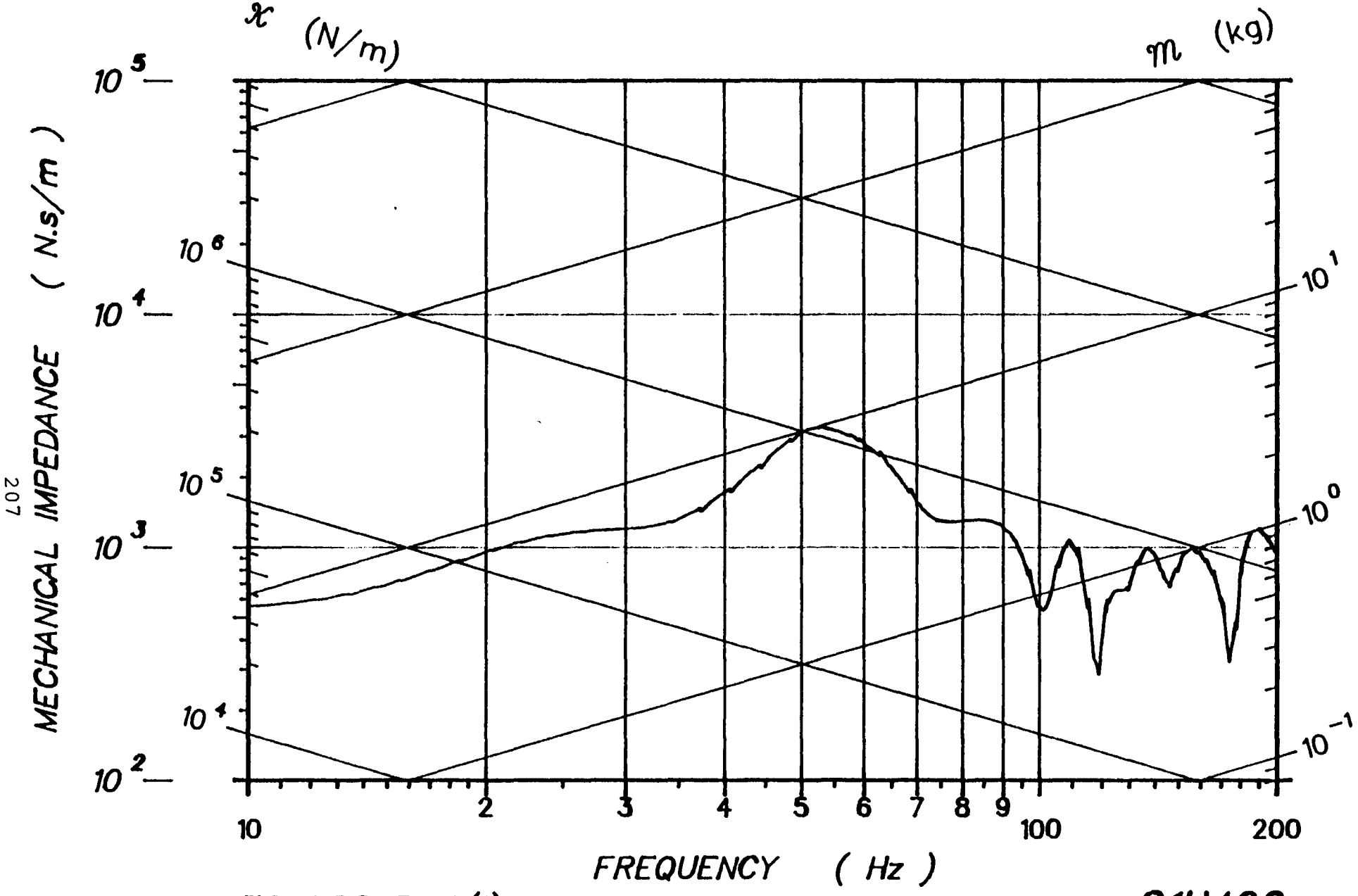
κ (N/m)
m (kg)
MECHANICAL IMPEDANCE (N.s/m)
10 5
10 4
10 3
10 2
10 6
10 5
10 4
10 1
10 0
10 -1
10
2
3
4
5
6
7
8
9
100
200
FREQUENCY (Hz)
T6 ACC P–A(I)
81H406

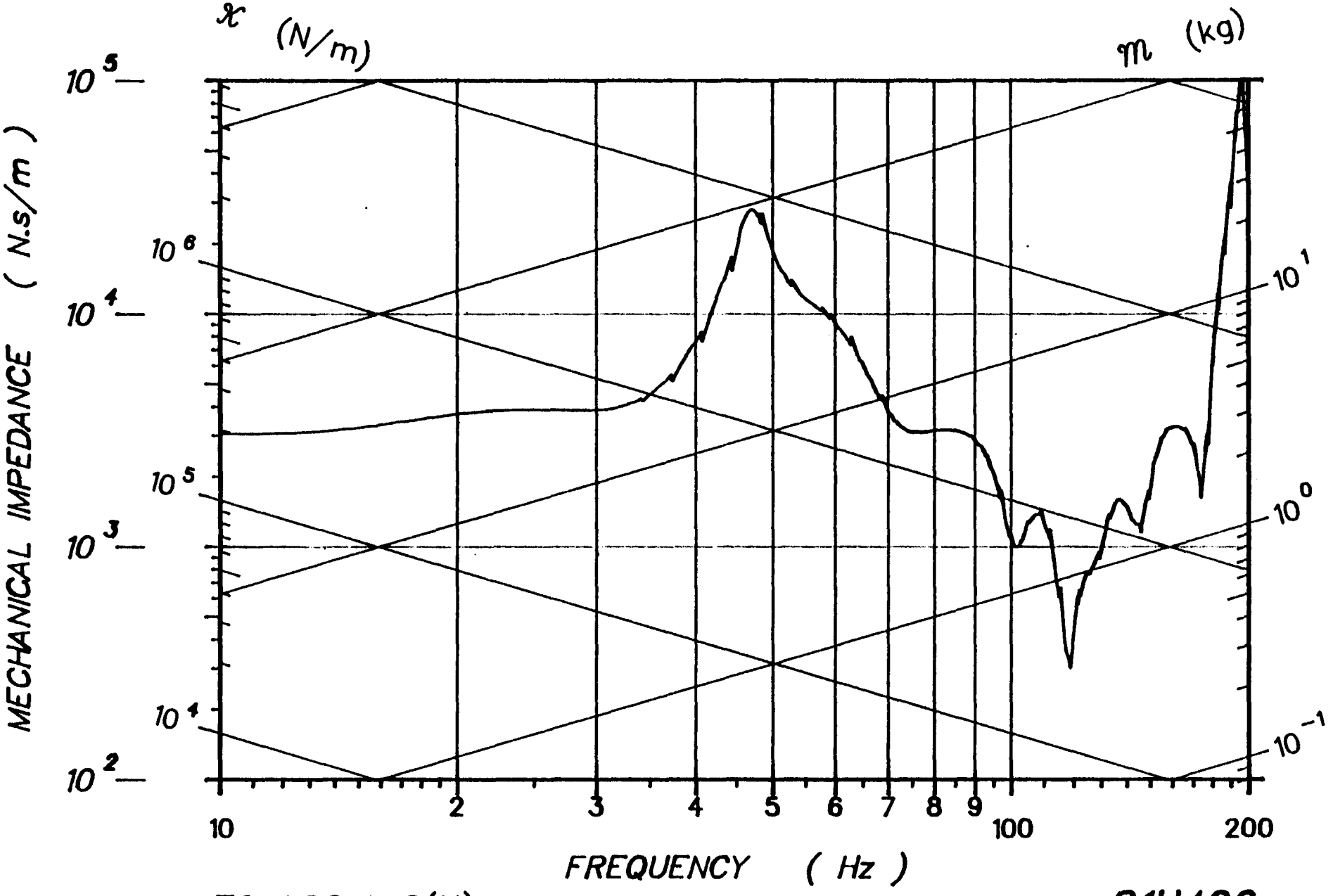
$\mathcal{K}$ (N/m)
$\mathcal{M}$ (kg)
MECHANICAL IMPEDANCE (N.s/m)
10^5
10^4
10^3
10^2
10^6
10^5
10^4
10^1
10^0
10^{-1}
10
2
3
4
5
6
7
8
9
100
200
FREQUENCY (Hz)
T6 ACC I–S(K)
81H406

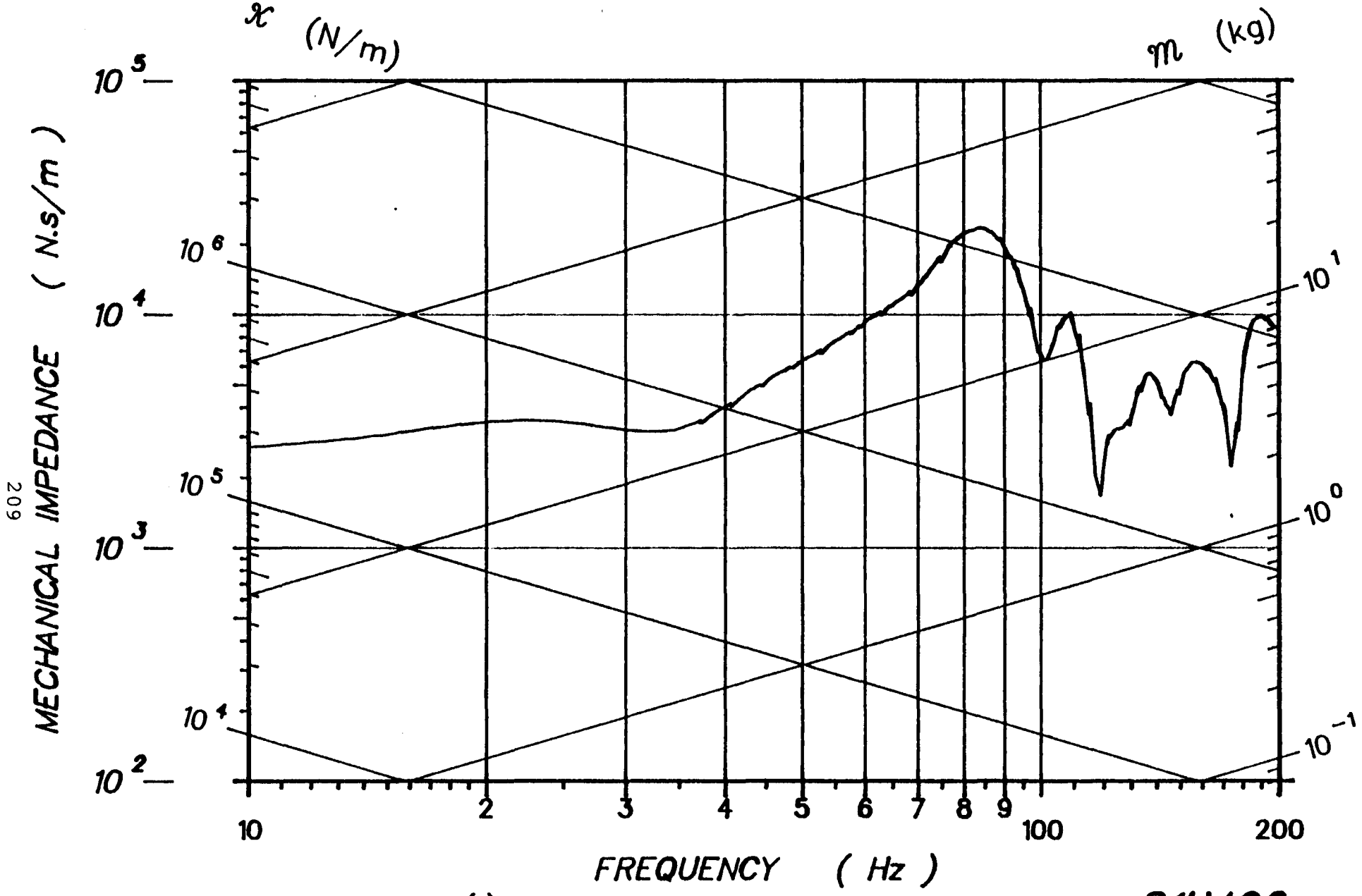

L1 ACC P--A(I)

81H406

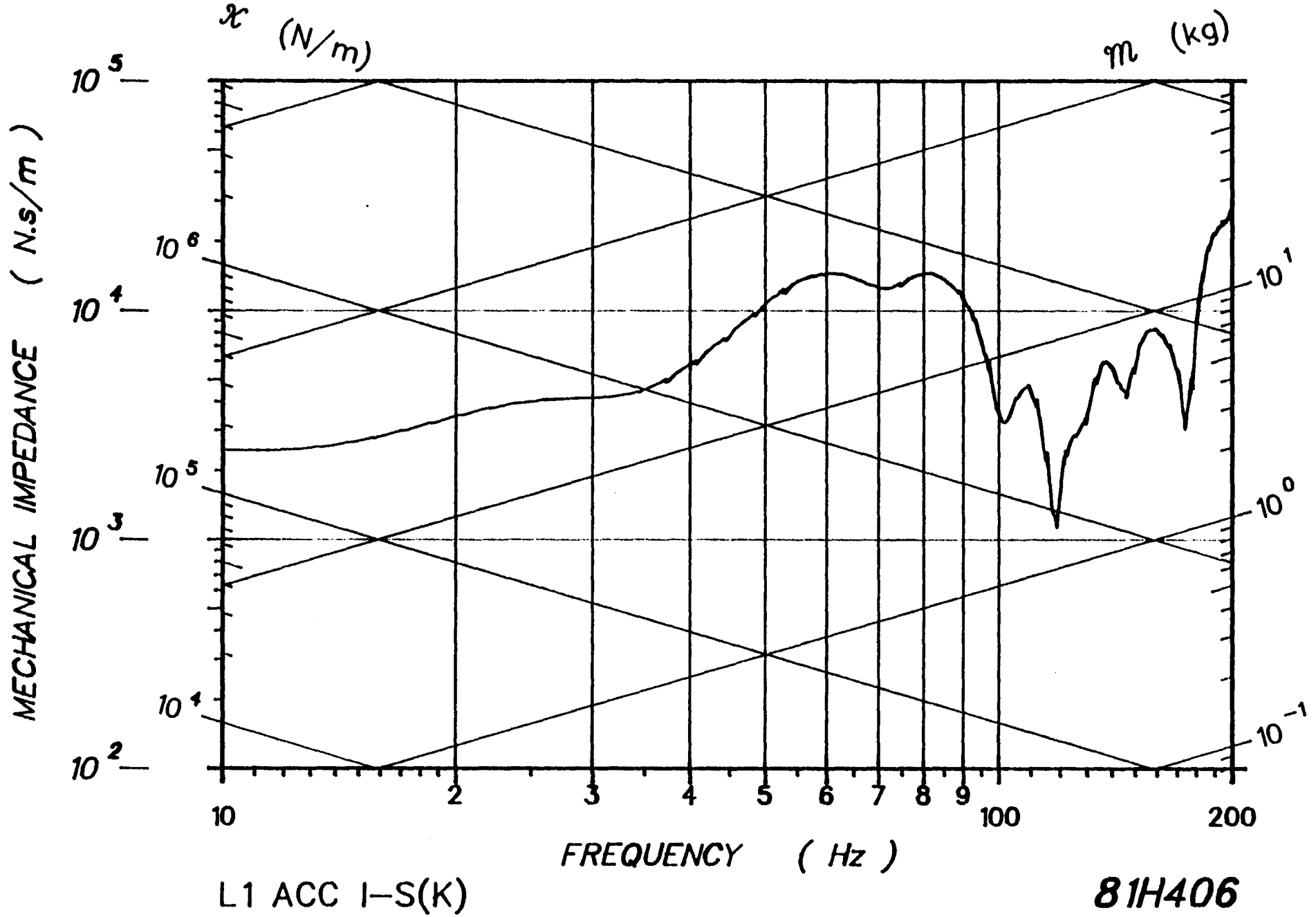
MECHANICAL IMPEDANCE (N.s/m)
FREQUENCY (Hz)
(N/m)
(kg)
10 5
10 4
10 3
10 2
10 6
10 5
10 4
10 1
10 0
10 -1
10
2
3
4
5
6
7
8
9
100
200
L1 ACC I–S(K)
81H406

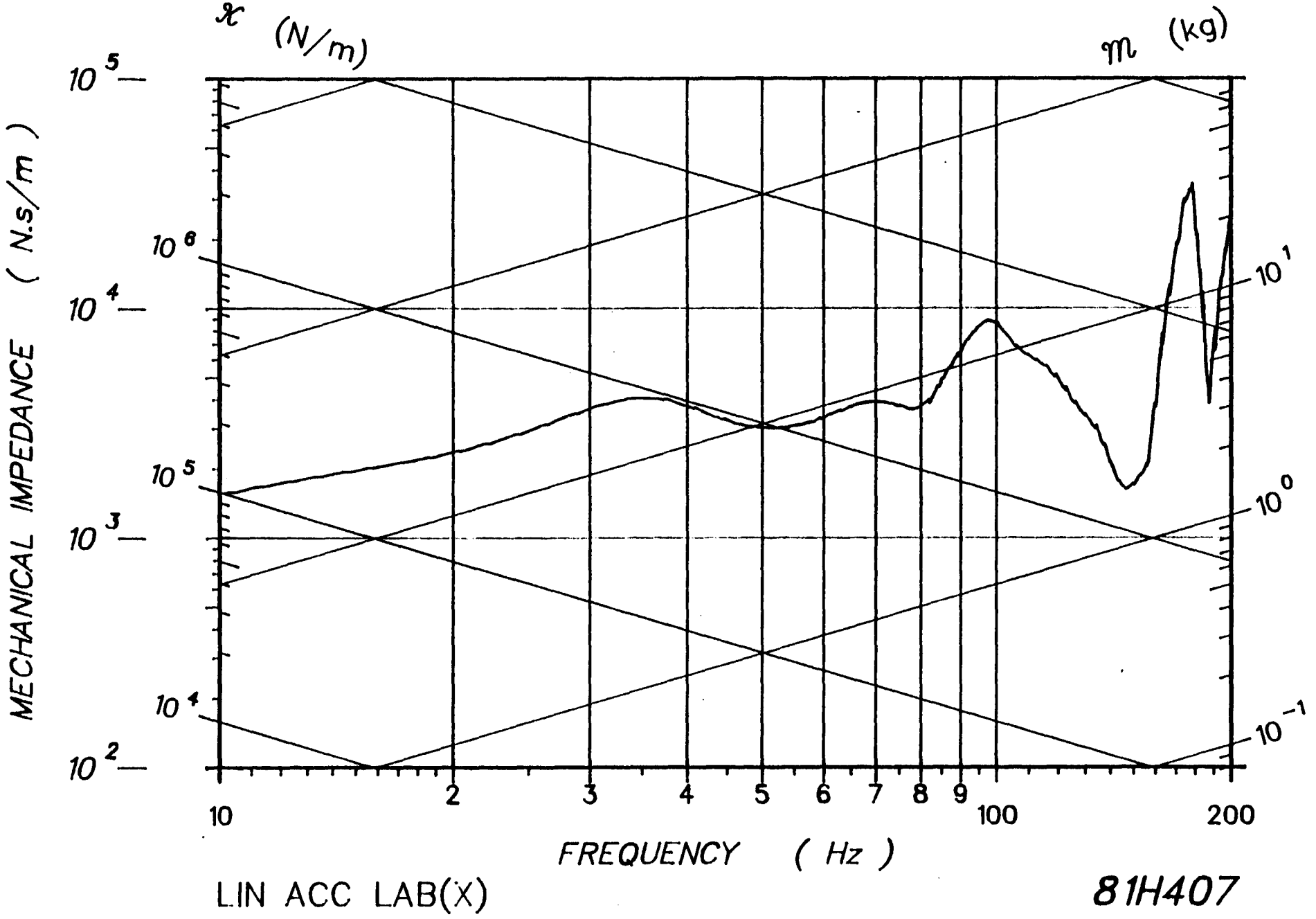
$\mathcal{K}$ (N/m)
$\mathcal{M}$ (kg)
10^5
10^4
10^3
10^2
10^6
10^5
10^4
10^1
10^0
10^{-1}
MECHANICAL IMPEDANCE (N.s/m)
10
2
3
4
5
6
7
8
9
100
200
FREQUENCY (Hz)
LIN ACC LAB(X)
81H407

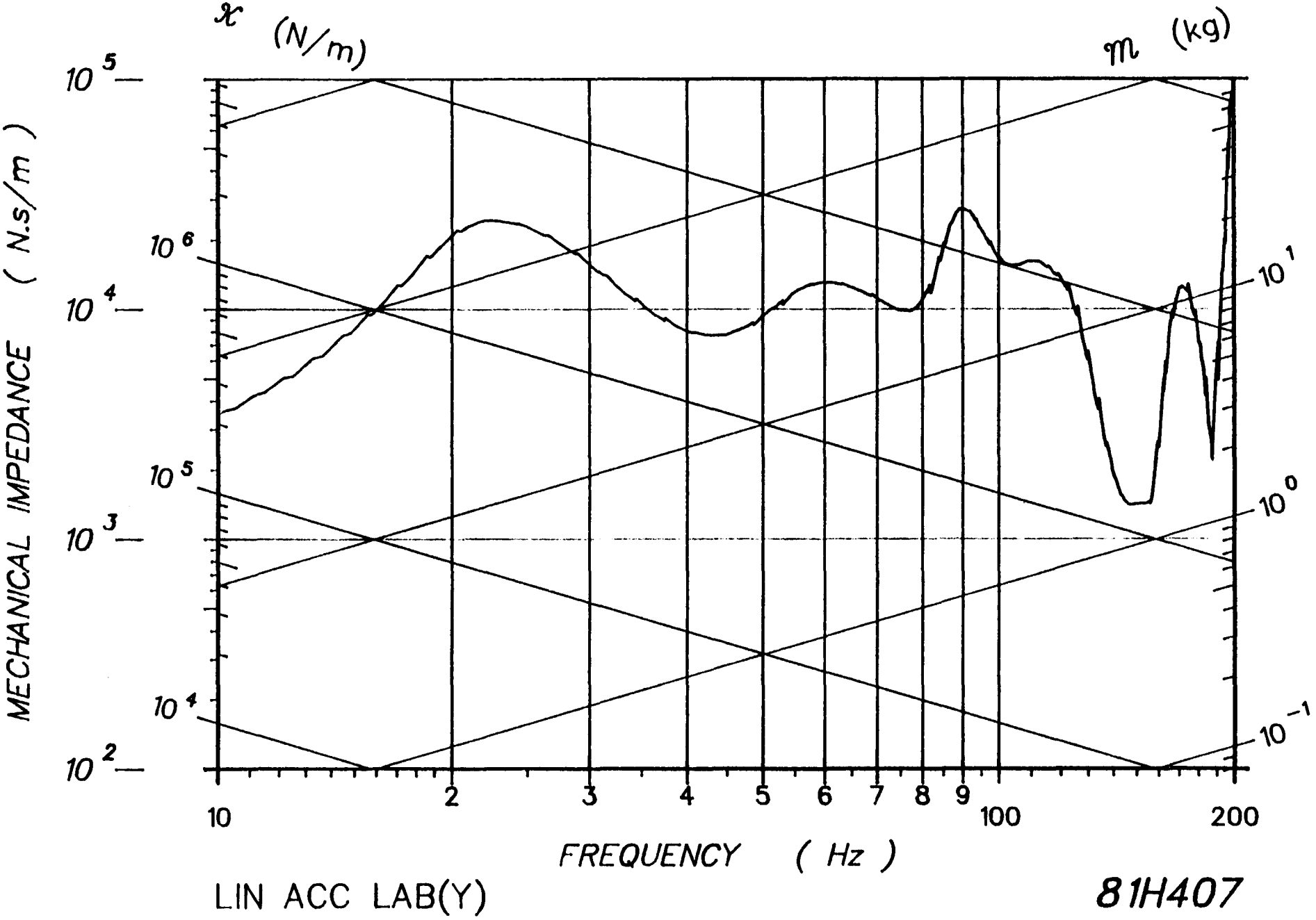
$\mathcal{K}$ (N/m)
$\mathcal{M}$ (kg)
10^5
10^4
10^3
10^2
10^6
10^5
10^4
10^1
10^0
10^{-1}
MECHANICAL IMPEDANCE (N.s/m)
10
2
3
4
5
6
7
8
9
100
200
FREQUENCY (Hz)
LIN ACC LAB(Y)
81H407

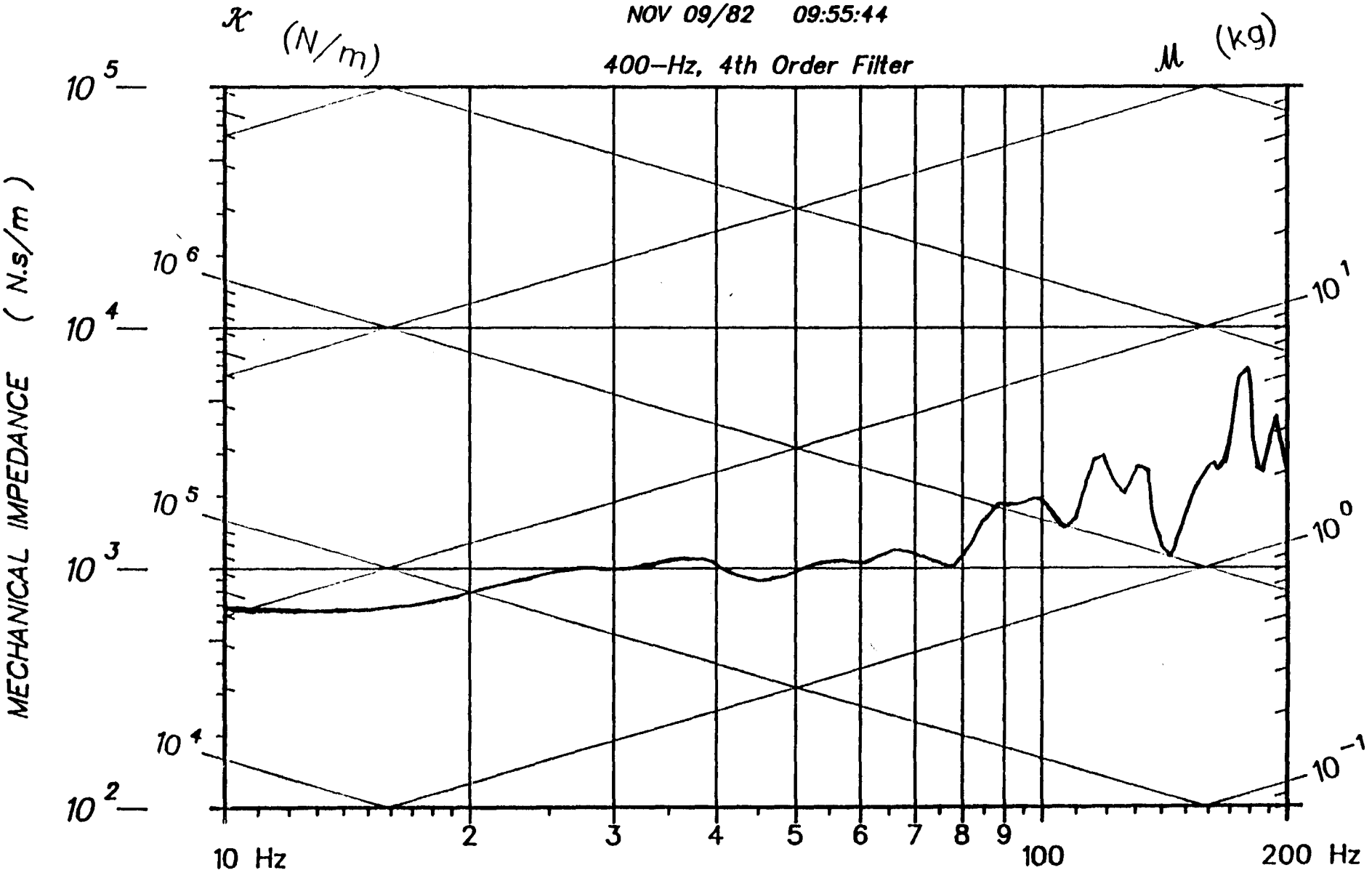

Z=F1/V1 for HEAD

81H407

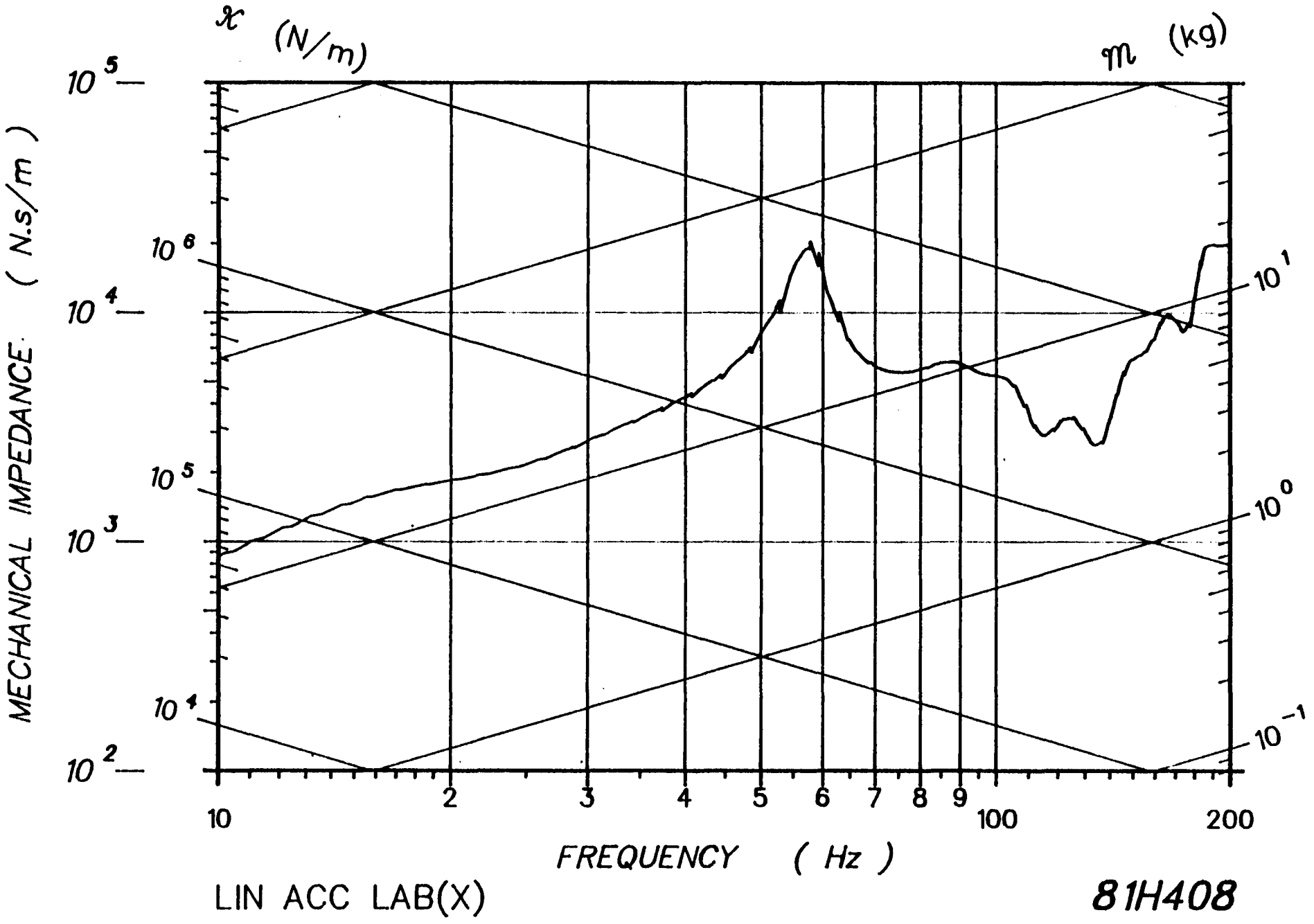
$\mathcal{K}$ (N/m)
$\mathcal{M}$ (kg)
MECHANICAL IMPEDANCE (N.s/m)
10^5
10^4
10^3
10^2
10^6
10^5
10^4
10^1
10^0
10^{-1}
10
2
3
4
5
6
7
8
9
100
200
FREQUENCY (Hz)
LIN ACC LAB(X)
81H408

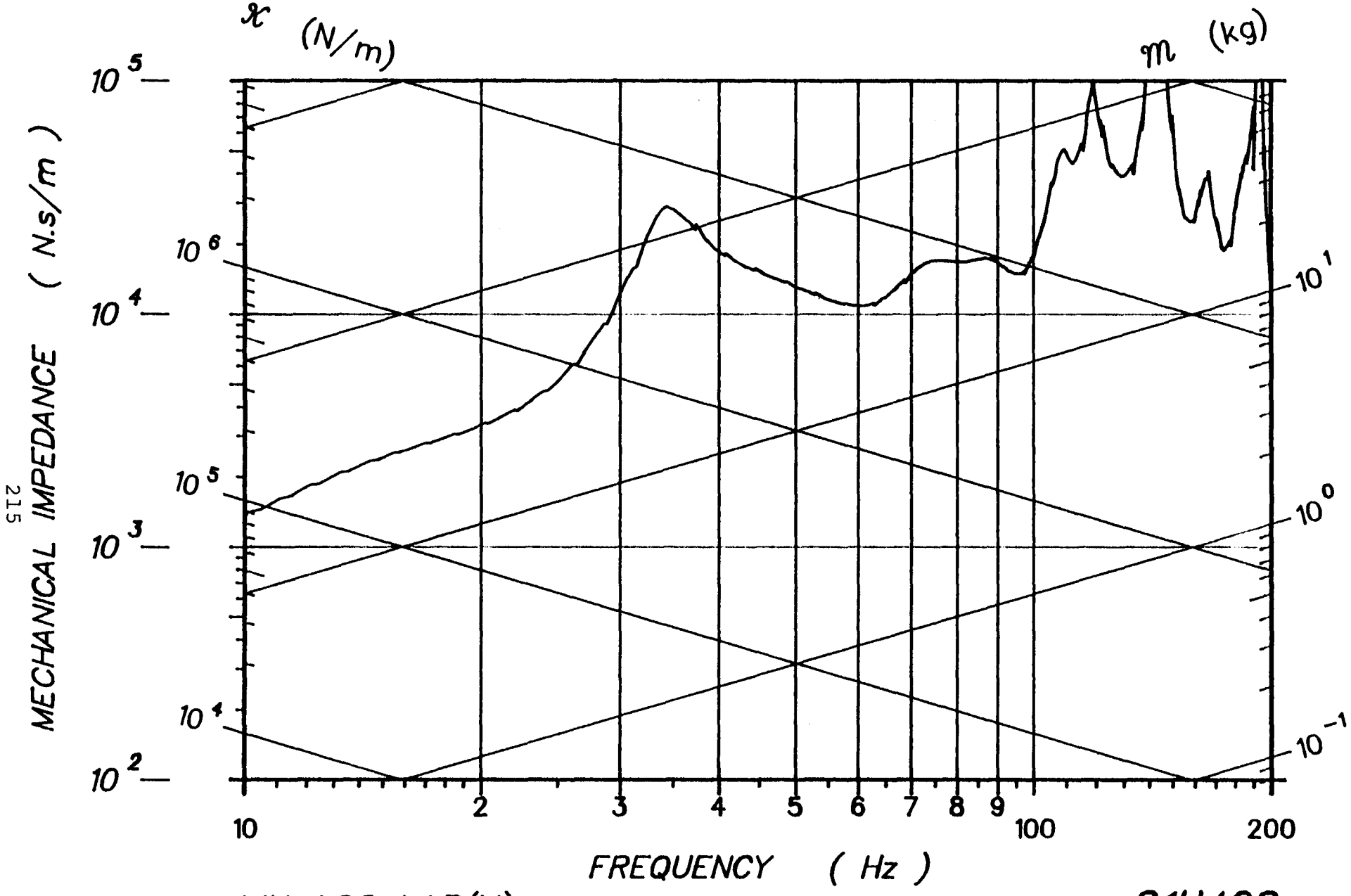

LIN ACC LAB(Y)

81H408

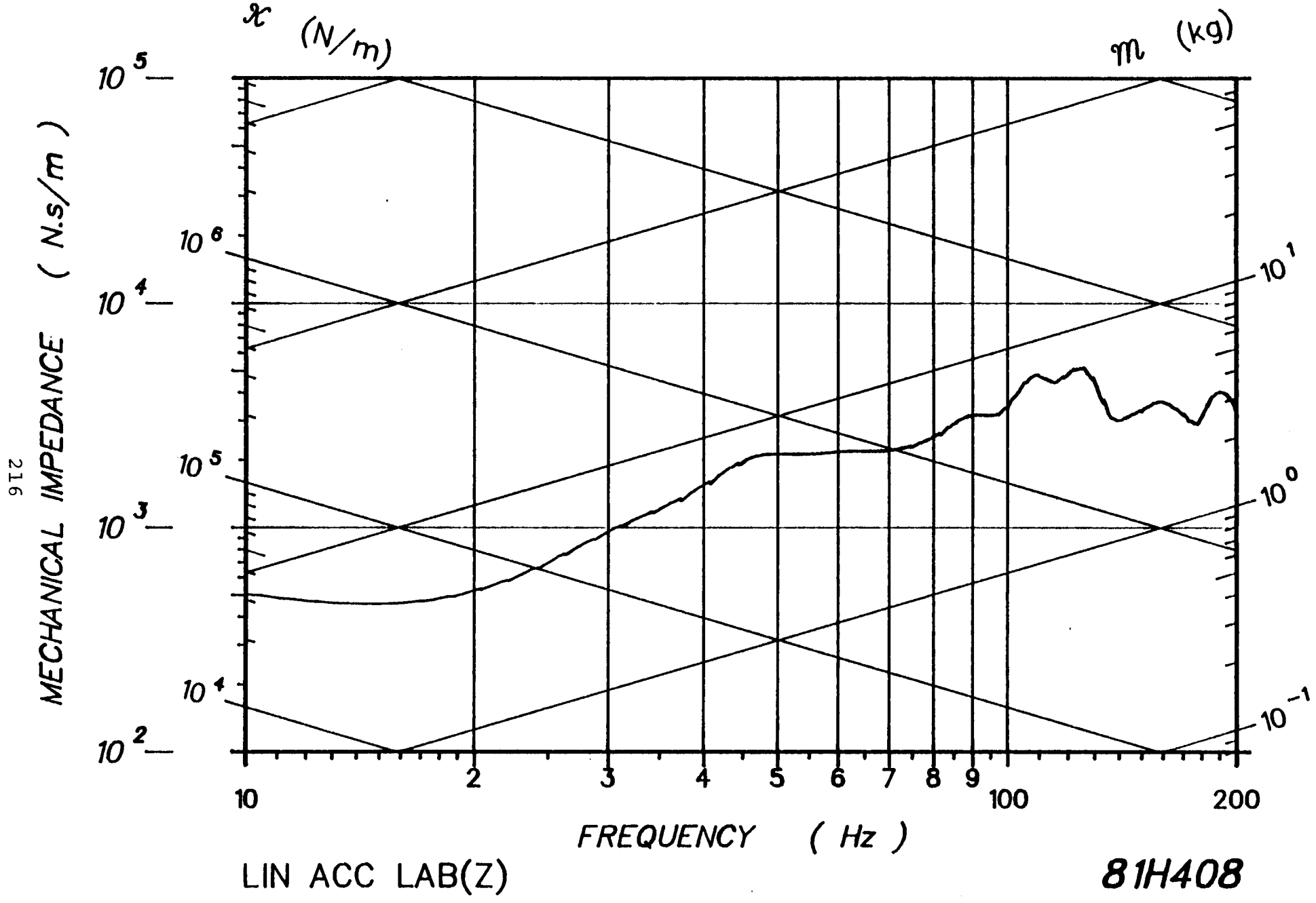
$\mathcal{K}$ (N/m)
$\mathcal{M}$ (kg)
MECHANICAL IMPEDANCE (N.s/m)
10^5
10^4
10^3
10^2
10^6
10^5
10^4
10^1
10^0
10^{-1}
10
2
3
4
5
6
7
8
9
100
200
FREQUENCY (Hz)
LIN ACC LAB(Z)
81H408

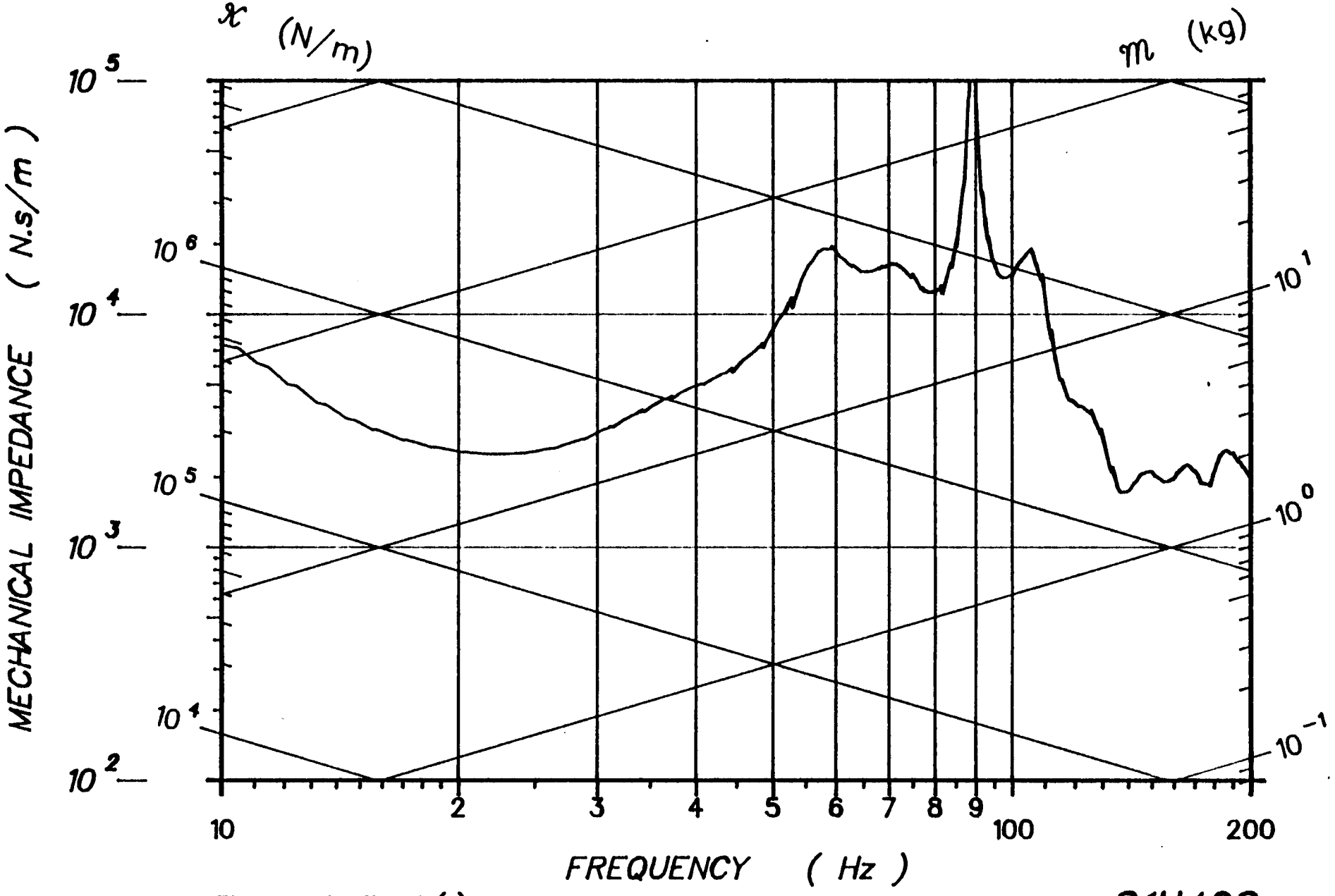
$\mathcal{K}$ (N/m)
$\mathcal{M}$ (kg)
10^5
10^4
10^3
10^2
10^6
10^5
10^4
10^1
10^0
10^{-1}
MECHANICAL IMPEDANCE (N.s/m)
10
2
3
4
5
6
7
8
9
100
200
FREQUENCY (Hz)
T1 ACC P–A(I)
81H408

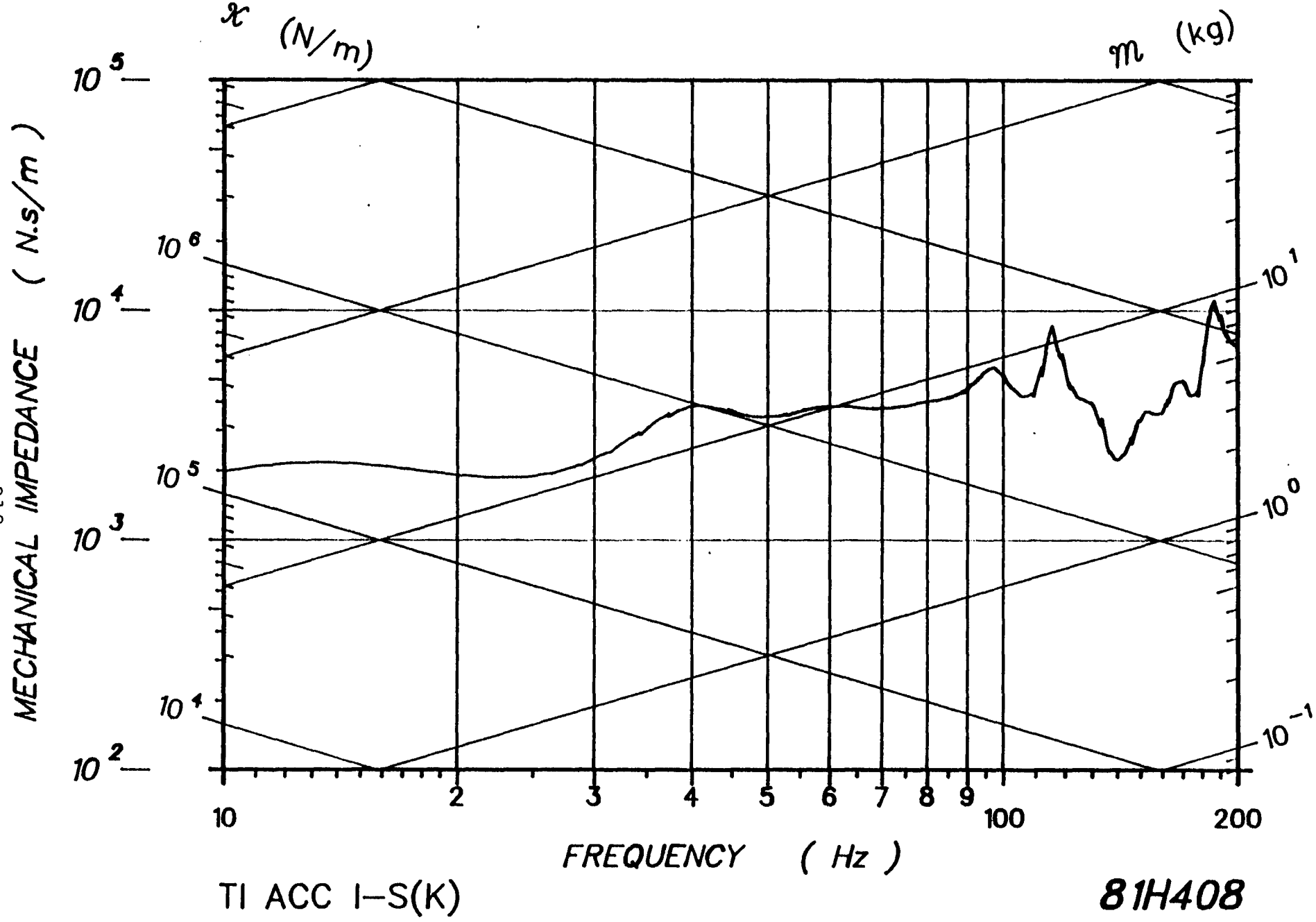
$\mathcal{K}$ (N/m)
$\mathcal{M}$ (kg)
MECHANICAL IMPEDANCE (N.s/m)
10^5
10^4
10^3
10^2
10^6
10^5
10^4
10^1
10^0
10^{-1}
10
2
3
4
5
6
7
8
9
100
200
FREQUENCY (Hz)
TI ACC I–S(K)
81H408

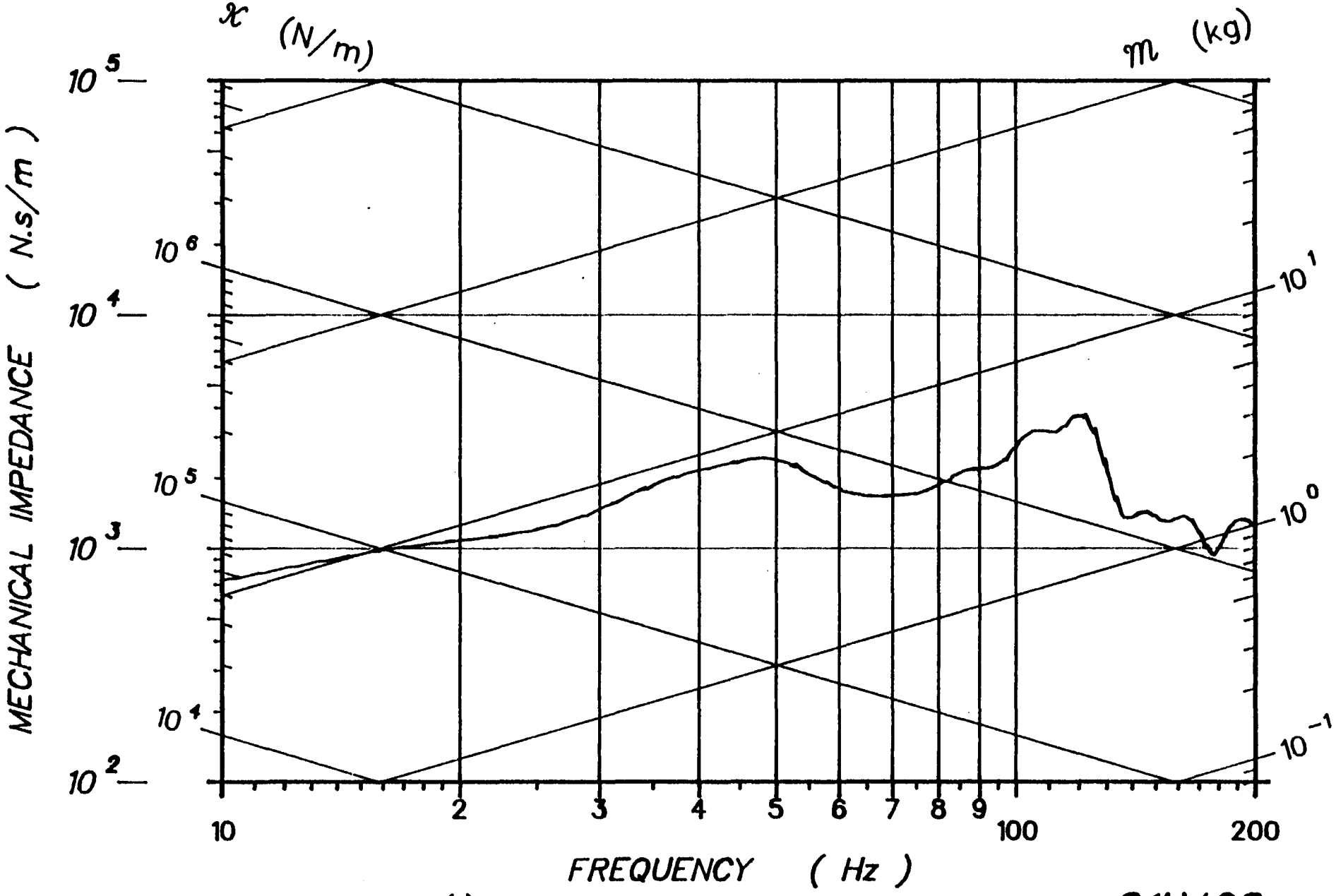
x (N/m)
m (kg)
MECHANICAL IMPEDANCE (N.s/m)
10 5
10 4
10 3
10 2
10 6
10 5
10 4
10 1
10 0
10 -1
10
2
3
4
5
6
7
8
9
100
200
FREQUENCY (Hz)
T6 ACC P-A(I)
81H408

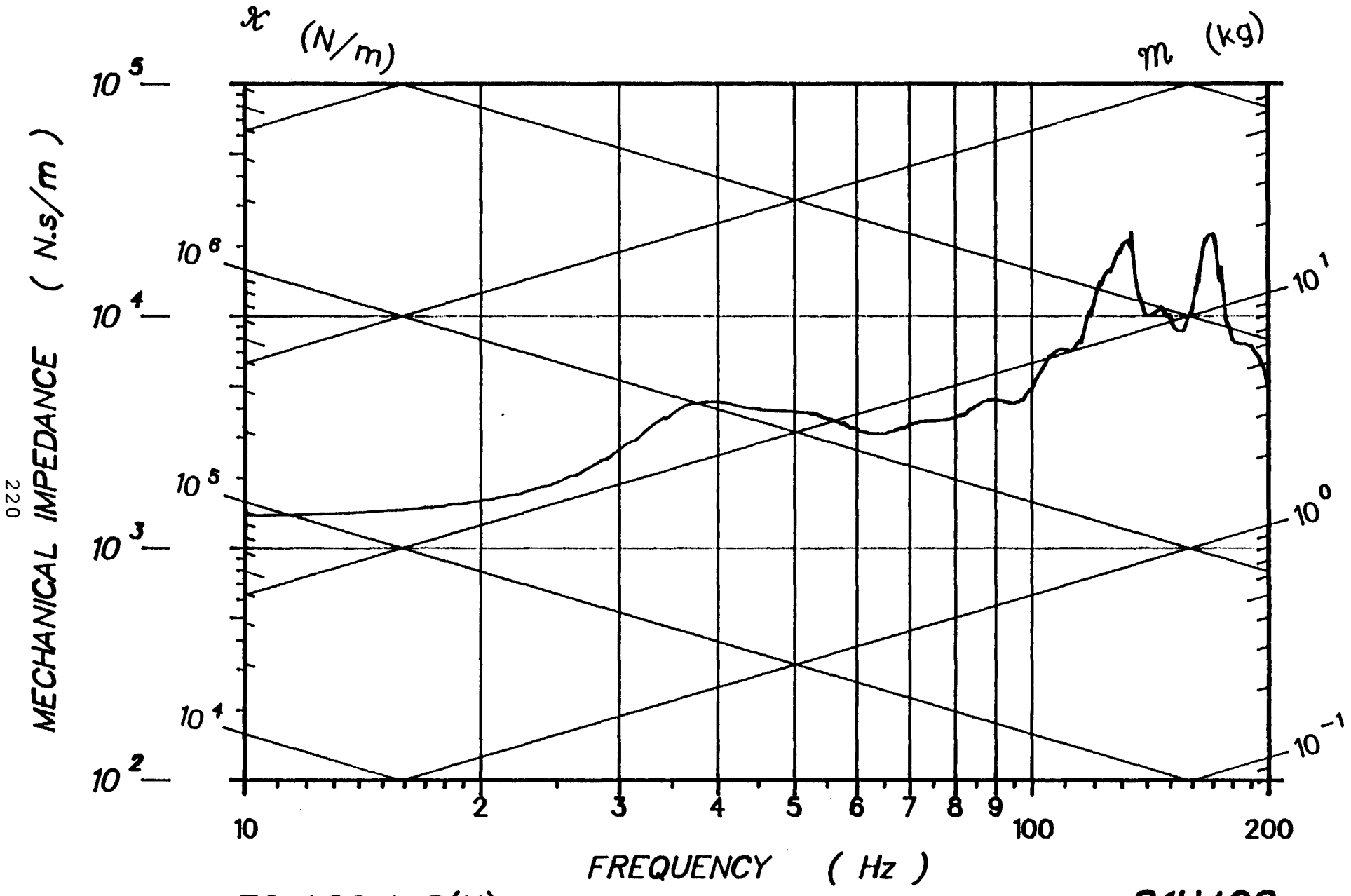

T6 ACC I–S(K)

81H408

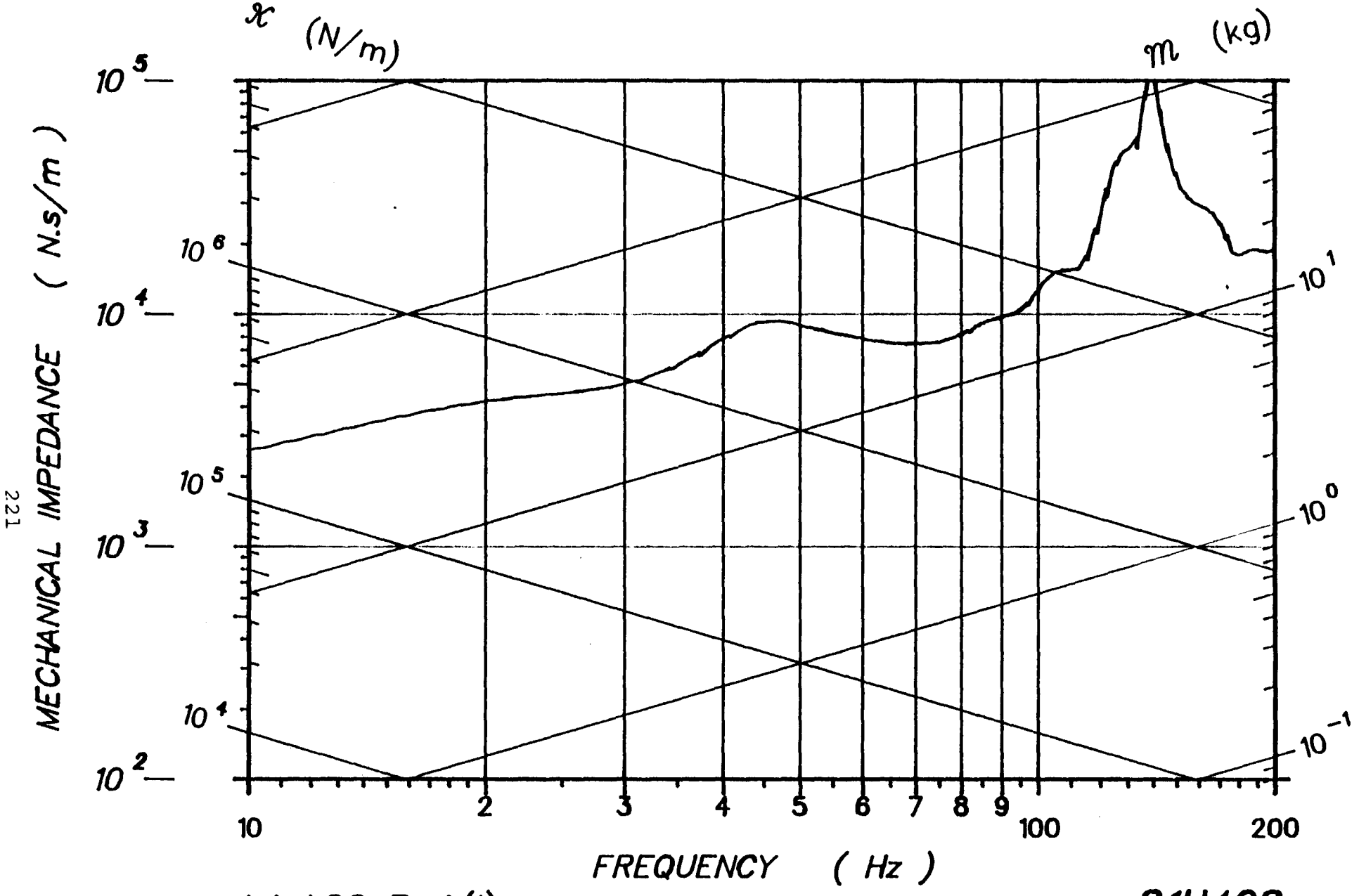

L1 ACC P–A(I)

81H408

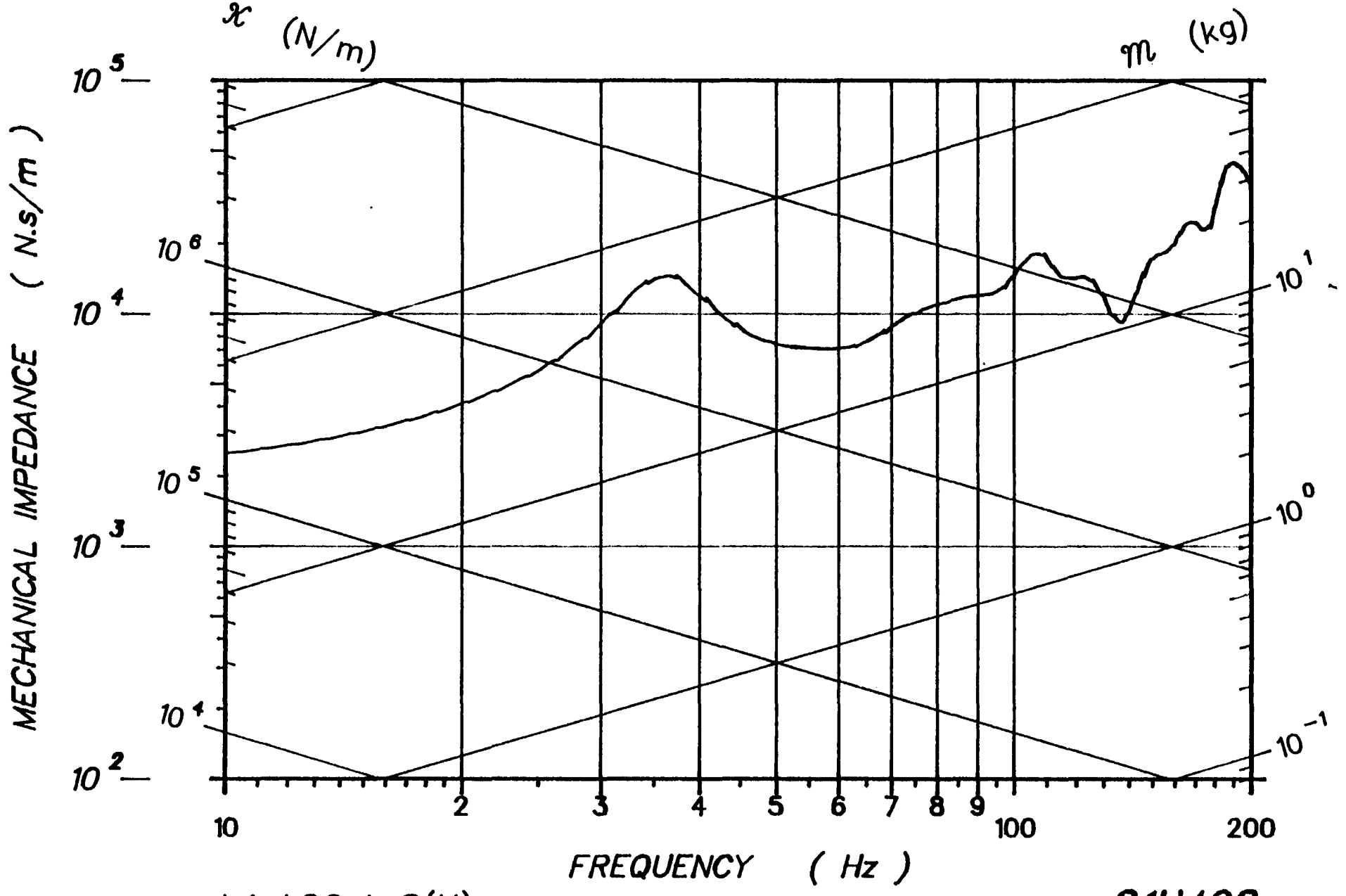

L1 ACC I–S(K)

81H408

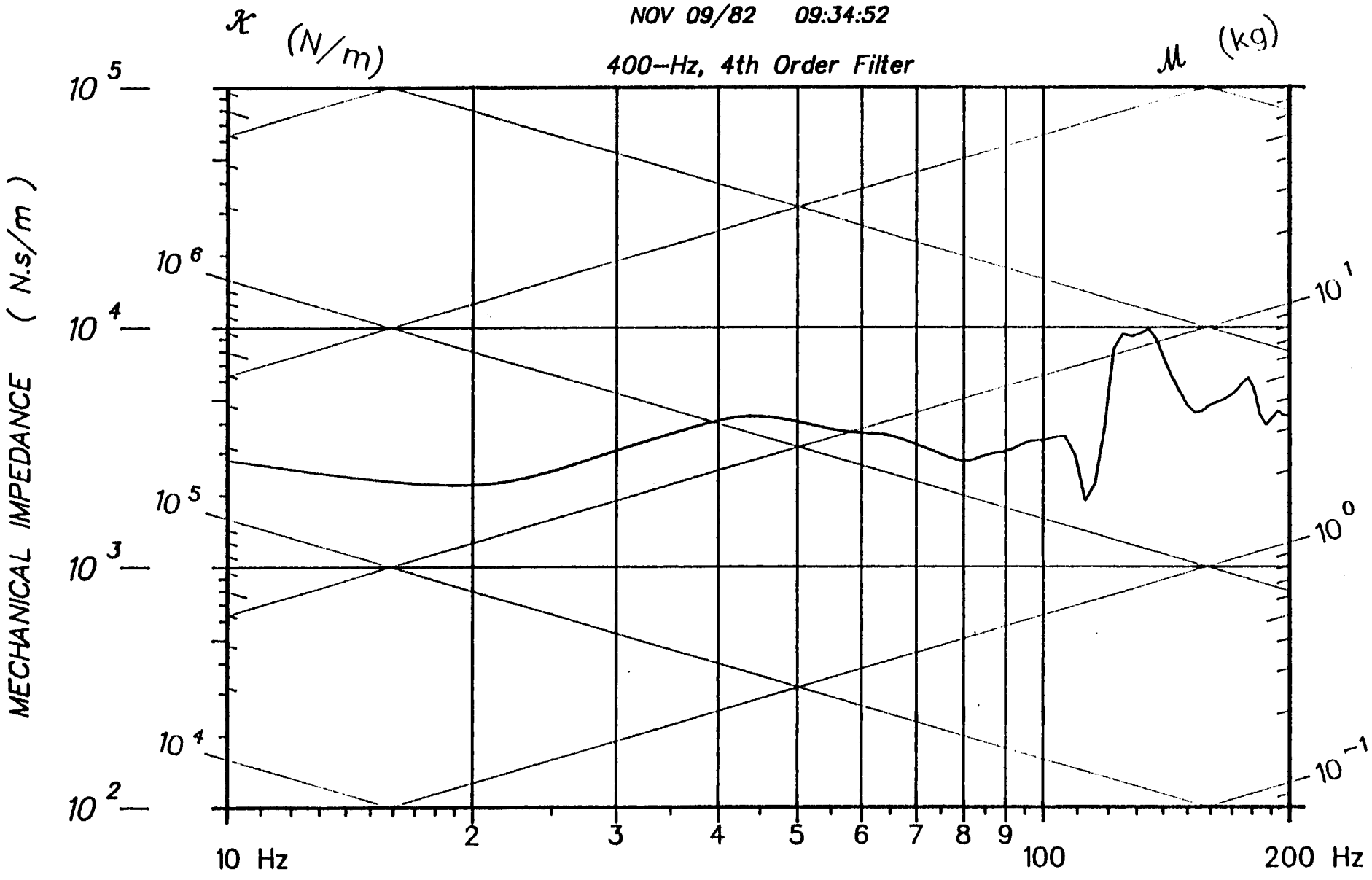

Z=F1/V1 for L1

81H410

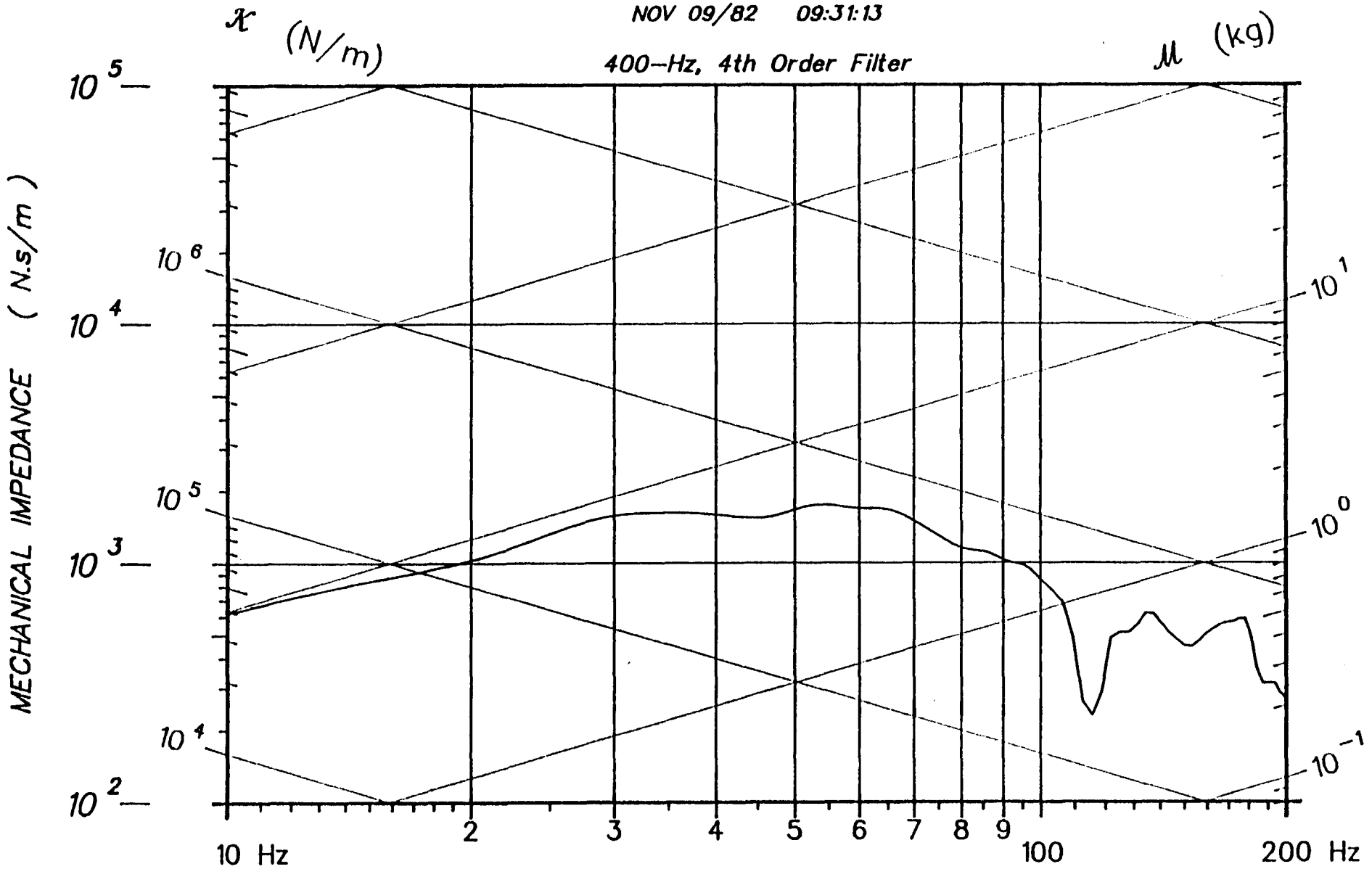

Z=F1/V1 for T1

81H410

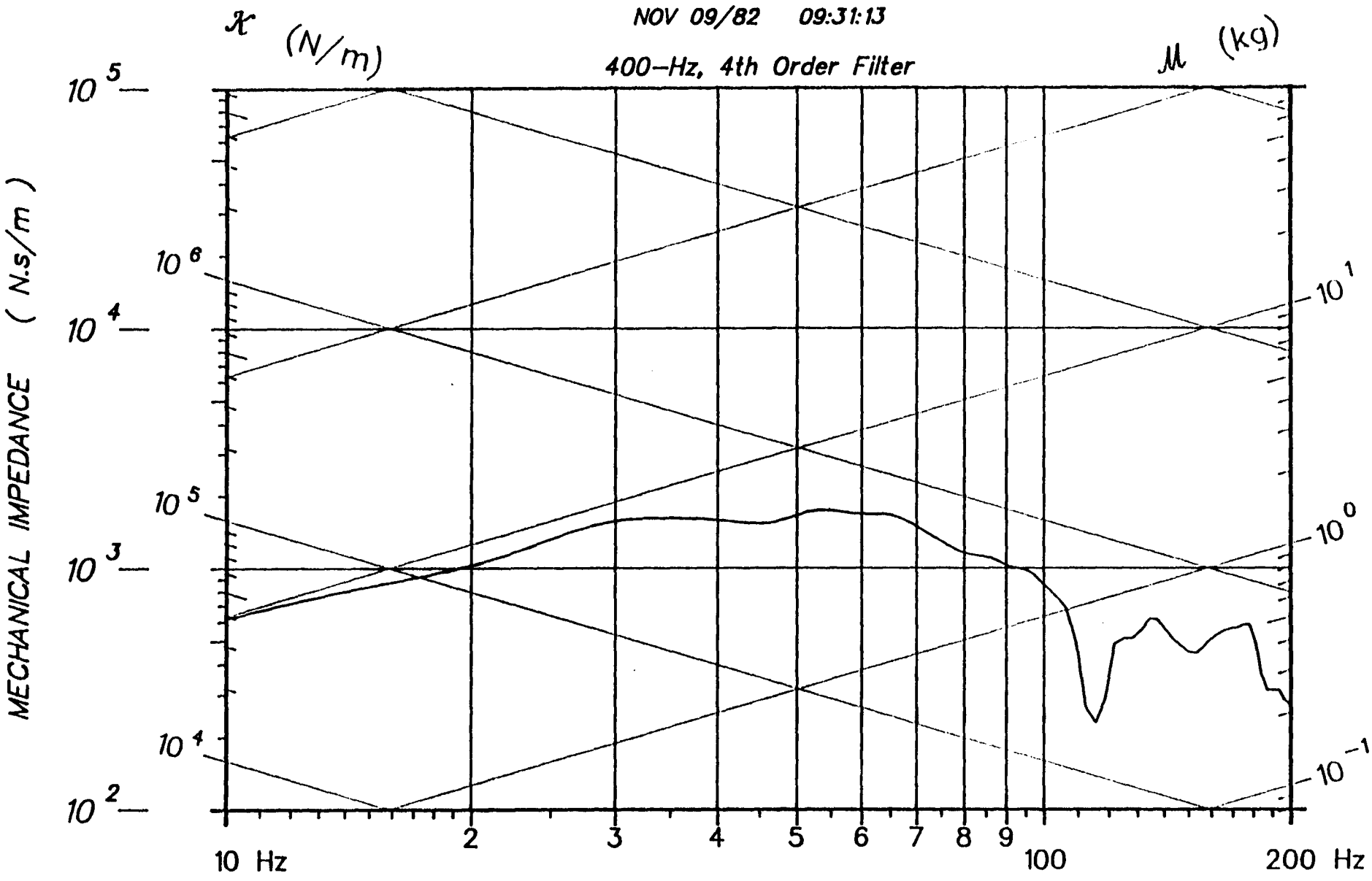

Z=F1/V1 for T1

81H410

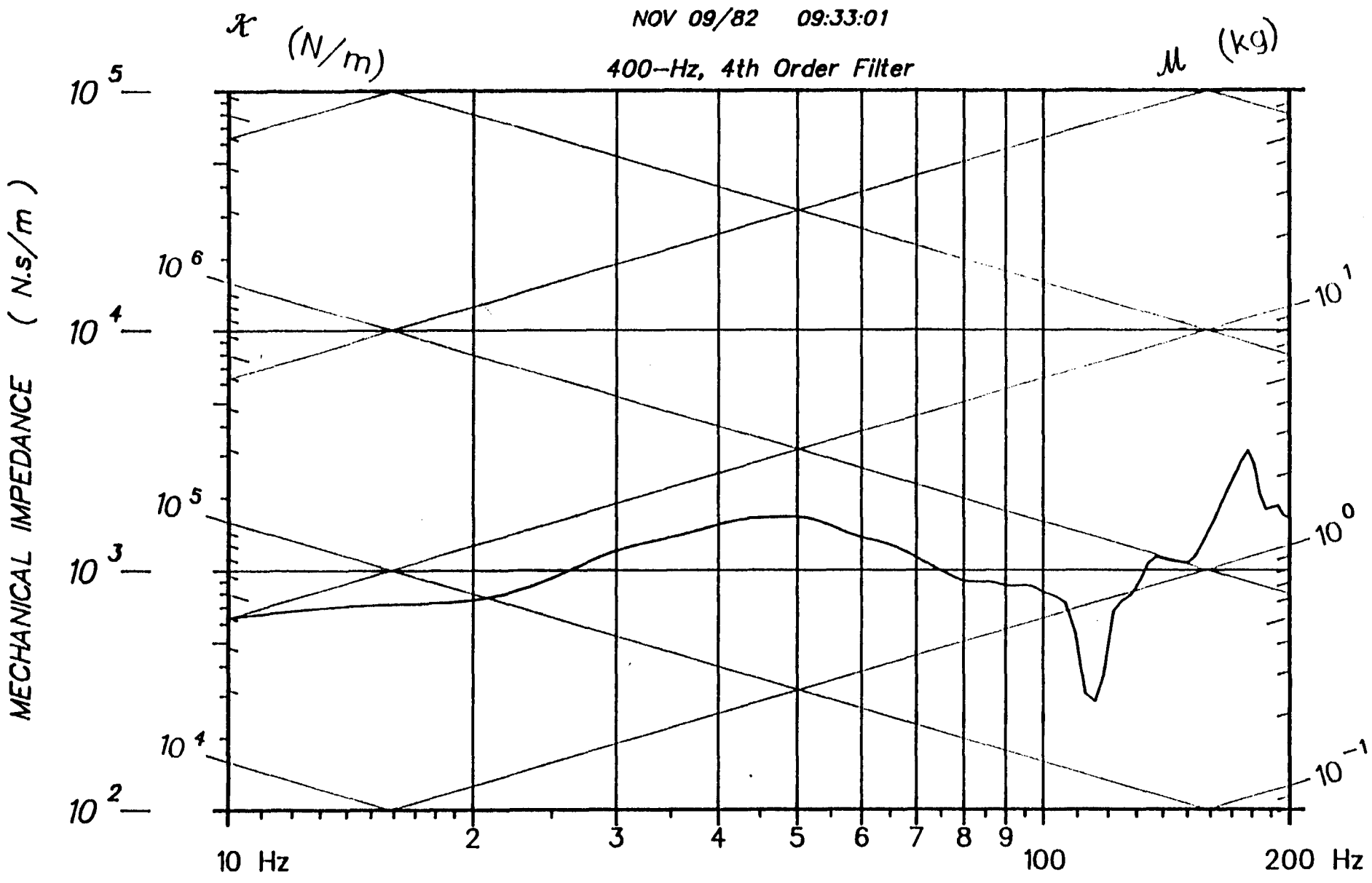

Z=F1/V1 for T6

81H410

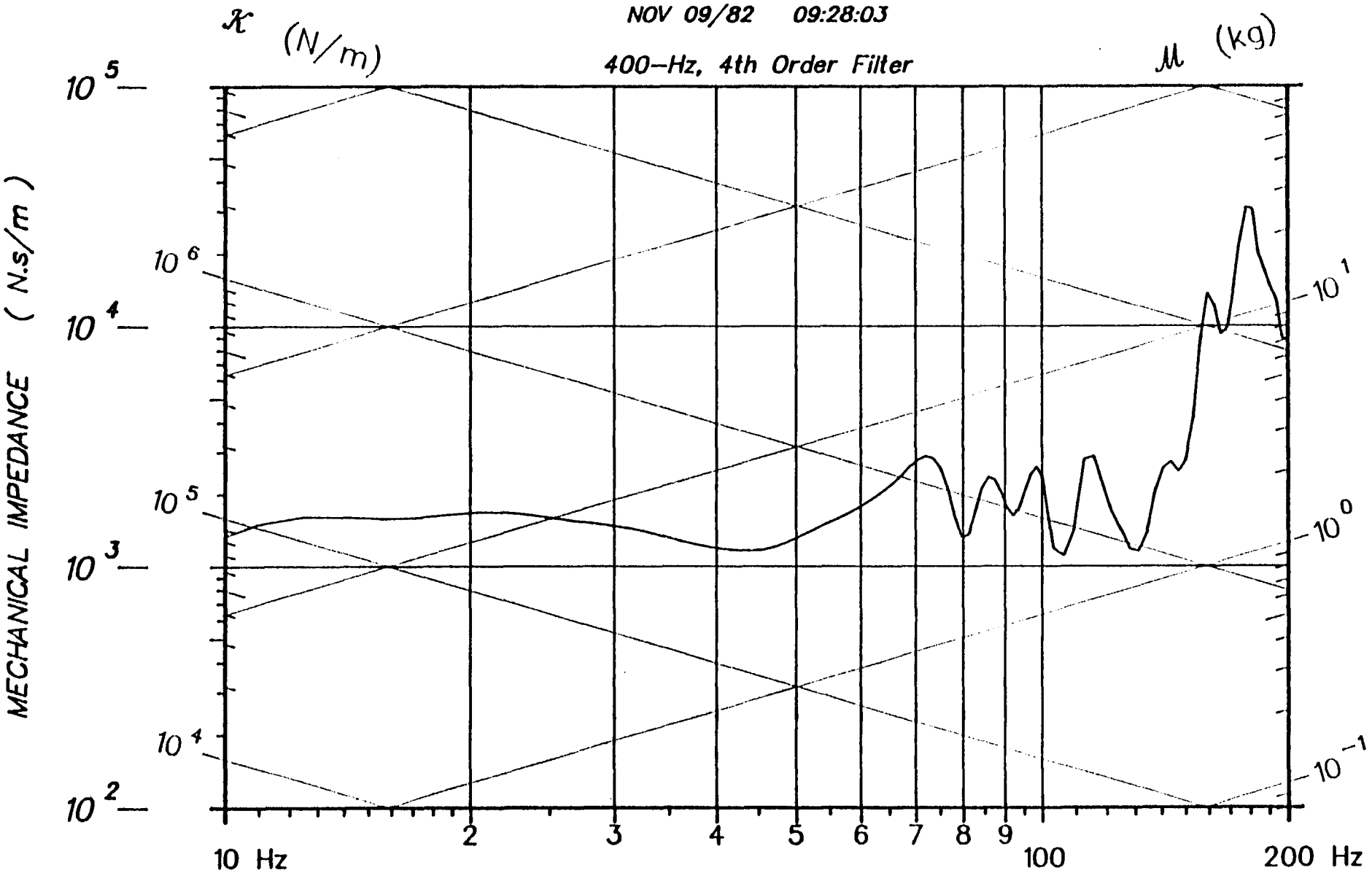

Z=F1/V1 for HEAD

81H410

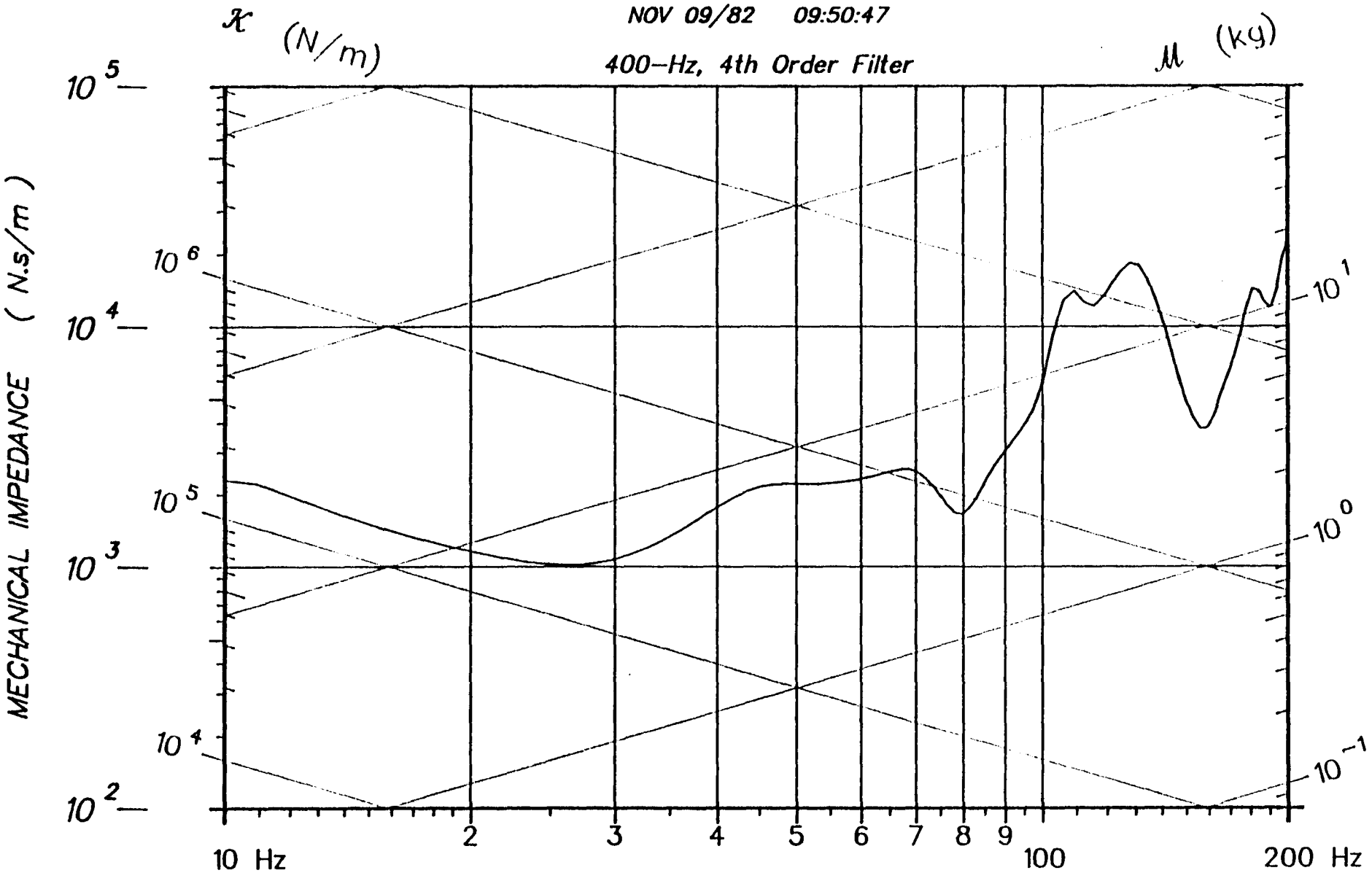

Z=F1/V1 for HEAD

81H411

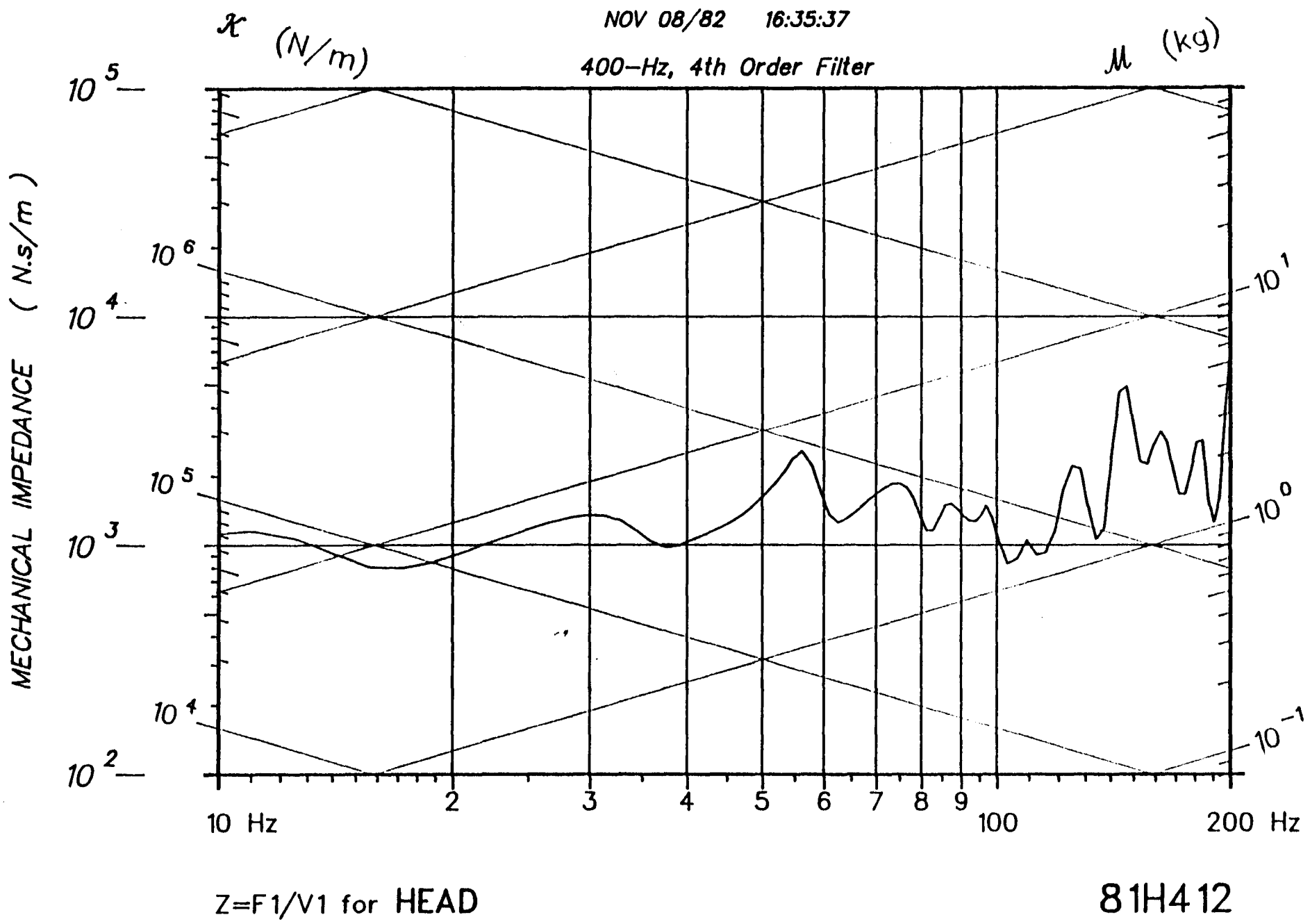

Z=F1/V1 for HEAD

81H412

APPENDIX D

TEST PROTOCOL

This appendix contains the test protocol that was originally developed to conduct both pressurized and non-pressurized S-I impact tests. Although no pressurized tests were conducted, major effort went into the development of the protocols for both types of tests. However, some tasks that were defined in the protocol were eventually modified as experience was gained in performing the sequence of tasks in the protocol.

The original protocol is included here for complete documentation of the work done under this project.

SUPERIOR-INFERIOR HEAD IMPACT

INJURY TOLERANCE LEVELS

(Test Series 80H300)

P R O T O C O L

TEST NO._____

TEST DATE_____

PERSONNEL	TASK ASSIGNMENTS
_____	_____
_____	_____
_____	_____
_____	_____
_____	_____
_____	_____

C H E C K L I S T O F T A S K S

NIOSH: S-I Head Impact Injury Tolerance Levels TEST NO.

TASK 1: ACCELEROMETERS FOR MOTION ANALYSIS

_____ A. Begin preparing instrumentation data sheet.

_____ B. Obtain 18 Endevco accelerometers.

_____ C. Obtain calibration factors. Calibrate if necessary.

_____ D. Wire the 18 Endevco accelerometers to the patch panel connecting the cannon lab to the sled lab.

_____ E. In the sled lab, wire each accelerometer to an amplifier.

_____ F. Check each accelerometer for balance and excitation. Replace if necessary.

_____ G. Assign each accelerometer to a mount, tape channel, patch panel cable and amplifier. Record in instrumentation data sheet.

_____ H. Obtain accelerometer gains. Record in instrumentation data sheet.

_____ I. Assemble 9 accelerometers in 3 triax packs for 9 accelerometer plate. Protect with pads.

_____ J. Assemble 9 accelerometers in 3 triax packs for spinal mounts. Protect with pads.

TASK 2: PRESSURE TRANSDUCERS

_____ A. Obtain 5 pressure transducers.

_____ B. Obtain calibration factors. Calibrate if necessary.

_____ C. Wire the 5 pressure transducers to the patch panel connecting the cannon lab to the sled lab.

_____ D. In the sled lab, wire each accelerometer to an amplifier.

_____ E. Check each accelerometer for balance and excitation. Replace if necessary.

_____ F. Assign each transducer to an anatomical position, patch panel cable, and amplifier. Record in instrumentation data sheet.

_____ G. Obtain pressure transducer gains. Record in instrumentation data sheet.

_____ H. Protect each transducer with padded tubes.

TASK 3: IMPACTOR TRANSDUCERS

_____ A. Prepare impactor head, load cell, accelerometer, and padding.

_____ B. Wire load cell and accelerometer to charge amplifier and check calibration.

_____ C. Compensate load cell.

_____ D. Assign force, compensated force, and acceleration to a patch panel cable and tape channel. Record in instrumentation data sheet.

_____ E. Obtain compensated force gain. Record in instrumentation data sheet.

TASK 4: PHOTOMETRICS (X-RAYS)

_____ A. Check out function of GE dental X-ray head and power supply.

_____ B. Wrenches, sockets and ratchets for frame bolts. (9/16" & 5/8" socket; 9/16" & 11/16" open ended wrench)

_____ C. Load 7 cassettes with fresh film.

_____ D. Prepare x-ray labels. (Test ID and x-ray no.)

_____ E. Check developer and fixer. Change if necessary.

TASK 5: POSITIONING

_____ A. Obtain initial test configuration.

_____ B. Adjustable "orange" table with 4 floor clamps, front and rear braces, and bolts.

_____ C. Two layers of 4" foam (18x60") and one layer (18x18") balsa wood.

_____ D. Several lengths of 4" thick balsa wood for pelvis support.

_____ E. Head suspension aluminum angle-iron attached to cannon.

_____ F. 1" and 1/2" masking tape. Duct tape, fiber tape, waxed string and two 4' rope pieces.

_____ G. Vise-grips, crank and other wrenches for table.

TASK 6: PRESSURIZATION SYSTEM

_____ A. Test out regulator.

_____ B. Test out plumbing system for water and air leaks.

_____ C. Mix new pressurization fluid.

_____ D. Check out pressurization system.

TASK 7: IMPACT DEVICE

_____ A. Obtain the following information to recycle and wire the cannon.

Striker weight _____ Bumper _____

Impactor weight _____ Bumper _____

Piston face _____ Padding _____

Piston rod _____ Post-test excursion _____

Pre-test gate zero _____ Gate duration _____

Approximate velocity _____

_____ B. Calculate:

Gate delay _____ Gate mag pick up _____

Crush tube length _____ X-ray trigger mag pick up _____

Pre-test travel _____ Velocity probe spacing _____

Cannon pressure _____

_____ C. Assign sequencer values and wire up appropriately. (See "TIMER BOX SET-UP" and "TIMER VALUES" tables below.)

_____ D. Wire up:
___Gate mag pickup
___Velocity mag pickup
___Chronograph
___Filter
___Strobe terminals
___Firing consoles
___Film switch
___Automatic firing

_____ E. Complete recycling of cannon 1-6 hours before test. Instructions are in cannon log book.

NIOSH: S-I Head Impact Injury Tolerance Levels TEST NO. _____

T I M E R B O X S E T - U P

Equipment		Source	Timing Sequence From	To
X-ray Standby	1			1
Cannon	2			2
Photosonics	3			3
X-ray Trigger	4			4
Pressure	5			5
	6			6
	7			7
	8			8

T I M E R V A L U E S

	1	2	3	4	5	6	7	8
Delay:								
Run:								

TASK 8: HIGH SPEED CINERADIOGRAPH

_____ A. Wire up:
___High voltage supply
___High voltage capacitor
___X-ray head
___Control console
___Image intensifier high voltage supply
___Gating circuit
___Camera mag pickup
___Mag pickup triggering unit
___Image intensifier
___Gating circuit test attenuator

_____ B. Connect cooling fan.

_____ C. Assign gating circuit to patch panel and record in instrumentation data sheet.

_____ D. Focus magnet.

_____ E. Bolt down photosonics and focus camera with boresight. Install cassettes with 2x negative film.

_____ F. Prepare power supplies and connect timing sights.

_____ G. Prepare strobe timing lights.

_____ H. Load 35 mm still cameras with B negatives and slides.

_____ I. Prepare developer and dark room for film.

_____ J. Obtain X-ray filter.

_____ K. Polaroid camera and 16 films.

TASK 9: ANATOMY LAB

_____ A. Anthropometer and metric measuring tape.

_____ B. Blue pads, gauze, and flat waxed string.

_____ C. Rolls of adhesive, masking, and duct tapes.

_____ D. 2 large and 2 small scalpel handles.

_____ E. Scalpel blades, 2 each of #15, #22, and #12

_____ F. Hemostats.

_____ G. Needles, 2 each: small/large -- curved/straight.

_____ H. Forceps, 2 each: plain and curved "meathooks".

_____ I. Surgical scissors, one each: small, medium, large.

_____ J. Electric hair clippers.

_____ K. Tampons (at least 20).

_____ L. Thermoknit longjohns.

_____ M. Cotton socks and gloves.

_____ N. Electric drill

_____ O. Screwdriver.

_____ P. 1/2", #8 panhead type A sheet metal screws.

_____ Q. 1-72 screws and screwdriver for 9-acc plate.

_____ R. 4-40 screws and screwdriver for spinal mounts.

_____ S. 2 ear targets (round, one with tail).

_____ T. 2 eye targets (square, one with tail).

_____ U. 2 ear plugs to carry ear targets and 2 eye plugs to carry eye targets.

_____ V. 1 small 9-acc plate and its feet.

_____ W. 2 spinal mounts and wood screws (various lengths).

_____ X. Modified peritoneal dialysis catheter.

_____ Y. Modified No. 18 and No. 20 Foley Catheter.

_____ Z. Pressure transducer catheter tubes - 1 long, 2 short.

_____AA. Pressurization fluid.

_____AB. Pressurization testing equipment, air hose, amplifier, D-volt meter.

_____AC. 7 spine vertebrae body targets.

_____AD. Three (3) 2-point spine targets in aluminum tubes.

TASK 10: IMPACT LAB CART

_____ A. Plastic garbage bag taped onto cart ring.

_____ B. Adhesive tape, black thread, and waxed string.

_____ C. Blue pads and gauze.

_____ D. 4 pairs of green gloves.

_____ E. Large and small scalpel handles.

_____ F. Scalpel blades, one each of no. 15, 22, 12.

_____ G. 2 hemostats, 2 forceps.

_____ H. Large surgical scissors.

_____ I. 2 trocar needles.

TASK 11: PRE-TEST TRIAL

A pre-test run is to be made to check out the function of each piece of equipment before the test. The cannon is recycled and a dummy system is tested. All transducers and signals to be recorded on tape must be checked to see that they are recorded.

_____ A. 18 accelerometers.

_____ B. 5 pressure transducers.

_____ C. Gate.

_____ D. Gating circuit.

_____ E. Velocity.

_____ F. Force.

_____ G. Acceleration.

_____ H. Comp force.

_____ I. Film developed with clear picture .

TASK 12: ANTHROPOMETRIC MEASUREMENTS

All measurements are in centimeters (cm) except weight in kilograms (kg). Most measurements pertain to head anthropometry. Accuracy should be within 2-3 mm.

Cadaver No. _____ Cadaver Sex _____

Height _____ Weight _____

Acromion Height: Left _____ Right _____

Mastoid to Vertex: Left _____ Right _____

Tragon to Vertex: Left _____ Right _____

Menton to Vertex _____ Bitragon Diameter _____

Head A-P Length _____ Head L-R Breadth _____

Head Circumference _____ Neck Circumference _____

TASK 13: PRE-TEST SPINAL X-RAYS

KVP	MA	SEC	DESCRIPTION
_____	_____	_____	_____
_____	_____	_____	_____
_____	_____	_____	_____
_____	_____	_____	_____

Use bag of lead shot to position head/neck in desired position. Repeat if necessary.

Examine x-rays to detect a broken skull or any broken vertebrae.

TASK 14: VASCULAR PRESSURIZATION

INCISIONS:

_____ A. Make a longitudinal incision in the neck above the carotid artery.

_____ B. Make a short longitudinal incision in the carotid artery just big enough for the catheter to pass through. It is best to make the incision in the artery closer to the head to allow for tying off the artery both above and below the incision.

INSERTION:

_____ C. Tie off the carotid artery above the incision (near the head) using waxed string. The waxed string can now be used to relocate the artery.

_____ D. Raise the artery to the surface by pulling slightly on the waxed string.

_____ E. Insert the catheter. Hemostats may be necessary to spread the incision enabling the catheter to then slide into the artery.

_____ F. Once the tip of the catheter is pushed into the artery, care is taken that the wire handle is pointing up. Continued insertion of the catheter will place it in the heart.

POSITIONING:

_____ G. Push the catheter into the heart.

_____ H. Pull the catheter back and rotate it so that the wire handle is pointing down and the tip of the catheter is pointing down the descending aorta.

TRANSDUCER:

_____ I. Once the catheter tip is pointing down the aorta, the catheter is slid along the wire and into the descending aorta.

____ J. The wire is then pulled out.

_____ K. The polyethylene tube used for the pathway of the pressure transducer is inserted into the common carotid and as close to the brain as possible.

_____ L. The polyethylene tube used as a fluid pathway has one end inserted into the carotid above the incision and one below.

_____ M. Wrap 3 pieces of waxed string around the artery with the one close to the heart tied down tight, but not tight enough to close off any of the tubes.

_____ N. Acrylic is injected into the carotid, not past the waxed string that has heen tightened.

_____ O. When the acrylic is almost hardened, the other 2 loops of waxed string are tightened.

_____ P. Allow the acrylic to harden, then close up the incision.

TASK 15: CERVICAL SPINE TARGETS

This task is done before closing the incision in the neck for the vascular pressurization.

_____ A. Locate the 7th Cervical vertebra

_____ B. Place a vertebra body target on the 7th body using modified 3/8" panhead screws with lead targets.

_____ C. After the 7th cervical vertebra has been targeted place a target on C-6, C-5, C-4, and C-3 the same way.

_____ D. Make an incision over C-7 to C-5. Place a 2-point target on the vertebral process of C-7 and C-5. Secure with lock wire and acrylic.

_____ E. Close all incisions.

TASK 16: HEAD ANATOMICAL TARGETS

EYE TARGETS: _____ LEFT _____ RIGHT _____

_____ A. Cadaver in supine position.

_____ B. Expose the two infraorbital ridges by making incisions.

_____ C. Drill two holes at lowest point in bone margin of each orbital cavity, to accept 3/8"x4 aluminum panhead screws. Screw them in.

_____ D. Use dental acrylic to secure the eye targets (both square, left with tail) to the two screws.

_____ E. Allow acrylic to dry. Close incisions by sewing over the targets.

EAR TARGETS: _____ LEFT _____ RIGHT _____

_____ F. Remove the outer ear with a scapel. Expose the bone opening of the ear canal.

_____ G. Put 3/8"x4 aluminum panhead screw in the posterior edge of the auditory canal.

_____ H. Use acrylic to hold the target to the screw. Both ear targets are round, with a tail on the left one.

TASK 17: EPIDURAL PRESSURE TRANSDUCERS

_____ A. Remove scalp from frontal, occipital and parietal regions where pressure transducers will be implanted.

_____ B. Core a 0.128" hole in skull . Record position of hole. Remove bone core with dental scoop. Screw the metal epidural pressure transducer fitting (EPTF) into the cored hole.

_____ C. Mix dental acrylic.

_____ D. Affix the EPTF to the skull with dental acrylic, making sure that it will not loosen.

TASK 18: 9-ACC PLATE

_____ A. Cadaver face down. Shave the head and remove a 2x2" square of scalp from the occiput.

_____ B. Drill 4 holes for 1/2"x8 panhead, type A sheet metal screws. Clean up and dry the bone; then insert the 4 screws.

_____ C. Install small 9-acc plate (#2) over the exposed occiput with 4 feet attached to the plate.

_____ D. Mold a single 2" diameter acrylic pillar around the 4 feet and the 4 screws. Allow the acrylic to dry (approximately 20 minutes)

TASK 19: SPINAL MOUNTS

THORACIC T-1: _____ THORACIC T-6: ____ LUMBAR L-1 _____

_____ A. Make an incision over each of the vertebrae. Separate the muscles and tissue to expose the bone. Remove the top half of each of the spinous processes.

_____ B. Prepare acrylic mix and use it between the mounts and the vertebrae to fill any air space.

_____ C. Secure the mounts to the vertebrae with wood screws. Use an appropriate size screw to make sure that the structural integrity of the vertebrae are not compromised.

_____ D. Mold more acrylic around the mounts to anchor them to the vertebrae. Keep fluid leakage to a minimum by filling the incisions with gauze and temporarily sealing them with duct tape.

TASK 20: POSITIONING OPERATION CHECKLIST

_____ A. Dress cadaver.

_____ B. Position on "orange" table with the head/neck overhanging; shoulders aligned with edge of foam.

_____ C. Brace against foot board.

_____ D. Hands stretched and tied to upper thighs.

_____ E. Feet tied together.

_____ F. Install 3 triax accelerometers on head plate.

_____ G. Install 3 triax accelerometer packages on spine.

_____ H. Align cadaver spine with the impact device.

_____ I. Pull out the piston to estimate contact point.

_____ J. Place the head and the neck in position and tape to cantilever.

_____ K. X-ray to determine head/neck/impactor orientation.

_____ L. Final position.

TASK 21: IN-PLACE X-RAYS OPERATION CHECKLIST

Prepare station labels and do the following x-rays. Each station is defined by locations of cassette holder and opposite head location. Record/modify KVP/MA/SEC as necessary.

While x-rays are being developed, move to next station.

KVP	MA	SEC	LABEL	
				Source LEFT OF CADAVER (Film in 1st quadrant)
____	____	____	_____	STATION: X _____ F _____
____	____	____	_____	STATION: X _____ F _____
____	____	____	_____	STATION: X _____ F _____
____	____	____	_____	STATION: X _____ F _____
				Source RIGHT OF CADAVER (Film in 2nd quadrant)
____	____	____	_____	STATION: X _____ F _____
____	____	____	_____	STATION: X _____ F _____
____	____	____	_____	STATION: X _____ F _____
____	____	____	_____	STATION: X _____ F _____

TASK 22: CANNON OPERATION CHECKLIST

_____ A. Calibration

_____ B. Chronograph zero and green light

_____ C. Piston status green

_____ D. Velocity probe 2.5" from impact

_____ E. Correct padding

_____ F. Load cell cables clear of all obstacles and strain relieved

_____ G. Pressure

_____ H. All doors locked and individuals in position

TASK 23: HIGH SPEED X-RAYS OPERATION CHECKLIST

_____ A. Turn on CineRadioGraph (CRG) focusing magnet. Check to see that it limits.

_____ B. Position the CRG.

_____ C. Position x-ray head approximately 40" from the screen of the CRG.

_____ D. Lock the wheels on the x-ray head and CRG table.

_____ E. Check filters.

_____ F. Set Polaroid camera at f/16.

_____ G. Clear lab of all individuals not wearing x-ray badges.

_____ H. Take Polaroid photo.

_____ I. If necessary, adjust the KVP and distance from the x-ray head to the CRG screen. Retake a second Polaroid photo to check if further adjustment is necessary. Record the number of Polaroids taken. Save and label the good ones.

_____ J. Exchange the high speed movie camera for the Polaroid in the CRG camera mount.

_____ K. Check alignment of movie camera with the output screen.

_____ L. Focus the movie camera.

_____ M. Set the lens opening of the movie camera at its largest aperture.

_____ N. Take setup photos. Make sure that the test number and targets are visible.

_____ O. Check the pulse width on the gating circuit. It should be at 255 microseconds.

_____ P. Set x-ray head to CRG screen distance. Record.

_____ Q. Measure and record the subject mid-line to CRG screen distance.

TASK 24: POST-TEST SPINAL X-RAYS

KVP	MA	SEC	DESCRIPTION

Use bag of lead shot to position head/neck in desired position. Repeat if necessary.

Examine x-rays to detect a broken skull or any broken vertebrae.

TASK 25: BRAIN AUTOPSY

_____ A. Check the accelerometer mounts on T-1, T-6 and L-1 for any looseness by grasping each mount and moving the vertebrae. Note any looseness here. _____

_____ B. Remove the head and neck down to T-3 by making bilateral cuts through the costo-vertebral joints R-1 - R-3 and the inter-vertebral disc between T-3 and T-4.

_____ C. Remove the skin and superficial fascia of the neck. Examine the external jugular veins, sterno-mastoid muscles, trachea, and carotid sheaths for signs of lacerations and/or hemorrhage.

_____ D. Insert a scalpel blade at the occiputal proterberance and proceed toward the glabella making a circumferential cut.

_____ E. Remove the skin and superficial fascia and examine the underlying tissues for hemorrhage and fracture.

_____ F. Remove the calvarium by making a circumferential cut with a Stryker saw. The saw cut should be down to but not penetrating

the dura.

_____ G. Pry the calvarium loose by twisting a T-shaped chisel in the saw cut at the forehead or using a chisel and hammer. Place a basin at the occiput to catch any free flowing blood or clot which may escape when the calvarium is pried loose.

_____ H. If present, record the location and measure the volume of epidural hematoma. Photograph, if the clot remains in situ. Usually the hematoma will fall away.

_____ I. If an acute epidural hematoma is present, after cleaning the hematoma, attempt to identify a point of rupture of the meningeal artery, most commonly beneath the temporal squama.

_____ J. If no epidural hematoma is present, look carefully for the telltale darkening of the dura of underlying acute subdural hematoma. Place a catch basin at the occiput before proceeding with the incision of the dura.

_____ K. Incise the dura along the saw cut anteriorly and bilaterally but not posteriorly until you are ready to deliver the brain from the cranial cavity.

_____ L. If an acute subdural hematoma is present, then the incision can be extended posteriorly so the dura can be reflected to expose the hematoma. Try to retain the hematoma in place and photograph. Remove and measure the volume of the hematoma.

_____ M. If a hematoma is not present, the dura is not cut posteriorly so as to provide support for the brain while it is being retracted in the process of cutting the blood vessels and cranial nerves.

_____ N. At the most anterior point, cut the falx cerebri down to the crista galli.

_____ O. Deliver the frontal poles using fingers to expose the olfactory bulbs which should be carefully lifted from the olfactory fossae. The now exposed optic nerves are cut as close to the optic canals as possible. The internal carotid arteries will then come into view just beneath the optic nerves. Cut them carefully at right angles. Cut the infundibular stalk. The oculomotor nerves will come into view which should then be examined for hemorrhage or bruising. Cut them as long as possible at a point where they enter the wall

of the cavernous sinus.

_____ P. Rotate the head to one side and allow the uppermost temporal pole to fall out of the middle fossa. This will expose the petrous ridge of the temporal bone, the tentorium, and the margin of the incisura tentorii. Inspect the tentorium for hemorrhage.

_____ Q. Open the posterior fossa by cutting the tentorium cerebelli, beginning from the free margin of the incisura and cutting along the posterior margin of the petrous ridge and laterally and posteriorly just inside the transverse sinus without entering the latter. The cut should be carried as close as possible to the falx posteriorly. Do the same on the opposite side.

_____ R. Straighten the head back to the neutral position and cut, in order, the following cranial nerves: 5th, 6th, 7th and 8th, 9th, 10th, 11th, and 12th.

_____ S. Identify the vertebral arteries and with scissors carefully cut them just proximal to the takeoff of the posterior-inferior cerebellar arteries. Do not make multiple slashes with the scalpel.

_____ T. Place fingers on either side of the cerebellar tonsils and slowly deliver the cerebellum from the posterior fossa. Cut the spinal cord at the floor of the cranium.

_____ U. Inspect the floor of the cranium for hemorrhage. Examine the cerebellar tentorium and sinuses for tears. Peel the dura from the base of the skull and look for fractures.

TASK 26: NECK AUTOPSY

_____ A. Using a Stryker saw make a circumferential cut around the foramen magnum. Separate the neck from the floor of the cranium.

_____ B. Following the posterior neck dissection, clean away the soft tissues from the spinous processes and laminae down to C-7.

_____ C. Before proceeding with a laminectomy, grasp each cervical spinous process with Kocher forceps and attempt to move the vertebrae in the anteroposterior direction. If laxity is present, note the degree of laxity.

_____ D. Unroof the spinal canal by performing a laminectomy from C-1 through C-7 using a Stryker saw.

_____ E. Look for epidural hematoma, and, if present, record the location and measure the volume.

_____ F. Examine the dura mater for tears, dural hemorrhage, and underlying discoloration.

_____ G. Make a button-hole in the dura at the highest exposed level. Slit the dura over its entire length along the posterior midline, taking care not to dislodge any underlying subdural hematoma. If a hematoma is present, indicate the level with a reference marker and a photograph.

_____ H. Transect the spinal cord at C-1 and free the cord from the dura by carefully cutting all the dentate ligaments and roots at the root sleeves.

_____ I. Inspect the fibrous ring and anterior and posterior longitudinal ligaments for tears and hemorrhages.

_____ J. Examine the vertebral bodies of C-2 through C-7 for fractures.

TASK 27: BONE ASHING

After doing the autopsy, remove from the calvarium a bone sample between 1 to 2 square inches. Save this "wet" sample in a tightly closed plastic bag, then deliver to the laboratory where bone ashing will be perfomed as follows:

_____ A. Blot sample with absorbent paper; then weigh it. Record this weight in milligrams (mg) as the "wet weight" or WETMG.

_____ B. Freeze-dry the sample for at least 36 hours.

_____ C. Oven-dry the freeze-dried sample at 75C for at least 48 hours and until the sample reaches a constant weight. Record this weight as the "dry matter weight" in mg, or DRYMG.

_____ D. The last stage is to ash the dry sample in a muffle at 700C for a minimum of 72 hours until all residues turn whitish and reach constant weight. Record this weight as the "total ash weight" or ASHMG.

WETMG = _____ DRYMG = _____ ASHMG = _____

_____ E. Calculate the ASH CONTENT in percent as follows:

WET ASH CONTENT(%) = 100x(ASHMG/WETMG) = _____

DRY ASH CONTENT(%) = 100x(ASHMG/DRYMG) = _____

I N S T R U M E N T A T I O N D I A G R A M S

NIOSH: S-I Head Impact Injury Tolerance Levels TEST NO.

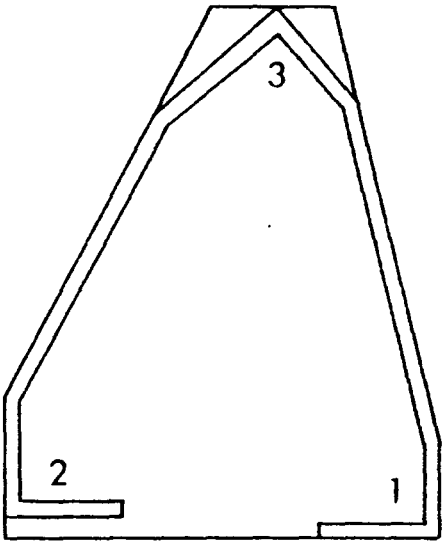

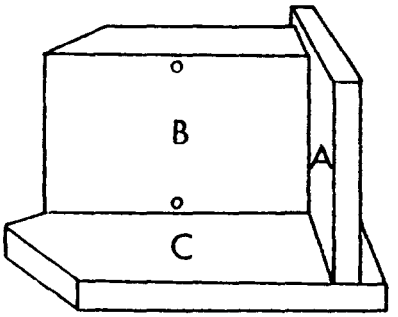

COMMENTS (Check threads on all mounts before assembly):

NIOSH: S-I Head Impact
Injury Tolerance Levels

TEST NO.

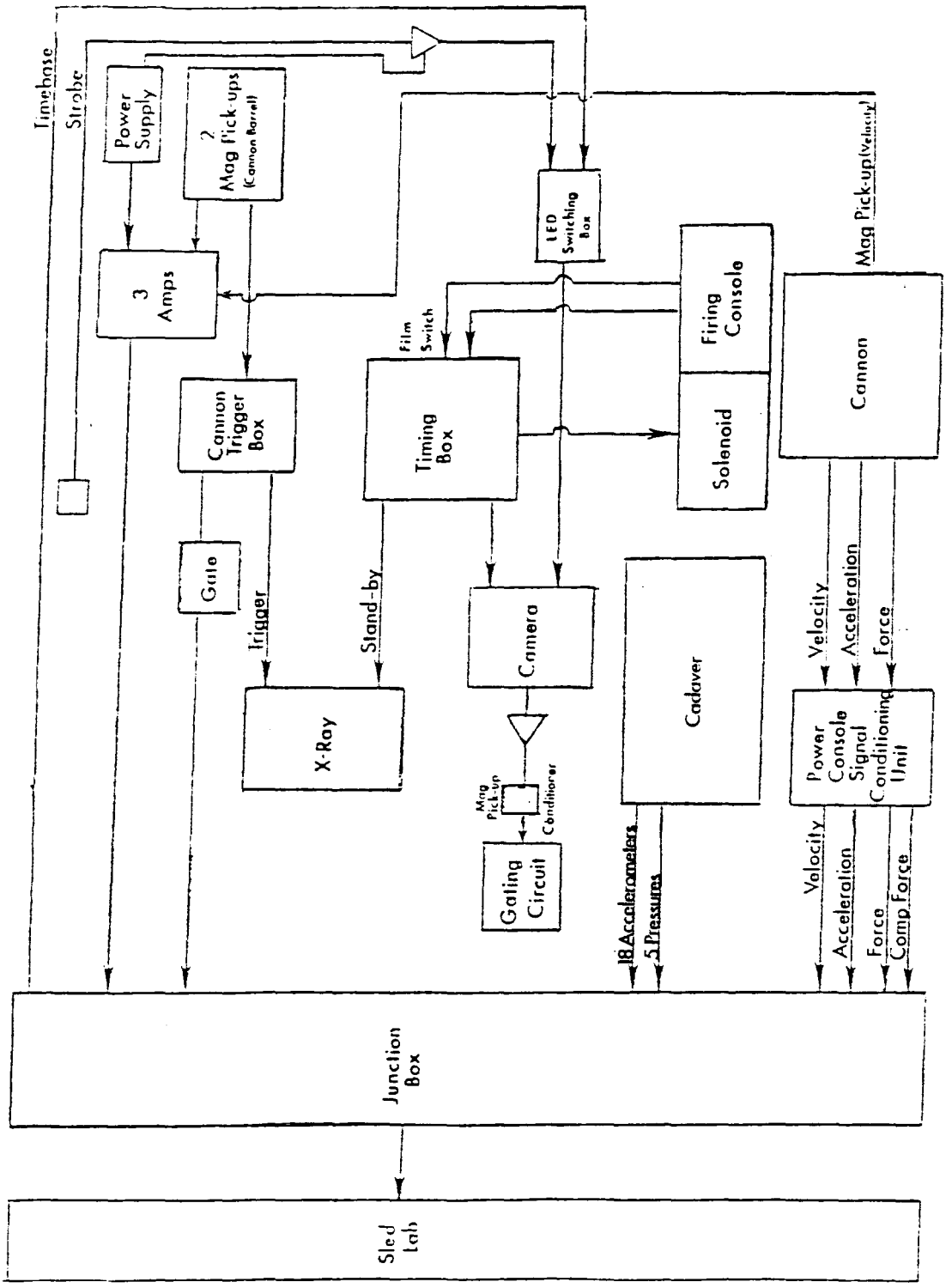

NIOSH: S-I Head Impact Injury Tolerance Levels TEST NO.

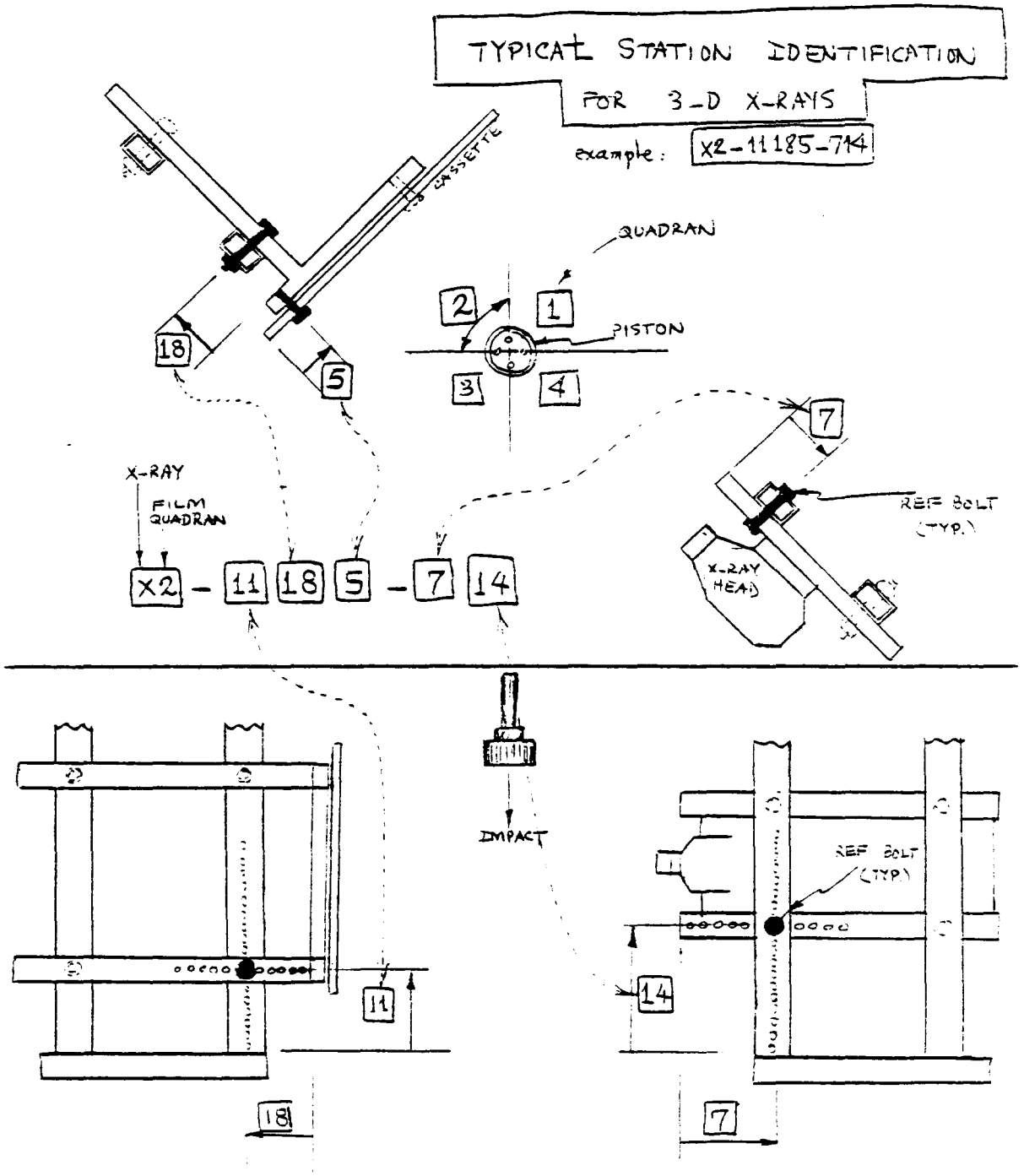

A U T O P S Y D I A G R A M S

NIOSH: S-I Head Impact TEST NO.
Injury Tolerance Levels

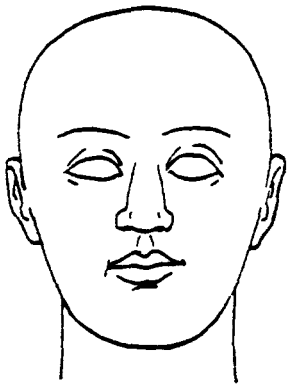

Anterior View

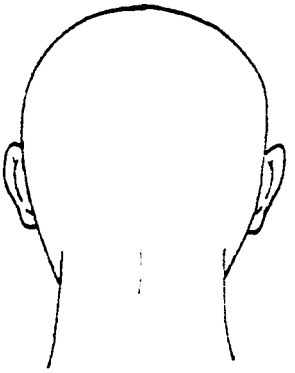

Posterior View

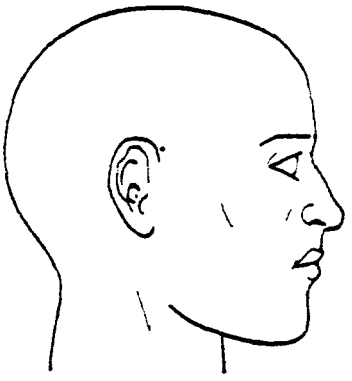

Right Lateral View

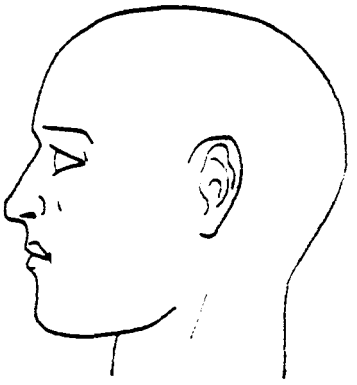

Left Lateral View

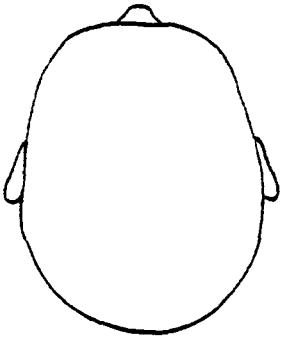

Superior View

NIOSH: S-I Head Impact Injury Tolerance Levels TEST NO.

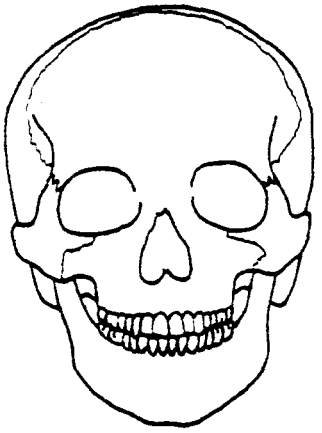

Anterior View

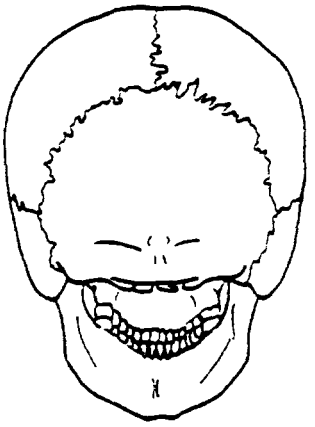

Posterior View

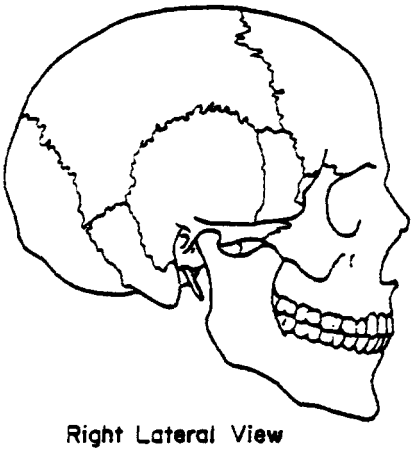

Right Lateral View

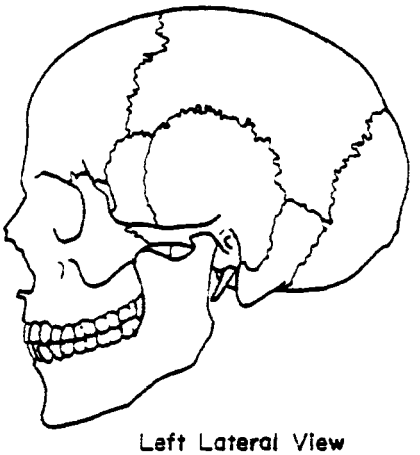

Left Lateral View

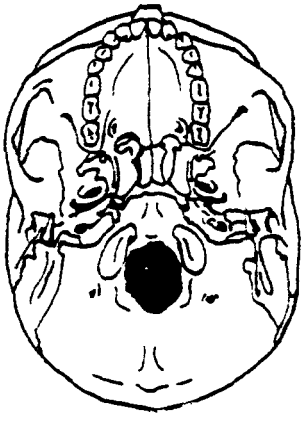

Inferior View

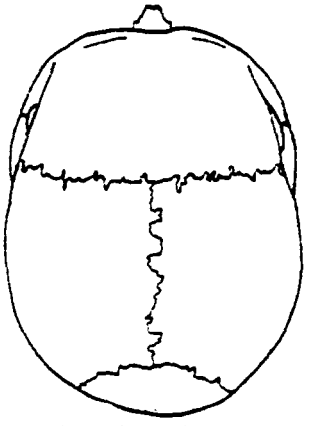

Superior View

NIOSH: S-I Head Impact TEST NO.
Injury Tolerance Levels

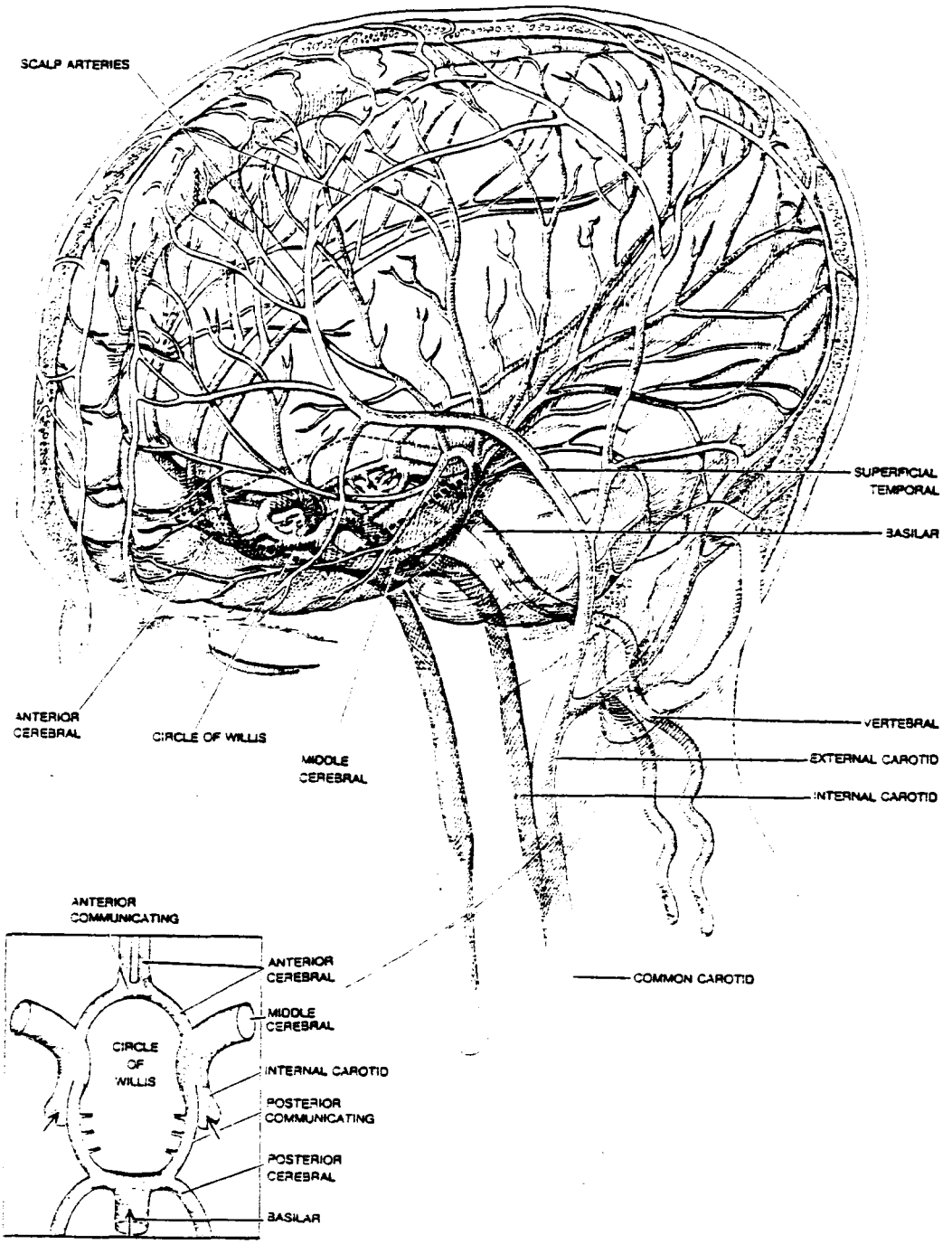

NIOSH: S-I Head Impact TEST NO.
Injury Tolerance Levels

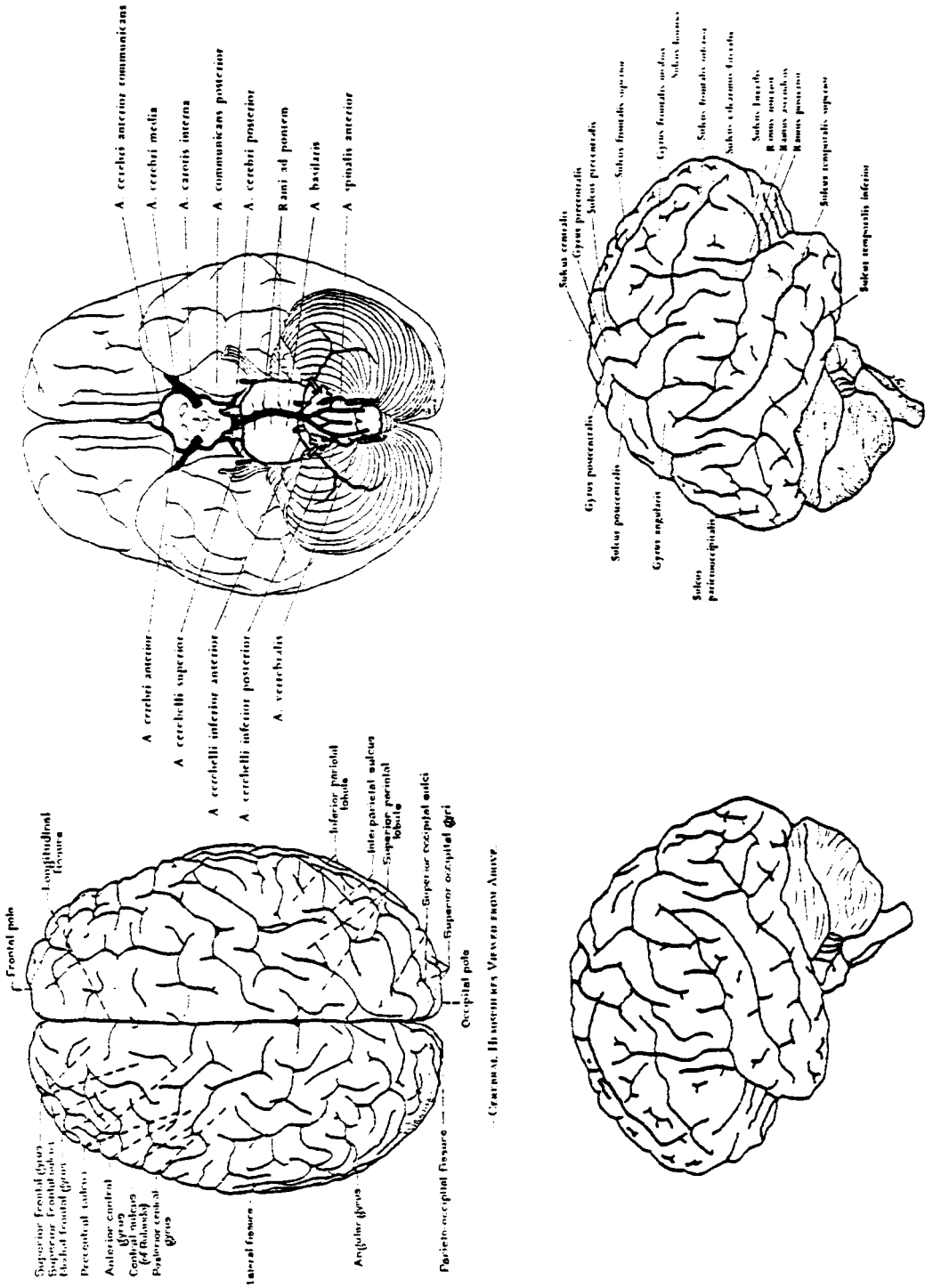

NIOSH: S-I Head Impact TEST NO.
Injury Tolerance Levels

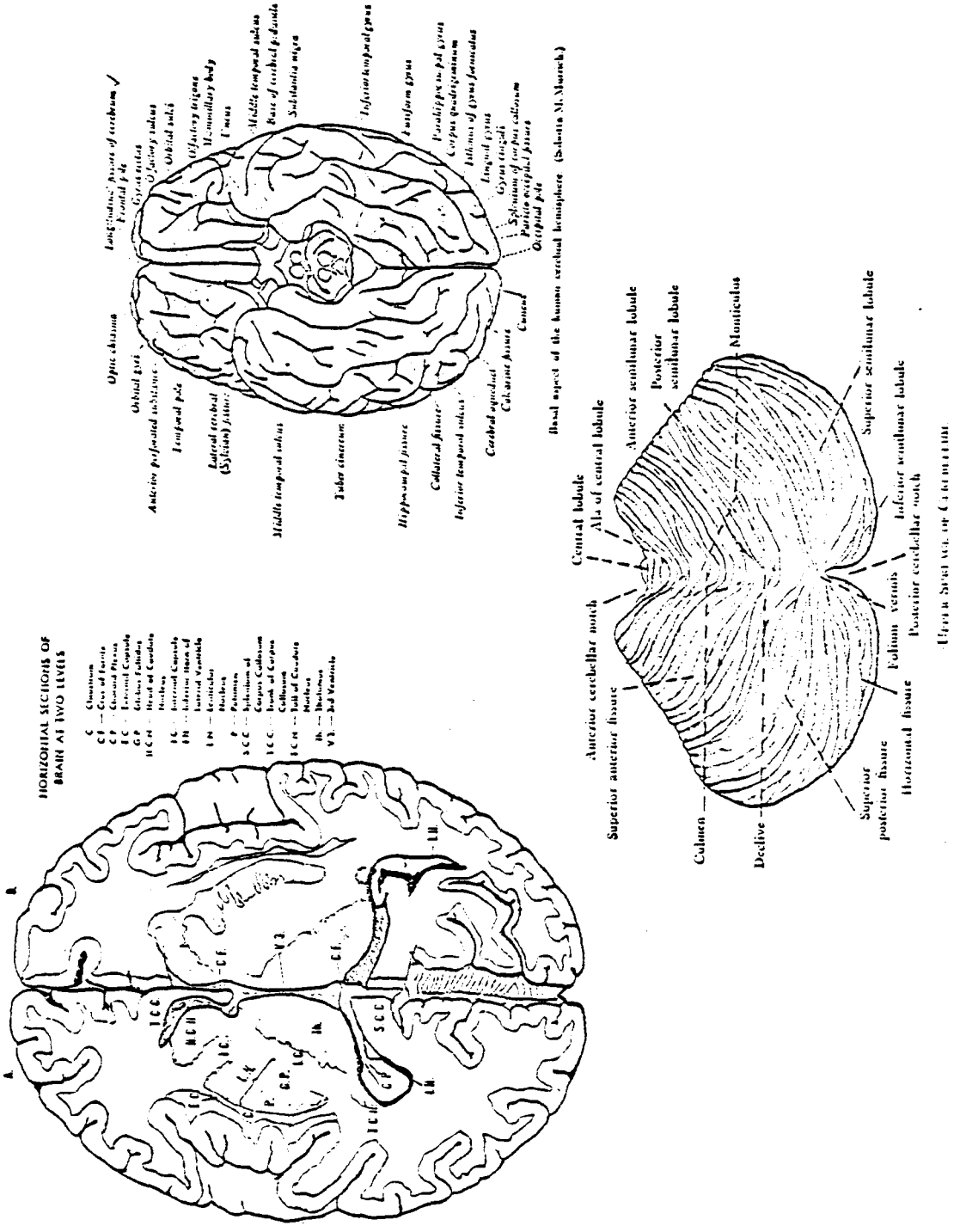

NIOSH: S-I Head Impact Injury Tolerance Levels TEST NO.

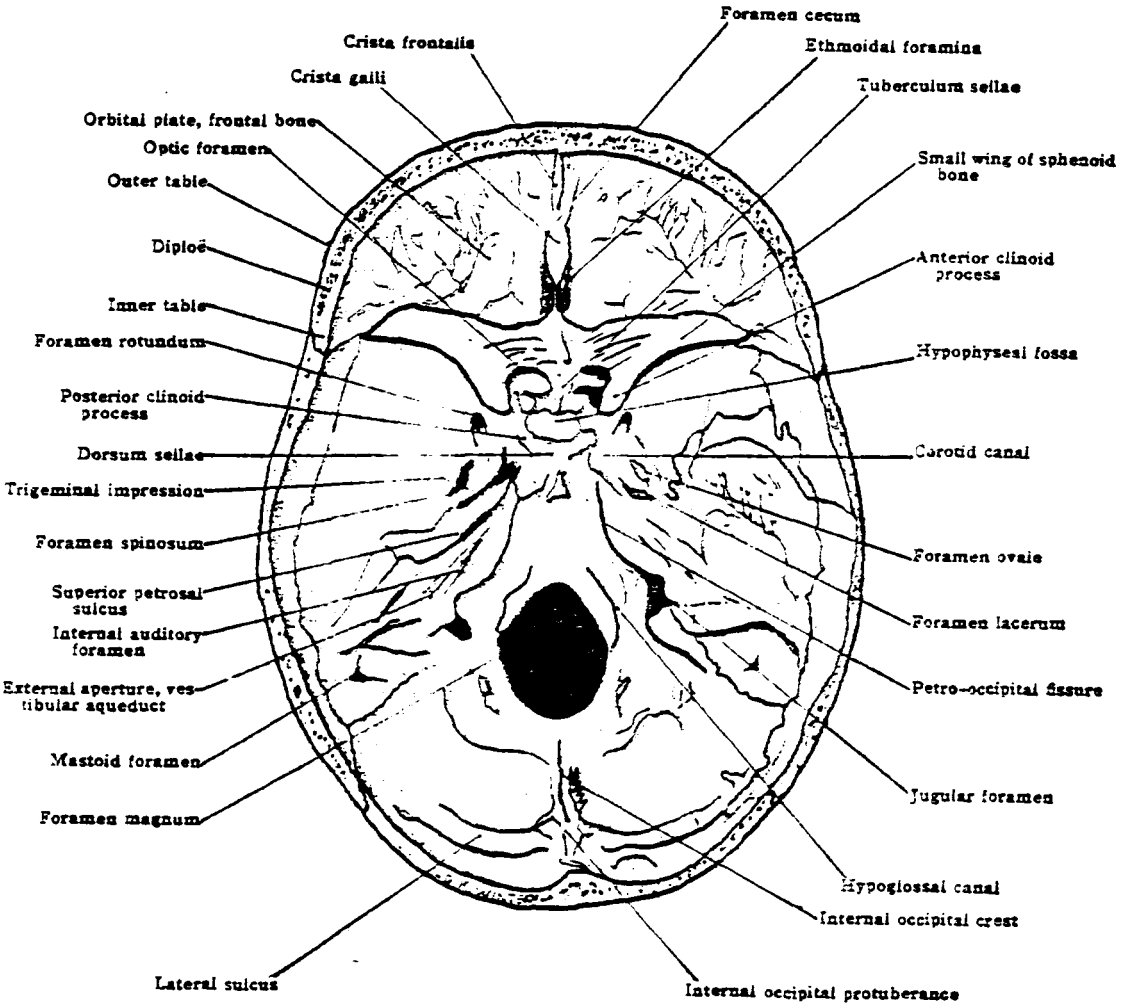

THE SKULL, INTERNAL ASPECT OF THE BASE.

NIOSH: S-I Head Impact TEST NO.
Injury Tolerance Levels

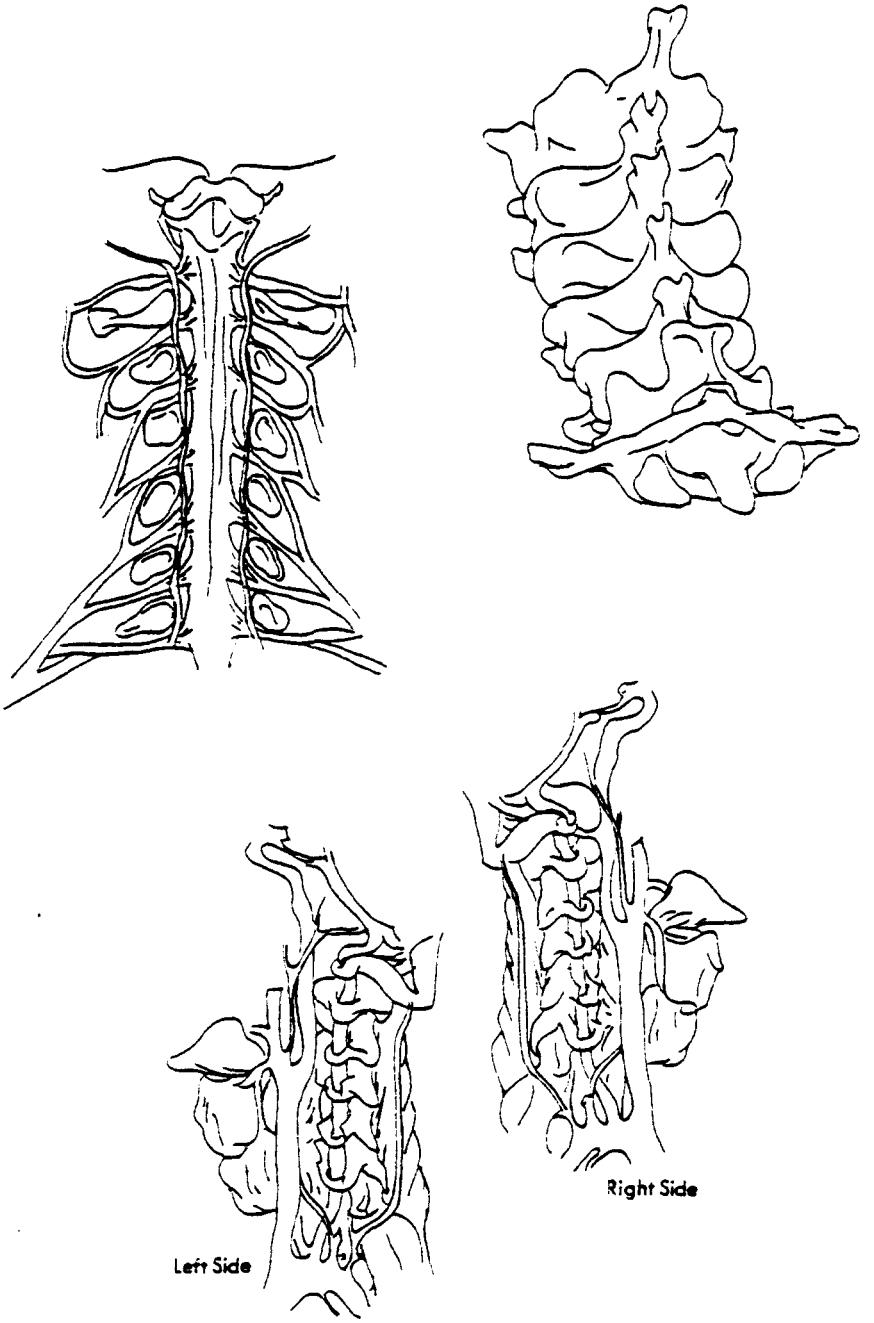

NIOSH: S-I Head Impact TEST NO.
Injury Tolerance Levels

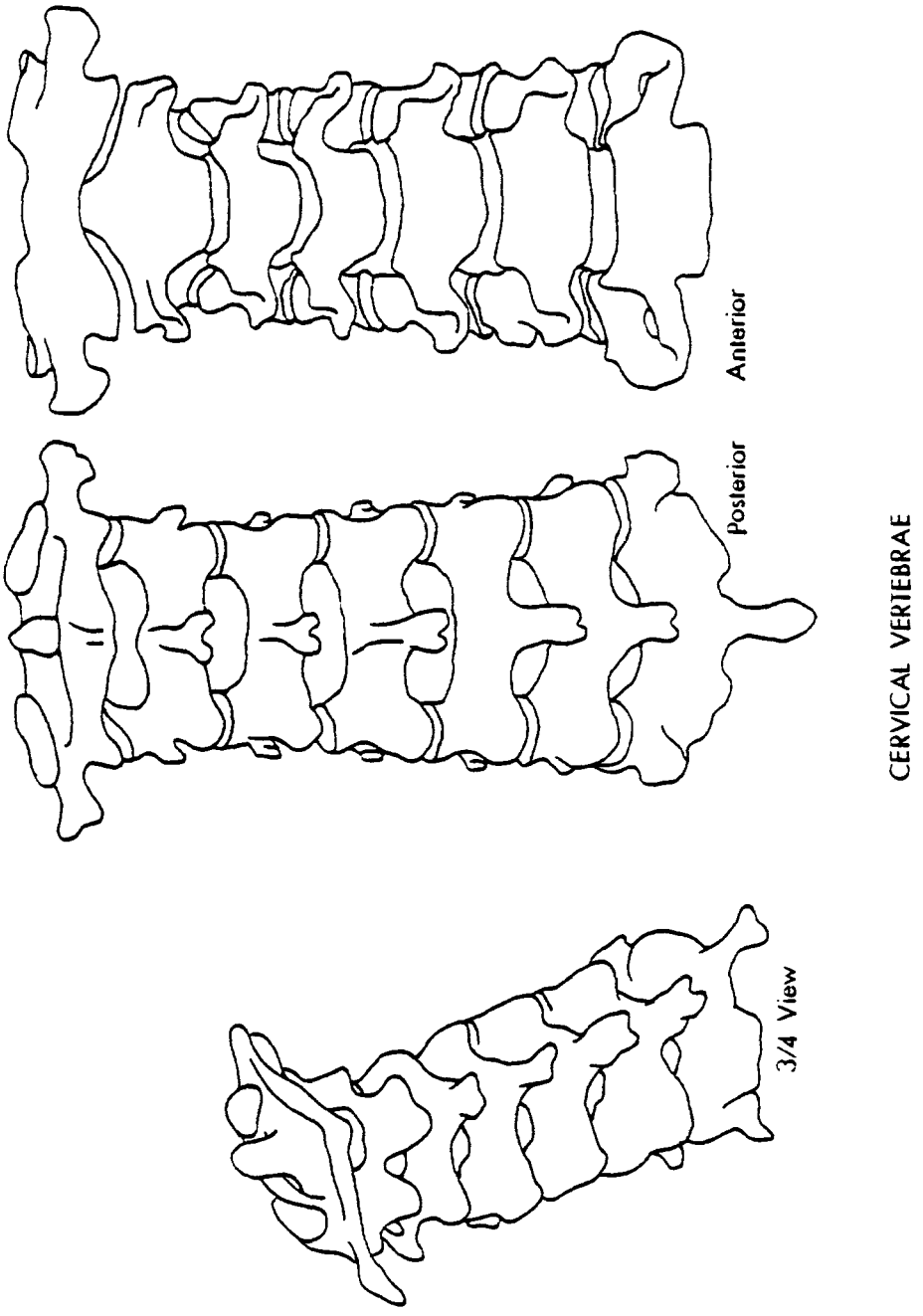

NIOSH: S-I Head Impact TEST NO.
Injury Tolerance Levels

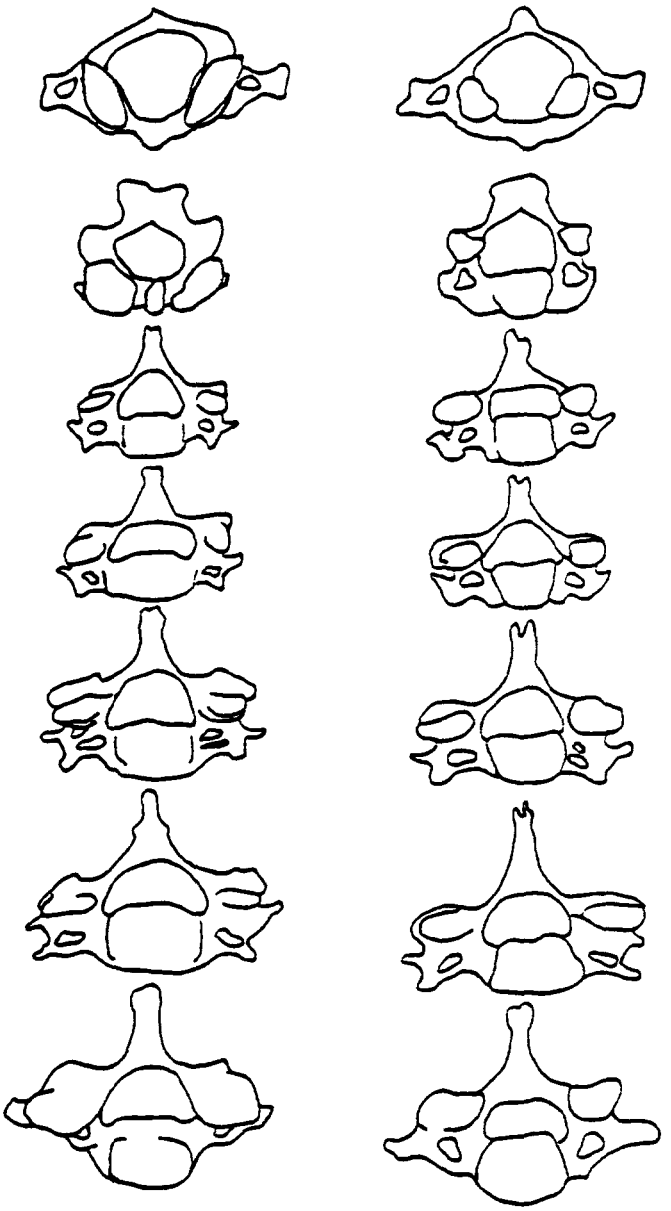

View from Above View from Below

NIOSH: S-I Head Impact TEST NO.
Injury Tolerance Levels